UNIVERSITY OF LONDON THESIS

Degree PhD Year 2006 Name of Author FREE, Paul Francis

COPYRIGHT

This is a thesis accepted for a Higher Degree of the University of London. It is an unpublished typescript and the copyright is held by the author. All persons consulting the thesis must read and abide by the Copyright Declaration below.

COPYRIGHT DECLARATION

I recognise that the copyright of the above-described thesis rests with the author and that no quotation from it or information derived from it may be published without the prior written consent of the author.

LOAN

Theses may not be lent to individuals, but the University Library may lend a copy to approved libraries within the United Kingdom, for consultation solely on the premises of those libraries. Application should be made to: The Theses Section, University of London Library, Senate House, Malet Street, London WC1E 7HU.

REPRODUCTION

University of London theses may not be reproduced without explicit written permission from the University of London Library. Enquiries should be addressed to the Theses Section of the Library. Regulations concerning reproduction vary according to the date of acceptance of the thesis and are listed below as guidelines.

A. Before 1962. Permission granted only upon the prior written consent of the author. (The University Library will provide addresses where possible).

B. 1962 - 1974. In many cases the author has agreed to permit copying upon completion of a Copyright Declaration.

C. 1975 - 1988. Most theses may be copied upon completion of a Copyright Declaration.

D. 1989 onwards. Most theses may be copied.

This thesis comes within category D.

☐ This copy has been deposited in the Library of UCL

☐ This copy has been deposited in the University of London Library, Senate House, Malet Street, London WC1E 7HU.

The role of Cathepsin E in the Antigen Processing and Presentation Pathway

A thesis submitted in requirement for the degree of Doctor of Philosophy in the University of London

Paul Francis Free

Department of Immunology and Molecular Pathology,
Department of Chemistry

University College London
2006

ProQuest LLC
789 East Eisenhower Parkway
P.O. Box 1346
Ann Arbor, MI 48106-1346

Abstract

Although much has been unravelled with regards to the mechanisms of proteolysis of exogenously derived antigen for presentation *via* histocompatibility class-II (MHC-II), key questions remain unresolved. The exact role of each proteolytic enzyme in this process is not understood. The aspartic proteinase cathepsin E is hypothesised to play an important role. The aim of this study is to examine this by the use of novel aspartic proteinase inhibitors based upon the aspartic proteinase inhibitor pepstatin A.

The first two inhibitors designed and synthesised included a mannose sugar molecule to improve solubility, a linker section and a single pepstatin molecule. The mannose derivative 3'-succinimidoxycarbonyl-propyl 2,3,4,6-tetra-*O*-acetyl-α-D-mannopyranoside was synthesised and linked *via* an amide bond to either *N*-(*t*-butyloxycarbonyl) propane-1,3-diamine or *N*-(*t*-butyloxycarbonyl) cystamine, the latter of these containing a cellularly cleavable disulphide bond. After deprotection, the amines of these two molecules were further reacted with pepstatin succinimide to form the precursors to the inhibitors *N*-(3-(α-D-mannopyranosyloxy) propylcarbonyl),*N*' (pepstat-inyl) propane-1,3-diamine (Mannose Pepstatin Conjugate 1, MPC1) and *N*-(3-(α-D-mannopyranosyloxy) propylcarbonyl),*N*'-(pepstatinyl) cyst-amine (MPC2), the final products being formed by selective removal of the mannopyranosyl acetyl protecting groups. The purified inhibitors were tested in a well-characterised *in vitro* model of antigen processing, in which ovalbumin is processed and presented by a B-cell line A20 to ovalbumin-specific T-cells, DO11-10.

Further studies aimed to address the role of cathepsin E within dendritic cells (DCs), one of the key cells involved in initiating and propagating immune response to antigen. Further inhibitors were designed with the

aim of improving solubility and cellular targeting. These inhibitors contained multiple mannose sugars attached either to a protein backbone bovine serum albumin (MPC5 and 6) or a poly-lysine backbone (MPC3 and 4). As for MPC2, a cleavable linker was included in the design of MPC4 and MPC6, to facilitate intracellular release of pepstatin from the carrier.

The full synthesis of MPC5 and MPC6 was achieved by the coupling of either *N*-(iodoacetyl),*N*'-(pepstatinyl) propane-1,3-diamine (MPC5) or *N*-(iodoacetyl),*N*'-(pepstatinyl) cystamine (MPC6) to the single free sulfhydryl of mannosylated bovine serum albumin (BSA) protein. The mannosylated BSA protein was achieved by the thiourea bond formation between the multiple lysine residues contained within BSA and the amine-reactive mannose derivative 4-isothiocyanatophenyl α-D-mannopyranoside. Biochemical tests showed that between 22 and 24 mannose units were coupled to each BSA protein. The inhibitors MPC5 and MPC6 were tested for their ability to block processing and presentation of ovalbumin by mouse bone-marrow derived DCs. Since pepstatin A inhibits not only cathepsin E but also the lysosomal proteinase cathepsin D, the inhibitors were further tested on DCs prepared from mice deficient in cathepsin D. The results suggest that cathepsin E has an important and non-redundant role in antigen processing of ovalbumin by dendritic cells.

This work was supported by funds supplied by the Department of Immunology and Molecular Pathology, UCL, and the Department of Chemistry, UCL. In addition, an Interdisciplinary Research Scholarship was provided by the UCL Graduate School, and a MONBUSHO Fellowship was provided by the Japanese Science & Education Ministry / British Council.

To my friends and family for their constant support and encouragement

Acknowledgements

I would like to thank both of my supervisors, Doctor Alethea Tabor and Professor Benny Chain. I appreciate their encouragement and wisdom in making this project possible, and helping me to develop the skills and foresight required for such a project. I am grateful for their patience and guidance in what has been a very difficult few years towards the final thesis submission. I appreciate the efforts made to get me to the end of this thesis. I would also like to thank Professor David Katz for his help and encouragement. In addition, I would like to thank Professor Takeshi Kagiyama for allowing me to work within his laboratory at the University of Kyoto, it was a very valuable experience.

I have had the pleasure to work with, and socialise with some amazing people during my time at UCL, many of which will always be good friends of mine. I would like to thank Luciene Lopez, Liljana Petrovska, Marienne Groussier and Piers Gaffney for their friendship and help with training in techniques used throughout my PhD. Several peptides were made on a MilliGen 9050 peptide synthesiser by my colleagues Erwann Guenin and Mike Miksa, to whom I gratefully acknowledge their contribution.

My eternal friends Charles Alderman and Jae Youl Cho, who started their PhDs with me in immunology, will always be remembered for their encouragement during bad times and our joy during good times. I would in addition like to thank the following from the department of chemistry for their help and friendship: Sarah Sheady, Linda McNamara, Firouz Mustapa, Frieder Mitzel, Chris Hurley, Paul Bell and Nives Bulic-Subanovic. Those in the department of immunology I would like to thank include: Pippa Newton, Peter Bunyard, Christina Lindved, Katharina Speidel, Remi Creusot, Gabriel Pollara, Ariel Rad, Clair Swetman, Paul

Kaye and Matthew Handley. Thanks to everyone who have helped on my long journey.

I would especially like to thank Professor Avrion Mitchison for being an excellent landlord for several years, and for introducing me to a truly outstanding academic and intellectual environment. It was a great pleasure to know his family, in particular his wife Lorna, and his eccentric neighbour Gerry Clarke. They have shown me the potential of what can be achieved with a bit of care, thought and determination.

Being a friendly character, and having my feet firmly attached to the ground, I had the great pleasure to get to know all of the staff that worked behind the scenes at both departments, and I would like to thank them all for there friendliness.

My close friends and family from my home in East London will always be important to me, being my roots and branches from which 'I am what I am'. Would also like to thank West Ham FC for having a great year and getting into the FA cup final!!

Declaration

The structure of this thesis contains both elements of a biological and a chemical thesis. I have tried to structure this thesis in a format that would lead to the reading of the project in a logical order that would aid in the understanding of the overall project.

I, Paul Francis Free, hereby declare that all of the work presented is entirely my own.

Paul Francis Free
May, 2006

Contents

Chapter 1

From Antigen to Immune Response – An Antigen Processing and Presentation Viewpoint

Chapter 2

Design of aspartic proteinase inhibitors for use within antigen presenting cells

Chapter 3

Chemical Synthesis

Chapter 4

Chemical Synthesis Results and Discussion

Chapter 5

Methods for Biological Study

Chapter 6

The Use of pepstatin inhibitors in dissecting the role of cathepsin E

List of Tables

List of Figures

Abbreviations

2-ME	2-Mercaptoethanol
AcOH	Acetic acid
AEP	Asparaginyl endopeptidase
Ag	Antigen
APC	Antigen presenting cell
B112 mice	C57BL/6J crossed Balb/c mice with I-A^d haplotype
BACE	β-Site amyloid precursor protein-cleaving enzyme
BSA	Bovine serum albumin
CD	Cathepsin D
CE	Cathepsin E
$CHCl_3$	Chloroform
CH_2Cl_2	Dichloromethane
CIITA	Class II transactivator
CIIV	Class II containing vesicle
CLIP	Class II-associated invariant chain peptide
Con A	Concanavalin A
COSY	Correlation spectroscopy
DC	Dendritic cell
DCM	Dichloromethane
Dde	1-(4,4-Dimethyl-2,6-dioxocyclohexylidene)ethyl
DEC-205	CD205
DEPT	Distortionless enhancement by polarisation transfer
DMSO	Dimethyl sulfoxide
DNA	Deoxyribonucleic acid
EDCI	1-(3-Dimethylaminopropyl)-3-ethylcarbodiimide hydrochloride
EDTA	Ethylene diamine tetraacetic acid, disodium salt
ELISA	Enzyme linked immunosorption assay
ER	Endoplasmic reticulum
EtOH	Ethanol
FACS	Fluorescence-activated cell sorting

FCS	Fetal calf serum
FITC	Fluorescein isothiocyanate
FITC-DX	FITC-dextran
G418	Geneticin
GILT	γ-Interferon-like thiol reductase
GM-CSF	Granulocyte-macrophage colony-stimulating factor
HBSS	Hanks buffered saline solution
HEPES	(*N*-2-Hydroxyethylpiperazine-*N*'-2-ethanesulphonic acid)
HSQC	Heteronuclear single quantum coherence
IFN-γ	Interferon-γ
Ig	Immunoglobulin
Ii	Invariant chain
IL-	Interleukin-
IL-2	Interleukin-2
LE	Late endosome
LIP	Leupeptin-induced peptide
LY	Lucifer yellow
MALDI-TOF MS	Matrix-assisted laser desorption time-of-flight mass spectrometry
MBP	Myelin basic protein
MeCN	Acetonitrile
MEM	Modified eagle medium
MHC class-I	Majorhistocompatibility class-I complex
MHC class-II	Majorhistocompatibility class-II complex
MIIC	MHC class-II compartment
MPC1 – 6	Mannose Pepstatin Conjugate 1 - 6
MR	Mannose Receptor
MMR	Macrophage Mannose Receptor, as MR
MTT	3-(4,5-Dimethylthiazol-2-yl)-2,5-diphenyltetrazolium bromide
MVB	Multivesicular body
NHS	*N*-Hydroxysuccinimide
NMR	Nuclear magnetic resonance
NOESY	Nuclear Overhauser effect spectroscopy

O.D.	Optical density
OVA	Chicken egg ovalbumin
OVA–peptide	Fragment 323 – 329 of chicken egg ovalbumin protein
p323	as OVA – peptide
PAMAM	Poly(amidoamine)
PBS	Phosphate buffered saline
PCR	Polymerase chain reaction
Pepstatin	Pepstatin A
PI-3	*Ascaris* pepsin inhibitor-3
PMA	Phosphomolybdic acid
PRR	Pattern recognition receptor
RER	Rough endoplasmic reticulum
RT	Retention time
s/n	Supernatant
SDS	Sodium dodecyl sulphate
SLIP	Small leupeptin-induced peptide
TCR	T-cell receptor
TEA	Triethylamine
THF	Tetrahydrofuran
TMB	3, 3', 5, 5' – Tetramethyl benzidine
Tween 20	Polyoxyethylene sorbitan monolaurate

Chapter 1

From Antigen to Immune Response – An Antigen Processing and Presentation Viewpoint

1.1 Introduction

The recognition of foreign particles such as proteins, peptides, lipids and carbohydrates (known as antigen) by effector cells expressing specific antigen receptors is paramount to forming a successful adaptive immune response. Antigen presenting cells (APCs) hold the key role of internalising, processing and presenting soluble antigen to T lymphocytes that occurs through the interaction of the T-cell receptor (TCR) complex with APC presented antigen on surface majorhistocompatibility complex (MHC) class-I or -II molecules.

The mechanisms involved in the antigen processing and presentation pathways of APCs are complex. These mechanisms are not a set of distinct predictable processes and have great diversity in their action. One protein can be proteolytically cleaved into numerous fragments, in theory to produce many antigenic peptides. However more often than not a single or several immunodominant peptides are produced. The mechanisms that control this process are still being studied, but it is known that the enzymes that proteolytically cleave antigenic proteins play a vital role. A successfully activated T-cell, by interaction with an APC peptide / MHC complex, will induce T-cells to mediate other immune responses, such as release of cytokines from helper $CD4^+$ T-cells or $CD8^+$ T-cell mediated cell killing.

The mechanisms of antigen processing and presentation can be broadly divided into two, major histocompatibility class-I (MHC class-I) and major histocompatibility class-II (MHC class-II) mediated antigen presentation. The discussion of MHC class-I antigen presentation is not within the scope of this research and will not be discussed further.

MHC class-II molecules are expressed on APCs and predominantly bind antigen taken in from without the cell. Antigens derived from invading organisms is efficiently internalised into APCs by specialised mechanisms that recognise common antigenic molecular patterns on pathogens.

The possible role of the enzyme cathepsin E (CE) within the formation of MHC class-II presented peptidic fragments is the concern of this thesis. To gain more insight into its possible role, and to highlight the complexity of the antigen processing and presentation system, several areas will be explained in this chapter. The pathway from antigen entry into an APC to antigenic peptide presentation on the surface, complexed with MHC class II will be examined. The participation of the proteolytic enzymes that generate the antigenic peptides will also be discussed, in particular the aspartic proteases cathepsin D and E. An overview of some inhibitors of such proteinases, followed by a discussion of an approach to study the proteinase cathepsin E will conclude the chapter.

An understanding of these concepts will highlight the major obstacles in the study and understanding of the antigen processing pathway. Chapter 2 will highlight some criteria that need to be considered in the design of aspartic proteinase inhibitors that can be used in the study of antigen processing. Chapter 2 will also propose some synthesis procedures and chemical structures of aspartic proteinase inhibitors. Chapter 3 details the synthesis of these compounds, with chapter 4 discussing the results of this synthesis. Chapter 5 explain the materials and methods used in the biological study of the synthesised inhibitors. The biological data obtained in the testing of the synthesised inhibitors upon several models of antigen processing are presented in Chapter 6. The conclusion to this thesis summarises the information obtained and discusses it in the context of current information on antigen processing, and details improvements that can be made for future work.

1.2 The 'professional' antigen presenting cells

The skin and absorptive epithelia are the first line of defence to intercept many invading organisms. The epithelium and most tissues of the body contain a class of "professional" APCs that are well suited to capture, internalise, degrade and present extracellular antigen. Professional APC express a variety of cell surface receptors that are involved in the internalisation of microbial antigens[5,6]. They contain acidic intracellular vesicles containing numerous proteolytic enzymes able to generate antigenic peptides for loading onto MHC class-II molecules[7,8]. The professional APCs can also express high levels of MHC class-II and costimulatory molecules for efficient CD4+ T-cell activation. The antigen presenting function of these cells is upregulated when pathogens are recognised by APC cell surface pattern recognition receptors (PRRs) such as the Toll-like receptors (TLRs)[9]. Epithelial cells themselves along with cells such as monocytes and astrocytes, do not constitutively express MHC class-II and other elements of the antigen processing machinery to allow presentation to activated CD4+ T-cells. These cells usually express this function only when activated by pro-inflammatory factors such as IFN-γ. These cells are sometimes referred to as "non-professional" APCs.

1.2.1 Dendritic Cells

Unlike the B-cell and the macrophage, the dendritic cell is mainly concerned with the efficient endocytosis, degradation and presentation of antigenic particles to both CD4+ and CD8+ T-cells. Their specialisation for this function is reflected by the fact that DCs are the only cells able to activate naïve T-cells, and hence are necessary for the establishment of the memory T-cell pool. There are numerous reviews on dendritic cell immunobiology[10,11] that can be read for more information.

The DC takes up antigen *via* receptor-mediated endocytosis, phagocytosis or macropinocytosis (see section 1.3). Receptor mediated endocytosis, like that of the macrophage, involves many different types of receptors including the mannose receptor, scavenger receptors or *via* FcγRII receptor mediated endocytosis[12,13]. Macropinocytosis is a specialised form of rapid fluid endocytosis, a function performed by immature dendritic cells as a means to sample large volumes of extracellular fluid[14]. The antigen sampling abilities of peripheral DCs can quickly change in the presence of microbial signals. TLRs are among a group of cellular receptors (PRRs) that play a major role in signalling the presence of pathogens to DCs[15]. The classical TLR interaction response of DCs is to mature and migrate from the tissue periphery to the T-cell zone of lymph node or spleen, and to express co-stimulation molecules[16]. Transient stimulation of antigen macropinocytosis and antigen processing occurs before the maturation events occur[17-19]. The interaction of TLRs on DCs with microbes is a key link between innate and adaptive immunity. Recognition of foreign particles by DC PRRs induces the secretion of cytokines and chemokines that causes inflammation and activation of other immune cells, or induces chemotaxis of immune cells to the infected region. In short, the innate recognition of pathogenic signals by immune cells, in particular DC, activates the adaptive immune response.

During DC migration and maturation, the cell function switches from antigen sampling to antigen presenting. The expression of antigen processing enzymes is at its maximum to increase the maximum amount of antigen presented by MHC class-II molecules, however during the maturation process, these enzymes are downregulated. Important co-receptors (such as CD80 / CD86 and CD40) are expressed to deliver the "second signal" costimulation that is required along with MHC / TCR / peptide to activate T cells. In addition, the cell morphology changes once within a lymphoid organ. DCs mature into cells that send out many dendrites to form contact with several T-cells, forming a characteristic DC / T-cell cluster.

1.3 Endocytosis - mechanisms involved in antigen uptake

The mechanisms employed by professional APC to endocytose or to phagocytose microorganisms are highly specialised to ensure maximum efficiency of antigen internalisation. Four main mechanisms have been described, macropinocytosis, phagocytosis, clathrin-mediated coated pit endocytosis and caveolae-mediated endocytosis. These are diagrammatically represented in fig. 1.1.

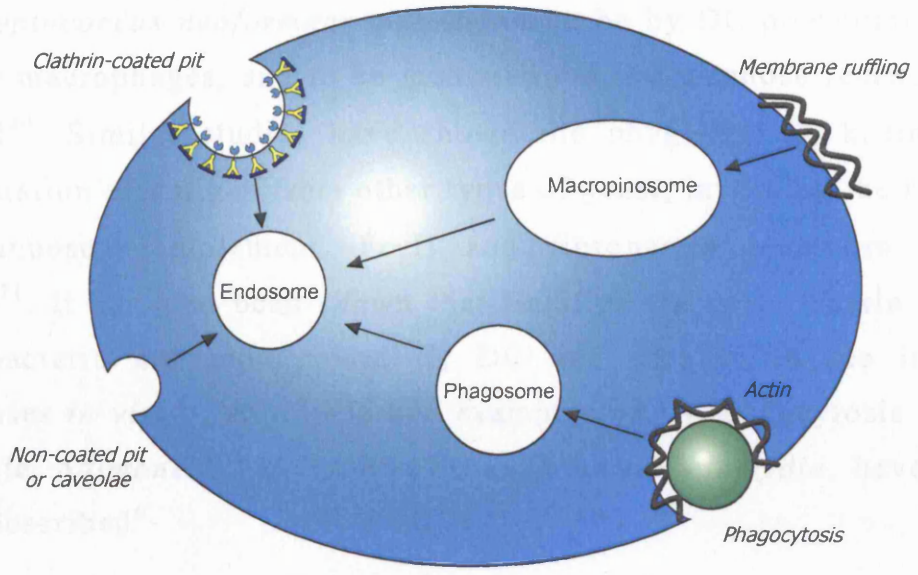

Figure 1.1: Schematic of pinocytosis mechanisms. Arrows signify movement of antigen towards the antigen containing vesicles of endosomes, although other mechanisms may exist to shuttle antigen to these or similar vesicles.

1.3.1 Macropinocytosis

DCs use macropinocytosis, which is the ability to endocytose non-specifically large volumes of extracellular fluid. Sallusto *et al* showed that the immature DC can endocytose approximately a cell volume within one hour by macropinocytosis[14]. Macropinosomes form around membrane ruffling sites, mediated by a rearrangement of the actin cytoskeleton and can form large vesicles with a diameter ranging from 0.5 – 3 μm. Such a large volume of internalisation requires that DCs also have a high rate of exocytosis[12]. Some fluid and antigen from macropinosomes is routed further into vesicles containing MHC class-

II, proteolytic enzymes such as cathepsin D, and lysosomal associated markers such as LAMP-1[14].

1.3.2 Phagocytosis

The macrophage is the classical phagocytic cell playing an important part in the removal of large pathogens. DCs can also actively phagocytose microbes such as yeast and bacteria *via* the many receptors expressed on the cell surface. For example, T-cell stimulation by *Cryptococcus neoformans* was shown to be by DC presentation and not by macrophages, and to be mediated *via* the mannose receptor and FcγRII[20]. Similar studies have shown the phagocytosis, killing and presentation of antigen from other types of yeast, involving the binding of mannose, complement, FcγII and fibronectin receptors among others[21]. It has also been shown that Bacillus Calmette-Guerin (BCG) mycobacteria are endocytosed by DC and able to induce immune responses *in vivo*[22], and numerous examples of DC endocytosis of, for example, *Salmonella*, *M. tuberculosis*, *E. coli*, *Chlamydia*, have since been described[6].

1.3.3 Clathrin and non-clathrin-mediated endocytosis

Clathrin-coated pits are a major organelle used by eukaryotic cells for the endocytosis of receptors and their ligands. These vesicles are formed by the formation of cage-like structures mediated by the formation and assembly of clathrin triskelions[23]. The endosomal vesicles formed are small (80 – 120nm) in comparison to macropinosomes. Many PRRs such as the mannose receptors [14] are known to be endocytosed *via* clathrin-coated pits. Receptors cluster during coated pit formation, internalise and sometimes release attached ligand (usually triggered by a lowering of endosomal pH), allowing receptor recycling back to the plasma membrane. These features of clathrin-coated pits can lead to a high quantity of antigen internalisation by APC.

Non-coated pits, including caveolae, are the least understood of the endocytosis mechanisms. It is believed that caveolae play a role in the endocytosis of certain antigens and bacteria into macrophages and dendritic cells, both of which express caveolin-1, an essential element of caveolae formation[24]. The size of caveolae are in the region of 50 – 80 nm diameter. The exact role of caveolae and their link to the endocytosis of antigen is unknown. However, several interesting observations have shown that caveolae may be important in immune functions or immune evasion by bacteria. Caveolae may play a particularly important role in internalisation of antigen when clathrin coated-pit formation is disrupted[25].

1.4 Mannose receptor and antigen uptake

The mannose receptor (MR) is a well-characterised receptor for the binding of mannose-fucose type sugars by macrophages and dendritic cells. Work by Stahl, Ezekowitz, Taylor, Drickamer and many others has elucidated both the structure and binding characteristics of the MR.

1.4.1 Mannose receptor function

The mannose receptor is found on mononuclear phagocytes such as macrophages and liver Kupffer cells, on antigen presenting DCs and on endothelial cells. The presence of these cells in most tissues leads to a wide tissue distribution of the mannose receptor including the liver, all epithelial surfaces such as the gastrointestinal tract and lungs, the spleen, lymph nodes and other lymphoid tissues. Its expression on DCs has created a lot of interest into its possible immunological function.

The MR is synthesised in the rough endoplasmic reticulum (RER) as an inactive 154 kDa precursor, and on its journey towards the cell surface is *N*-and *O*-glycosylated, maturing to a 162 kDa active form[26]. The location of glycosylation on the MR is thought to be between the

carbohydrate recognition domains (CRDs) and may function to induce conformational changes and affect MR binding.

Endocytosis of the mannose receptor concentrates the receptor mainly into early endosomes, with some also being detectable in late endosomes[27]. This has the effect of concentrating antigen into early endosomes, the first intracellular step where degradation of protein antigen occurs. The MR is endocytosed *via* clathrin-coated pits, as suggested by its association with surface α-adaptin[27]. An estimated 100,000 MR molecules are found on the plasma membrane of GM-CSF / IL-4 cultured DCs, with approximately four times this amount in intracellular pools. The MR requires 2 Ca^{2+} ions and a neutral pH to internalise attached sugars[28]. Once the receptor and ligand enter endosomes of a sufficiently low pH, the receptor releases the sugar and is recycled back to the plasma membrane[29]. By contrast, FcγR and scavenger receptors on APCs and membrane Ig molecules on B-cells are targeted for degradation upon endocytosis, possibly suggesting an important role for the MR in antigen endocytosis. Approximately 2 x 10^6 molecules can be endocytosed by the MR every hour, suggesting a turnover of 15 min for the receptor to recycle back to the surface. In DCs, MR internalisation of antigen was found to enhance presentation to T-cells 100 fold[30], compared to antigen internalisation *via* fluid phase uptake. Tan *et al*[31] reported a 200-10,000-fold enhanced potency of mannosylated *versus* non-mannosylated peptides in ability to stimulate HLA class-II-restricted peptide-specific T-cell clones.

1.4.2 MR homologues as endocytic receptors

The DEC-205 receptor is a 205 kDa membrane protein shown to be expressed on mouse dendritic and thymic epithelial cells[32] and certain subsets of DCs[33]. Like the MR, DEC-205 is able to endocytose glycosylated antigens very efficiently[32]. DEC-205 has a low surface expression on human immature monocyte-derived DCs, with expression increasing as the cells mature, the opposite situation to the MR[33], but like the MR, DEC-205 is endocytosed *via* clathrin-coated pits. A C-

terminal cytoplasmic sequence within DEC-205 targets DEC-205 to MHC class-II positive late endosomal / lysosomal vesicles and not to early endosomes as for the MR and most other endocytic vesicles[34]. Recently Steinman *et al* have shown that targeting antigens to maturing DCs *via* DEC-205 improves T-cell vaccination[5]. The exact type of carbohydrate ligand for DEC-205 is unknown, but is suggested to be more complex than simple mannose ligands. This suggests a specialised recognition and function of DEC-205 that may or may not involve antigen endocytosis.

The DC-specific ICAM-grabbing non-integrin (DC-SIGN) receptor family have so far only been found to be expressed on DCs, in particular DCs in the sub-mucosa and dermis. The yeast *Candida albicans* is known to enter *via* these tissues, and Cambi *et al* have proposed that like the MR, DC-SIGN is a receptor for *C. albicans*[35]. DC-SIGN has been shown to bind to a whole range of viruses, such as HIV-1/2, Ebola, Hepatitis C and Dengue virus. It is clear that the multitude of recently discovered C-type lectins expressed by DCs may perform various functions including antigen internalisation. Extensive reviews on these and other C-type lectins expressed on DCs can be found elsewhere[36-38].

1.4.3 MR structure and binding characteristics

Figure 1.2 shows a schematic of the macrophage MR structure. The cytoplasmic tail of the receptor contains an amino acid sequence (FENTLY) that is involved in signalling for internalisation *via* clathrin-coated pits. At the N-terminus are two cysteine-rich domains and the fibronectin type II repeat. Neither of these are involved in the recognition of mannosylated targets[39] but are suggested to perform a different function, possibly also in antigen recognition. After the N-terminal domains are eight CRDs that are involved in the recognition of specific types of sugars.

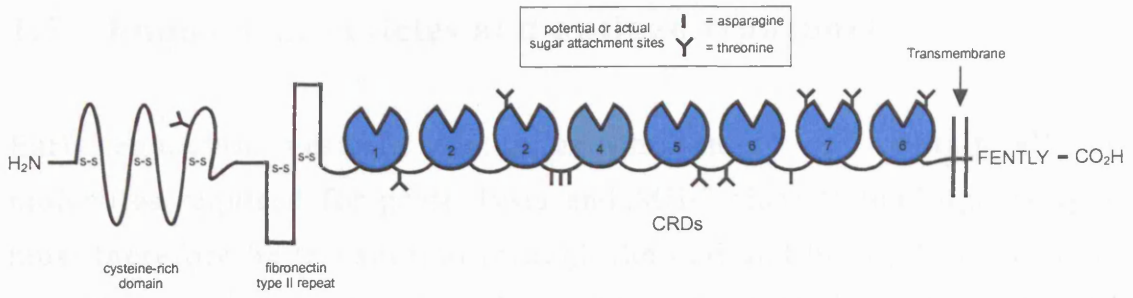

Figure 1.2: Structure of the macrophage mannose receptor. Diagram adapted from Taylor *et al*[39]

At present, little is known about the relationship between these CRDs in terms of binding ligands, although it is believed that the domains cluster together, reinforcing multiple weak interactions with individual oligosaccharides to give high-avidity of binding. CRD4 is the only MR domain that is able to bind mannose ligands on its own [39] and is essential for binding to many carbohydrate complexes[39-41]. CRD4-8 shows the same binding as the whole receptor and CRD1-3 do not appear to be needed for binding. In complex carbohydrates, CRD5-7 also show binding activity. It is clear that binding of complex oligosaccharides is dependent on many of the CRDs.

1.5 Endosomal vesicles and antigen transport

Early endocytic vesicles containing antigen do not contain all the molecules required for proteolysis and MHC class-II loading. Antigen must therefore be transported through the cell and brought into contact with these molecules by vesicular fusion[7]. A simplified scheme for the transport of vesicles through a typical APC is shown in figure 1.3.

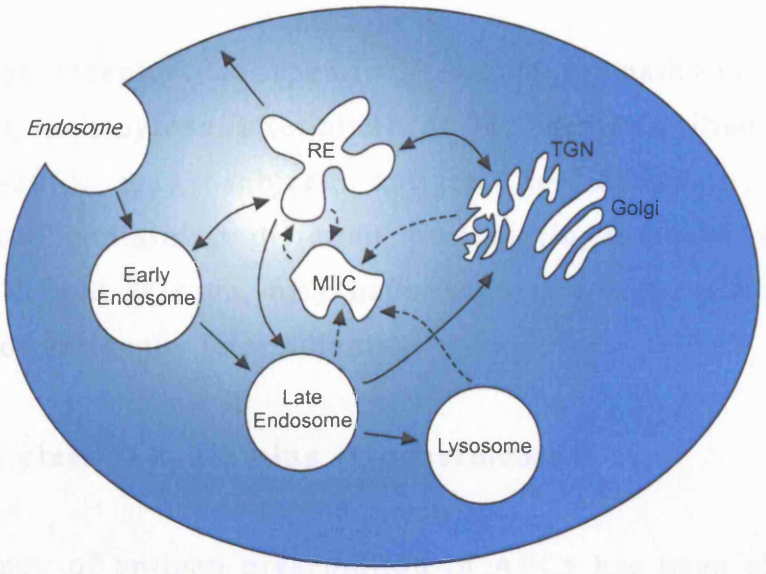

Figure 1.3: Schematic of endosomal vesicular transport. Solid lines denote vesicle maturation, fusion or membrane / solute transport. The existence of what are termed MHC class-II compartments is also included with dotted arrows denoting possible links with other vesicles. MIIC = MHC class-II compartment, RE = Recycling Endosome, TGN = Trans-Golgi Network

1.5.1 Endosome transport

An important early step of endosome transport is the fusion of newly created endosomes with the pre-existing early endosome. Early endosomes have a pH of ~6.0, and possibly contain the first enzymes involved in the proteolysis of antigen such as asparaginyl endopeptidase (AEP) and thio reductases such as γ-interferon-like thiol reductase (GILT) (see section 1.7, page 47). Early endosomes can then form late endosomes and then lysosomes, a process called vesicular maturation. However, vesicle maturation is also accompanied by the shuttling of membrane and / or intravesicular contents throughout all

endosomal pathways. This fluidity of endosomal movement makes it difficult to associate some important cellular functions to particular organelles, such as the location of acid proteases required for antigen processing, or the loading of MHC class-II molecules. Recycling or sorting endosomes have also been described in the literature[42] which adds to the overall complexity. The movement and maturation of different vesicles is controlled by a whole series of GTP-binding Rab GTPases, information on lies outside the scope of this thesis [42].

Targeting of receptors to specific vesicles or pathways by signal sequences in their cytosolic terminal (as has been described for the MR and DEC–205) may subject antigen to different proteolytic environments, containing different proteolytic enzymes and altered vesicular pH, and as such, may have important consequences for the generation of antigenic determinants.

1.5.2 MHC class-II containing compartments

The efficiency of antigen presentation in APCs has been attributed in part to the existence of specialised MHC class-II containing compartments, called MIICs[43]. These compartments, along with a similarly described class-II vesicle (CIIV), exhibit all the properties expected of a vesicle involved in the efficient loading of MHC class-II molecules. MIICs contain MHC class-II and HLA-DM for exchange of invariant chain (Ii) with antigen peptides (see section 1.6), have an acidic pH which allows proteolytic degradation of Ii and antigen, are accessible to endosomes and allow export of antigen loaded MHC class-II molecules to the cell membrane. Although such organelles have been described as multivesicular or multilaminar late endosomes, it is still unclear if MIIC are specialised or conventional endocytic compartments, these issues being highlighted by several groups[43,44]. The role of these multivesicular endosomes is still not fully understood, but it is clear from recent reports that they are important in antigen presentation[7,45].

1.5.3 Antigen transport within APC endosomes

Vesicular kinetics within dendritic cells have been analysed, and compartments positive for MHC class-II, LAMP-1, antigen and cathepsin D are present in DCs[14,46]. Similar studies within macrophages[47] and B-cells[48,49] have also shown the co-localisation of antigen with lysosomal markers, MHC class-II associated molecules and proteolytic enzymes. DCs however, display a difference to macrophages and B-cells in the speed upon which they are able to present MHC class-II / antigen complexes to responder T-cells. Kleijmeer *et al* showed that presentation of hen egg-white lysozyme protein (HEL) antigen to HEL-specific T hybridomas by mouse spleen dendritic cells occurred after only 2 hours, with a maximal response after 6 hours[50]. Studies with an immature DC cell line (FSDC) showed that macropinocytosed and clathrin coated-pit endocytosed antigen displayed a long-lasting retention of unprocessed antigen for up to 24 hours within large, mildly acidic vesicles[51]. Similar long-lasting antigen retention has recently been reported *in vivo*[52].

1.6 MHC class-II molecules and antigen presentation

The major histocompatibility class-II complex (MHC class-II) is a set of highly polymorphic cell membrane proteins that bind antigen for presentation to T-cells. They play a major role in all of the steps from antigen proteolysis to presentation of antigen on the cell surface to T-cells, and as such, have an their important role in the antigen processing and presentation pathway. Class-II MHC molecules and their role in antigen processing and presentation have been reviewed elsewhere[53,54].

1.6.1 MHC class-II structure

MHC class-II molecules are comprised of the glycoprotein chains α (34 kDa) and β (29 kDa). A crystal structure drawing of the MHC class-II molecule I-A^d in complex with the ovalbumin peptide 323 – 339 is shown in figure 1.4. These two chains each contain two domains (α_1, α_2, and β_1, β_2), and the chains are non-covalently bound to form the full MHC class-II molecule as a heterodimer[55]. The α_1 and β_1 domains form the peptide binding cleft where antigenic peptides are bound allowing presentation to the TCR. The binding groove is lined at the base by eight strands of anti-parallel β-sheets (four from each chain) with two sides lined by long α-helices (one from each chain). The binding groove has "open-ends", allowing binding of peptides of differing lengths, typically between 12-20 amino acids[56]. It has been suggested that this allows for MHC-guided processing of antigen by allowing the binding of long antigenic fragments that can later be trimmed at the ends by proteases[57]. Binding of peptides occurs by hydrophobic, electrostatic and Van der Waals forces, by interacting with both invariant and polymorphic parts of the binding cleft. There are many different variations of the MHC class-II genes, such that each individual may express a different set of alleles (a term that refers to each individual gene variation) within a population. The combination of MHC polygeny (a human can express four different MHC class-II

genes) and polymorphism leads to great variations in the expression of MHC class-II genes within a population. The potential to respond to antigens differently depends on the ability of different MHC to bind an antigen.

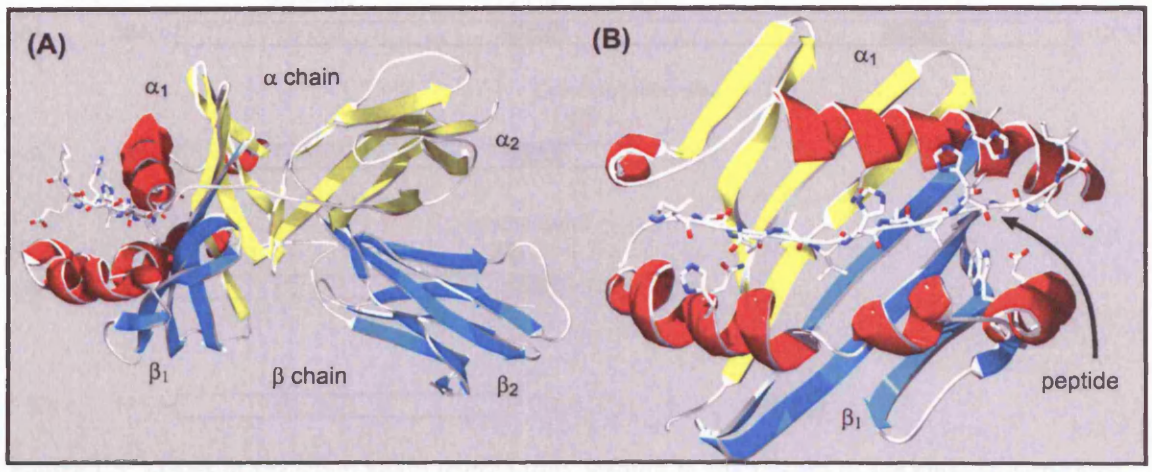

Figure 1.4: MHC class-II molecule I-A^d in complex with ovalbumin peptide 323 – 339. The β-sheets of the two chains (α and β chains) are shown in yellow and blue, respectively, with α-helices shown in red. A) Side view of the molecules, B) A top-down view of the α_1 and β_1 domains showing the peptide binding groove with bound peptide. Some amino acid side chains of the α-helices are also shown to display possible interactions of MHC class-II with peptide. Diagram drawn from PDB file (PDB accession number 1IAO)[58].

1.6.2 MHC class-II and the invariant chain

Empty MHC class-II molecules that arrive within the ER are unstable without the binding of a specialised protein called the invariant chain (Ii). The invariant chain fulfils several functions; stabilisation of MHC class-II molecules, provision of a targeting signal to help transport MHC class-II molecules towards appropriate endosomal vesicles, and prevention of peptides binding to MHC class-II with the ER. The invariant chain is a non-polymorphic type II integral membrane protein, with a short 30 amino acid cytosolic domain, 24 amino acid transmembrane region and ~ 150 amino acid luminal domain (fig. 1.5). Ii exists as a trimer and is able to bind three MHC class-II molecules of any allele type (referred to as an $(\alpha\beta Ii)_3$ complex)[59]. Within the ER, a region of Ii, called the class-II-associated Ii chain peptide (CLIP) fits into the MHC class-II peptide-binding groove and stops binding of any other antigen peptide fragments. Ii facilitates the targeting of the

$(\alpha\beta Ii)_3$ complex into low pH late endosomes such as MIICs. Targeting towards these vesicles is mediated by the cytoplasmic tail of the Ii.

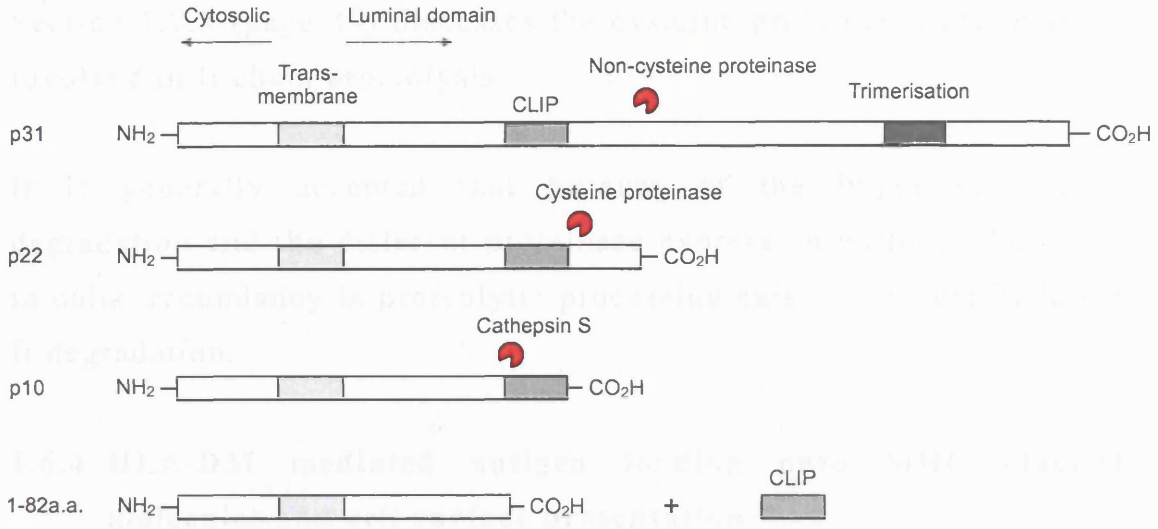

Figure 1.5: Stages of invariant chain degradation leading to the release of the class-II-associated Ii chain peptide (CLIP). Figure adapted from Matza *et al*[60].

1.6.3 Invariant chain proteolysis

During transport or upon arrival into vesicles where antigen loading occurs, Ii is degraded by a stepwise process. Aspartic, cysteine and possibly other proteinases are implicated in this processing, but the exact details remain unclear (fig. 1.5). Blum and Cresswell were first to analyse the proteolysis of Ii[61]. They found that the Ii degradation during passage through the endosomal pathway was inhibited by the cysteine proteinase inhibitor leupeptin, resulting in an accumulation of Ii fragments dubbed LIPs (leupeptin induced polypeptides) and SLIPs (small leupeptin induced polypeptides). Maric *et al* found that the formation of these LIP / SLIP fragments was a two stage process that required a cysteine proteinase to generate the final CLIP / MHC class-II complex, but that also required an aspartic proteinase to perform initial Ii degradation[62]. It has been shown using cathepsin D (CD) knockout mice that degradation of Ii still occurs, suggesting that CD is not involved, or its activity can be replaced by another proteinase[63]. The cysteine proteinase cathepsin S has been shown to be a major enzyme involved in the generation of CLIP fragments. However, this is

MHC class-II haplotype dependent, and other proteinases such as cathepsin B are also involved[63]. Cathepsin L has been shown to be important in Ii degradation within cortical thymic epithelial cells[64]. Section 1.7.3 (page 49) discusses the cysteine proteinases that may be involved in Ii chain proteolysis.

It is generally accepted that because of the importance of Ii degradation and the different proteinase expression patterns that exist in cells, redundancy in proteolytic processing exists to ensure efficient Ii degradation.

1.6.4 HLA-DM mediated antigen loading onto MHC class-II molecules and cell surface presentation

To facilitate the removal of the CLIP fragment, an MHC class-II encoded protein called HLA-DM (H-2M in the mouse) catalyses the removal of the CLIP protein and replacement by antigen. HLA-DM is a non-polymorphic MHC class-II like molecule that does not bind peptide, and is found predominantly in vesicles that contain MHC class-II molecules. HLA-DM can catalyse the removal of antigen from MHC class-II molecules containing weakly associated antigen. Higher affinity antigen peptides and longer antigenic peptides are more resistant to HLA-DM induced dissociation[65]. HLA-DM may function by binding to unstable conformations of MHC class-II molecules. L-cells (which do not contain HLA-DM) transfected with genes for MHC class-II and Ii were able to present one dominant epitope of HEL and elicit a T-cell response, but also two cryptic epitopes of HEL (i.e., antigenic peptides that can be generated by proteolysis but not presented). However, L-cells also transfected with HLA-DM were unable to present the cryptic epitopes and only elicited a T-cell response to the dominant epitope of HEL[66].

The morphology of MIICs as being multivesicular or multilaminar is thought to provide the segregation and controlled association of the large array of molecules involved in antigen processing[8]. It has been

suggested that this may be the reason why immature DCs are able to store antigen for long periods of time by segregating the machinery that is required to efficiently load and present antigen[45]. The transport of MHC class-II molecules to the cell surface is believed to occur via vesicular budding from MIIC-derived tubules, which are thought to fuse with the outer cell membrane[8]. Figure 1.6 summarises the pathways that are involved in MHC class-II transport through to the cell surface.

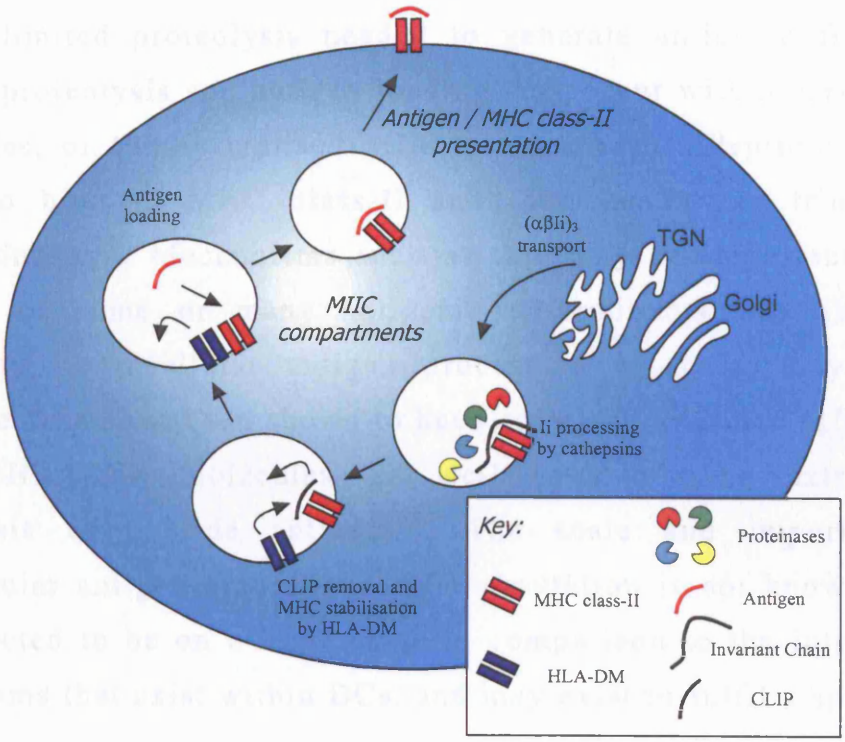

Figure 1.6: Schematic representation of the process of MHC class-II transport to the cell surface. The processes of Ii degradation, MHC class-II stabilisation by HLA-DM, CLIP removal for loading of antigen and MHC class-II presentation on the surface of APCs are represented.

1.7 Antigen proteolysis

Following capture of antigen *via* one of the endocytic mechanisms previously mentioned, an APC needs to proteolytically degrade antigen to generate class-II specific peptide MHC class-II complexes for recognition by CD4+ T-cells. Proteins may require disulphide bond reduction, denaturation as well as cleavage to generate small peptide fragments. In addition, the invariant chain Ii also requires cleavage. The degradative environment of the lysosome may be too aggressive for the limited proteolysis needed to generate antigenic fragments. Instead, proteolysis and antigen loading may occur within early or late endosomes, or the specialised MIIC compartments. Peptidic antigens may also bind to MHC class-II and then be further trimmed by exoproteinases[57]. Mechanisms such as this may be important for the survival of some or many antigenic determinants. An alternative possibility, extracellular antigen processing by DCs, may exist[67]. Immature DCs have been shown to have empty cell surface MHC class-II and HLA-DM molecules, as well as displaying extracellular proteolysis of peptide antigens[68]. The scale and importance of extracellular antigen processing and presentation is not known, but is not expected to be on a large scale in comparison to the intracellular mechanisms that exist within DCs, and may exist to fulfil a specialised function.

Several proteolytic enzymes have been implicated in antigen processing, with most having broad substrate specificity and an acidic pH optimum, consistent with their distribution within endocytic and lysosomal compartments of APCs[69,70]. However, there are exceptions to these rules, and proteolytic expression can differ between APC cell types or different T-cell activation / maturation stages.

The cathepsin family forms the major group of proteins involved in antigen processing. Dependent on the proteinase active site amino acid required for the catalytic cleavage, the enzymes in the cathepsin family can be classified as either aspartic proteinases, such as cathepsin D and E, or cysteine proteinases, such as cathepsins B, L, and S. Although

other classes of hydrolases exist within lysosomal compartments such as serine proteinases and metalloproteinases, no evidence exists for their involvement in antigen processing within APCs. Figure 1.7 shows the stages of antigen proteolysis that occurs within APCs as it is currently understood. Several techniques have been used to identify proteinase enzymes and their specificities, such as mutagenesis of processing sites, the use of specific inhibitors, gene-knockout mice, and more recently techniques utilising fluorescent active-site directed probes[71].

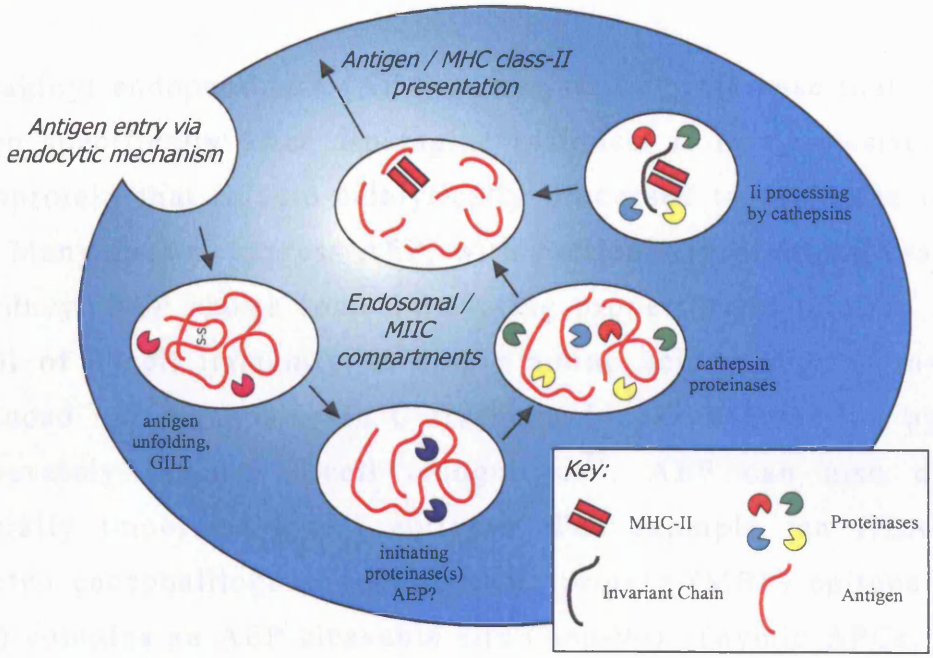

Figure 1.7: Antigen and Invariant chain (Ii) processing within a typical APC. Antigen is first unfolded by the action of γ-interferon-inducible thiol reductase (GILT), then an initiating proteinase (AEP) and then further degraded by the cathepsins to produce small antigenic peptides for loading onto MHC class-II molecules. At the same time, MHC class-II / Ii processing occurs to allow removal of stabilising Ii.

1.7.1 γ-Interferon-inducible thiol reductase (GILT)

The reduction of disulphide bonds may be required to open up a protein sufficiently to allow proteolysis and release of immunodominant T-cell epitopes. Most studies on antigen processing that look at the role of disulphide bond reduction shows this to be an essential step[72,73]. The identification of γ-interferon-inducible thiol reductase (GILT) resolved

the problem of the protein involved in disulphide reductive cleavage[74]. GILT is constitutively expressed in APCs and expression can be induced in other cells by IFN-γ, suggesting the enzyme has an immune function. It is expressed as a 35 kDa precursor that is transported to endosomal compartments where N-terminal and C-terminal propeptides are cleaved to generate the 30 kDa mature form[75]. The importance of GILT in immune responses was shown by generation of GILT-deficient mice which displayed defective antigen processing[76].

1.7.2 Asparaginyl Endopeptidase

Asparaginyl endopeptidase (AEP) is a cysteine proteinase that cleaves antigen specifically after asparagine residues. It is synthesised as a preproprotein that is auto-catalytically processed to yield the mature form. Many tissues express AEP, with particularly high expression in the kidney. AEP shows some interesting properties in relation to the control of T-cell immunity. A single amino acid change (Asn-1219) introduced into tetanus toxin C fragment blocks degradation by AEP and severely impairs T-cell recognition[77]. AEP can also destroy potentially important T-cell epitopes. For example, an HLA-DR2-restricted encephalitogenic myelin basic protein (MBP) epitope (MBP 85-99) contains an AEP cleavable site (Asn-94). Thymic APCs, which express AEP, possibly destroy this epitope during thymic T-cell development, limiting negative selection of self-reactive T-cells to this epitope[78] and allowing potentially autoreactive T-cells to survive. Another study has shown with OVA and myelin oligodendrocyte glycoprotein antigens containing asparagine within or near to relevant epitopes that presentation were not impaired in AEP-deficient mice[79].

Manoury *et al* have recently shown that the initiation of Ii degradation in B-cells can be performed by AEP, as inhibition of AEP slows (but does not stop) the processing of Ii[80]. The generation of AEP-deficient mice has shown that the generation of the two-chain mature forms of cathepsins B, H, and L are impaired, suggesting AEP is important in processing the immature forms of these enzymes[79]. At least in the case

of cathepsin L, this does not necessarily lead to impairment of its function[79]. A review by Watts *et al* describes more information on AEP[81].

1.7.3 Cysteine cathepsins

There are numerous cysteine cathepsins within lysosomes of cells, that play a part in "house-keeping" protein degradation. Cathepsins B, L and S are the most characterised cysteine cathepsins involved in antigen processing, and along with other cysteine cathepsins have been located within endosome / lysosome compartments of APCs[69]. They are synthesised in the endoplasmic reticulum as pro-enzymes, with a propeptide occupying the active-site, which is removed autocatalytically or by another enzyme[82]. Like other classes of proteinases, cysteine proteinases can act as endoproteinases (cathepsin L, S, F) or exoproteinases (cathepsin H, Z)[83], cathepsin B may act as both.

1.7.3.1 Cathepsin B

Cathepsin B, a lysosomal papain-like proteinase, is a potent carboxypeptidase, involved in cellular protein turnover, that may have a role in antigen processing[84]. Cathepsin B is synthesised as a pro-enzyme, and targeted to late endosomes / lysosomes by the mannose-6-phosphate receptor. The mature single chain form is generated in these compartments by autocatalysis. The administration of the cathepsin B-specific inhibitor CA-074 2 hours before and after HBV vaccination of mice suppressed anti-HBV IgG production[84]. In the same study, CA-074 was shown to suppress antigen processing and presentation by macrophages of rabies antigens to specific T-cell clones. In contrast to these inhibitor studies, analysis of cathepsin B deficient mice suggested that cathepsin B (as well as cathepsin D) is dispensible for processing and presentation of antigens[85].

1.7.3.2 Cathepsin L

Another lysosomal cysteine proteinase, cathepsin L, has been shown to be important in Ii degradation within cortical thymic epithelial cells, the cells which mediate positive selection of CD4+ T-cells[64]. There is evidence that cathepsin L is regulated by a degradation product of the p41 isoform of Ii, which binds to, and inhibits specifically, the proteolytic abilities of cathepsin L[86]. This degradation product has no effect on cathepsin B or S. Although there is no direct evidence for the involvement of cathepsin L within antigen processing by direct antigen cleavage, its involvement has been suggested[84,87]. A study by Hsieh *et al* showed that fibroblasts expressing either cathepsin L or S generated significantly altered levels of some peptide antigens compared with fibroblasts not expressing cathepsin L / S. The antigenic peptide levels expressed were also different between these two fibroblasts expressing either of these Ii degrading enzymes, an observation that may suggest an involvement in more than Ii-processing alone[87]. The authors do point out, however, that it cannot be dismissed that this effect could be related to differences in the rate of Ii degradation, and as such antigen loading and proteolysis within different T-cellular compartments.

1.7.3.3 Cathepsin S

Cathepsin S has been identified in APCs such as B-cells, macrophages, DCs and epithelial cells. It is known to be essential in the degradation of Ii in some alleles, particularly I-A^b. Cathepsin S deficient mice have B-cells and DCs with accumulated MHC class-II / Lip10 complexes, and it is suggested that in these cells cathepsin S is essential, although as mentioned, this is dependent on the allelic type as some alleles are less dependent on invariant chain processing[88]. In human epithelial cells, cathepsin S is the only cysteine proteinase able to degrade the Ii-p10 fragment[89]. Cathepsin S may contribute a role in autoantigen generation within several immunological diseases. In mouse models of Sjogren's Syndrome, a specific inhibitor of cathepsin S (CLIK-60) dramatically reduced the signs of symptoms[84]. In another study, the N-

terminal generation *in vitro* of a major autoantigen from Myelin basic protein, was wholly controlled by cathepsin S[90]

1.7.3.4 Other cysteine cathepsins

In recent years some additional cysteine cathepsins which could be implicated in antigen processing have been identified[70]. Cathepsin H for example, is an aminopeptidase shown to localise within early endosomal compartments and has a near neutral pH optimum. However no data yet associates it to antigen processing. Cathepsins F and Z are expressed in many cell types, but among APCs this distribution is restricted to macrophages. *In vitro*, Cathepsin F is able to generate the Ii10 fragment of Ii as efficiently as cathepsin S, and in cathepsin S deficient mice, macrophages were shown to cleave Ii fragments as well as wild-type mice. These observations suggest cathepsin F may substitute for cathepsin S in degradation of Ii in cathepsin S deficient mice[91], highlighting the redundancy that exists in proteolytic enzymes.

1.7.4 Aspartic proteinases

The aspartic proteinase family is a diverse family of enzymes, involved in a whole range of important biological functions[92], and implicated in a number of diseases[93]. Many pathogens rely on aspartic proteinases to function correctly, and the interest in specific aspartic proteinase inhibitors is therefore huge[94]. Of particular interest in this study is their role in antigen processing. The distribution of the aspartic proteinases within cells or tissues varies. Some recently discovered human aspartic proteinases may not be relevant to antigen processing within antigen presenting cells[92]. The napsins are a family of aspartic proteinases so far shown to be predominantly expressed within lung and kidney[95]. Another family recently discovered, called the β-site amyloid precursor protein-cleaving enzyme (BACE), has been suggested to have a role in antigen processing as low levels are found within most human organs. However, BACE is insensitive to the aspartic proteinase pepstatin A[96], and as will become apparent

throughout this section, suggests that BACE is not implicated in antigen processing.

Cathepsin D (CD) and cathepsin E (CE) are the only two aspartic proteinases identified to date expressed within the endosomal / lysosomal compartments of APCs, and have been implicated in several studies of antigen processing[69,97,98]. They are widely distributed in many tissues, and in particular APCs, of most mammalian species. Human CD and CE are 51 % homologous at the amino acid level, however the two enzymes have different tissue distributions and sub-cellular localisation, and are therefore likely to perform different roles[99].

1.7.4.1 Cathepsin D

CD is a ubiquitous proteinase that primarily functions as a "house-keeping" enzyme, degrading intra- and extracellular proteins. It is usually expressed in lysosomes and late endosomes, but can also be found in early endosomes of macrophages where it is membrane-bound[100]. Its expression varies with different cell types[101]. CD has a wide distribution amongst various mammalian tissues, but it is particularly high in adrenal, spleen and lung tissues[102].

The transport of CD from the ER is mediated by the N-terminal pre sequence of CD. The 44-residue propeptide of CD stabilises the enzyme until its transport to endosome or lysosome compartments *via* mannose-6-phosphate targeting[103], where it is cleaved to generate an active 44kDa cathepsin D enzyme[104]. The crystal structures of CD identified the active site within a deep cleft that is flanked by an N-linked oligosaccharide[103,105].

A wide variety of proteins have been shown to be degraded by CD *in vitro*, including extracellular matrix components such as pro-collagen [106], hormones such as β-endorphin, β-lipoprotein and parathyroid hormone, and inactivation of the cysteine proteinase inhibitor cystatin.

Over-expression of CD has been associated with inflammation, tumour progression, and β-amyloid peptide release from amyloid precursor protein in Alzheimer's disease[107]. Recent work has associated CD with the caspase cascade in apoptosis, essential for homeostasis. CD has been shown to be involved in the programmed cell death induced by IFN-γ, Fas and TNF-α[108]. Ceramide, a second messenger in the transduction of apoptotic signalling has been shown to interact with preprocathepsin D and induce its autocatalytic cleavage to enzymatically active isoforms[109].

1.7.4.2 Cathepsin D deficient mice

The cathepsin D deficient mouse (CD–/–) generated by homologous gene targeting has given some interesting insights into the role and importance of CD. CD–/– mice develop a progressive atrophy of the intestinal mucosa and lymphoid tissue. These mice develop normally within the first few weeks, but stop thriving and decrease weight in the third week, and usually die at 25 +/– 2 days of age[110]. They also display neurological seizures near terminal stages, with cells of the central nervous tissue displaying autophagosome / autolysosome-like bodies[99]. The Balb/c CD–/– mice generated as part of the present study (see section 6.5, page 213) displayed a similar abnormalities and die around weaning.

General lysosomal proteolysis is not impaired in CD–/– mice. Stimulation of antigen-specific T-cells[110] and the degradation of invariant chain in MHC class-II expressing APCs[85] are not affected. This suggests that CD is not essential for antigen processing in the mouse. A recent study looked at the aspartyl proteinase substrate myoglobin presentation to T-cells by DCs. Presentation of two different myoglobin T cell epitopes was enhanced rather than hindered in CD–/– mice[111]. This was concluded to be due to the destructive processing of cathepsin D. It was also shown that pepstatin-sensitive myoglobin processing activity persists in lysosomes from CD–/– mice, being likely due to cathepsin E. A role for CD in antigen processing

cannot be ruled out however, as the complexity and degeneracy inherent in antigen processing may allow adequate antigen processing of certain antigens to occur by any of the proteolytic enzymes found within APCs, but this may not be the case for all antigens. The presence of another aspartic enzyme, cathepsin E, that has similar cleavage specificity, may provide a large contribution to antigen proteolysis in the absence of CD. Indeed in the murine B lymphoblastoid cell line A20, cathepsin E is the main aspartic proteinase[112]. Species other than mice, including humans, may rely more on CD.

1.7.4.3 Cathepsin E

Cathepsin E has a limited distribution compared with that of CD, being found in lymphoid tissues, gastrointestinal tracts, urinary organs, some red blood cells in some species, and microglia[113]. Of particular interest is its expression in APCs, including DCs, B-cells and epithelial cells[114-116]. The CE gene has been shown to be expressed in many mammalian species[117] and has been cloned from many species[118-120].

CE, unlike CD and other aspartic proteinases such as pepsin, renin, napsin, and BACE, is neither secreted nor lysosomal. CE has been shown to be localised to endosomal compartments and the ER[113]. CE is synthesised as a preproenzyme in the RER. A signal peptide of 17 amino acids in length is cleaved upon entry into the ER, where an intracellular pool of procathepsin E is retained. This is mediated by a region of 48 amino acids at the N-terminus of the mature cathepsin E[121]. Entry into the endosome is associated with autocatalytic activation of the mature enzyme. Position 4 of the mature enzyme contains a cysteine residue that forms a disulphide bond with another CE chain to form a homodimer of 85 kDa in size, although the monomeric form is also found. The cysteine residue is highly conserved amongst various mammalian species[122]. This residue may also play a role in the retention of CE within the ER, possibly *via* interaction of the homodimer with a membrane bound receptor within

the ER. The monomeric form of CE is less stable to pH and temperature changes[123]. Unlike CD, CE can retain activity at slightly acidic or even neutral pH, when in the presence of ATP[124]. N-Linked glycosylation was also shown to be essential for CE to remain stable to changes in pH and temperature[125]. In human cells and mouse lymphoblasts, the sub-cellular localisation of CE has been shown to be limited to endosomal compartments with a higher pH than late endosomes[112,121].

Recently the structure of cathepsin E in complex with its pro-sequence was solved at 2.35Å[126]. Unlike other aspartic proteinases, cathepsin E does not appear to cleave its pro-sequence, which remains attached to the mature enzyme as a β-strand. In addition, the N-terminal section from a different, nearby cathepsin E pro-sequence, blocks the active site[126]. Cathepsin D is inactive at neutral pH, due to the N-terminal section of mature enzyme blocking the active site. In cathepsin E, the active site is blocked by the bound pro-sequence. This difference may help to explain the reason for the differences in pH optima between cathepsin D and E. A combination of crystal structure data and a model of substrate binding for cathepsin D and cathepsin E show that the binding sites of both enzymes are almost identical. As such both enzymes, as appears so far from substrate binding studies[127], are likely to have very similar substrate binding preferences, making it very difficult to design cathepsin D or E specific inhibitors[126].

There are a number of biologically important molecules shown to be cleavable by CE *in vitro*, although this does not necessarily imply a biological significance. α_2-Macroglobulin, an important plasma glycoprotein, is involved in the capture and cellular targeting of a range of molecules, including cytokines, growth factors and hormones. Recent evidence has shown that CE, and not CD, is able to cleave α_2-macroglobulin into three major proteins[128]. In line with the expression of CE within the brain and gastrointestinal tissue, the hormones substance P, neurokinin A, eledoisin and neurotensin have also been shown to be selectively or more efficiently cleaved by CE, compared to

CD[120,129,130]. The B chain of oxidised insulin and big endothelin-1 have both been reported to be cleaved by CE[131,132]. There are two potential processing sites within human invariant chain that can be cleaved by cathepsin E[133], suggestive of a possible role in Ii chain degradation.

The substrate specificity of CE has been explored and, as predicted from crystal structure, shares many similarities in substrate preference with other aspartic proteinases. CE prefers hydrophobic bulky amino acids at P_1 and P_1',[†] examples being Phe and Nph (4-nitrophenylalanine). However, CE is also able to cleave peptides containing Phe-X, Tyr-X and Leu-X (where X = any amino acid) around the scissile bond[131,134]. Val and Ile are not tolerated at the P_1 position, and there is a preference for Pro at the P_4' position[135]. The S_4 subsite[‡] of CE prefers proline or leucine, whereas the S_3 subsite prefers large a.a.'s. The S_2 and S_2' subsite can accommodate hydrophobic amino acids (S_2 also accepts hydrogen bonding residues). When Ile is present at P_3, the influence of the P_2 residue becomes less important[134]. Recent work by Liu *et al* have shown through mutational analysis of specific residues of CE, that the amino acids Asp-98, Asp-283 and Thr-284 are critical for the catalysis of peptide cleavage[136].

1.7.4.4 Cathepsin E deficient mice

The cathepsin E deficient mouse (CE–/–) has recently been generated by homologous gene targeting[137]. The function and study of a potential role in antigen processing by CE was not explored, however a change in immune function was noted. CE deficient mice primarily develop severe atopic dermatitis (AD) when bred under conventional conditions but not under specific pathogen free (SPF) conditions. CE deficient mice have a higher expression of the cytokines IL-18 and IL-1β, both

---

[†] Nomenclature for naming peptide substrate for proteolytic enzyme is:

substituent – NH – P_1 – P_1' – CO – substituent

where the bond between P_1 – P_1' is the scissile bond. The next residue in the direction of the amino terminal is the P_2 residue, and P_2' for the next residue towards the carboxy terminal and so on

[‡] The enzyme subsite that is involved in the binding of the corresponding peptide residue, e.g. S_2 is the subsite for the peptidic P_2 residue

important in the polarisation of naïve T-cells to T_H2 cells. Such cytokines can induce the production of IL-4 and IL-5 by T_H2 cells, and increased levels of IgE, all of which were observed in the CE deficient mice. These results suggest that the turnover of IL-18 and IL-1β is reduced, and as such may implicate CE in the deactivation of these cytokines. It is noted that humans with AD have an observed decrease in CE expression.

1.7.4.5 Role of CE and CD in antigen and Ii processing

The expression of CE within APC, given its limited expression in other cell types is suggestive of a role in antigen processing. M cells of follicle associated epithelium in the gut express CE but do not express MHC class-II. Such cells are the main, if not the only way, for complex antigens to gain access to the intestinal immune system, and may function to pass on antigen to intestinal APCs[138]. CE expression in HeLa cells can be induced by IFN-γ via a class II transactivator (CIITA) independent manner (CIITA induces the expression of MHC class-II, HLA-DM and Ii) [139]. It is thought that CIITA independent IFN-γ action is required for the generation of an antigen presenting phenotype in non-professional APCs[140]. Recently it has been shown that an isoform of CIITA negatively regulates CE expression[141]. CE is also the major aspartic proteinase in a human B-cell lymphoblastoid cell line[112]. Its expression in DC is particularly significant, and CE has been shown to be expressed in human Langerhans and interdigitating reticulum cells[115], and murine microglia[142].

Both CD and CE have been shown to generate known T-cell epitopes by *in vitro* protein digestion. Tetanus toxin contains numerous CD / CE cleavage sites and several previously described T-cell epitopes, such as between residues 1273 and 1284, which are flanked by CD and CE cleavage sites[143]. The generation of H-2^d-restricted OVA epitopes, in particular $OVA_{323-339}$, as recognised by the DO11-10 hybridoma has been shown to be mediated by CD and CE[144,145]. This model forms the basis of the work presented within this thesis.

More direct evidence for the role of CE in APC comes from several studies. In the A20 B-cell line, 70 % of the aspartic proteinase activity could be blocked by the CE-specific *Ascaris* pepsin inhibitor-3 or by pre-incubation of cell lysates with anti-CE antibody[112]. Processing of OVA by A20 cells for presentation to the DO 11-10 T-cell line was dramatically reduced by the *Ascaris* inhibitor, but the presentation of peptide was unaffected. The responses of T-cells primed *in vivo* by administration of OVA were also reduced (63%) by the addition of the inhibitor to A20 cells[112]. The approach used and presented within this thesis has also recently been applied elsewhere. The inhibitor pepstatin A significantly inhibited the interleukin-2 (IL-2) production from an OVA-(266-281)-specific T helper cell hybridoma upon stimulation with native OVA presented by IFN-γ-treated microglia isolated from CD–/– mice[113,142]. IL-2 production was not inhibited by OVA peptide 266 – 281. Microglia from CD deficient mice retained the ability for antigen presentation when not in the presence of pepstatin A. Another study confirmed that CD was dispensable for antigen processing as APCs from spleens of CD deficient mice were able to generate T-cell epitopes from a number of antigens, including OVA, hen egg lysozyme, pigeon cytochrome C, and myelin basic protein[85]. This study did not specifically address the role of CE. As previously mentioned, cathepsin E has been suggested to play a role in myoglobin presentation by murine DCs in CD–/– mice, with better myoglobin antigen presentation by CD–/– mice than wildtype cathepsin D-expressing mice[111].

Other studies have implicated endosomal aspartic proteinases in the processing of Ii[62]. Zhang *et al* found mice infected with *Leishmania major* were more susceptible to disease when treated with pepstatin A *in vivo*[97], and attributed this to a CD-like proteinase mediating processing of Ii. In the presence of pepstatin A, LIP and SLIP Ii fragments accumulate within A20 cells[97], this effect being mainly attributed to the inhibition of CE[112]. The same group showed that Pepstatin A was found to inhibit the processing of a 28kDa fragment of soluble leishmania antigen within splenocytes from naïve mice *in vitro*.

They also attributed the degradation of Ii by an aspartic proteinase with the observation that pepstatin A suppressed the degradation of Ii in OVA immunized mice *in vivo* and *in vitro*[146]. Riese *et al* however, showed that the culture of a B-cell lymphoblastoid cell line with an aspartic proteinase inhibitor (CGP 53437) did not lead to the accumulation of Ii fragments from αβIi MHC class-II dimers, suggesting Ii processing by aspartic proteinases was not essential[147]. The specificity of this inhibitor for all classes of aspartic proteinase was not mentioned other than to say it inhibits cathepsin D at nanomolar concentration, so other proteinases such as CE may still participate. An alternative is that the processing of Ii by cysteine proteinases within this B-cell lymphoblastoid cell line is sufficient such that aspartic proteinase-mediated Ii degradation is redundant. Different APCs express different levels of proteolytic enzymes or even different enzymes, making it difficult to derive general principals from the conflicting data.

1.7.5 Aspartic proteinase inhibitors

Ideally, the design of a cathepsin E specific peptide inhibitor would allow for the discrimination between cathepsin D and E. Such an approach however is not within the scope of this project. This problem can be addressed in other ways with the use of cell lines containing a significantly larger expression of CE than CD[112], or with the use of cathepsin D knockout mice[110].

Initial studies into protease inhibitors concentrated on screening microorganisms for inhibitors that were relatively small and generally resistant to animal metabolism[148]. One particular inhibitor from *Streptomyces testaceus* n.sp., called pepstatin A, is a particularly potent inhibitor of a broad range of aspartic proteases including CD and CE. Pepstatin will be used as the most readily available, highly potent broad-spectrum aspartic proteinase specific inhibitor. Its small size and ease of chemical modification is attractive from a synthesis

point of view. The use of pepstatin and pepstatin analogues will be discussed further, along with some other inhibitor options.

1.7.5.1 Pepstatin A

Several variants of pepstatin (differing in the molecule attached to the N-terminal amide group) are synthesised by *Streptomyces* species, the most studied and well known of which is the pepstatin A molecule containing the isovaleryl residue (from here onwards just referred to as pepstatin). Pepstatin is a pentapeptide, the structure of which is shown in figure 1.8. The availability of a single C-terminal carboxylic acid and a lack of other highly reactive molecules makes pepstatin an highly attractive target for chemical conjugation.

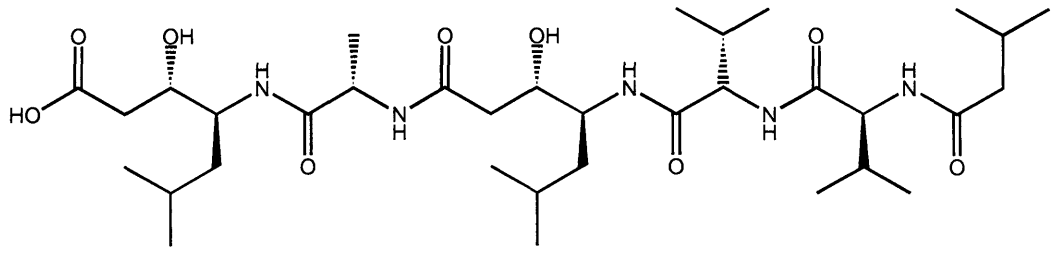

Figure 1.8: Structure of pepstatin from *Streptomyces testaceus* n.sp. containing isovaleryl residue

Pepstatin is a very potent inhibitor with a K_i value in the 1-10 nM range. The unusual amino acid statine provides pepstatin with its high potency. The proposed mechanism for aspartic protease cleavage of a scissile peptide bond involves a tetrahedral intermediate (fig. 1.9). Structure-based subsite specificity of aspartic proteases with pepstatin analogues[149-151] and crystal structures of cathepsin D bound to pepstatin[105] and *Rhizopus* aspartic proteinase bound to pepstatin[152] has lead to the proposed cathepsin D – peptide binding and bond cleavage mechanism as shown in figure 1.9. The acidic environment in which aspartic proteases optimally work allows two aspartic acid residues to hydrogen bond to, and hydrolyse, a carboxyl of a suitable peptide bond (fig. 1.9a). This leads to an equilibrium involving a tetrahedral

intermediate (fig. 1.9b) and subsequent bond cleavage (fig. 1.9c) to yield two separate peptide fragments (fig. 1.9d). It is believed that all aspartic proteases exhibit a mechanism similar to that shown in figure 1.9, and that the statine residue mimics the tetrahedral intermediate. More information on the structure and mechanism of pepsin-like aspartic proteinases can be found elsewhere[92].

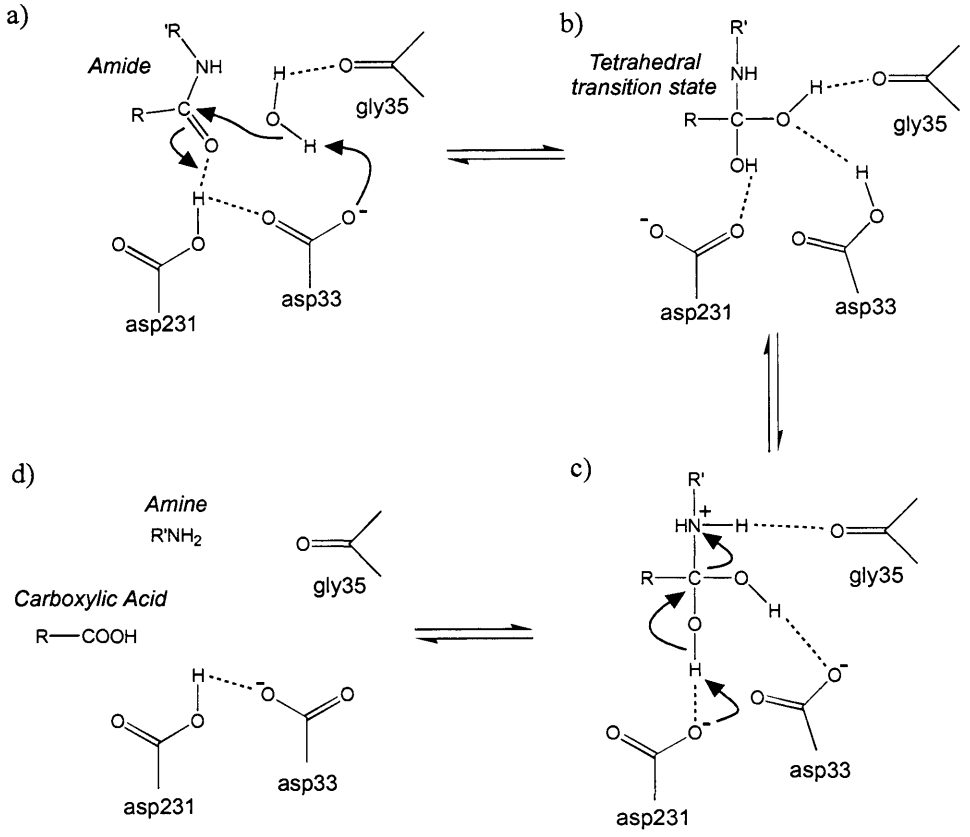

Figure 1.9: Proposed mechanism of peptide bond cleavage by cathepsin D as deduced from the cathepsin D – pepstatin crystal structure of Baldwin *et al.*[105]. The separate stages of peptide binding, intermediate formation and cleavage of peptide bond are represented from a) to d). Diagram adapted from Bott *et al*[152].

1.7.5.2 Pepstatin inhibitor analogues

Many groups have also used the C-terminal carboxy group of pepstatin to synthesis analogues with varied properties. For example, Hamdaoui *et al*[153] synthesised mannose-6-phosphate pepstatin analogues that showed anti-proliferative activity on breast-cancer cell strains by targeting pepstatin to mannose-6-phosphate receptors and subsequent inhibition of cathepsin D within lysosomes. The work of Brygier *et al*[154] showed that a methoxypoly (ethylene glycol) conjugate of

pepstatin inhibited hog pepsin *in vitro* with a K_i 400 times higher than pepstatin. A similar idea was adopted by Campbell *et al*[155] who conjugated pepstatin to poly (L-lysine) to show increased inhibition of protein degradation within Balb/c 3T3 fibroblasts. The labelling of pepstatin has been used previously to probe for the localisation of cathepsin D. Knight *et al*[156] conjugated pepstatin to dinitrophenyl and used an anti-dinitrophenyl antibody to localise cathepsin D. The same group synthesised a fluorescent bimane-labelled pepstatin[157]. It should be noted however that these studies do not mention cathepsin E inhibition, which is equally likely in all cases mentioned. The crystal structure of cathepsin E, recently solved at 2.35Å, suggests that it would be difficult to design a substrate specific for either cathepsin D or E[126].

1.7.5.3 Statine-related aspartic proteinase inhibitors

Pepstatin is by far the most well-known and studied aspartic proteinase inhibitor, but its active component, the amino acid statine, has been derivatised to synthesise new aspartic protease-specific inhibitors. The variation in binding pockets of different aspartic proteases and subsequent binding or steric hindrance of particular statine inhibitor analogues makes this possible, and this has been achieved for some aspartic proteases such as plasmepsin[158], BACE[159] and cathepsin D[151,160-163], although to date there is no data to suggest that these CD-specific inhibitors are not also CE inhibitory. A compound originally tested as a BACE inhibitor was found to be more potent towards CE than pepstatin, however no data was shown of its effects upon CD[164]. Very recently, two bis-trifluoromethyl analogues of pepstatin displayed good inhibition of CD and CE, the inhibition (IC_{50}, nM) of CE being 10-fold lower than that for CD[165].

1.7.5.4 *Ascaris* pepsin inhibitor-3

The *Ascaris* pepsin inhibitor-3 (PI-3) along with inhibiting porcine pepsin, also inhibits the function of cathepsin E, but not cathepsin D[166]. PI-3 has until recently been difficult to obtain in sufficient quantities for functional studies of antigen processing. Structural studies have shown that PI-3 uses the N-terminal β-strand to block several binding pockets of porcine pepsin, and that approximately 17% of its surface interacts with porcine pepsin[167]. The mechanism of inhibition of cathepsin E is likely to be similar, and it may therefore be difficult to synthesise a smaller peptidic version of PI-3 comparable to pepstatin.

1.8 Aims for studying antigen processing using inhibitors

There is a great potential for the use of aspartic proteinase inhibitors, such as pepstatin, in the study of antigen processing. However, the use of pepstatin is limited due to its poor solubility and inability to cross the cell membrane at concentrations that do not affect cell viability. The aim of this research is to chemically modify the structure of the proteinase inhibitor pepstatin to overcome some of the restrictions of the use of pepstatin *in vitro* and *in vivo* (discussed in chapter 2).

Several options are available that could help to address the role of cathepsin E in antigen processing. A well understood model of antigen processing, in which the A20 B-cell murine lymphoma[112] is used to process and present a specific peptide epitope of ovalbumin to DO11-10 T-cells, has been used to assess the role of cathepsin E within antigen proteolysis. A20 cells have been shown to express mostly cathepsin E as their aspartic proteinase.

Another approach is to study antigen processing by cathepsin E deficient mice. Such a model would not only address the role of cathepsin E within antigen processing but also help to address if it also has an importance for other critical cellular processes, as has been suggested by its enzymatic cleavage of a number of key endocrine mediators. Work towards the generation of a cathepsin E deficient mouse has been achieved (section 1.7.4.4, page 56)[137]. An alternative option would be to use a cathepsin E specific protease inhibitor. As previously mentioned, the *ascaris* inhibitor is cathepsin E and not cathepsin D specific[166]. However it is difficult to obtain sufficient quantities for *in vitro* or *in vivo* studies. Alternatively, the chemical synthesis of a cathepsin E specific inhibitor could help to address this problem. A different approach, and one used within this study, is the use of mice deficient in cathepsin D. Antigen presenting cells from such mice should express cathepsin E, but not cathepsin D. Inhibitors such as pepstatin, or pepstatin derivatives, which do not distinguish

between cathepsin D and E could be used to probe selectively the function of cathepsin E.

Published functional studies of antigen processing using the aspartic proteinase inhibitor pepstatin (see section 1.7.5.1, page 60) suffer from a number of limitations: Pepstatin is insoluble in most solvents except DMSO, a solvent that can itself markedly affect T-cellular activities. The concentrations of pepstatin required to achieve biological effects is often extremely high (up to 100 μM) raising the possibility of non-specific/toxic activity. At these concentrations, pepstatin is likely to target any cell and cellular compartment present in the culture (or *in vivo*), further complicating the interpretation of the results. Chapter 2 details these problems and introduces a series of chemical strategies that could be used to address the aforementioned problems and lists a series of modified pepstatin inhibitors that may improve both the solubility and cell / compartmental targeting.

Chapter 2

Design of aspartic proteinase inhibitors for use within antigen presenting cells

2.1 Introduction

There are a number of studies in which inhibitors of proteolytic enzymes, including those of the aspartic proteases cathepsin D and E, have shown an involvement of cathepsins in the MHC class-II processing pathway (refer to section 1.7). However, several major problems have limited the value and interpretation of these studies, and have in particular precluded any *in vivo* pharmacological analysis of these inhibitors in processing activity.

i) There is no low molecular weight inhibitor that discriminates between cathepsin D and E. As both enzymes are found within the cellular vesicles upon which antigen may travel during its processing lifetime, interpretation of any data involving a non-specific aspartic proteinase inhibitor cannot be entirely attributed to one or the other cathepsin.

ii) Almost all aspartic proteinase inhibitors are poorly soluble in aqueous medium, limiting their potential use *in vivo* and in culture.

iii) Many inhibitors are poorly accessible to the correct intra-cellular compartment and rely on fluid-phase uptake alone. Attachment *via* a membrane specific molecule would both aid uptake into an appropriate cell compartment (i.e. the endosome as opposed to the cytoplasm which could lead to non-specific effects on other enzymes) and increase cellular availability of the inhibitor.

iv) Inhibitors usually have no cell-specific targeting, leading to systemic distribution of inhibitor. This would give rise to unfavourable

inhibition within non-antigen presenting cells and a greatly reduced availability of inhibitor. The higher doses of inhibitor needed in this case could produce toxic effects within any *in vivo* model.

There is a need to design inhibitors that are soluble in aqueous medium, specific for cathepsin E, and that are cell-specific and specific for an appropriate intracellular compartment. Such inhibitors would help to obtained data on the effect of cathepsin E within the class II MHC antigen processing pathway of professional antigen presenting cells. These problems are explored further in this chapter, and an approach to help solve these problems is discussed. A rational chemical design strategy based upon these ideas is presented with the design of some appropriate classes of inhibitors. The chemistries available to achieve the synthetic goals will also be discussed.

2.2 The choice of cathepsin inhibitor – pepstatin A

As mentioned in section 1.7.5, there are a few choices for the inhibitor moiety that can be used, however it is clear from the research that has been previously been done in relation to cathepsin D / E inhibitors, that the best and easiest option is to use pepstatin A itself. There are several advantages of using pepstatin A. Firstly, it is available in sufficient quantities for chemical synthesis procedures. Secondly, the presence of a single terminal carboxylic acid and no other highly reactive chemical groups means that derivatives of pepstatin can be easily achieved without the need for complex side chain protection strategies for the rest of the compound (fig. 2.1).

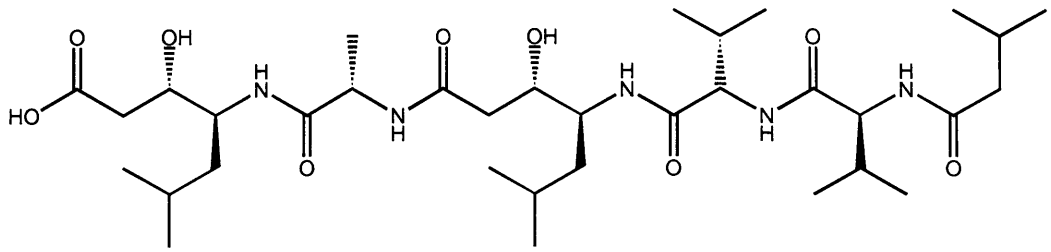

Figure 2.1: Structure of pepstatin from *Streptomyces testaceus* n.sp. containing isovaleryl residue

Two disadvantages of using pepstatin A is that it is not specific to either cathepsin D or E, and that it is a very insoluble inhibitor in aqueous solutions. The first problem, in the context of this research, will be accomplished by selecting a model of antigen processing that can overcome the need to distinguish the difference between cathepsin D and E. Two models are to be used for this; the use of B-cell hybridomas that have a very high expression of cathepsin E and low expression of cathepsin D, and the use of cathepsin D knockout mice. Both of these approaches will be described elsewhere in the chapters 5 and 6. The second problem of pepstatin solubility can be overcome by chemically synthesising derivatives of pepstatin that have a solubilising compound attached.

2.3 Inhibitor solubility and cellular targeting

Solubility is an essential criterion in the design of a modified pepstatin inhibitor. The presence of hydrophobic residues in pepstatin (fig. 2.1) explains its insolubility. For its use *in vitro*, the inhibitor is usually dissolved in DMSO and then diluted into aqueous solution. DMSO is toxic to cells at high concentrations, and from data presented (see section 6.1.2, page 185), may directly inhibit the function of aspartic proteinases. The usual method for increasing solubility is to attach hydrophilic molecules such as sugars or certain peptides as discussed below. Another consideration given the poor solubility of pepstatin is its bioavailability. The insolubility characteristics of pepstatin mean that it is likely to be poorly endocytosed into cells, in fact this has been shown to be the case *in vitro* and *in vivo*[168]. The selection criteria for overcoming these problems are thus to improve the bioavailability of pepstatin by improving its solubility and possibly cell targeting.

Synthetic derivatives of pepstatin attached to either carbohydrates or hydrophilic peptides are two good choices for improving solubility and bioavailability of any pepstatin analogues. Carbohydrates, however, have some advantages. Certain carbohydrates can promote cell targeting *via* their recognition by cell surface lectins. As discussed in section 1.4, the mannose receptor provides a way to allow endocytosis into some types of APCs, and into the vesicles that are likely to fuse with aspartic proteinase containing vesicles. Carbohydrates are also less likely to interact with target proteinases than peptides. The sugar mannose fulfils the requirements of improving solubility and cell targeting in this context.

2.4 Initial aspartic proteinase inhibitor design

From the requirements mentioned above, it is clear that a synthetic conjugate containing a single mannose and pepstatin molecule linked together are the minimum requirement for the design of a more potent aspartic protease inhibitor with improved solubility in aqueous solution. It is expected however that this will not be sufficient to overcome the problems described, and a more flexible design would need to allow the addition of multiple mannose sugars to be attached to a pepstatin molecule. The inclusion of a framework with a higher amount of mannosylation introduces the potential for steric hindrance between the mannosylation unit and the binding of pepstatin to an aspartic proteinase. Therefore, the design of a soluble aspartic proteinase needs to also include the possibility to allow cleavage between the two halves of the soluble aspartic proteinase inhibitor molecule. In addition, the aspartic proteinase inhibitor should include careful design that would allow for the inclusion of a label to improve the usefulness of such an inhibitor. Figure 2.2 illustrates these design requirements. Further consideration of the mannosylation unit and the linker section is required to aid in our final synthetic design.

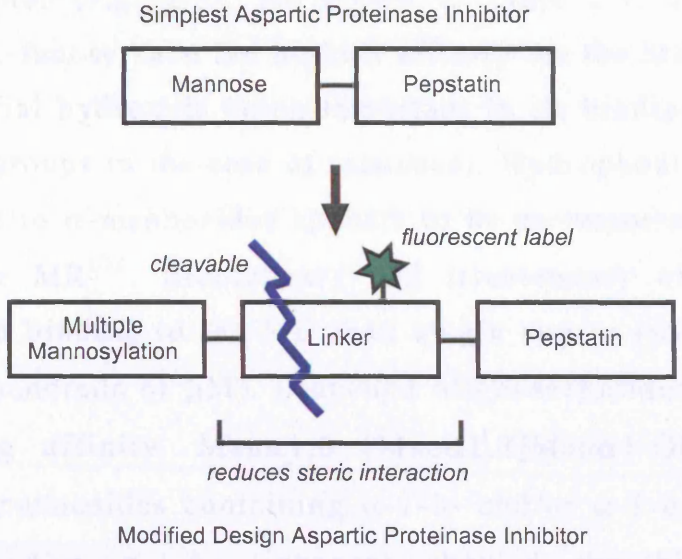

Figure 2.2: Schematic of aspartic proteinase design

2.5 Mannosylation design considerations

Improving aqueous solubility using multiple mannose units is quite straightforward, however the ideal ligands for binding to the mannose receptor have to be considered.

2.5.1 Mannose receptor binding

Many oligosaccharides and glycodendrimers have been studied for binding characteristics to lectins[169]. It was through such studies that the "cluster glycoside" effect was established, i.e. that the affinity of multivalent glycosides for polyvalent binding ligands is significantly higher than that of the individual glycosides[170]. There has been much research on the structure and sugar binding characteristics of the mannose receptor. There is still uncertainty as to the "ideal" ligand for the MR and how the multiple carbohydrate recognition domains (CRDs) cooperate in the binding. There are however a whole series of natural and artificial ligands with good binding to the MR.

Mannose is not the only sugar monomer that is able to bind to the mannose receptor (fig. 2.3). As shown in table 2.1, sugars such as mannose and L-fucose have the highest affinity for the MR, the presence of two equatorial hydroxyls being important in its binding (the C-2 and C-3 hydroxyl groups in the case of mannose). Hydrophobicity in the C-1 position linked to α-mannosides appears to be an important factor in its binding to the MR[171]. Biantennary and triantennary oligosaccharides show increased binding to the MR than single sugars (with typical IC_{50} values in the hundreds of μM). Branched oligosaccharides show an even higher binding affinity. Manα1,6 [Manα1,3]Manα1-OMe and other similar oligo-mannosides containing α-1-3- and/or α-1-6- linkages (i.e. not α-1-2- and/or α-1-4- linkages) showed the highest affinity characteristics of simple branched or straight oligosaccharides. α-Linked

sugars showed higher affinity than β-linked sugars[171]. Mannose has the added advantage of being a reasonably easy carbohydrate upon which to do chemical synthesis in comparison to some other sugar monomers.

Sugar Ligand	*IC_{50} (μM)*
L-Fucose	3,200
D-Mannose	5,500
D-Glucose	6,000
α-Man1-OMe	1,000
D-Man-6-P	13,500
D-GlcNAc	13,000
D-Galactose	19,000
D-GalNAc	60,000

Table 2.1: Inhibition (IC_{50}, mM) of MR binding to mannan coated micro-plates by sugar monomers. Diagram adapted from Kéry *et al*[171].

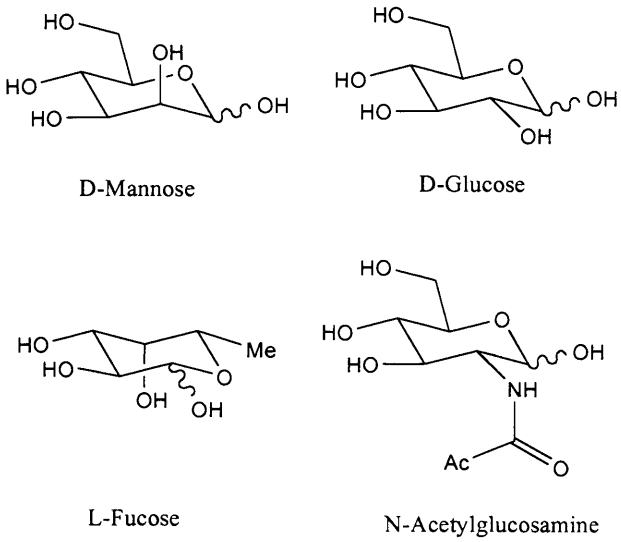

Figure 2.3: MR binding sugars

2.5.2 Natural and synthetic MR ligands

There are a whole range of pathogens that are able to bind to the MR, including yeasts[14,172] and mycobacteria[27,173]. Yeast mannan is the most well understood microbial ligand for the MR. Mannan is the name for a mannosylated structure found in yeast cell walls, with a conserved α-(1→6)-linked polymannosylated backbone with varied length α-(1→2)-linked mannoses. Strategies to synthesise such ligands have been developed by Ley and co-workers using novel one-pot synthesis methodologies[174,175]. Others have also synthesised mannan derivatives using trichloroacetimidate, thiophenyl and / or *n*-pentenyl

methodologies[176-179]. There is however a simpler way to achieve mannose receptor binding by using the cluster glycoside effect.

Several different approaches have been used to synthesis high mannose containing glycosynthons with good binding affinity for lectins such as the MR. These approaches have either incorporated multiple copies of single mannosyl structures, or multiple copies of oligosaccharides, such as mannan structures. The dendritic structures of the glycosynthons have in general been based upon either well known dendrimeric structures such as poly(amidoamine) (PAMAM) or β-cyclodextrin, or based upon peptides such as polylysine, or even upon proteins such as bovine serum albumin (BSA). These latter two approaches will be considered in more detail.

2.5.3 Peptide-based carriers

The first attempts to design small glycopeptide substrates for endocytosis by macrophage MR came from Robbins *et al*[1], who developed mannosyl analogues such as that shown in figure 2.4. These contained multiple mannose groups linked to the α and ε amino group of lysine, dilysine (Man_3Lys_2) and trilysine (Man_4Lys_3) with inhibition constants (K_i) in the μM range. For comparison, Man_{43}-BSA is quoted as having a K_d of between 0.5-4 nM[180].

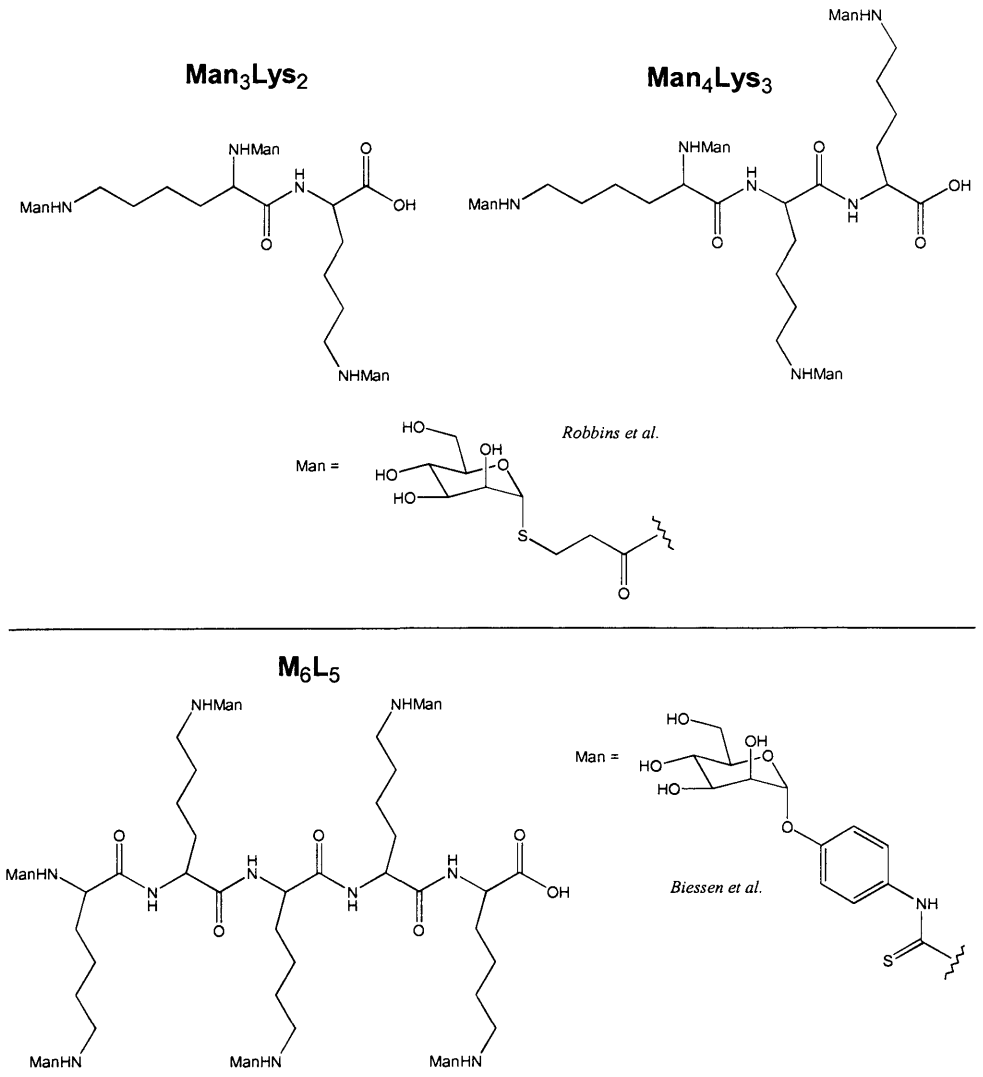

Figure 2.4: Mannosylated polylysines as synthesised by Robbins *et al*[1;2] and Biessen *et al*[3]

Subsequent research lead to the development of cluster mannosides such as M_6L_5 (fig. 2.4)[3]. Competition studies showed an increase in mannoside binding for mannosides ranging from M_2L to M_6L_5[3], the mannoside M_6L_5 is reported as the most potent synthetically designed mannoside with nanomolar affinity. The affinity of the M_6L_5 is comparable with mannosylated BSA.

The improved affinity of the M_6L_5 oligolysine mannoside ligands over those designed by Robbins *et al*[1] is due to the length of the spacer connecting the mannose sugars to the polylysine backbone and in the

nature of the spacer. M_6L_5 mannosides contain an aromatic group, which may help the binding affinity to the CRD protein residues[181].

2.5.4 Protein-based carriers

Over the last 20 years, two neoglycoproteins have been used a great deal, these being Man_{23}-BSA[39,180,182] and Man_{40}-HSA (Human Serum Albumin)[183]. The advantage of these protein conjugates is that they are easy to prepare and can be labelled with fluorescent probes or radiolabelled[184].

As a choice of protein carrier, bovine serum albumin (BSA) contains between 30 – 35 free lysine side chains for conjugation. Another useful feature of BSA is that it contains one free cysteine sulfhydryl side chain[185], that can be used for attachment of a pepstatin molecule. One concern with the conjugation of proteins to pepstatin is solubility. Given the dramatic difference of solubility between a protein and pepstatin, it will be essential to use a protein that allows the use of some pepstatin solubilising solvent, such as DMSO. BSA has a tolerance towards precipitation at up to 35 % DMSO.

2.6 Linker design considerations

The possibility of steric interactions between the mannosyl unit and pepstatin is an important consideration in the design of an aspartic proteinase inhibitor. Considering the initial design of inhibitor (fig. 2.2, page 70), the inclusion of a spacer unit would help to reduce this risk. An improvement on this idea is to allow inhibitor cleavability within an APC, thus avoiding the steric interaction altogether. Ensuring that the design is flexible enough to incorporate other molecules if needed (i.e. fluorochrome or radio-label) would greatly increase the usefulness of any synthesised inhibitors that may appear potentially useful after biological testing (i.e. due to high solubility, high targeting to appropriate cells / compartments, or high potency). All of these considerations for linker design are discussed below.

2.6.1 Reducing steric interaction

In the synthesis of anti-adhesion agents, Toyokuni and Hakomori used several different length benzyl esters to provide space between various carbohydrate molecules and a lysyllysine framework[4]. This kind of approach, originally designed by Lemieux *et al*[186], is useful for attaching an activated carbohydrate at one end to an amino compound at the other end while providing extra space to reduce steric interactions (fig. 2.5a). An alternative approach is to conjugate mannose monomers to a suitable carrier *via* a 4-nitrophenol spacer, as used in the M_6L_5 (fig. 2.5b) synthesis of Biessen *et al*[3]. This approach would have the advantage of improving affinity for the mannose receptor.

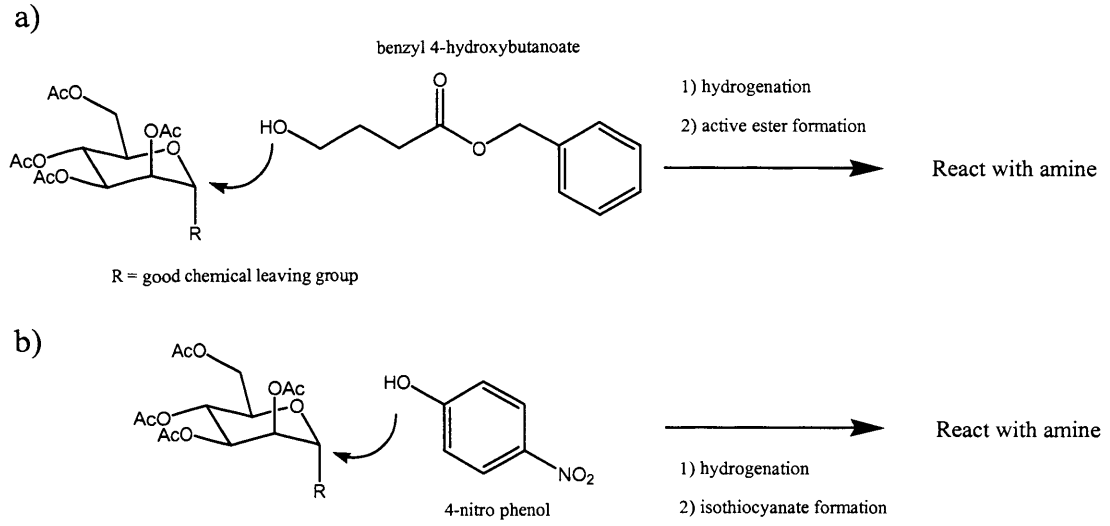

Figure 2.5: Use of a) benzyl ester[4] or b) 4-nitrophenol[3], as a molecular spacer to reduce steric interactions

2.6.2 Intracellular cleavable linker

Cleavable linkers have been used in prodrug design and can contain either acid-labile bonds or enzyme cleavable bonds (cleaved by enzymes such as esterases, lipases and proteinases). Endocytosis of ligands *via* the mannose receptor introduces an endocytosed ligand into a vesicular environment that has a decreased pH towards lysosomal vesicles, using acid-labile bonds in a cleavable linker would be a good choice. Examples of intracellular acid-labile bonds include vinyl ethers[187], aryl esters[188] hydrazone linkages[189,190], and disulphide bonds[191,192].

Disulfide bond reduction plays a key role in the production of antigenic peptides by antigen processing[72,73,193,194]. Recently an enzyme involved in disulphide reduction within APCs has been identified (GILT)[74] and shown to be constitutively expressed within endosomes and lysosomes of APCs such as macrophages and dendritic cells[195]. A disulphide will be considered in our design of cleavable linkers. A full review of the use of

cellular reduction of disulfide linked conjugates is provided by Saito *et al*[196].

Based upon the information of mannosylated carrier that will be used in the inhibitor design, and upon an inclusion of a spacer section, and upon the reactivity of pepstatin (i.e. a terminal carboxylic acid) then a good choice for desired functionality on either side of the linker is provided by the use of a diamine linker. A diamine linker can be attached to carboxy groups *via* active esters, or to other amines *via* a thiourea linkage. A diamine disulfide (cystamine, fig. 2.6) is readily available as a convenient cleavable linker. It is proposed that a non-cleavable linker is also chosen to allow for the potential comparison of inhibition potency with cleavable linkers. For simplicity, this was selected to be 1,3-diaminopropane (fig. 2.6).

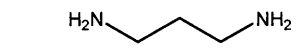

1,3-diaminopropane

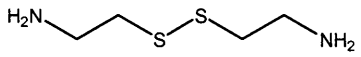

cystamine

Figure 2.6: Cleavable (cystamine) and non-cleavable (1,3-diaminopropane) linkers

2.6.3 Flexibility for further chemical modification

In the situation whereby a particular inhibitor has proven to be valuable in terms of cell targeting, solubility or inhibitor potency, it would be useful to include a design that would allow for modifications. This is particularly important with the testing in DCs, whereby various labelling studies could be extremely useful with successfully tested inhibitors. The ideas so far discussed using peptide and protein-based carriers (sections 2.5.3 and 2.5.4) would use the side chain of lysine to introduce

the mannosylation unit. There is no reason why the ε-amino group of lysine could not also be used for the potential to introduce extra inhibitor functionality.

For a protein carrier, there are a sufficient number of lysine side chains on the protein BSA to accommodate both mannose moieties and any additional functionality. For poly-L-lysine peptides, the synthesis of which is most likely to be by standard peptide synthesis procedures, introduction of a single orthogonally protected lysine group is possible. Standard peptide synthesis uses Boc-protected lysine groups. Literature shows that the lysine side chain protecting group ivDde is stable under a large range of reaction conditions but is easily cleaved by the use of 2 % hydrazine solution[197], and would be compatible with the use of Boc-protected lysine.

2.7 Final aspartic proteinase inhibitor design

With all of the considerations mentioned so far in this chapter, it is possible to propose a series of separate modules that could be synthesised and conjugated together to provide different aspartic proteinase inhibitors, from here onwards referred to as Mannose Pepstatin Conjugates (MPCs). Three classes of inhibitors will be synthesis, the simplest being a link between a single mannose and pepstatin, with or without a cleavable linker (MPC1 and MPC2 respectively, fig. 2.7). The other two classes will incorporate a larger number of mannose units, a peptide-based (MPC3 / 4) or protein-based carrier (MPC5 / 6), and a cleavable or non-cleavable linker (fig. 2.8).

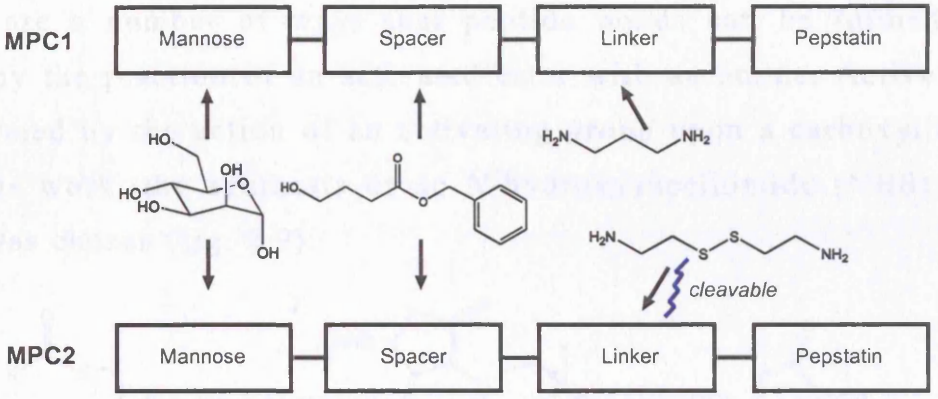

Figure 2.7: Design of MPC1 and MPC2 inhibitors

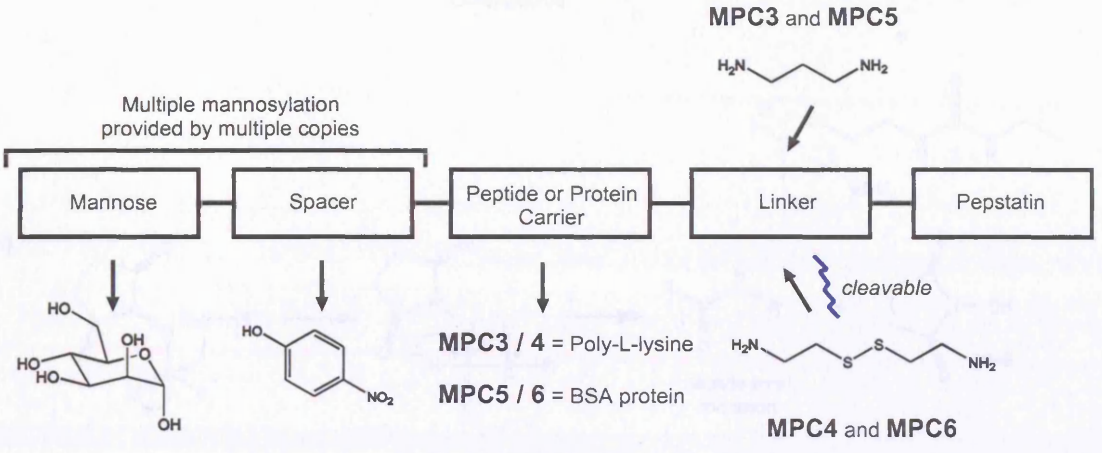

Figure 2.8: Design of MPC3 to MPC6 inhibitors

2.8 Chemical strategy for inhibitor synthesis

Within the previous sections are clear sets of defined chemical building blocks that will lead to the final structures of the inhibitors MPC1 to MPC6. Coupling modules together requires methods that are simple, selective and likely to work under various synthesis situations. For this, three types of bond formation methods were chosen: peptide, isothiourea and thioether bonds. In addition, mannose sugar derivatives need to be activated so that they are able to react with suitable targets (i.e. the hydroxyl of the spacer sections).

2.8.1 Peptide bond formation using NHS esters

There are a number of ways that peptide bonds can be formed[198,199], often by the reaction of an activated ester with an amine. Active esters are formed by the action of an activating group upon a carboxylic acid. For this work, the synthesis of an *N*-hydroxysuccinimide (NHS) active ester was chosen (fig. 2.9).

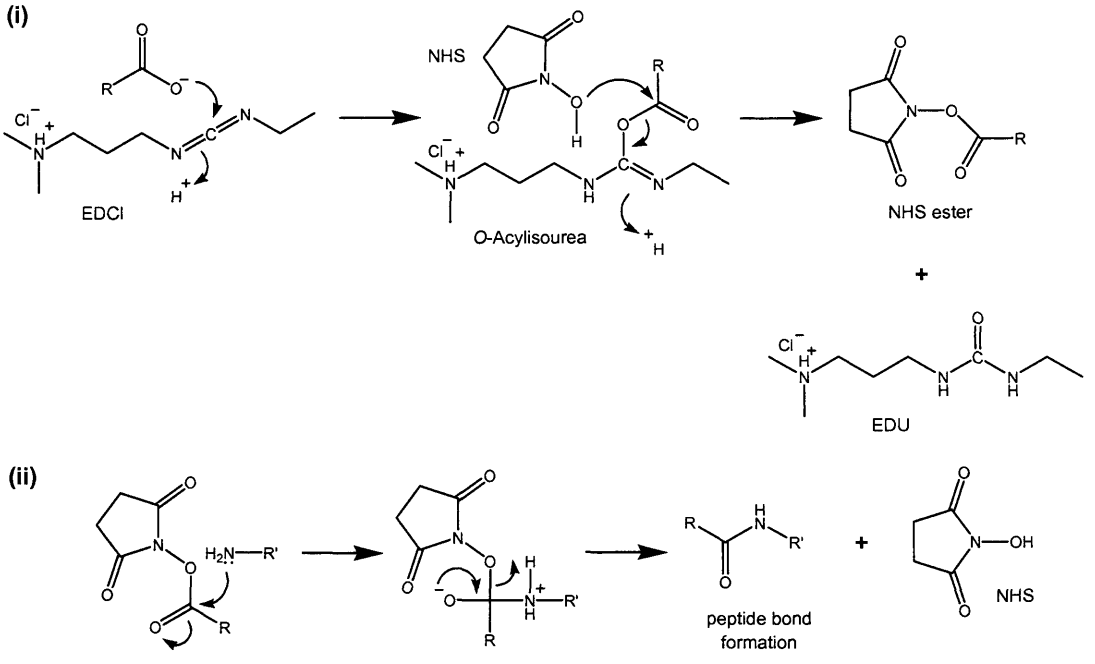

Figure 2.9: (i) NHS ester synthesis and (ii) coupling of amine and an NHS active ester to form a peptide bond between R and R'

Figure 2.9 shows the synthetic steps required for making NHS esters. It is possible to make a peptide bond by reacting an amine directly with an *O*-acylisourea, however, at the stage of *O*-acylisourea formation, there is a competing reaction of intramolecular acyl transfer to nitrogen, to form an *N*-acylurea. As the reactivity of an amine (especially if using a sterically hindered amine) cannot be assured, it would be wiser to choose an attacking nucleophile (such as NHS) that would rapidly attack the *O*-acylisourea and reduce the possibility of any side reactions occurring.

There are several carbodiimides to choose from including the more widely used dicyclohexylcarbodiimide (DCC)[185] and many possibilities for the active ester (including 1-hydroxybenzotriazole)[200]. The choice of EDCI and NHS was mainly based on the need for water solubility. The urea by-product of DCC (DCU) is partially soluble in most solvents, and as such difficult to remove by filtration. EDCI is more water-soluble than DCC, and EDU and NHS are both removable by an aqueous workup after a reaction. As the NHS ester derivatives are soluble in organic solvents, this allows for easy removal of starting materials and the urea biproduct.

2.8.2 Isothiourea bond formation using isothiocyanates

Isothiocyanates are made by the reaction of an amine with thiophosgene. Although not as reactive as isocyanates (where sulphur is replaced by oxygen), they are still highly reactive towards nucleophiles, much more stable, and avoid the use of the highly toxic phosgene gas. Isothiocyanates react with amines to form an isourea bond. This is particularly useful for reaction with the ε-terminal of lysine[201] and can be used for the attachment of mannose derivatives to MPC3 – MPC6. This is illustrated in figure 2.10. The reaction is simple, and involves the attack of an amine towards the highly electrophilic carbon of the

isothiocyanate. The resulting electron shift and proton loss results in a very stable thiourea linkage[202,203].

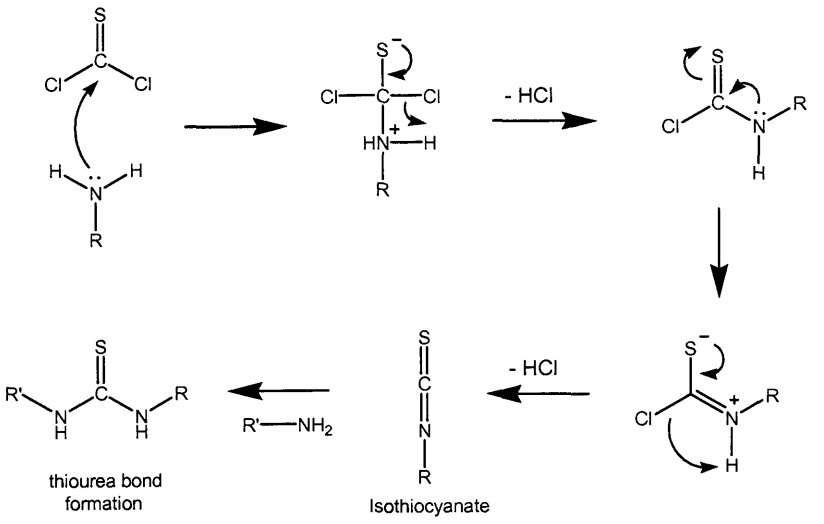

Figure 2.10: Isothiocyanate formation and reaction with amine

2.8.3 Thioether bond formation with iodoacetamides

Thioether bonds may be formed by the reaction of a haloacetamide with a sulfhydryl group. The most reactive haloacetamide is iodoacetamide; these can be synthesised by the reaction of an amine with iodoacetic anhydride. This method was selected for attachment of pepstatin – linker intermediates to a single cysteine sulfhydryl group found on the surface of bovine serum albumin (BSA)[185] for the formation of MPC5 and MPC6[204].

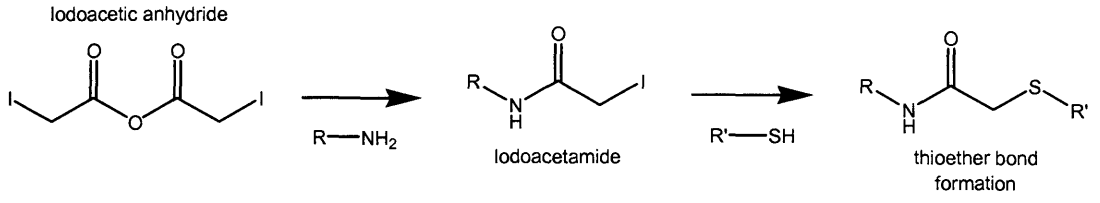

Figure 2.11: Formation of iodoacetamide and reaction with a sulfhydryl to create a thioether bond

2.8.4 Activation of mannose C-1 hydroxyl group

Mannose, like other aldopyranose sugars, contains five hydroxyl groups. In order to activate the C-1 hydroxyl for reaction with for example the hydroxyl group of a spacer element (section 2.6.1, page 76), it is necessary to protect the others from reaction. Mannose derivatives containing acetyl protecting groups in these other positions are highly stable and often crystalline. In addition, these protecting groups are removable under mild reaction conditions. α-Anomer derivatives of mannose have higher affinity for the mannose receptor than corresponding β-anomer derivatives[171], and conveniently, reactions involving the anomeric C-1 position of mannose derivatives containing acetyl protection mostly prefer α-anomer compounds due to the influence of both the anomeric effect and neighbouring group participation.

2.8.4.1 The anomeric effect and neighbouring group participation

The anomeric effect[205] is due to two main influences[206,207], a favourable interaction between the lone pair of the ring oxygen and the antibonding σ*-orbital of the C-1 – C-X bond (fig. 2.12i), and an electrostatic effect favouring formation of an axial substituent, with less repulsive interactions between the oxygen lone pairs and Xa than with Xe (fig. 2.12ii). Taken together, the anomeric affect influence on mannose is to favour the α-anomer.

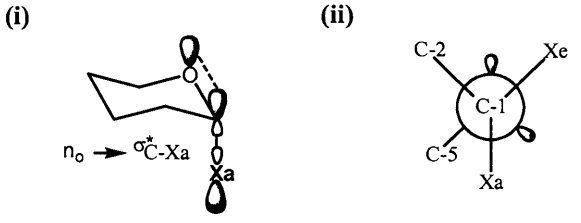

Figure 2.12: Factors that lead to the anomeric effect

The neighbouring group effect occurs when the C-2 hydroxy group of aldopyranose sugars are protected by an acetyl group. For reactions that involve removal of a leaving group from the C-1 position (as would occur for the reaction of a spacer group with a mannose derivative, section 2.6.1, page 76), a C-2 acetoxy group helps to stabilise the intermediate oxonium ion formed by the formation of an acetoxonium ion (fig. 2.13). The acetoxonium intermediate, being more stable than an oxonium ion, is the species under attack by a nucleophile, and as such, effectively blocks the β-face of the sugar from nucleophilic attack, and forces the incoming nucleophile to approach the α-face.

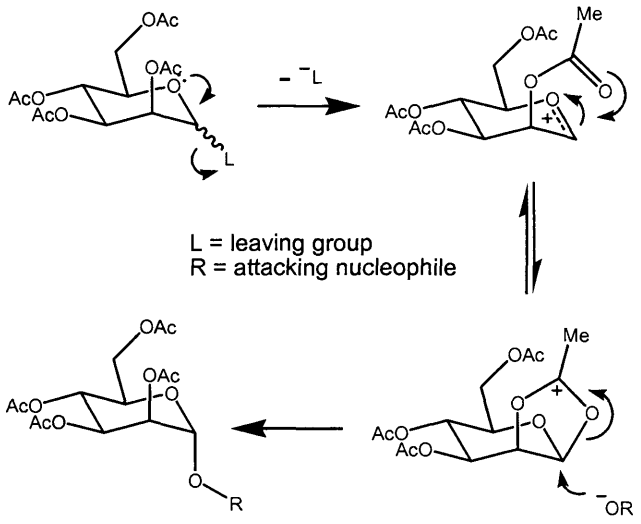

Figure 2.13: Neighbouring group effect on α-anomer formation

2.8.4.2 Bromo and trichloroacetimidyl activated mannopyranosides

Two choices for the formation of activated mannopyranosides will be used in the synthesis of activated mannopyranosides, these being bromo[208,209] and acetimidate[210] activated mannopyranosides. The formation of mannosyl bromides[208,209] is efficient with the use of per-*O*-acetylated mannopyranose. The process involves the displacement of the acetoxy group by halide ion to give exclusively the α-anomer in high yields. The synthesis of α-mannosyl trichloroacetimidates is used to

obtain pure, readily isolable and highly reactive glycosylation intermediates. They can be formed easily by the reaction of 2,3,4,5-tetra-*O*-acetyl-α-D-mannopyranose with trichloroacetonitrile. The α-anomer trichloroacetimidate is formed as reaction involves the deprotonation of the hydroxyl group by a base and then attack of the nucleophilic oxygen on the carbon of the electron deficient nitrile group of trichloro-acetonitrile.

2.9 Structure of MPC1 – MPC6 inhibitors

The chemical strategies mentioned throughout this chapter have led to the design of the inhibitors MPC1 to MPC6, the structure of which are shown in figure 2.14. Chapter 3 details the chemical syntheses used to make these inhibitors and chapter 4 discusses the results of the syntheses.

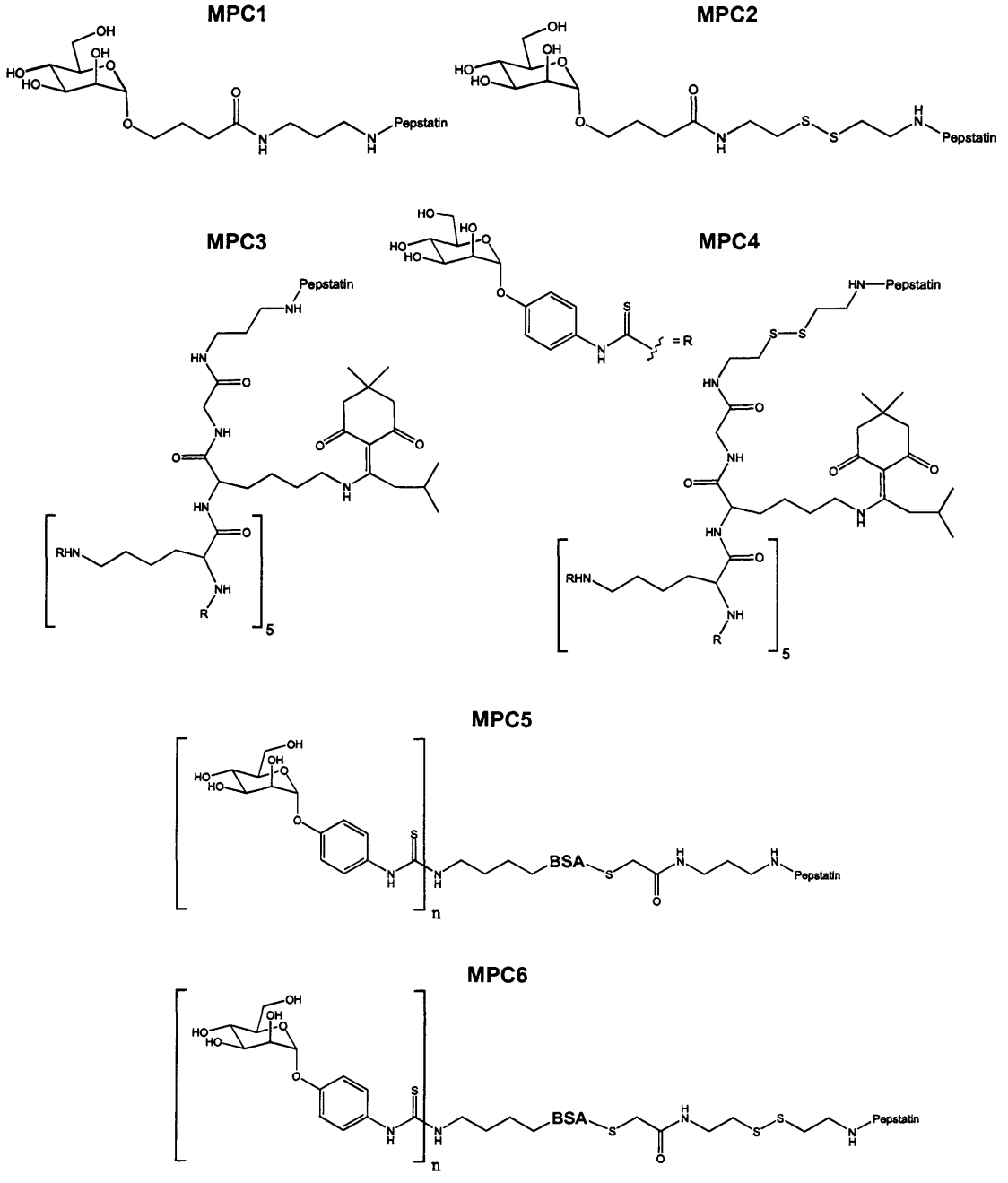

Figure 2.14: Structure of the inhibitors MPC1 to MPC6

Chapter 3

Chemical Synthesis

All abbreviations used in the experimental section are listed on page 25. Unless specified, all reagents were purchased from commercial suppliers and were used without further purification. Pepstatin was obtained from Calbiochem and Bachem. Hydrazine acetate and 4-nitrophenyl α-D-mannopyranoside were supplied by Acros.

^{1}H and ^{13}C NMR spectra were recorded on Bruker AC 300, 400 and 500 instruments. The chemical shift data for each signal is given in units of δ relative to tetramethylsilane (TMS) where δ (TMS) = 0. The multiplicity of the signals is indicated as: br – broad, s – singlet, d – doublet, t – triplet, m – multiplet, quin – quintet, dd – doublet of doublets. CI and FAB mass spectra (MS) were recorded using a VG ZAB SE mass spectrometer. APCI and ES mass spectra were recorded on a Micromass Quattro mass spectrometer. Most acetylated sugar compounds gave some or all of the fragmentation ions of 169, 229, 289 and 331. These correspond to fragmentations of tetraacetyl mannoside. Table 3.1 shows the major fragment ions for **[2]** (RMM 348) (see section 3.1.2, page 92).

Structure	Ion	Fragmentation
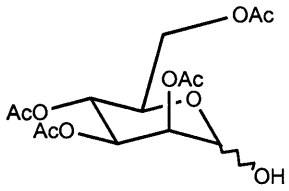	169	compound [2] – 3 x Acetate
	229	compound [2] – 2 x Acetate
	289	compound [2] – Acetate
	331	compound [2] – OH

Table 3.1: Compound [2] structure and acetylated sugar fragmentation ions

Optical rotation was recorded using an AA-10 automatic polarimeter (Optical Activity Ltd, UK) and a 5cm length, 1.5ml cell (d = 0.5). Melting point determination was carried out using a Gallenkamp melting point apparatus. Infra-red (IR) spectroscopy (ν_{max}) was carried out using a Shimadzu FTIR-8700 Fourier transform infra-red spectrometer and analysed with Shimadzu FT IRS software. Abbreviations used in reporting IR data are: w – weak, m – moderate, s – strong, br – broad. Characteristic absorptions are seen across many compounds with minor changes of approx. +/– 15 cm^{-1}. These are listed below for brevity:
3500 – 3000 (br, -OH, NH_2 or H_2O), 3030 – 2830 (s, C-H), 1780 – 1720 (s, C=O), 1660 (m, amide C=O), 1595 (s, aromatic), 1530 – 1510 (m, amide N-H), 1500 (s, aromatic), 1450 – 1430 (w, C-H), 1370 (m, C-H), 1255 - 1230 (acetyl C-O-COMe) cm^{-1}.

Analytical HPLC (flow rate 1 ml/min) was carried out using a Millipore Waters 600E system controller and pump system, Pye Unicam PU4025 UV detector, Shimadzu C-R6A chromatopac and a Vydac 218TP54 protein & peptide C18 column, 4.6 mm x 25 cm. Preparative HPLC (flow rate 15 ml/min) was carried out using a Millipore Waters 600E system controller and pump system, Gilson Holochrome UV detector, Millipore Waters 745B data module and a Vydac 218TP1022 protein & peptide C18 column, 21.4 mm x 25 cm. Samples applied to preparative HPLC were dissolved at a maximum of 20 mg / ml and dissolved in the starting HPLC solvent or the closest equivalent if solubility was a problem. T.l.c. was carried out on pre-coated 0.25 mm thick Merck 60 F_{254} silica plates. Reverse phase silica plates used were Merck RP-8 $F_{254}S$. Silica for chromatography was obtained from BDH. In some instances (where mentioned) plates were pre-soaked in t.l.c. solvent. Visualisation of t.l.c. plates was either by absorption of U.V. light, anisaldehyde or phosphomolybdic acid (PMA) stains for sugars, ninhydrin for amines, bromocresol green for organic acids, or permanganate solution as a universal reagent.

Dialysis was performed using 12,000 molecular weight cut-off dialysis tubing. Before use, the tubing was prepared by first boiling for 10 mins in a large volume of 2% (w/v) sodium bicarbonate and 1mM EDTA (pH 8.0), then rinsing the tubing thoroughly in 1mM EDTA (pH 8.0), before boiling again for 10 minutes in 1mM EDTA (pH 8.0). The tubing was allowed to cool before use, and was stored in solution (water or buffer) at 4°C. Centrifugal filtration devices used were either Millipore centriplus YM-30 (Millipore (UK) Ltd) with a maximum 15 ml capacity and used within a Beckman J2-21 swing bucket centrifuge, or Millipore ultrafree-4 filtration unit (5 ml maximum capacity) using a fixed 35° angle centrifuge (Jouan MR 1812, Jouan S. A., France).

Tetrahydrofuran (THF) was dried by distillation from a suspension of THF with sodium and benzophenone. Dimethyl formamide (DMF) was dried by distillation from a suspension of DMF and calcium hydride. Acetic anhydride was purified by a three step process of drying with P_2O_5 (added very slowly) until no more P_2O_5 turned from white to brown/black. Then this was dried over potassium carbonate for a few hours, and then distilled into a flask under N_2 containing anhydrous activated molecular sieves (4Å) for storage. Dichloromethane, triethylamine and ethanol were dried over CaH_2 powder and stored over molecular sieves. Where used as drying agents, sodium sulphate or magnesium sulphate are anhydrous. With all reactions that used dry solvents, an inert atmosphere of nitrogen or argon was used. Where reaction stirring is required, it is assumed that a stirrer bar is included at the beginning of the reaction unless otherwise stated. All reaction vessels used were round-bottomed flasks of a volume at least twice the capacity of the solvent used for the reaction. Ether refers to diethyl ether. Pet. ether refers to petroleum spirit 40 – 60 °C. Brine refers to a saturated solution of sodium chloride, and as such an aqueous brine solution refers to 50 % ddH_2O, 50 % saturated sodium chloride solution. Bicarbonate refers to a saturated solution of sodium bicarbonate.

3.1 Sugar Derivatives

3.1.1 1,2,3,4,6-Penta-*O*-acetyl-*α/β*-D-mannopyranose [1][211]

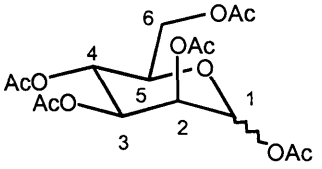

Anhydrous TEA (46 ml) and anhydrous acetic anhydride (15.7 ml, 166 mmol, 5 equiv.) were added to D-mannose (6.03 g, 33.5 mmol). The reaction was stirred overnight under anhydrous conditions. The TEA and unreacted acetic anhydride were removed *in vacuo* to obtain a sticky viscous orange oil. This oil was dispersed in a mixture of iced-water (200 ml) / $CHCl_3$ (200 ml) and then solid potassium bicarbonate was added until the aqueous layer reached neutral pH, ensuring careful mixing of the two layers upon addition of the bicarbonate. The aqueous layer was separated and then washed with $CHCl_3$ (3 x 30 ml). The combined $CHCl_3$ extracts were combined with the original organic layer, and dried over $MgSO_4$ overnight. The $CHCl_3$ was removed *in vacuo* to obtain the title compound as a viscous yellow/orange oil (12.6 g, 33.2 mmol, 99 %) identical by NMR to the literature[211], and used without further purification.

R_f 0.8 [1:2 ethanol – $CHCl_3$; anisaldehyde and permanganate stain].
MS (FAB+): *m/z* = 169 (17 %), 331 (5 %), 413 (100 %, $[M + Na]^+$).
ν_{max} ($CHCl_3$): 3500 – 3200 (br s), 3028 (m), 3005 (s), 2945 (s), 2833 (m), 1774 – 1726 (s), 1448 (m), 1429 (m), 1371 (s) cm^{-1}.
^1H NMR ($CDCl_3$, 300 MHz): δ 1.94 (3H, s), 1.95 (3H, s), 2.0 (3H, s), 2.02 (3H, s), 2.03 (3H, s), 2.10 (3H, s), 2.11 (3H, s), 2.14 (3H, s), 3.75 (1H, ddd, *J* 2.4, 5.0 & 9.8 Hz, H-5β), 3.96 – 4.04 (2H, m, H-5α & H-6aβ), 4.08 (1H, dd, $J_{6a,5}$ 2.4 $J_{6a,6b}$ 12.2 Hz, H-6aα), 4.21 (1H, dd, $J_{6b,5}$ 4.8 $J_{6b,6a}$ 12.2 Hz, H-6b'α), 4.24 (1H, dd, $J_{6b,5}$ 5.3 $J_{6b,6a}$ 12.5 Hz, H-6bβ), 5.08 (1H, dd, *J* 3.3, 10.0 Hz, H-β), 5.19 – 5.32 (4H, m, H-β, H-2α, H-3α

& H-4α), 5.42 (1H, dd, $J_{2,1}$ 1.1 $J_{2,3}$ 3.3 Hz, H-2β), 5.81 (1H, d, $J_{1,2}$ 1.1 Hz, H-1β), 6.02 (1H, d, $J_{1,2}$ 1.9 Hz, H-1α).

^{13}C NMR ($CDCl_3$, 75.4 MHz): δ 20.0, 20.2, 20.31, 20.33, 20.35, 20.38, 20.39, 20.42, 20.44, 20.5, 53.3, 61.7, 65.1, 65.2, 67.9, 68.0, 68.4, 70.3, 70.3, 72.8, 90.2, 90.3, 167.8, 168.0, 169.2, 169.3, 169.4, 169.5, 169.6, 169.9, 170.2, 170.3.

3.1.2 2,3,4,6-Tetra-*O*-acetyl-α-D-mannopyranose [2][212;213]

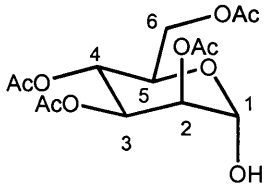

1,2,3,4,6-Penta-*O*-acetyl-α/β-D-mannopyranose **[1]** (17.04 g, 43.7 mmol) was added to anhydrous DMF (300 ml) in a three necked flask equipped with a Youngs tap, Suba-seal and stopper. Hydrazine acetate (4.82 g, 87.4 mmol, 2 equiv.) was added portionwise to the reaction mixture and then stirred for 4 hours under N_2 or until the starting material was judged to have been consumed by t.l.c. The reaction mixture was diluted with ethyl acetate (100 ml) and then washed with water (3 x 100 ml). The organic layers were dried overnight with Na_2SO_4, filtered and then concentrated *in vacuo*. Purification by flash chromatography (4 cm, gradient, 100 % $CHCl_3$ to 50 % acetone in $CHCl_3$) gave the title compound as a yellow oil (11.77 g, 33.8 mmol, 77 %) spectroscopically identical to the literature[213,214] with less than 1 % of the β-anomer by ^1H NMR. With time, pure samples crystallised at – 20 °C.

R_f 0.35 [1:2 ethanol – $CHCl_3$; anisaldehyde and permanganate stain].

m.p. 93 – 95 °C (lit. ref. 95 – 97 °C)[215].

$[\alpha]_D^{21}$ + 21.0° (c 1, $CHCl_3$), (lit. ref. + 19.8°)[213].

MS (FAB+): *m/z* = 169 (92 %), 331 (93 %), 349 (8 %, $[M + H]^+$).

ν_{max} (KBr): 3500 – 3100 (br), 3030 – 2830 (s), 1780 – 1720 (s), 1371 (m), 1255 (s) cm^{-1}.

^{1}H NMR ($CDCl_3$, 400 MHz): δ 1.96 (3H, s), 2.01 (3H, s), 2.07 (3H, s), 2.12 (3H, s), 3.98 (1H, d, *J* 4.2 Hz), 4.18 – 4.23 (2H, m), 5.19 – 5.20 (1H, m, H-5), 5.22 (1H, dd, *J* 1.9 & 3.3 Hz), 5.26 (1H, t, *J* 9.9 Hz, H-4), 5.37 (1H, dd, *J* 3.3 & 10.1 Hz).

^{13}C NMR (100.6 MHz, $CDCl_3$): δ 20.6, 20.7, 20.9, 62.5, 66.1, 68.3, 68.8, 70.0, 92.1, 169.8, 170.1, 170.3, 170.9.

Missing 1 CH_3 ^{13}C signal, overlapping with 20.7 ppm.

3.1.3 2,3,4,6-Tetra-*O*-acetyl-α-D-mannopyranosyl trichloroacetimidate [3][212;214]

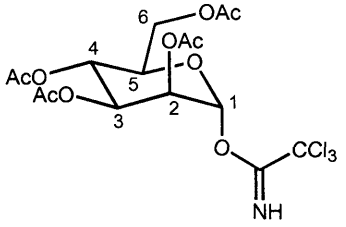

2,3,4,6-Tetra-*O*-acetyl-α-D-mannopyranose **[2]** (11.04 g, 31.7 mmol) was dissolved in a flask with anhydrous CH_2Cl_2 (200 ml). Potassium carbonate (5.26 g, 38 mmol, 1.2 equiv.) was added and stirred for 10 mins. The reaction mixture was cooled to 4 °C and covered with foil to exclude light. Trichloroacetonitrile (15.8 ml, 158 mmol, 5 equiv.) was dissolved in anhydrous CH_2Cl_2 (50 ml) and slowly added to the reaction vessel. The reaction was stirred overnight and monitored by t.l.c. After the reaction was judged complete, the mixture was filtered and the CH_2Cl_2 and trichloroacetonitrile were removed *in vacuo* to obtain the title compound as a yellow oil (15.01 g, 30.5 mmol, 96 %) identical by NMR and IR to the literature[212,214].

R_f 0.7 [1:2 ethanol – $CHCl_3$; anisaldehyde and permanganate stain].

$[\alpha]_D^{21}$ + 49.0° (c 1, $CHCl_3$), (lit. ref. + 50.0°)[216].

MS (FAB+): *m/z* = 169 (100 %), 331 (62 %), 514.5 (92 %, $[M + Na]^+$).

ν_{max} ($CHCl_3$): 3026 (s), 1761 – 1732 (s), 1678 (m, C=N), 1369 (s), 1255 (s) cm^{-1}.

^{1}H NMR (400 MHz, $CDCl_3$): δ 1.96 (3H, s), 2.02 (3H, s), 2.04 (3H, s), 2.15 (3H, s), 4.11 (1H, dd, $J_{6a,5}$ 2.2 $J_{6a,6b}$ 11.9 Hz, H-6a), 4.13 – 4.16 (1H, m, H-5), 4.23 (1H, dd, $J_{6b,5}$ 4.7 $J_{6b,6a}$ 12.0 Hz, H-6b), 5.34 – 5.36 (2H, m, H-3 & H-4), 5.42 (1H, dd, $J_{2,1}$ 1.9 $J_{2,3}$ 3.0 Hz, H-2), 6.23 (1H, d, $J_{1,2}$ 1.9 Hz, H-1), 8.76 (1H, s, C=NH).

^{13}C NMR (100.6 MHz, $CDCl_3$): δ 20.5, 20.6, 20.7, 61.9, 65.3, 67.7, 68.7, 71.1, 90.4, 94.4, 159.6, 169.5, 169.6, 169.7, 170.5.

Missing 1 CH_3 ^{13}C signal, overlapping with 20.6 ppm.

3.1.4 2,3,4,6-Tetra-*O*-acetyl-α-D-mannopyranosyl bromide [4][217]

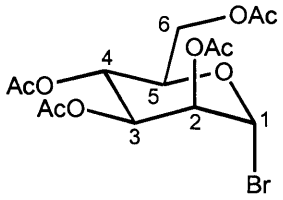

1,2,3,4,6-Penta-*O*-acetyl-α-D-mannopyranose **[1]** (3.112 g, 8 mmol) was placed into a round-bottomed flask and dissolved with acetic acid (9 ml). Hydrogen bromide (45 % solution in acetic acid, 9 ml) was added slowly while stirring and the reaction stirred for a further 3 hours. The reaction mixture was diluted with CH_2Cl_2 (100 ml) and washed with cold 1 % HBr solution (3 x 100 ml) and then dried over Na_2SO_4. Filtration and removal of the solvent *in vacuo* gave a brown oil containing some acetic acid. The acetic acid was removed azeotropically with toluene to obtain the title compound as an orange oil (3.22 g, 7.8 mmol, 97 %) identical by NMR to the literature[217].

$[\alpha]_D^{21}$ + 123.0° (c 1, $CHCl_3$). lit. ref. +123.5° (c 1, $CHCl_3$).

^{1}H NMR ($CDCl_3$, 300 MHz): δ 1.98 (3H, s), 2.05 (3H, s), 2.08 (3H, s), 2.15 (3H, s), 4.11 (1H, dd, $J_{6a,5}$ 2.1 $J_{6a,6b}$ 12.3 Hz, H-6a), 4.16 – 4.22 (1H, m, H-5), 4.30 (1H, dd, $J_{6b,5}$ 4.8 $J_{6b,6a}$ 12.4 Hz, H-6b), 5.34 (1H, t, J 10.1 Hz, H-4), 5.42 (1H, dd, $J_{2,1}$ 1.3 $J_{2,3}$ 3.4 Hz, H-2), 5.69 (1H, dd, $J_{3,2}$ 3.4 $J_{3,4}$ 10.2 Hz, H-3), 6.27 (1H, d, $J_{1,2}$ 1.3 Hz, H-1).

^{13}C NMR ($CDCl_3$, 75.4 MHz): δ 20.5, 20.6, 20.7, 20.7, 61.4, 65.2, 67.9, 72.1, 72.8, 83.0, 169.5, 170.5. Missing 2 C=O ^{13}C signals.

3.1.5 4-Nitrophenyl 2,3,4,6-tetra-*O*-acetyl-β-D-mannopyranoside [5][218;251]

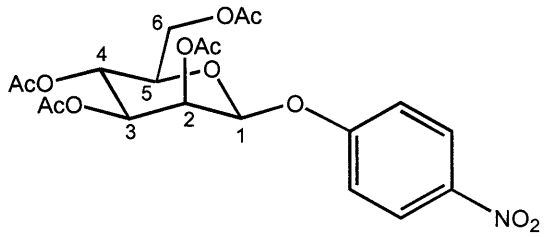

To a flask containing 2,3,4,6-tetra-*O*-acetyl-α-D-mannopyranosyl bromide **[4]** (968 mg, 2.3 mmol) and 4-nitrophenol (650 mg, 4.6 mmol, 2 equiv.) was added anhydrous MeCN (5 ml). N^1,N^1,N^3,N^3-tetramethyl-guanidine (442 µl , 3.5 mmol, 1.5 equiv.) was added slowly and the reaction stirred continually overnight. The solvent was removed *in vacuo* at room temperature and the residue redissolved in ethyl acetate. This was washed with water / 1 % sodium carbonate solution (2 x 200 ml), aqueous brine / 1 % sodium carbonate solution (2 x 200 ml) and aqueous brine (2 x 200 ml). Drying over Na_2SO_4 for 2 hours and then removal of the solvent *in vacuo* (at room temperature) gave a white crystalline product. The product was successively recrystallised from EtOH and $CHCl_3$ to give the title compound (628 mg, 1.34 mmol, 57 %) as yellowish crystals, identical by NMR to the literature[251].

R_f 0.5 [1:9 acetone – toluene + 1 % acetic acid; PMA stain and UV].

m.p.: 182 – 184 °C (lit. ref. 183 °C)[218].

$[\alpha]_D^{23}$ + 24.0° (c 1, MeOH), (lit. ref. + 24.5°)[218].

Found: M+Na, 492.1121. $C_{20}H_{23}NO_{12}$ requires M+Na, 492.1118 (ES).

ν_{max} (KBr): 3600 – 3100 (br), 1749 (s), 1596 (s), 1519 (s, C-NO_2), 1500 (s), 1371 (s), 1340 (s, C-NO_2), 1229 (s) cm^{-1}.

^1H NMR ($CDCl_3$, 500 MHz): δ 1.87 (3H, s), 2.04 (3H, s), 2.06 (3H, s), 2.11 (3H, s), 3.70 (1H, ddd, $J_{5,6a}$ 2.9 $J_{5,6b}$ 5.3 $J_{5,4}$ 9.4 Hz, H-5), 4.15 (1H,

dd, $J_{6a,5}$ 2.8 $J_{6a,6b}$ 12.2 Hz, H-6a), 4.22 (1H, dd, $J_{6b,5}$ 5.4 $J_{6b,6a}$ 12.2 Hz, H-6b), 4.45 (1H, dd, $J_{2,1}$ 2.8 $J_{2,3}$ 4.0 Hz, H-2), 5.13 (1H, dd, $J_{3,2}$ 4.0 $J_{3,4}$ 9.4 Hz, H-3), 5.29 (1H, t, J 9.4 Hz, H-4), 5.48 (1H, d, $J_{1,2}$ 2.7 Hz, H-1), 7.22 (2H, d, J 9.3 Hz, phenyl), 8.15 (2H, d, J 9.3 Hz, phenyl).

^{13}C NMR ($CDCl_3$, 125.7 MHz): δ 20.6, 20.68, 20.7, 23.5, 62.4, 65.4, 69.7, 71.8, 76.0, 97.3, 121.2, 125.3, 143.8, 158.4, 169.5, 170.1, 170.6. Missing 1 ^{13}C signal, possibly quaternary.

3.1.6 4-Nitrophenyl 2,3,4,6-tetra-*O*-acetyl-α-D-mannopyranoside [6][219;220]

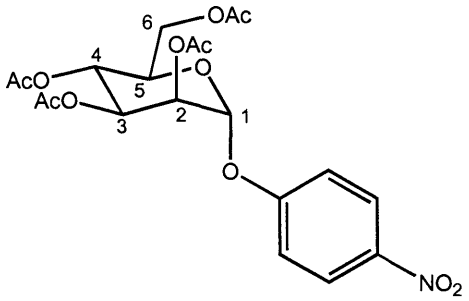

1,2,3,4,6-Penta-*O*-acetyl-α-D-mannopyranose **[1]** (334 mg, 860 μmol) and 4-nitrophenol (179 mg, 1.29 mmol, 1.5 equiv.) were added to a flask and any water present was removed azeotropically with anhydrous MeCN. The reagents were dissolved into anhydrous CH_2Cl_2 (10 ml) and cooled to ~ 0 °C. $BF_3.Et_2O$ (325 μl, 2.56 μmol, 3 equiv.) was dropped slowly into the reaction mixture while stirring. The reaction was then stirred and allowed to reach room temperature over 16 hours. t.l.c. of the reaction mixture showed approximately 50 % of the starting material remaining. An extra portion of $BF_3.Et_2O$ (0.5 ml, 4.6 equiv.) was added slowly and the reaction stirred at r.t. for a further 24 hours. The reaction was washed with water / brine / sodium bicarbonate solution (7 x 50 ml), until all of the yellow 4-nitrophenol had been removed from the organic layer. The product was dried over $MgSO_4$, filtered and the solvent removed *in vacuo*. The final crude product was recrystallised from CH_2Cl_2 / cyclohexane to obtain the title compound as a pure yellowish

crystalline compound (359 mg, 764 mmol, 89 %) with approximately 5 % of the incorrect anomer present as shown by NMR[220].

R_f 0.5 [1:9 acetone – toluene + 1 % acetic acid; PMA stain and UV], compound **[1]** R_f 0.4, 4-nitrophenol R_f 0.45.
m.p. 159 – 161 °C, (lit. ref. 154 – 156 °C)[220].
$[\alpha]_D^{23}$ + 72.0° (c 1, MeOH), (lit. ref. + 103° [c 1, $CHCl_3$])[252].
MS (ES+): *m/z* = 169 (84 %), 331 (100 %), 470 (12 %, $[M + H]^+$), 492 (68 %, $[M + Na]^+$).
ν_{max} ($CHCl_3$): 3025 (w), 1751 (s), 1594 (m), 1521 (m, C-NO_2), 1495 (m), 1370 (m), 1346 (m, C-NO_2), 1235 (s) cm^{-1}.
^1H NMR ($CDCl_3$, 400 MHz): δ 1.99 (3H, s), 2.01 (3H, s), 2.02 (3H, s), 2.18 (3H, s), 3.94 (1H, ddd, $J_{5,6a}$ 2.3 $J_{5,6b}$ 5.4 $J_{5,4}$ 10.0 Hz, H-5), 3.98 (1H, dd, $J_{6a,5}$ 2.3 $J_{6a,6b}$ 12.3 Hz, H-6a), 4.19 (1H, dd, $J_{6b,5}$ 5.4 $J_{6b,6a}$ 12.3 Hz, H-6b), 5.30 (1H, t, *J* 10.0 Hz, H-4), 5.38 (1H, dd, $J_{2,1}$ 1.7 $J_{2,3}$ 3.5 Hz, H-2), 5.45 (1H, dd, $J_{3,2}$ 3.5 $J_{3,4}$ 10.0 Hz, H-3), 5.57 (1H, d, $J_{1,2}$ 1.7 Hz, H-1), 7.18 (2H, d, *J* 12.5, phenyl), 8.19 (2H, d, *J* 12.6, phenyl).
^{13}C NMR ($CDCl_3$, 125.7 MHz): δ 20.57, 20.58, 20.6, 20.7, 61.9, 65.5, 68.5, 68.9, 69.8, 95.6, 116.4, 125.8, 143.1, 160.1, 169.6, 169.9, 170.0, 170.3.

3.1.7 Conversion of 4-nitrophenyl 2,3,4,6-tetra-*O*-acetyl-β-D-manno-pyranoside [5] to 4-nitrophenyl 2,3,4,6-tetra-*O*-acetyl-α-D-mannopyranoside [6]

4-Nitrophenyl 2,3,4,6-tetra-*O*-acetyl-β-D-mannopyranoside **[5]** (113 mg, 241 μmol) was placed in a flask and dissolved in anhydrous CH_2Cl_2 (5 ml). The flask was cooled to ~ 0 °C and $BF_3.Et_2O$ (92 μl, 726 μmol, 3 equiv.) was added slowly drop-wise with stirring. After 4 hours, t.l.c. (40 % ethyl acetate / hexane) showed the presence of the nitrophenol (R_f 0.6, UV and strong yellow colour) implying that anomerisation was occurring. The solvent was removed *in vacuo* and the residue redissolved

in ethyl acetate. The organic layer was washed with water / 1 % brine / 1 % bicarbonate solution (6 x 50 ml). The organic layer was dried over Na_2SO_4, the solvent removed *in vacuo* and the crude product re-crystallised from ethanol to obtain the α-anomer mannoside **[6]** (22 mg, 48 μmol, 20 %) as identified by NMR[220].

3.1.8 4-Aminophenyl 2,3,4,6-tetra-*O*-acetyl-*α*-D-mannopyranoside [7]

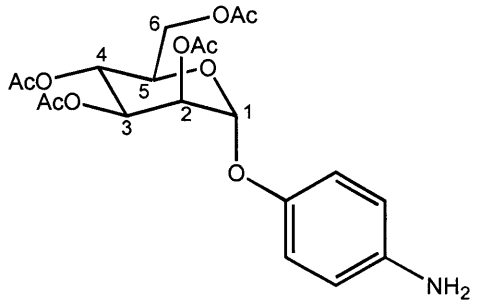

4-Nitrophenyl 2,3,4,6-tetra-*O*-acetyl-*α*-D-mannopyranoside **[6]** (199 mg, 420 μmol) was dissolved in anhydrous THF (5 ml) and 10 % Pd / C (100 mg) was added. Hydrogenation was carried out under standard conditions using an atmospheric pressure hydrogenator over 4 hours in the presence of an excess of H_2 gas. The mixture was filtered through Celite and the solvent removed *in vacuo*. Flash column chromatography (4 cm, isocratic, 5 % ethanol in $CHCl_3$) gave the title compound as a yellowish oil (185 mg, 336 μmol, 85 %), identical by NMR to literature values[220,221].

R_f 0.2 [1:19 acetone – toluene + 1 % acetic acid, ninhydrin, PMA stain and UV].

$[\alpha]_D^{23}$ + 71.0° (c 1, $CHCl_3$), (lit. ref. + 71.2°)[221].

MS (APCI): m/z = 169 (100%), 331 (34%), 440 (14%, $[M + H]^+$).

ν_{max} (neat): 3460 (s), 3373 (s), 3230 (w), 3045 (w), 2960 (m), 1733 (s), 1627 (s), 1511 (s), 1435 (s), 1372 (s), 12220 (s br) cm^{-1}.

^1H NMR ($CDCl_3$, 400 MHz): δ 1.97 (3H, s), 1.99 (3H, s), 2.0 (3H, s), 2.13 (3H, s), 3.51 (2H, br s, NH_2), 4.03 (1H, dd, $J_{6a,5}$ 2.3 $J_{6a,6b}$ 12.1 Hz, H-6a), 4.10 (1H, ddd, $J_{5,6a}$ 2.2 $J_{5,6b}$ 5.0 $J_{5,4}$ 10.0 Hz, H-5), 4.23 (1H, dd,

$J_{6b,5}$ 5.3 $J_{6b,6a}$ 12.1 Hz, H-6b), 5.29 (1H, t, J 10.1 Hz, H-4), 5.30 (1H, d, $J_{1,2}$ 1.7 Hz, H-1), 5.37 (1H, dd, $J_{2,1}$ 1.8 $J_{2,3}$ 3.4 Hz, H-2), 5.47 (1H, dd, $J_{3,2}$ 3.5 $J_{3,4}$ 10.0 Hz, H-3), 6.56 (2H, d, J 8.8 Hz, phenyl), 6.82 (2H, d, J 8.8 Hz, phenyl).

^{13}C NMR ($CDCl_3$, 100.6 MHz): δ 20.4, 20.6, 20.8, 20.9, 62.1, 68.8, 76.7, 77.0, 77.3, 96.8, 115.6, 116.1, 117.6, 118.2, 142.1, 148.4, 170.5, 169.7, 169.8, 169.9.

3.1.9 4-Isothiocyanatophenyl 2,3,4,6-tetra-*O*-acetyl-α-D-manno-pyranoside [8][222]

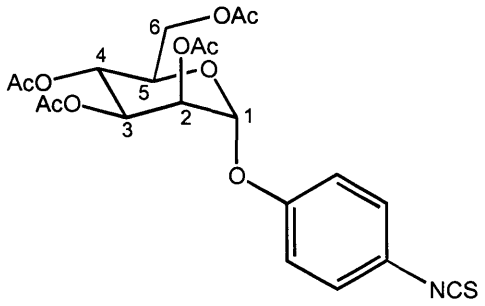

Extreme caution was taken with this procedure due to the toxicity and volatility of the thiophosgene reagent. A 250 ml, single neck, round bottomed flask containing a stirrer bar and fitted with a pressure equalised dropping funnel under argon was prepared before the procedure was started. A continuous flow of argon through the vessel and out into a mild bleach solution was used for ventilation and quenching of gaseous thiophosgene and hydrogen chloride produced in the reaction. All equipment and removed solvents were deactivated by the addition of methylamine for several hours.

Thiophosgene (286 µl, 3.75 mmol, 5 equiv.) was dissolved in anhydrous THF (10 ml) and added to a flask containing a pressure equalised dropping funnel under argon. Anhydrous TEA (1 ml) and 4-aminophenyl 2,3,4,6-tetra-*O*-acetyl-α-D-mannopyranoside **[7]** (329 mg, 750 µmol) in anhydrous THF (9 ml) were added to the dropping funnel. The mixture

was slowly added to the flask with vigorous stirring. During the course of the reaction, the mixture turned cloudy, producing hydrogen chloride gas. After several hours the mixture turned dark brown and the gaseous layer disappeared. By 4 hours, t.l.c. showed complete formation of product. The solvent was removed *in vacuo* and the reaction redissolved in ethyl acetate (100 ml), washed with water (2 x 100 ml) and with brine (1 x 100 ml). The partitions during workup showed a brown membrane in between, which was included in each subsequent ethyl acetate wash fraction. The organic layer was dried over anhydrous $MgSO_4$ for 2 hours and the solvent removed *in vacuo* to obtain a crude brown crystalline product (358 mg). Further purification by dissolving the product in ethyl acetate and refluxing for 1 minute with some decolourising charcoal, and removal of the solvent *in vacuo* gave the title compound as a lighter brown crystalline product (333 mg, 690 μmol, 92 %) identical to the literature[222].

R_f 0.7 [1:1 ethyl acetate – hexane].

m.p.: 134 – 136 °C (lit. ref. = 134 – 136 °C)[222].

$[\alpha]_D^{23}$ + 56.0° (c 1, MeOH) (lit. ref. = + 55.0°)[222].

MS (ES+): m/z = 169 (100 %), 331 (19 %), 504 (54 %) $[M + Na]^+$).

ν_{max} ($CHCl_3$): 3025 (w), 2170 – 2000 (br, -N=C=S), 1751 (s), 1502 (s), 1370 (m), 1234 (s) cm^{-1}.

^1H NMR ($CDCl_3$, 300 MHz): δ 1.93 (3H, s), 1.94 (3H, s), 1.96 (3H, s), 2.10 (3H, s), 3.93 – 4.02 (2H, m, H-5 and H-6a), 4.17 (1H, dd, $J_{6b,5}$ 5.7 $J_{6b,6a}$ 12.4 Hz, H-6b), 5.27 (1H, t, *J* 10.1 Hz, H-4), 5.35 (1H, dd, 1.8 & 3.5 Hz, H-2), 5.42 – 5.46 (2H, m, H-1 & H-3), 7.0 (2H, d, *J* 9.1 Hz, phenyl), 7.11 (2H, d, *J* 9.1 Hz, phenyl).

^{13}C NMR ($CDCl_3$, 75.4 MHz): δ 18.7, 21.0, 21.1, 62.5, 66.2, 69.1, 69.6, 69.8, 96.3, 117.9, 127.4, 135.8, 154.7, 169.9, 170.0, 170.2, 170.7. Missing 1 CH_3 ^{13}C signal, overlapping.

3.1.10 4-Nitrophenyl α-D-mannopyranoside [9][223]

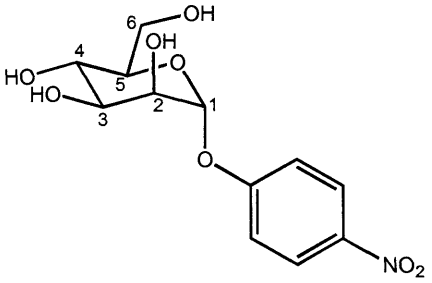

4-Nitrophenyl 2,3,4,6-tetra-*O*-acetyl-α-D-mannopyranoside **[6]** (1.125 g, 2.4 mmol) and methanol (10 ml) were added to a flask. LiOH (1M, aq) was added drop-wise with stirring until pH 11 was reached. During this time the starting material slowly dissolved to form a yellow solution, which was then stirred for a further 2 hours during which time a yellow precipitate was formed. The solvent was removed *in vacuo* to give a off-white solid. This was then purified by flash chromatography (2cm, isocratic, 20% methanol in $CHCl_3$) to give the title compound as a off-white powder (0.502 g, 1.68 mmol, 70%). This was recrystallised from hot methanol to give elongated yellowish needles, identical by NMR[223] to reference compounds.

R_f 0.5 [1:4 methanol – $CHCl_3$, PMA stain and UV].

m.p. 175 – 177 °C, (lit. ref. 182 – 184 °C)[223].

$[\alpha]_D^{23}$ + 160.0° (c 1, MeOH), (lit. ref. + 155.0°)[223].

MS (ES+): m/z = 323 (100%, $[M + Na]^+$).

ν_{max} (KBr): 3500 – 3100 (br), 2960 – 2850 (m), 1600 (s), 1520 (s, C-NO_2), 1500 (s), 1350 (s, C-NO_2), 1150 – 995 (s) cm^{-1}.

^{1}H NMR (CD_3OD, 500 MHz): δ 3.49 (1H, ddd, $J_{5,6a}$ 2.4 $J_{5,6b}$ 5.7 $J_{5,4}$ 9.7 Hz, H-5) 3.68 (1H, dd, $J_{6b,5}$ 5.8 $J_{6b,6a}$ 12.1 Hz, H-6b) 3.69 – 3.72 (1H, m, H-4) 3.75 (1H, dd, $J_{6a,5}$ 2.3 $J_{6a,6b}$ 12.1 Hz, H-6a) 3.88 (1H, dd, $J_{3,2}$ 3.4 $J_{3,4}$ 9.5 Hz, H-3) 4.02 (1H, dd, $J_{2,1}$ 1.8 $J_{2,3}$ 3.4 Hz, H-2) 5.64 (1H, d, $J_{1,2}$ 1.8 Hz, H-1) 7.29 (2H, d, *J* 9.3 Hz, phenyl) 8.21 (2H, d, *J* 9.3 Hz, phenyl).

^{13}C NMR (CD_3OD, 125.7 MHz): δ 62.6, 68.1, 71.6, 72.2, 76.0, 100.1, 117.8, 126.7, 143.8, 162.8.

3.1.11 4-Aminophenyl α-D-mannopyranoside [10][223]

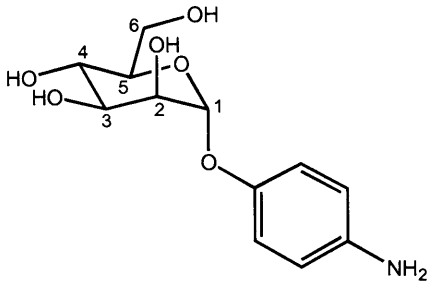

4-Nitrophenyl α-D-mannopyranoside **[9]** (1 g, 3.3 mmol) and 10 % Pd / C (200 mg) were added to a flask with anhydrous MeOH (50 ml). The flask was attached to an atmospheric pressure hydrogenator over 4 hours in the presence of an excess of H_2 gas. The flask contents were filtered through Celite and the solvent removed *in vacuo* to obtain a yellowish solid. This was then dissolved in CH_2Cl_2 with a small amount of MeOH until soluble and filtered through a pad of silica. The silica was washed with 40% EtOH / CH_2Cl_2 and the filtrates combined. The solvent was removed *in vacuo* to obtain the title compound as an off-white powder (0.89 g, 3.26 mmol, 99 %). NMR data as literature[223].

m.p. 147 – 149°C (lit. ref. 158°C)[224].

$[\alpha]_D^{23}$ + 124.0° (c 1, MeOH) (lit. ref. + 128.0°)[223].

MS (ES+): m/z = 272 (37%, $[M + H]^+$).

ν_{max} (KBr): 3600 – 3000 (br), 2940 – 2890 (w), 1630 (m), 1514 (s) cm^{-1}.

^1H NMR ($CDCl_3$, 300 MHz): δ 3.67 – 3.80 (4H, m, H-4, H-5 & H-6) 3.88 (1H, dd, *J* 3.3 & 8.7 Hz, H-3) 3.98 (1H, m, H-2) 5.29 (1H, s, H-1) 6.71 (2H, d, *J* 8.8 Hz, phenyl) 6.92 (2H, d, *J* 8.8 Hz, phenyl).

^{13}C NMR ($CDCl_3$, 75.4 MHz): δ 62.7, 68.5, 72.2, 72.5, 75.1, 101.4, 117.9, 119.3, 144.0, 151.1.

3.1.12 4-Isothiocyanatophenyl α-D-mannopyranoside [11][201;225]

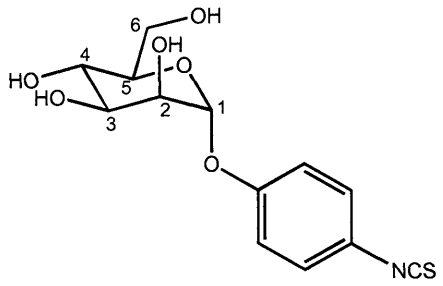

4-Aminophenyl α-D-mannopyranoside **[10]** (800 mg, 2.95 mmol) was added to a flask with ethanol (80 ml) and water (20 ml) and a dropping funnel attached. Thiophosgene (1.7 ml, 14.76 mmol, 5 equiv.) was carefully added dropwise *via* the dropping funnel to the flask while vigorously stirring. After 1 hour the reaction appeared to be complete. T.l.c. UV visualisation and ninhydrin were used to ensure that the starting material had been consumed. Removal of the solvent *in vacuo* gave a brown semi-solid that was purified by flash chromatography (6 cm, isocratic, 20 % methanol in $CHCl_3$) to give the desired product as a white solid (0.90 g, 2.86 mmol, 97 %). This was recrystallised from $CHCl_3$ / cyclohexane to obtain a crystalline white solid of the title compound. All equipment and removed solvent were deactivated by the addition of methylamine for a period of 2 hours. Literature does not contain analytical data.

R_f 0.5 [1:4 methanol – $CHCl_3$, PMA stain and UV], amine compound **[10]** at baseline.

$[\alpha]_D^{23}$ + 12.0° (c 1, MeOH).

m.p. 168 – 170°C.

MS (ES+): m/z = 336 (20%, $[M + Na]^+$).

ν_{max} (KBr): 3650 – 3150 (br), 2980 – 2880 (s), 2800 – 2430 (s), 2133 (br, -N=C=S), 1475, 1444 cm^{-1}.

^1H NMR (CD_3OD, 300 MHz): δ 3.53 (1H, ddd, *J* 2.7, 5.0 & 9.7 Hz, H-5), 3.66 – 3.80 (3H, m, H-4, H-6), 3.86 (1H, dd, $J_{3,2}$ 3.4 $J_{3,4}$ 9.4 Hz, H-3),

3.99 (1H, dd, $J_{2,1}$ 1.9 $J_{2,3}$ 3.3 Hz, H-2), 5.48 (1H, d, $J_{1,2}$ 1.8 Hz, H-1), 7.15 (2H, d, J 9.1 Hz, phenyl) 7.23 (2H, d, J 9.1 Hz, phenyl).
^{13}C NMR (CD_3OD, 75.4 MHz): δ 62.7, 68.3, 71.8, 72.4, 75.6, 100.3, 114.5, 119.0, 127.9, 157.0. Missing 1 ^{13}C.

3.2 Linker Synthesis

3.2.1 Benzyl 4-hydroxybutanoate [12][226]

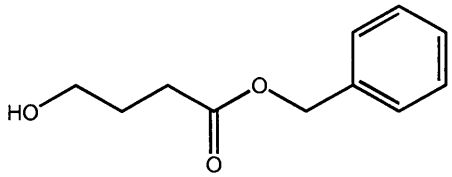

To a flask containing γ-butyrolactone (4.20 g, 48.8 mmol) was added sodium hydroxide (1M, 1.95g in 49 ml water, 48.8 mmol). A condenser was attached and the mixture was stirred and heated at 70 °C overnight. Water was azeotropically removed with toluene or alternatively by freeze-drying for between 24 and 48 hours. The salt was loosened from the sides of the reaction vessel and made as fine a powder as possible with a mortar and pestle. To the sodium salt were added anhydrous acetone (40 ml), tetrabutylammonium bromide (1.57 g, 4.87 mmol, 0.1 equiv.), and benzyl bromide (3.30 ml, 27.7 mmol, 0.6 equiv.). This mixture was refluxed under a nitrogen atmosphere for 24 hours. The reaction mixture was cooled and concentrated *in vacuo* to remove the acetone. The reaction contents were partitioned between ethyl acetate (200 ml) and 0.4M $NaHSO_4$ (200 ml). The organic layer was washed with aqueous brine (3 x 200 ml) and then with saturated brine (3 x 200 ml) and dried over $MgSO_4$. Removal of the solvent *in vacuo* gave the title compound as a yellow oil (5.81 g, 29.9 mmol, 61 %) identical by NMR to the literature[226].

R_f 0.3 [2:3 ethyl acetate – hexane; UV and permanganate stain], benzyl bromide R_f 0.7 (UV only).

MS (APCI+): *m/z* = 195 (100%, $[M + H]^+$).

ν_{max} ($CHCl_3$): 3550 – 3100 (br), 3010 – 3008 (s), 3050 – 2900 (w), 1780 – 1700 (s), 1454 (m), 1377 (m), 1229 (s) cm^{-1}.

^1H NMR ($CDCl_3$, 300 MHz): δ 1.86 (2H, m, H-3), 2.27 (2H, t, *J* 7.2 Hz, H-2), 3.60 (2H, t, *J* 6.1 Hz, H-4), 5.08 (2H, s, benzyl), 7.31 (5H, m).

^{13}C NMR ($CDCl_3$, 75.4 MHz): δ 27.5, 30.8, 61.7, 66.5, 128.1, 128.4, 135.7, 173.7. Missing 1 ^{13}C, may be quaternary.

3.2.2 *N*-(*t*-Butyloxycarbonyl) propane-1,3-diamine [13][227]

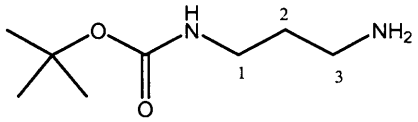

Anhydrous THF (20 ml) was added to a flask containing diaminopropane (4 ml, 47.4 mmol, 4 equiv.) and stirred vigorously. Di-*t*-butyl dicarbonate (2.56 g, 11.8 mmol) was dissolved in anhydrous THF (2 ml) and added slowly. The mixture was stirred vigorously for 3 hours, by which time the Boc anhydride had completely reacted (t.l.c. 20 % MeOH / $CHCl_3$ + 1 % TEA, Boc anhydride R_f 0.9, product R_f 0.2). The THF was removed *in vacuo* and the crude product redissolved in 100 ml ether. The ethereal layer was washed with water (1 x 100 ml), water / 1 % brine / 1 % 0.2M sodium acetate buffer (2 x 100 ml) and then with brine (1 x 100 ml). The organic layer was dried with $MgSO_4$, and the solvent removed to give 389 mg of a white powder. This gave, not the title compound, but *N,N*-(di-*t*-butyloxycarbonyl) propane-1,3-diamine. To the aqueous layer was added 80 ml (i.e. 20 %) of 50 % saturated brine / 50 % of saturated bicarbonate solution, and organic material was extracted with $CHCl_3$ (200 ml, then 3 x 50 ml). The solvent was removed *in vacuo* from the combined $CHCl_3$ layers to give 1.175 g (6.73 mmol, 57 %) of the title product as a yellow oil identical by NMR to the literature[153,227].

R_f 0.5 [1:1 ethyl acetate – hexane; ninhydrin stain].

MS (APCI+): *m/z* = 175 (65 %, $[M + H]^+$).

ν_{max} ($CHCl_3$): 3454 (w, N-H), 3009 – 2870 (s), 1711 – 1691 (s), 1512 (s) cm^{-1}.

^1H NMR ($CDCl_3$, 300 MHz): δ 1.36 (9H, s, t-butyl), 1.54 (2H, q, *J* 6.6 Hz, H-2), 1.72 (2H, s, NH_2), 2.68 (2H, t, $J_{1,2}$ 6.5 Hz, H-1), 3.12 (2H, q, $J_{3,2}$ 6.4 Hz, H-3), 4.97 (1H, br s, NH).

3.2.3 *N*-(*t*-Butyloxycarbonyl) cystamine [14][250]

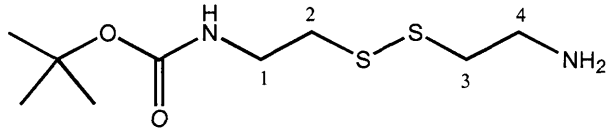

To a flask containing water (5 ml) and dioxane (4 ml) was added cystamine dihydrochloride (1.29 g, 5.7 mmol, 4 equiv.) and sodium bicarbonate (0.48 g, 5.7 mmol, 4 equiv.) with vigorous stirring. Di-*t*-butyl dicarbonate (313 mg, 1.43 mmol) was dissolved in dioxane (1 ml) and added slowly. The mixture was stirred vigorously. By 2 hours a residue had formed which was re-dissolved by the addition of MeCN (5 ml). After 4 hours the organic solvents were removed *in vacuo* to give an insoluble mixture in water. To the mixture was added a few drops of acetate buffer (0.2 M) and the solid filtered and washed several times with 10 % saturated brine and 10 % saturated bicarbonate solution (50 ml total). All organic products were removed from the filtrate by extraction with CH_2Cl_2 (4 x 50 ml) and the combined organic layers dried over $MgSO_4$. Removal of the solvent *in vacuo* gave the title compound as a viscous yellow oil (154 mg, 0.61 mmol, 43 %), similar to the literature by NMR.

R_f 0.2 [1:4 ethanol – CH_2Cl_2; ninhydrin stain].

MS (APCI+): *m/z* = 252.9 (56%, $[M + H]^+$).

Found: M+H, 253.1010. $C_9H_{20}N_2O_2S_2$ requires M+H, 253.1044 (F.A.B.).

ν_{max} ($CHCl_3$): 3454 (w), 3000 – 2900 (w), 1720 – 1680 (s), 1506 (s) cm^{-1}.

^1H NMR ($CDCl_3$, 400 MHz): δ 1.39 (9H, s, t-butyl), 1.78 (2H, s, NH_2), 2.72 (2H, t, *J* 6.2 Hz, H-2 or H-3), 2.73 (2H, t, *J* 6.3 Hz, H-2 or H-3), 2.96 (2H, t, *J* 6.1 Hz, H-1), 3.38 – 3.44 (2H, m, H-4), 5.03 (1H, br s, NH).

^{13}C NMR ($CDCl_3$, 100.6 MHz): δ 28.3, 38.4, 39.3, 40.4, 42.5, 155.7.

Missing 1 ^{13}C, may be quaternary.

3.3 Mannose Linker Conjugates

3.3.1 3'-Benzyloxycarbonylpropyl 2,3,4,6-tetra-*O*-acetyl-α-D-mannopyranoside [15]

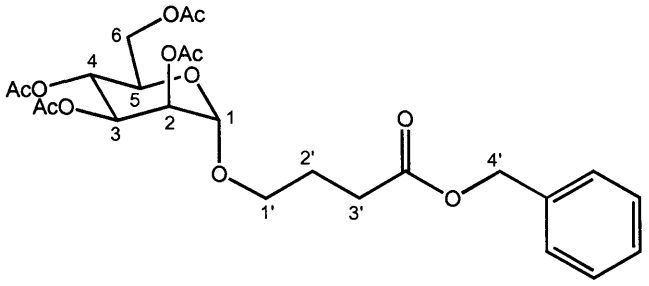

Benzyl 4-hydroxybutanoate **[12]** (2.68 g, 5.4 mmol) and 2,3,4,6-tetra-*O*-acetyl-α-D-mannopyranosyl trichloroacetimidate **[3]** (2.11 g, 10.8 mmol, 2 equiv.) were added to a flask, and azeotroped with anhydrous toluene (4 x 10 ml). Anhydrous CH_2Cl_2 (30 ml) was added and the mixture stirred vigorously and cooled to -40 °C using an MeCN / $CO_{2\ (S)}$ bath. $BF_3.Et_2O$ (1.4 ml, 10.9 mmol, 2 equiv.) was added slowly to this reaction mixture over 10 min during which time the reaction mixture turned yellow. The disappearance of the acetimidate **[3]** was monitored by t.l.c. with maximum conversion to the title product in 4 hours. The reaction mixture was washed with ice-cold 50 % sodium bicarbonate solution (3 x 60 ml) and then with ice-cold 50 % brine solution (3 x 60 ml). The organic layer was dried over $MgSO_4$ and filtered. Removal of the CH_2Cl_2

in vacuo gave 3.75 g of a yellow oil. Flash chromatography (4 cm, gradient, reverse-phase, 100 % water to 80 % MeOH / water) column fractions were pooled and the MeOH removed *in vacuo*. Addition of CH_2Cl_2 (50 ml) to extract the organic material from the aqueous layer plus a re-extraction (50 ml) turned the organic layer yellow. Drying of the organic layer over anhydrous $MgSO_4$, filtration and removal of the CH_2Cl_2 *in vacuo* gave the title product as a yellow wax (1.57 g, 3.0 mmol, 55 %).

R_f 0.35 [3:1 MeOH – water; reverse-phase plates, anisaldehyde stain and UV], acetimidate **[3]** R_f 0.45.

$[\alpha]_D^{21}$ + 38.0° (c 1, $CHCl_3$).

MS (APCI+): *m/z* = 169 (100 %), 331 (29 %), 547 (16 %, $[M + Na]^+$).

Found: M+Na, 547.1796. $C_{25}H_{32}O_{12}$ requires M+Na, 547.1792 (F.A.B.).

ν_{max} ($CHCl_3$): 3024 – 3014 (w), 1751 – 1740 (s), 1454 – 1429 (w), 1369 (m), 1240 (s) cm^{-1}.

^1H NMR (500 MHz, $CDCl_3$): δ 1.94 – 19.60 (2H, m, H-2'), 1.96 (3H, s), 2.01 (3H, s), 2.07 (3H, s), 2.13 (3H, s), 2.45 (2H, t, $J_{3',2'}$ 8.5 Hz, H-3'), 3.37 (1H, ddd, *J* 5.7, 6.6 & 9.7 Hz, H-1'), 3.72 (1H, ddd, *J* 5.7, 6.9 & 9.8 Hz, H-1'), 4.05 (1H, ddd, $J_{5,6a}$ 2.4 $J_{5,6b}$ 5.3 $J_{5,4}$ 9.6 Hz, H-5), 4.08 (1H, dd, $J_{6a,5}$ 2.4 $J_{6a,6b}$ 12.3 Hz, H-6a), 4.25 (1H, dd, $J_{6b,5}$ 5.3 $J_{6b,6a}$ 12.2 Hz, H-6b), 4.76 (1H, d, $J_{1,2}$ 1.7 Hz, H-1), 5.12 (2H, s, H-4'), 5.21 (1H, dd, $J_{2,1}$ 1.8 $J_{2,3}$ 3.3 Hz, H-2), 5.24 (1H, t, *J* 9.8 Hz, H-4), 5.29 (1H, dd, $J_{3,2}$ 3.4 $J_{3,4}$ 10.0 Hz, H-3), 7.34 (5H, s).

^{13}C NMR (100 MHz, $CDCl_3$): δ 20.58, 20.59, 20.62, 20.8, 24.5, 30.8, 62.3, 66.0, 66.3, 67.1, 68.4, 69.0, 69.4, 97.3, 128.2, 128.5, 135.8, 169.6, 169.8, 169.9, 170.5, 172.7. Missing 1 ^{13}C, possibly quaternary.

3.3.2 3'-Oxycarbonylpropyl 2,3,4,6-tetra-*O*-acetyl-α-D-mannopyranoside [16]

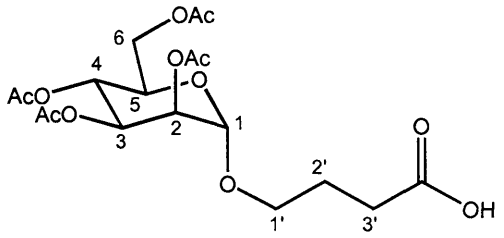

To a flask containing 3'-benzyloxycarbonylpropyl 2,3,4,6-tetra-*O*-acetyl-α-D-mannopyranoside **[15]** (1.16g, 2.2 mmol) was added anhydrous EtOH (30 ml) and 10% Pd/C (0.1g). This was hydrogenated under standard atmospheric pressure hydrogenation conditions over 4 hours in the presence of an excess of H_2 gas. Filtering of the mixture through Celite and removal of the ethanol *in vacuo* yielded the title compound as an opaque viscous yellow oil (0.82 g, 1.89 mmol, 85 %).

R_f 0.6 [1:4 ethanol – CH_2Cl_2; anisaldehyde and bromocresol green stain], compound **[15]** R_f 0.7.

$[\alpha]_D^{22}$ + 36.0° (c 1, $CHCl_3$).

MS (ES+): *m/z* = 169 (8 %), 331 (5 %), 457 (100 %, $[M + Na]^+$).

Found: M+Na, 557.1316. $C_{18}H_{26}O_{12}$ requires M+Na, 557.1322 (F.A.B.).

ν_{max} ($CHCl_3$): 3024 – 3014 (w), 1757 – 1730 (s), 1429 (w), 1369 (m), 1252 (s) cm^{-1}.

^1H NMR (300 MHz, $CDCl_3$): δ 1.94 – 2.02 (2H, m, H-2') 1.98 (3H, s), 2.03 (3H, s), 2.08 (3H, s), 2.13 (3H, s), 2.44 (2H, t, *J* 6.9 Hz, H-3'), 3.49 (1H, dt, $J_{1'a,2'}$ 5.9 $J_{1'a,1'b}$ 9.6 Hz, H-1'a), 3.68 (1H, dt, $J_{1'b,2'}$ 5.9 $J_{1'b,1'a}$ 9.6 Hz, H-1'b), 3.93 – 3.99 (1H, m, H-5), 4.07 (1H, dd, $J_{6a,5}$ 2.3 $J_{6a,6b}$ 12.2 Hz, H-6a), 4.25 (1H, dd, $J_{6b,5}$ 5.3 $J_{6b,6a}$ 12.3 Hz, H-6b), 4.79 (1H, d, $J_{1,2}$ 1.6 Hz, H-1), 5.21 (1H, dd, $J_{2,1}$ 1.6 $J_{2,3}$ 3.0 Hz, H-2), 5.25 – 5.31 (2H, m, H-3 & H-4), 7.98 (1H, br, COOH).

^{13}C NMR (100 MHz, $CDCl_3$): δ 20.6, 20.7, 20.8, 24.4, 30.7, 62.4, 66.0, 67.0, 67.2, 68.5, 69.1, 69.4, 97.5, 169.8, 170.1, 170.8, 176.7, 177.9.

3.3.3 3'-Succinimidoxycarbonylpropyl 2,3,4,6-tetra-O-acetyl-α-D-mannopyranoside [17]

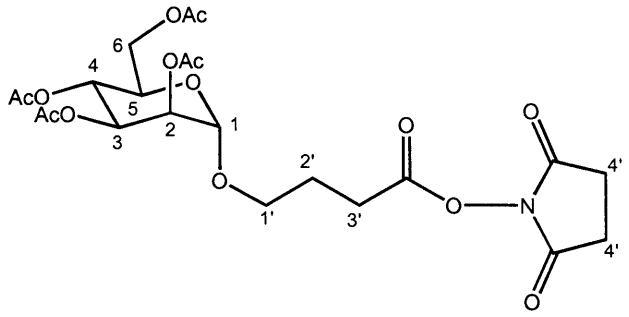

3'-Oxycarbonylpropyl 2,3,4,6-tetra-*O*-acetyl-α-D-mannopyranoside **[16]** (1.4 g, 2.7 mmol) was dissolved in anhydrous CH_2Cl_2 (30 ml), added to a flask and then cooled using an ice - water bath. To the reaction mixture was added EDCI (1 g, 5.4 mmol, 2 equiv.) and NHS (0.62 g, 5.4 mmol, 2 equiv.). The reaction was stirred overnight, allowing the flask to reach room temperature. The reaction mixture was washed with 20 % brine (3 x 50 ml), dried over Na_2SO_4, filtered and the solvent removed *in vacuo* to obtain the title compound as a pale yellow oil (1.55 g, 2.9 mmol, 107 %) with the excess in yield due to the presence of urea. This was used without further purification.

R_f 0.55 [1:4 ethanol – CH_2Cl_2; anisaldehyde, PMA and bromocresol green stain], butanoic acid **[16]** R_f 0.6.

$[\alpha]_D^{22}$ + 46.0° (c 0.5, $CHCl_3$).

MS (ES+): *m/z* = 331 (8 %), 554 (100 %, $[M + Na]^+$).

Found: M+Na, 554.1491. $C_{22}H_{29}NO_{14}$ requires M+Na, 554.1486 (F.A.B.).

ν_{max} ($CHCl_3$): 3024 – 3014 (w), 1741 (s), 1431 (w), 1369 (w), 1229 (s), 1203 (s) cm^{-1}.

^1H NMR (300 MHz, $CDCl_3$): δ 2.01 – 2.12 (2H, m, H-2') 1.97 (3H, s), 2.02 (3H, s), 2.08 (3H, s), 2.13 (3H, s), 2.73 (2H, t, $J_{3',2'}$ 7.0 Hz, H-3'), 2.80 – 2.82 (4H, m, H-4'), 3.52 (1H, dt, $J_{1'a,2'}$ 5.9 $J_{1'a,1'b}$ 10.1 Hz, H-1'a), 3.81 (1H, dt, $J_{1'b,2'}$ 6.1 $J_{1'b,1'a}$ 9.9 Hz, H-1'b), 3.92 – 3.96 (1H, m, H-5), 4.07 (1H, dd, $J_{6a,5}$ 2.4 $J_{6a,6b}$ 12.3 Hz, H-6a), 4.27 (1H, dd, $J_{6b,5}$ 5.1

$J_{6b,6a}$ 12.3 Hz, H-6b), 4.81 (1H, d, $J_{1,2}$ 1.4 Hz, H-1), 5.22 – 5.31 (3H, m, H-2, H-3 & H-4).

^{13}C NMR (100 MHz, $CDCl_3$): δ 13.9, 13.94, 20.7, 20.9, 24.5, 25.4, 30.8, 62.5, 66.0, 67.3, 68.6, 69.3, 69.4, 97.5, 169.8, 170.2, 170.3, 170.9, 172.2, 177.1. Missing 1 carbonyl, possibly overlapping for NHS.

3.3.4 *N*-(3-(2,3,4,6-Tetra-*O*-acetyl-α-D-mannopyranosyloxy)-propylcarbonyl),*N*'-(*t*-butyloxycarbonyl) propane-1,3-diamine [18]

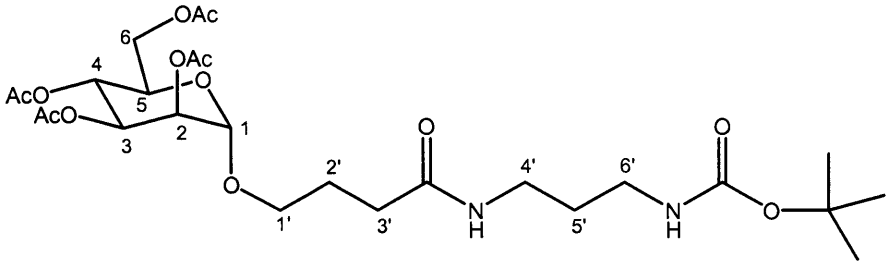

To a round-bottomed flask was added 3'-succinimidoxycarbonylpropyl 2,3,4,6-tetra-*O*-acetyl-α-D-mannopyranoside **[17]** (1 g, 1.9 mmol, 1.2 equiv.) and dissolved in anhydrous CH_2Cl_2 (10 ml). *N*-(*t*-butyloxycarbonyl) propane-1,3-diamine **[13]** (279 mg, 1.6 mmol) was dissolved into anhydrous CH_2Cl_2 (2 ml) and added to the stirred reaction mixture at r.t. A further 8 ml of anhydrous CH_2Cl_2 was added to the reaction vessel along with three drops of anhydrous TEA. The reaction was monitored by t.l.c. for the disappearance of the starting material amine (visualised by ninhydrin stain) and appearance of a spot of different R_f (visualised by PMA stain). After 2 hours, most of the amine had disappeared however the reaction was stirred continuously overnight. The reaction was washed with 20 % brine (3 x 50 ml) and the organic layer dried over $MgSO_4$. Removal of the solvent *in vacuo* gave an oil. Flash chromatography (4 cm, isocratic, ethyl acetate) gave the title compound as an oil (0.78 g, 1.31 mmol, 82 %) that crystallised in part after 16h at 4 °C.

R_f 0.35 [1:19 EtOH – CH_2Cl_2; PMA stain], compound **[17]** R_f 0.30.

$[\alpha]_D^{22}$ + 23.2° (c 2.5, $CHCl_3$).

MS (ES+): m/z = 331 (24 %), 629 (100 %, $[M + Na]^+$).

ν_{max} ($CHCl_3$): 3024 – 3014 (w), 1745 (s), 1700, 1662 (m), 1512 (m), 1440 – 1433 (br w), 1367 (w), 1230 (s) cm^{-1}.

^1H NMR (300 MHz, $CDCl_3$): δ 1.33 (9H, s), 1.52 (2H, quin, J 5.9 Hz, H-5'), 1.79 – 1.92 (2H, m, H-2') 1.89 (3H, s), 1.94 (3H, s), 2.0 (3H, s), 2.05 (3H, s), 2.20 (2H, t, $J_{3',2'}$ 7.3 Hz, H-3'), 3.05 (2H, q, J 6.1 Hz, H-4' or H-6'), 3.18 (2H, m, H-4' or H-6'), 3.39 (1H, dt, $J_{1'a,2'}$ 6.2 $J_{1'a,1'b}$ 9.8 Hz, H-1'a), 3.66 (1H, dt, $J_{1'b,2'}$ 6.0 $J_{1'b,1'a}$ 9.8 Hz, H-1'a), 3.86 – 3.91 (1H, m, H-5), 3.97 – 4.02 (1H, m, H-6a), 4.18 (1H, dd, $J_{6b,5}$ 5.2 $J_{6b,6a}$ 12.2 Hz, H-6b), 4.70 (1H, d, $J_{1,2}$ 1.4 Hz, H-1), 5.11 – 5.22 (3H, m, H-2, H-3 & H-4), 6.44 (1H, m, NH).

^{13}C NMR (100 MHz, $CDCl_3$): δ 20.7, 20.71, 20.8, 25.1, 28.3, 30.1, 32.8, 62.4, 66.1, 67.5, 68.5, 69.1, 69.5, 97.5, 169.7, 170.0, 170.1, 170.7, 172.5. Missing 2 CH_2 ^{13}C signals, possibly overlapped, 1 C=O signal and a quaternary signal.

3.3.5 *N*-(3-(2,3,4,6-Tetra-*O*-acetyl-α-D-mannopyranosyloxy)-propylcarbonyl),*N*'-(*t*-butyloxycarbonyl) cystamine [19]

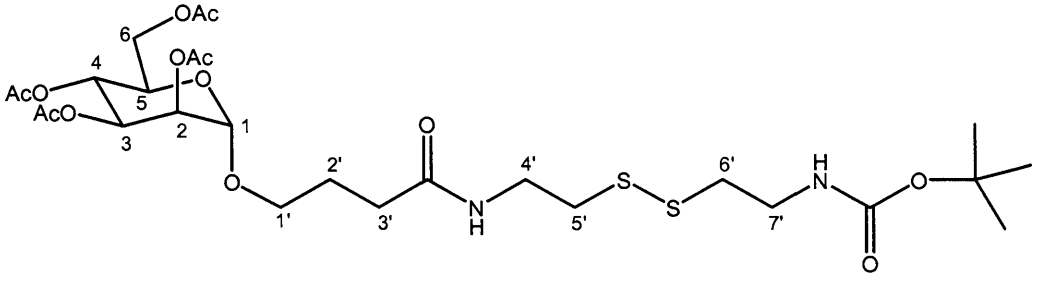

To a round-bottomed flask was added 3'-succinimidoxycarbonylpropyl 2,3,4,6-tetra-*O*-acetyl-α-D-mannopyranoside **[17]** (500 mg, 0.94 mmol, 1.7 equiv.) and dissolved into anhydrous CH_2Cl_2 (10 ml). *N*-(*t*-butyloxycarbonyl) cystamine **[14]** (140 mg, 550 μmol) was dissolved into anhydrous CH_2Cl_2 (2 ml) and added to the stirred reaction mixture while stirring at r.t. A further 8 ml of anhydrous CH_2Cl_2 was added to the reaction vessel along with three drops of anhydrous TEA to improve solubility. The reaction was monitored by t.l.c. for the disappearance of

amine starting material (visualised by ninhydrin stain) and appearance of a spot of different R_f (visualised by PMA stain). The reaction was stirred continuously overnight. The reaction was then washed with 20 % brine (3 x 50 ml) and the organic layer dried over $MgSO_4$. Removal of the solvent *in vacuo* gave an oil. Flash chromatography (4 cm, gradient, 50 % hexane / ethyl acetate to 10 % hexane / ethyl acetate, change in 10 % hexane every 50 ml) gave the title compound as an oil (244 mg, 363 μmol, 66 %).

R_f 0.3 [1:9 hexane – ethyl acetate, PMA stain], compound **[17]** R_f 0.5.

$[\alpha]_D^{23}$ + 22.4° (c 2.5, $CHCl_3$).

Found: M^+, 669.2371. $C_{27}H_{44}NO_{13}S_2$ requires M^+, 669.2363 (F.A.B.).

ν_{max} (Neat): 3400 – 3100 (s), 2980 – 2900 (s), 1760 – 1650 (s), 1550 – 1504 (m), 1435 (w), 1367 (w), 1280 – 1220 (m) cm^{-1}.

^1H NMR (400 MHz, $CDCl_3$): δ 1.38 (9H, s), 1.88 – 1.94 (2H, m, H-2') 1.94 (3H, s), 2.0 (3H, s), 2.05 (3H, s), 2.10 (3H, s), 2.27 (2H, t, $J_{3',2'}$ 7.2 Hz, H-3'), 2.73 (2H, t, *J* 6.7 Hz, H-5' or H-6'), 2.79 (2H, t, *J* 5.9 Hz, H-5' or H-6'), 3.38 (2H, q, *J* 6.4 Hz, H-4' or H-7'), 3.41 – 3.47 (1H, m, H-1'), 3.51 (2H, q, *J* 6.0 Hz, H-4' or H-7'), 3.70 (1H, dt, *J* 5.9 & 9.8 Hz, H-1'), 3.90 – 3.95 (1H, m, H-5), 4.02 – 4.07 (1H, m, H-6a), 4.27 (1H, dd, $J_{6b,5}$ 5.2 $J_{6b,6a}$ 12.2 Hz, H-6b), 4.75 (1H, d, *J* 1.5 Hz, H-1), 5.11 (1H, br, NH), 5.16 – 5.27 (3H, m, H-2, H-3 & H-4), 6.53 (1H, br, NH).

^{13}C NMR (100 MHz, $CDCl_3$): δ 20.6, 20.7, 20.8, 25.0, 28.3, 32.5, 37.7, 38.1, 38.2, 39.4, 62.4, 66.0, 67.4, 68.4, 69.0, 69.4, 97.4, 155.9, 169.6, 169.9, 170.1, 170.6, 172.4. Missing 1 C=O ^{13}C signal.

3.3.6 *N*-(3-(2,3,4,6-Tetra-*O*-acetyl-α-D-mannopyranosyloxy)-propylcarbonyl),*N*'-(trifluoroacetyl) propane-1,3-diamine [20]

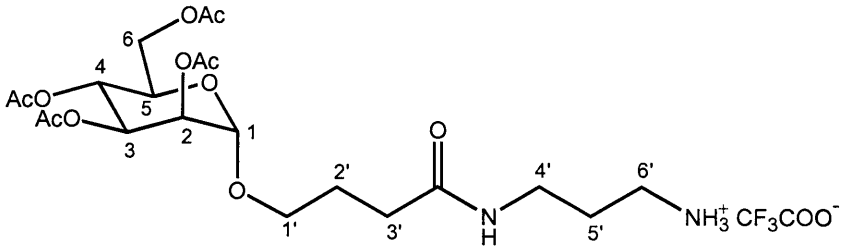

N-(3-(2,3,4,6-Tetra-*O*-acetyl-α-D-mannopyranosyloxy)propylcarbonyl), *N*'-(*t*-butyloxycarbonyl) propane-1,3-diamine **[18]** (650 mg, 1.1 mmol) was added to a flask and dissolved in anhydrous CH_2Cl_2 (20 ml). TFA (2 ml) was added slowly to the flask while stirring. After 30 mins the reaction was stopped and 10 ml of CH_2Cl_2 was added. The reaction mixture turned greenish. The solvent and TFA were removed *in vacuo* during which time the colour gradually disappeared to obtain the title compound as a viscous oil (0.7 g, 1.1 mmol, 100 %), contaminated by residual TFA and used without further purification.

MS (APCI+): *m/z* = 491.2 (100%, $[M - CF_3COO^-]^+$).

ν_{max} ($CHCl_3$): 3030 – 3018 (w), 1755 – 1742 (s), 1700 – 1660 (br m), 1530 (br w), 1437 (br w) cm^{-1}.

^1H NMR (300 MHz, $CDCl_3$): δ 1.80 – 2.00 (4H, m, H-2' & H-5') 1.98 (3H, s), 2.03 (3H, s), 2.08 (3H, s), 2.13 (3H, s), 2.31 – 2.37 (2H, m, H-3'), 3.05 (2H, m, H-4'), 3.41 – 3.49 (3H, m, H-1' & H-6'), 3.72 – 3.75 (1H, m, H-1'), 3.95 – 3.97 (1H, m, H-5), 4.10 (1H, dd, $J_{6a,5}$ 2.3 $J_{6a,6b}$ 12.2 Hz, H-6a), 4.24 (1H, dd, $J_{6b,5}$ 5.2 $J_{6b,6a}$ 12.2 Hz, H-6b), 4.77 (1H, s, H-1), 5.16 – 5.30 (3H, m, H-2, H-3 & H-4), 6.88 (1H, br, NH), 12.18 (br, 1H).

3.3.7 *N*-(3-(2,3,4,6-Tetra-*O*-acetyl-α-D-mannopyranosyloxy)-propylcarbonyl),*N*'-(trifluoroacetyl) cystamine [21]

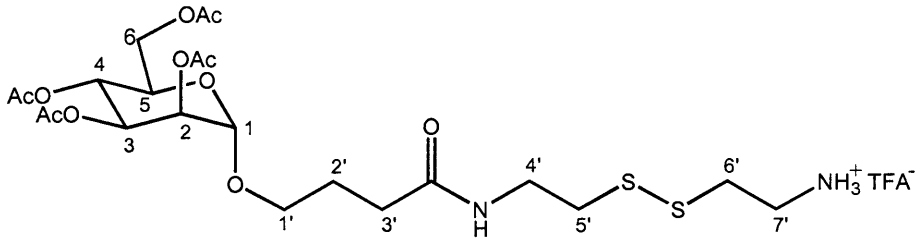

N-(3-(2,3,4,6-Tetra-*O*-acetyl-α-D-mannopyranosyloxy)propylcarbonyl), *N*'-(*t*-butyloxycarbonyl) cystamine **[19]** (183 mg, 270 μmol) was added to a flask and dissolved in anhydrous CH_2Cl_2 (5 ml). TFA (0.5 ml) was added slowly to the flask while stirring. The reaction was monitored by t.l.c. After 4 hours the solvent was removed *in vacuo* and purified by flash chromatography (4 cm, isocratic, 10 % EtOH / CH_2Cl_2) to obtain the title product as a yellow / orange oil (141 mg, 202 μmol, 75 %).

R_f 0.3 [1:9 EtOH – CH_2Cl_2; PMA stain], compound **[19]** R_f 0.7.

MS (APCI+): *m/z* = 569.3 (100%, $[M - CF_3COO^-]^+$).

ν_{max} ($CHCl_3$): 3030 – 2930 (br w), 1747 (s), 1662 (br m), 1521 (br w), 1454 – 1433 (br w), 1371 (m), 1234 (s) cm^{-1}.

^1H NMR (300 MHz, $CDCl_3$): δ 1.97 (2H, m), 2.03 (3H, s), 2.08 (3H, s), 2.13 (3H, s), 2.31 – 2.33 (2H, m), 2.79 – 2.88 (2H, m), 3.06 – 3.13 (4H, m), 3.46 – 3.62 (3H, m), 3.66 – 3.73 (1H, m), 3.96 (1H, m), 4.08 (1H, br d, *J* 12.1 Hz), 4.26 (1H, dd, *J* 4.3, 12.1 Hz), 4.78 (1H, s), 5.20 – 5.45 (3H, m), 7.01 (1H, br, NH). NMR shows the presence of *t*-butyl side product.

^{13}C NMR (75.4 MHz, $CDCl_3$): δ 18.4, 20.7, 20.78, 20.82, 26.5, 33.8, 35.6, 38.4, 39.6, 58.4, 63.7, 67.3, 68.6, 69.9, 70.8, 79.6, 99.0, 171.4, 171.6, 171.7, 172.4. Missing 1 C=O ^{13}C signal.

3.4 Pepstatin analogues, MPC1, MPC2, MPC5, MPC6

3.4.1 Pepstatin succinimide [22][153]

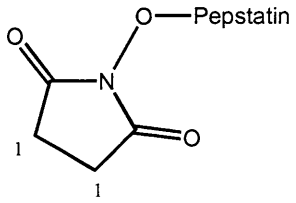

Pepstatin A (176 mg, 260 μmol), EDCI (493 mg, 2.6 mmol, 10 equiv) and NHS (296 mg, 2.6 mmol, 10 equiv) were placed in a flask. To this was added anhydrous DMF (5 ml) and the reaction stirred overnight. The DMF was removed in high *vacuo*. The solid was loosened from the vessel walls, washed with water (20ml) and collected by filtration. The solid was further washed with water (180 ml) and then with ether (50 ml). The wet solid was then dried for 24 hours under vacuum over anhydrous phosphorus pentoxide (1 g). This gave 187 mg (239 μmol, 93 %) of the title product as a white solid. Literature compound is not isolated but used *in situ*[153].

m.p.: 227 – 229 °C.

MS (APCI+): *m/z* = 215.4 (83 %), 283.4 (33 %), 511.6 (67 %), 668.7 (100 %), 783.7 (33 %, $[M + H]^+$).

Found: M+Na, 805.4194. $C_{38}H_{66}N_6O_{11}$ requires M+Na, 805.4687 (ES).

ν_{max} (KBr): 3500 – 3200 (s), 2959 – 2871 (m), 1818 (w), 1785 (w), 1740 (s), 1650 – 1617 (s), 1534 (s) cm^{-1}.

^1H NMR (DMSO, 300 MHz): δ 0.50 – 0.70 (30H, m, CH_3), 0.98 (3H, d, *J* 6.81 Hz), 0.95 – 1.25 (4H, m), 1.25 – 1.40 (2H, m), 1.70 – 1.85 (3H, m), 1.85 – 1.95 (2H, m), 2.25 – 2.33 (4H, m), 2.60 (4H, s), 3.55 – 3.77 (4H, m), 3.90 – 4.10 (3H, m), 4.58 (1H, d, *J* 4.4 Hz, OH), 5.04 (1H, d, *J* 9.6 Hz, OH), 7.42 (2H, m, NH), 7.73 (1H, d, *J* 9.6 Hz, NH), 7.78 (1H, d, *J* 9.1 Hz, NH), 7.87 (1H, d, *J* 6.7 Hz, NH).

^{13}C NMR (DMSO, 75.4 MHz): δ 18.1, 18.2, 18.3, 18.38, 18.4, 18.41, 19.28, 19.33, 21.6, 21.8, 22.3, 23.3, 23.5, 24.2, 24.8, 25.5, 25.7, 30.1,

30.2, 30.3, 44.4, 48.3, 50.5, 57.8, 169.2, 169.3, 169.7, 170.2, 170.5, 170.6, 171.6, 172.4. Missing several ^{13}C signals due to overlapping.

3.4.2 *N*-(3-(2,3,4,6-Tetra-*O*-acetyl-α-D-mannopyranosyloxy)-propylcarbonyl),*N*'-(pepstatinyl) propane-1,3-diamine [23]

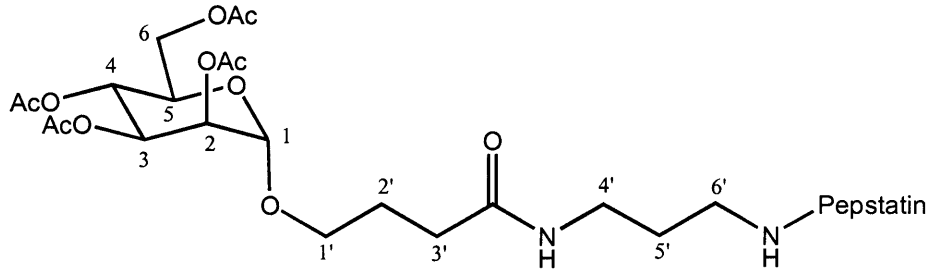

Pepstatin succinimide **[22]** (30 mg, 38 μmol, containing significant amount of pepstatin dimethylamine) and *N*-(3-(2,3,4,6-tetra-*O*-acetyl-α-D-mannopyranosyloxy)propylcarbonyl),*N*'-(trifluoroacetyl) propane-1,3-diamine **[20]** (83 mg, 137 μmol, > 5.6 equiv) were both dissolved in anhydrous DMF (1 ml), transferred to a flask and the volume of DMF increased to 5 ml. While the reaction contents were stirred, anhydrous TEA (1 ml) was added and the stirring continued overnight. The DMF and TEA were removed *in vacuo*, and the crude product dissolved in MeOH and filtered through cotton wool to remove the methanol insoluble pepstatin dimethylamine. Purification by reverse-phase preparative HPLC (gradient, 60 % MeOH / water to 95 % MeOH / water over 25 mins) gave the title product (RT 11 min). Removal of the MeOH *in vacuo*, and removal of the water by lyophilisation gave 20 mg (17.3 μmol, 45 %) of the title product as a white powder.

R_f 0.2 [1:9 MeOH – CH_2Cl_2; PMA stain].

m.p.: 120 – 130 °C, decomposes > 180 °C.

MS (APCI+): *m/z* = 169.0 (100 %), 331.2 (14 %), 810.7 (5 %, *[M – mannopyranoside]*$^+$), 1158.9 (7 % *[M + H]*$^+$).

Found: M+Na, 1180.6886. $C_{55}H_{95}N_7O_{19}$ requires M+Na, 1180.6580 (ES).

ν_{max} ($CHCl_3$): 3400 – 3200 (w, amide), 3024 – 2855 (m), 2401 (w), 1747 (s), 1647 (s), 1537 (m), 1466 – 1435 (br m), 1371 (w), 1227 – 1213 (s) cm^{-1}.

^1H NMR (CD_3OD, 500 MHz): δ 0.84 – 0.98 (30H, m, CH_3), 1.30 - 1.36 (2H, m, H-11' or H-20'), 1.37 (3H, d, $J_{16',15'}$ 7.2 Hz, H-16'), 1.54 – 1.65 (4H, m, H-12', H-21' & [H-11' or H-20']), 1.69 (2H, quin, *J* 6.8 Hz, H-5'), 1.93 – 1.95 (2H, m, H-2'), 1.95 (3H, s), 2.03 (3H, s), 2.05 (3H, s), 2.13 (3H, s), 2.02 – 2.10 (3H, m, H-25', H-29' & H-33'), 2.11 – 2.14 (2H, m, H-32'), 2.27 (2H, d, *J* 6.7 Hz, H-8' or H-17'), 2.31 (2H, t, *J* 7.4 Hz, H-3'), 2.34 – 2.36 (2H, m, H-8' or H-17'), 3.17 – 3.26 (4H, m, H-4' & H-6'), 3.51 (1H, ddd, *J* 5.9, 6.5, 9.8 Hz, H-1'), 3.75 (1H, ddd, *J* 6.0, 6.5, 9.8 Hz, H-1'), 3.90 – 3.96 (2H, m, H-10' & H-19'), 3.98 – 4.03 (3H, m, H-5, H-9' & H-18'), 4.09 (1H, dd, $J_{6a,5}$ 2.5 $J_{6a,6b}$ 12.2 Hz, H-6a), 4.13 (1H, d, *J* 7.8 Hz, H-24' or H-28'), 4.15 (1H, d, *J* 8.1 Hz, H-24' or H-28'), 4.23 – 4.28 (2H, m, H-6b & H-15'), 4.82 (1H, d, $J_{1,2}$ 1.4 Hz, H-1), 4.88 (1H, s, OH), 5.20 – 5.24 (3H, m, H-2, H-3 & H-4).

^{13}C NMR (CD_3OD, 125.7 MHz): δ 18.1 (C-16'), 18.9, 19.1, 19.9, 20.0, 20.6, 20.64, 20.7, 22.39, 22.4, 22.77, 22.8, 23.7, 23.8, 25.8 & 25.9 (C-12' & C-21'), 26.6 (C-2'), 27.5 (C-33'), 30.1 (C-5'), 31.4 & 31.5 (C-25' & C-29'), 33.7 (C-3'), 37.8 (2C, C-4' & C-6'), 41.3, 41.4, 41.6 & 42.0 (4C, C-8', C-11', C-17' & C-20'), 46.0 (C-32'), 51.4 (C-15'), 52.3 & 52.8 (C-10' & C-19'), 60.7 & 60.9 (C-24' & C-28'), 63.6 (C-6), 67.8 (C-4), 68.6 (C-1'), 69.8 (C-5), 70.7, 70.8, 71.1 & 71.5 (4C, C-2, C-3, C-9' & C-18'), 98.9 (C-1), 171.5, 171.52, 171.6, 172.4, 173.8, 173.9, 174.1, 174.2, 175.4, 175.5, 174.8.

3.4.3 *N*-(3-(2,3,4,6-Tetra-*O*-acetyl-α-D-mannopyranosyloxy)-propylcarbonyl),*N*'-(pepstatinyl) cystamine [24]

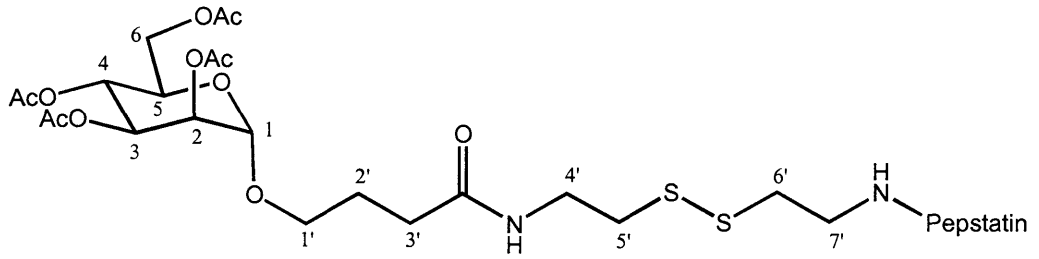

Pepstatin succinimide **[22]** (36 mg, 46 μmol, contains significant amount of pepstatin dimethylamine) and *N*-(3-(2,3,4,6-tetra-*O*-acetyl-α-D-mannopyranosyloxy)propylcarbonyl),*N*'-(trifluoroacetyl) cystamine **[21]** (33 mg, 48 μmol, > 1 equiv) were both dissolved in anhydrous DMF (1 ml), transferred to a flask and the volume of DMF increased to 4 ml. While the reaction contents were stirred, anhydrous TEA (1 ml) was added and the stirring continued for 16h. The DMF and TEA were removed *in vacuo*, and the crude product dissolved in MeOH and filtered through cotton wool to remove the MeOH insoluble pepstatin dimethylamine. Purification by reverse-phase preparative HPLC (gradient, 60 % MeOH / water to 95 % MeOH / water over 25 mins) gave the title product (RT 11 min). Removal of the MeOH *in vacuo*, and removal of the water by lyophilisation gave 28.5 mg (23 μmol, 55 %) of the title product as a white powder.

R_f 0.2 [1:9 MeOH – CH_2Cl_2; PMA stain].

m.p.: 125 – 135 °C, decomposes > 180 °C.

MS (ES+): *m/z* = 1236.6 (30 %, $[M + H]^+$), 1258.6 (100 %, $[M - H + Na]^+$).

Found: M+Na, 1258.6237. $C_{56}H_{97}N_7O_{19}S_2$ requires M+Na, 1258.6178 (ES).

ν_{max} ($CHCl_3$): 3400 – 3200 (m), 2962 – 2850 (m), 1746 (s), 1652 (s), 1540 (m), 1466 – 1438 (br m), 1370 (w), 1231 – 1225 (s) cm^{-1}.

^1H NMR (CD_3OD, 500 MHz): δ 0.87 – 0.98 (30H, m, CH_3), 1.28 - 1.35 (2H, m), 1.38 (3H, d, *J* 7.2 Hz), 1.54 – 1.64 (4H, m), 1.92 – 1.97 (2H,

m), 1.95 (3H, s), 2.03 (3H, s), 2.06 (3H, s), 2.13 (3H, s), 2.02 – 2.12 (3H, m), 2.12 – 2.14 (2H, m), 2.30 – 2.37 (6H, m), 2.82 (2H, t, *J* 6.8 Hz), 2.83 (2H, t, *J* 6.6 Hz), 3.40 – 3.55 (5H, m), 3.73 – 3.78 (1H, m), 3.90 – 4.03 (5H, m), 4.10 (1H, dd, *J* 2.6 & 12.3 Hz), 4.12 – 4.16 (2H, m), 4.23 – 4.29 (2H, m), 4.82 (1H, d, *J* 1.0 Hz), 4.89 (1H, s, OH), 5.20 – 5.26 (3H, m), 7.45 (1H, d, *J* 9.4 Hz, NH), 7.67 (1H, d, *J* 9.1 Hz, NH), 7.96 (1H, d, *J* 8.4 Hz, NH), 8.01 (1H, d, *J* 7.9 Hz, NH), 8.06 (1H, t, *J* 5.6 Hz, NH), 8.17 (1H, t, *J* 5.6 Hz, NH), 8.20 (1H, d, *J* 5.7 Hz, NH).

^{13}C NMR (CD_3OD, 125.7 MHz): δ 18.1, 18.9, 19.1, 20.0, 20.1, 20.6, 20.64, 20.66, 20.7, 22.4, 22.7, 22.8, 23.7, 23.8, 25.85, 25.9, 26.5, 27.5, 31.4, 31.5, 33.6, 38.3, 38.6, 39.6, 39.7, 41.3, 41.4, 41.6, 41.9, 46.0, 51.4, 52.3, 52.7, 60.8, 60.9, 63.6, 67.3, 68.5, 69.8, 70.7, 70.8, 71.1, 71.5, 98.9, 171.5, 171.55, 171.6, 172.4, 173.7, 173.9, 174.1, 174.2, 175.4, 175.6, 175.8. Missing 1 pepstatin CH_3, overlapped at 22.4 ppm.

3.4.4 *N*-(3-(α-D-Mannopyranosyloxy)propylcarbonyl),*N*'-(pepstatinyl) propane-1,3,-diamine (MPC1) [25]

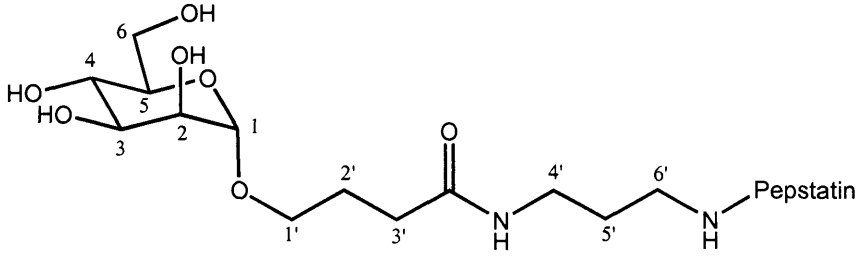

N-(3-(2,3,4,6-Tetra-*O*-acetyl-α-D-mannopyranosyloxy)propylcarbonyl), *N*'-(pepstatinyl) propane-1,3-diamine **[23]** (20 mg, 17.3 μmol), was dissolved in MeOH (5 ml) in a 25 ml round-bottomed flask and stirred. To this was added LiOH (1M, aq) solution drop wise until the reaction mixture was pH 11. Stirring was continued for 6 hours before removal of the solvents *in vacuo*. The crude product was purified by reverse-phase preparative HPLC (gradient, 20 % MeCN / water to 60 % MeCN / water over 25 mins, RT = 13 mins). Removal of the MeCN *in vacuo* and lyophilisation gave the title product as a white powder (12 mg, 70 %, 12 μmol).

m.p.: 120 – 130 °C, decomposes > 180 °C.

MS (ES+): *m/z* = 828.6 (32 %, *[M – mannopyranoside]*$^+$), 990.7 (100 %, *[M + H]*$^+$), 1012.8 (44 %, *[M + Na]*$^+$).

Found: M+Na, 1012.6140. $C_{47}H_{87}N_7O_{15}$ requires M+Na, 1012.6157 (ES).

ν_{max} (KBr): 3400 – 3200 (br s), 2960 – 2880 (s), 2500 – 2380 (w), 1685 – 1632 (s), 1560 – 1542 (m), 1468 – 1437 (m), 1206 – 1187 (s), 1138 (s) cm^{-1}.

^{1}H NMR (CD_3OD, 400 MHz): δ 0.86 – 0.99 (30H, m, CH_3), 1.28 – 1.34 (2H, m), 1.38 (3H, d, *J* 7.2 Hz), 1.53 – 1.64 (4H, m), 1.68 (2H, m), 1.85 – 1.92 (2H, m), 2.02 – 2.10 (3H, m), 2.12 (2H, d, *J* 6.5 Hz), 2.26 – 2.36 (6H, m), 3.20 – 3.23 (4H, m), 3.42 – 3.52 (2H, m), 3.59 (1H, t, *J* 9.5 Hz), 3.66 – 3.75 (3H, m), 3.78 (1H, dd, *J* 1.7 & 3.3 Hz), 3.82 (1H, dd, *J* 2.2 & 11.7 Hz), 3.93 – 4.03 (4H, m), 4.11 – 4.15 (2H, m), 4.26 (1H, q, *J* 7.1 Hz), 4.72 (1H, d, *J* 1.5 Hz), 4.85 (1H, s, OH), 7.47 (1H, d, *J* 9.4 Hz, NH), 7.70 (1H, d, *J* 9.3 Hz, NH), 7.99 (2H, m, NH).

^{13}C NMR (CD_3OD, 125.7 MHz): δ 18.1, 18.9, 19.2, 20.0, 20.1, 22.4, 22.5, 22.8, 22.9, 23.8, 23.9, 25.9, 26.0, 26.9, 27.5, 30.1, 31.5, 31.6, 34.0, 37.9, 41.3, 41.5, 41.7, 42.0, 46.0, 51.4, 52.4, 52.8, 60.8, 60.9, 63.0, 67.8, 68.7, 71.2, 71.5, 72.2, 72.7, 74.7, 101.7, 173.8, 174.0, 174.1, 174.2, 175.5, 175.7, 175.8. Missing 1 ^{13}C, overlapped at 37.9 ppm.

3.4.5 *N*-(3-(α-D-Mannopyranosyloxy)propylcarbonyl),*N*'-(pepstatinyl) cystamine (MPC2) [26]

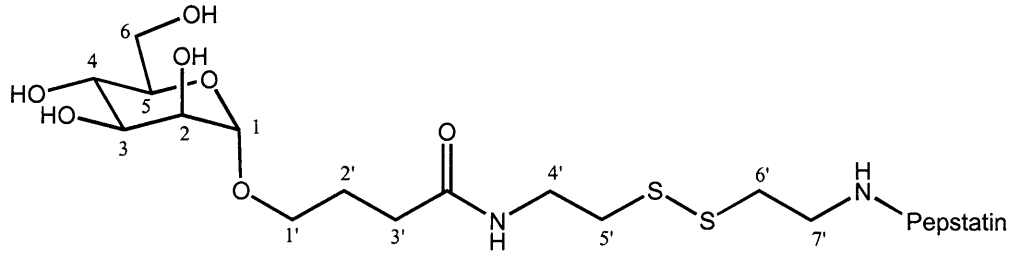

N-(3-(2,3,4,6-Tetra-*O*-acetyl-α-D-mannopyranosyloxy)propylcarbonyl), *N*'-(pepstatinyl) cystamine **[24]** (25 mg, 20.2 μmol), was dissolved in MeOH (5 ml) in a 25 ml round-bottomed flask and stirred. To this was

added LiOH (1M, aq) solution drop wise until the reaction mixture reached pH 11. Stirring was continued for 6 hours before removal of the solvents *in vacuo*. The crude product was purified by reverse-phase preparative HPLC (gradient, 20 % MeCN / water to 60 % MeCN / water over 25 mins, RT = 12.8 mins). Removal of the MeCN *in vacuo* and lyophilisation gave the title product as a white powder (14.3 mg, 13.4 μmol, 66 %).

m.p.: 135 – 145 °C, decomposes > 180 °C.
MS (ES+): *m/z* = 283.2 (38 %), 906.5 (22 %, *[M – mannopyranoside]*$^+$), 1068.4 (20 %, *[M + H]*$^+$).
Found: M+Na, 1090.5787. $C_{48}H_{89}N_7O_{15}S_2$ requires M+Na, 1090.5755 (ES).
ν_{max} (KBr): 3600 – 3200 (br s), 2965 – 2930 (w), 1690 – 1630 (s), 1565 – 1534 (m), 1455 – 1430 (m), 1208 (s), 1146 (s) cm^{-1}.
^{1}H NMR (CD_3OD, 500 MHz): δ 0.87 – 0.99 (30H, m, CH_3), 1.28 – 1.36 (2H, m, H-11' or H-20'), 1.39 (3H, d, $J_{16',15'}$ 8.0 Hz, H-16'), 1.58 – 1.63 (4H, m, H-11', H-12', H-20' & H-21'), 1.85 – 1.92 (2H, m, H-2'), 2.04 – 2.11 (3H, m, H-25', H-29' & H-33'), 2.14 (2H, d, $J_{32',33'}$ 6.7 Hz, H-32'), 2.29 – 2.38 (6H, m, H-3', H-8' & H-17'), 2.83 (4H, t, *J* 6.7 Hz, H-5' & H-6'), 3.47 – 3.53 (6H, m, H-5, H-1', H-4' & H-7'), 3.61 (1H, t, *J* 9.6 Hz, H-4), 3.64 – 3.72 (3H, m, H-3, H-6b & H-1'), 3.79 (1H, dd, *J* 1.7 & 3.3 Hz, H-2), 3.88 (1H, dd, $J_{6a,5}$ 2.5 $J_{6a,6b}$ 11.5 Hz, H-6a), 3.94 – 4.02 (4H, m, H-9', H-10', H-18' & H-19'), 4.12 – 4.17 (2H, m, H-24' & H-28'), 4.27 (1H, m, H-15'), 4.74 (1H, d, $J_{1,2}$ 1.7 Hz, H-1), 4.92 (1H, s, OH).
^{13}C NMR (CD_3OD, 125.7 MHz): δ 18.1, 19.0, 19.2, 20.0, 20.1, 22.5, 22.8, 22.9, 23.8, 23.9, 25.9, 26.0, 26.9, 27.5, 31.5, 31.6, 33.9, 38.4, 38.6, 39.7, 39.74, 41.3, 41.4, 41.6, 42.0, 46.0, 51.4, 52.4, 52.8, 60.9, 61.0, 63.0, 67.8, 68.7, 71.1, 71.5, 72.2, 72.7, 74.7, 101.6, 173.9, 174.0, 174.1, 174.2, 175.5, 175.9, 180.9. Missing 1 pepstatin CH_3, overlapped at 22.4 ppm.

3.4.6 *N*-(*t*-Butyloxycarbonyl),*N*'-(pepstatinyl) propane-1,3-diamine [27][153]

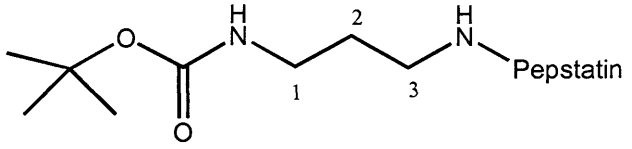

N-(*t*-Butyloxycarbonyl) propane-1,3-diamine **[13]** (111 mg, 640 μmol, 10 equiv), pepstatin succinimide **[22]** (50 mg, 64 μmol) and anhydrous DMF (6 ml) were added to a round-bottomed flask and stirred continuously for 2 days. The solvent was removed *in vacuo* and the crude product purified by flash chromatography (1 cm^3, isocratic, 10 % MeOH/CH_2Cl_2). T.l.c. visualisation was possible by using either permanganate solution or by dipping in TFA and leaving for ~5 mins (to remove the Boc group), heating to remove the TFA and then staining with ninhydrin. The column fractions collected with R_f 0.5 were pooled and the solvent removed *in vacuo* to give an off-white solid. This was re-crystallised from $CHCl_3$/cyclohexane to obtain a white powder (48 mg, 57 μmol, 89 %).

R_f 0.5 [1:9 MeOH – $CHCl_3$; TFA treatment, then ninhydrin stain].
m.p.: 219 – 221 °C (lit. ref. 215 – 217 °C)[153].
MS (ES+): *m/z* = 842.6 (100 %, $[M + H]^+$), 864.6 (27 %, $[M + Na]^+$).
Found: M+Na, 864.5785. $C_{42}H_{79}N_7O_{10}$ requires M+Na, 864.5786 (ES).
ν_{max} (KBr): 3400 – 3200 (s, amide), 2960 – 2872 (s), 2360 – 2331 (m), 1652 – 1634 (s), 1533 (m), 1465 – 1437 (m), 1171 (m) cm^{-1}.
^1H NMR (DMSO, 500 MHz): δ 0.77 – 0.85 (30H, m, CH_3), 1.18 (3H, d, *J* 7.1 Hz), 1.21 – 1.26 (2H, m), 1.33 – 1.37 (2H, m), 1.36 (9H, s), 1.46 – 1.52 (2H, m), 1.92 – 1.98 (3H, m), 2.00 – 2.05 (4H, m), 2.11 (2H, d, *J* 6.2 Hz), 2.90 (2H, q, *J* 6.4 Hz), 2.97 – 3.05 (2H, m), 3.27 – 3.34 (2H, m), 3.75 – 3.83 (4H, m), 4.11 (1H, dd, *J* 7.2 & 8.9 Hz), 4.17 (1H, dd, *J* 7.4 & 8.7 Hz), 4.24 (1H, quin, *J* 7.2 Hz), 4.82 (1H, d, *J* 4.8 Hz, OH), 4.83 (1H, d, *J* 4.9 Hz, OH), 7.30 (1H, d, *J* 9.2 Hz, NH), 7.43 (1H, d, *J*

8.8 Hz, NH), 7.75 (1H, d, *J* 8.9 Hz, NH), 7.79 (1H, d, *J* 8.8 Hz, NH), 7.89 (1H, d, *J* 7.4 Hz, NH). NMR data not quoted in the literature[153].

^{13}C NMR (DMSO, 125.7 MHz): δ 18.1, 18.2, 19.2, 19.3, 21.6, 21.9, 22.2, 23.2, 23.4, 24.1, 25.6, 28.2, 30.0, 30.3, 36.1, 37.5, 38.6, 39.6, 39.8, 39.9, 40.1, 40.2, 44.4, 48.3, 50.4, 50.7, 54.8, 57.8, 58.0, 69.0, 69.1, 77.4, 155.5, 170.6, 170.7, 170.78, 170.8, 171.1, 171.5, 172.1.

3.4.7 *N*-(*t*-Butyloxycarbonyl),*N*'-(pepstatinyl) cystamine [28]

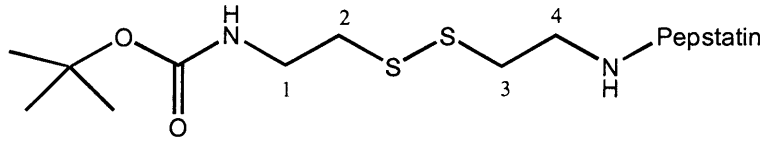

N-(*t*-Butyloxycarbonyl) cystamine **[14]** (161 mg, 640 μmol, 10 equiv), pepstatin succinimide **[22]** (50 mg, 64 μmol) and anhydrous DMF (6 ml) was added to a round-bottomed flask and stirred continuously for 2 days. The solvent was removed *in vacuo*. Purification by flash chromatography (1 cm^3, isocratic, 10 % MeOH/CH_2Cl_2, R_f 0.55) gave a white powder from the pooled fractions, which was re-crystallised from hot EtOH to obtain a white solid (47 mg, 64 μmol, 80 %).

R_f 0.5 [1:9 MeOH – $CHCl_3$; TFA treatment, then ninhydrin stain].

m.p.: 244 – 246 °C.

MS (ES+): *m/z* = 920.6 (100 %, $[M + H]^+$), 942.6 (53 %, $[M - H + Na]^+$).

Found: M+Na, 942.5378. $C_{43}H_{81}N_7O_{10}S_2$ requires M+Na, 942.5384 (ES).

ν_{max} (KBr): 3600 – 3100 (s), 2959 – 2871 (s), 1635 (s), 1534 (s), 1466 – 1437 (m), 1171 (m) cm^{-1}.

^{1}H NMR (DMSO, 500 MHz): δ 0.77 – 0.85 (30H, m, CH_3), 1.18 (3H, d, $J_{16',15'}$ 7.1 Hz, H-16'), 1.20 – 1.26 (2H, m, H-11' or H-20'), 1.33 – 1.38 (2H, m, H-12' & H-21'), 1.36 (9H, s, *t*-butyl), 1.48 – 1.52 (2H, m, H-11' or H-20'), 1.90 – 1.99 (3H, m, H-25', H-29' & H-33'), 2.00 – 2.08 (4H, m, H-32' & [H-8' or H-17']), 2.11 (2H, d, *J* 6.2 Hz, H-8' or H-17'), 2.72 (2H, t, *J* 6.5 Hz, H-2 or H-3), 2.73 (2H, t, *J* 6.5 Hz, H-2 or H-3), 3.16 –

3.20 (2H, m, H-1 or H-4), 3.25 – 3.31 (2H, m, H-1 or H-4), 3.74 – 3.81 (4H, m, H-9', H-10', H-18' & H-19'), 4.11 (1H, d, *J* 7.2 Hz, H-24' or H-28'), 4.11 (1H, d, *J* 7.3 Hz, H-24' or H-28'), 4.23 (1H, q, $J_{15',16'}$ 7.0 Hz, H-15'), 4.82 (1H, d, *J* 5.3 Hz, OH), 4.83 (1H, d, *J* 5.2 Hz, OH), 7.32 (1H, d, *J* 9.2 Hz, NH), 7.45 (1H, d, *J* 8.8 Hz, NH), 7.77 (1H, d, *J* 9.0 Hz, NH), 7.81 (1H, d, *J* 8.8 Hz, NH), 7.91 (1H, d, *J* 7.4 Hz, NH).

^{13}C NMR (DMSO, 125.7 MHz): δ 18.2, 18.3, 19.2, 19.3, 21.6, 21.9, 22.2, 23.3, 23.5, 24.2, 25.7 (C-33'), 28.2 (*t*-butyl), 30.1 & 30.3 (C-25' & C-29'), 37.1, 37.6, 37.9, 38.0, 38.6, 39.7, 39.8, 40.0, 40.1, 40.2, 44.3, 48.3 (C-15'), 50.4, 50.7, 57.7 & 57.9 (C-24' & C-28'), 69.0, 69.1, 77.8, 155.5, 170.7, 170.8, 170.9, 171.0, 171.02, 171.6, 172.2.

3.4.8 *N*-(Pepstatinyl) propane-1,3-diamine [29][153]

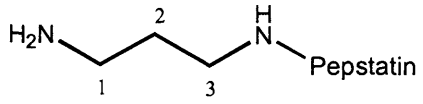

To a flask containing *N*-(*t*-butyloxycarbonyl),*N'*-(pepstatinyl) propane1,3-diamine **[27]** (75 mg, 89 μmol) was added TFA (4 ml), water (125 μl, 6.9 μmol), triethylsilane (125 μl, 0.77 μmol), thioanisole (250 μl, 2.1 μmol) and phenol (250 μl, 2.8 μmol) and stirred vigorously for 4 hours. The TFA was removed *in vacuo*, and the resulting solid purified by preparative HPLC (50 % MeOH / water to 100 % MeOH over 25 mins) to give the major product with RT = 14-15 mins (60 mg, 81 μmol, 91 %) as a white powder.

Other fractions (RT 12 mins and 16 mins) showed the presence of the title product but were impure.

R_f 0.2 [1:9 MeOH – $CHCl_3$; ninhydrin stain].

m.p.: 214 – 216 °C (lit. ref. 207 – 210 °C)[153].

MS (ES+): *m/z* = 742.6 (100 %, $[M + H]^+$).

Found: M+H, 742.5440. $C_{37}H_{71}N_7O_8$ requires M+H, 742.5442 (ES).

ν_{max} (KBr): 3500 – 3200 (s), 3079 (w), 2960 – 2872 (s), 2416 (w), 1700 – 1600 (s), 1537 (s), 1467 – 1417 (m), 1204 – 1138 (m) cm^{-1}.

^{1}H NMR (CD_3OD, 500 MHz): δ 0.86 – 0.98 (30H, m, CH_3), 1.27 – 1.35 (2H, m, H-11' or H-20'), 1.39 (3H, d, $J_{16',15'}$ 7.3 Hz, H-16'), 1.55 – 1.64 (4H, m, H-12', H-21' & [H-11' or H-20']), 1.84 (2H, quin, J 7.0 Hz, H-2), 2.02 – 2.10 (3H, m, H-25', H-29' & H-33'), 2.14 (2H, d, J 6.8 Hz, H-32'), 2.30 – 2.38 (4H, m, H-8' & H-17'), 2.98 (2H, t, $J_{3,2}$ 7.1 Hz, H-3), 3.20 – 3.25 & 3.32 – 3.36 (2H, m, H-1), 3.92 – 3.97 (2H, m, H-10' & H-19'), 3.99 – 4.03 (2H, m, H-9' & H-18'), 4.10 – 4.14 (2H, m, H-24' & H-28'), 4.21 (1H, q, $J_{15',16'}$ 7.2 Hz, H-15'), 4.97 (1H, s, OH). NMR data not quoted in the literature[153].

^{13}C NMR (CD_3OD, 125.7 MHz): δ 18.0 (C-16'), 18.9, 19.2, 19.9, 20.0, 22.3, 22.4, 22.7, 22.8, 23.7 & 23.8 (10C, CH_3), 25.8 & 25.9 (C-12' & C-21'), 27.4 (C-33'), 28.7 (C-2), 31.3 & 31.4 (C-25' & C-29'), 36.8 (C-3), 38.2 (C-1), 41.2, 41.3 & 41.6 (C-8', C-11', C-17' & C-20'), 46.0 (C-32'), 51.6 (C-15'), 51.9 & 52.7 (C-10' & C-19'), 61.0 (C-24' & C-28'), 71.0 & 71.3 (C-9' & C-18'), 173.9, 174.1, 174.3, 174.5, 175.5, 175.9. Missing 2 ^{13}C signals, overlapped at 41.6 & 61.0 ppm.

3.4.9 *N*-(Pepstatinyl) cystamine [30][157]

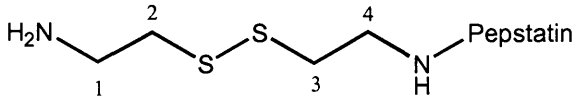

To a flask containing *N*-(*t*-butyloxycarbonyl),*N'*-(pepstatinyl) cystamine **[28]** (65 mg, 70 μmol) was added TFA (4 ml), water (125 μl, 6.9 μmol), triethylsilane (125 μl, 0.77 μmol), thioanisole (250 μl, 2.1 μmol) and phenol (250 μl, 2.8 μmol) and stirred vigorously for 4 hours. The TFA was removed *in vacuo*, and purified by preparative HPLC (40 % MeCN / water to 80 % MeCN over 30 mins) to obtain a major product with RT = 5 mins (37 mg, 45 μmol, 64 %) as a white powder. Other fractions (RT 12 mins and 16 mins) showed the presence of product but were impure. Literature does not quote any analytical data for comparision[157].

R_f 0.2 [1:9 MeOH – $CHCl_3$; ninhydrin stain].

m.p.: 219 – 221 °C.

MS (ES+): m/z = 820.5 (100 %, $[M + H]^+$).

Found: M+H, 820.5039. $C_{38}H_{73}N_7O_8S_2$ requires M+H, 820.5040 (ES).

ν_{max} (KBr): 3500 – 3200 (s), 2960 – 2872 (m), 1700 – 1600 (s), 1540 (s), 1470 – 1419 (w), 1203 – 1138 (m) cm^{-1}.

^1H NMR (CD_3OD, 400 MHz): δ 0.86 – 0.98 (30H, m, CH_3), 1.27 – 1.35 (2H, m), 1.38 (3H, d, *J* 7.3 Hz), 1.55 – 1.63 (4H, m), 2.02 – 2.10 (3H, m), 2.13 (2H, d, *J* 6.5 Hz), 2.28 – 2.38 (4H, m), 2.87 (2H, t, *J* 6.7 Hz), 2.97 (2H, t, *J* 6.8 Hz), 3.24 – 3.32 (2H, m), 3.42 – 3.62 (2H, m), 3.91 – 4.04 (4H, m), 4.10 – 4.17 (2H, m), 4.23 (1H, q, *J* 7.3 Hz), 4.93 (1H, s, OH), 7.47 (1H, d, *J* 9.4 Hz, NH), 7.63 (1H, d, *J* 9.7 Hz, NH), 7.67 (1H, d, *J* 9.1 Hz, NH), 7.97 (1H, d, *J* 8.3 Hz, NH), 8.05 (1H, d, *J* 7.6 Hz, NH), 7.6 (1H, s, NH).

^{13}C NMR (CD_3OD, 100.6 MHz): δ 18.0, 18.9, 19.2, 20.0, 20.1, 22.4, 22.7, 22.8, 23.7, 23.8, 25.8, 25.9, 27.5, 31.3, 31.5, 35.6, 38.3, 39.4, 39.5, 41.2, 41.3, 41.6, 41.9, 46.0, 51.5, 52.2, 52.7, 60.9, 71.0, 71.5, 173.8, 173.9, 174.2, 174.3, 175.5, 175.9. Missing 2 ^{13}C signals, overlapped at 22.4 & 60.9 ppm.

3.4.10 *N*-(Iodoacetyl),*N*'-(pepstatinyl) propane-1,3-diamine [31]

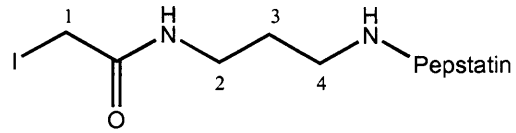

To a flask was added *N*-(pepstatinyl) propane-1,3-diamine **[29]** (10 mg, 13.5 μmol). Any water present was removed by azeotroping with anhydrous MeCN (3 x 1 ml). The amine was dissolved in anhydrous DMF (3 ml) and stirred while adding iodoacetic anhydride (5.3 mg, 15 μmol, 1.1 equiv). The flask was covered with aluminium foil to exclude all light and the reaction stirred continuously for 2 hours. The DMF was removed *in vacuo* and the crude product stored overnight in a fridge. The next day the flask contents were washed with water containing 1% v/v saturated bicarbonate solution and 10 % v/v saturated potassium iodide (KI) solution (to stop the possibility of iodine exchange). The product

precipitated and was filtered through cotton wool. The solid product was washed again with the aqueous KI/bicarbonate solution (40 ml) and once with water before being dissolved in EtOH and eluted into a round-bottomed flask (in an alternative method ethyl acetate was used to both crystallise and wash the crude product). Removal of the EtOH *in vacuo* gave the title compound as a white powder (6mg, 6.6 μmol, 49 %), which was stored in a fridge under argon and used in the next reaction as soon as possible.

m.p.: 189 – 191 °C.

MS (ES+): m/z = 932.3 (83 %, $[M + Na]^+$).

Found: M+Na, 932.4311. $C_{39}H_{72}IN_7O_9$ requires M+Na, 932.4334 (ES).

ν_{max} (KBr): 3500 – 3150 (s), 3079 (w), 2959 – 2871 (m), 1700 – 1635 (s), 1550 – 1507 (s) cm^{-1}.

^1H NMR (CD_3OD, 500 MHz): δ 0.86 – 0.98 (30H, m, CH_3), 1.32 – 1.39 (2H, m), 1.38 (3H, d, *J* 7.2 Hz), 1.54 – 1.65 (4H, m), 1.70 (2H, quin, *J* 6.8 Hz), 2.02 – 2.10 (3H, m), 2.13 (2H, d, *J* 6.7 Hz), 2.27 (2H, d, *J* 6.7 Hz), 2.34 – 2.37 (2H, m), 3.20 – 3.34 (4H, m), 3.69 (2H, s), 3.93 – 4.01 (4H, m), 4.13 (1H, d, *J* 7.9 Hz), 4.15 (1H, d, *J* 8.1 Hz), 4.26 (1H, q, *J* 7.3 Hz), 4.89 (1H, s, OH), 7.32 (1H, d, *J* 9.3 Hz, NH), 7.45 (1H, s, NH), 7.68 (1H, d, *J* 9.0 Hz, NH), 7.89 (1H, s, NH).

^{13}C NMR (CD_3OD, 125.7 MHz): δ -2.0 (CH_2-I), 18.1, 18.9, 19.1, 20.0, 20.1, 22.4, 22.7, 22.8, 23.7, 23.8, 25.8, 25.9, 27.5, 29.8, 31.4, 31.5, 37.8, 38.4, 41.3, 41.4, 41.7, 42.0, 46.0, 51.4, 52.3, 52.8, 60.7, 60.9, 71.1, 71.4, 171.4, 173.8, 173.9, 174.1, 174.2, 175.4, 175.8. Missing 1 pepstatin CH_3, overlapped at 22.4 ppm.

3.4.11 *N*-(Iodoacetyl),*N*'-(pepstatinyl) cystamine [32]

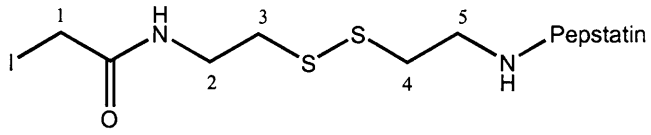

To a flask was added *N*-(pepstatinyl) cystamine **[29]** (7 mg, 8.3 μmol). Any water present was removed by azeotroping with anhydrous MeCN (3 x 1 ml). The amine was dissolved in anhydrous DMF (3 ml) and stirred while adding iodoacetic anhydride (3.3 mg, 9.4 μmol, 1.1 equiv). The flask was covered with aluminium foil to exclude all light and the reaction stirred continuously for 2 hours. The DMF was removed *in vacuo* and the crude product stored overnight in a fridge. The next day the flask contents were washed with water containing 1% v/v saturated bicarbonate solution and 10 % v/v saturated potassium iodide (KI) solution. The product precipitated and was filtered through cotton wool. The solid product was washed again with the aqueous KI/bicarbonate solution (40 ml) and once with water before being dissolved in EtOH and eluted into a round-bottomed flask (in an alternative method ethyl acetate was used to both crystallise and wash the crude product). Removal of the EtOH *in vacuo* gave the title compound as a white powder (6mg, 6.1 μmol, 83 %), which was stored in a fridge under argon and used in the next reaction as soon as possible.

m.p.: 198 – 201 °C.

MS (ES+): *m/z* = 988.2 (56 %, $[M + H]^+$), 1010.3 (100 %, $[M - H + Na]^+$).

ν_{max} (KBr): 3600 – 3100 (m), 2959 – 2871 (m), 1700 – 1617 (m), 1540 (w), 1067 (s) cm^{-1}.

^1H NMR (CD_3OD, 500 MHz): δ 0.87 – 0.99 (30H, m, CH_3), 1.28 – 1.36 (2H, m), 1.38 (3H, d, *J* 7.3 Hz), 1.57 – 1.62 (4H, m), 2.03 – 2.11 (3H, m), 2.13 (2H, d, *J* 6.7 Hz), 2.28 (2H, d, *J* 6.7 Hz), 2.34 – 2.37 (2H, m), 2.83 (4H, t, *J* 6.6 Hz), 3.43 – 3.61 (4H, m), 3.71 (2H, s), 3.91 – 4.04 (4H, m), 4.12 (1H, d, *J* 7.8 Hz), 4.15 (1H, d, *J* 8.0 Hz), 4.26 (1H, q, *J* 9.3

Hz), 4.89 (1H, s, OH), 7.43 (1H, s, NH), 7.45 (1H, s, NH), 7.68 (1H, d, *J* 9.0 Hz, NH).

^{13}C NMR (CD_3OD, 125.7 MHz): δ -2.1 (CH_2-I), 18.1, 18.9, 19.1, 20.0, 20.1, 22.4, 22.7, 22.8, 23.7, 23.8, 25.8, 25.9, 27.5, 31.4, 31.6, 38.2, 38.3, 39.7, 40.1, 41.3, 41.4, 41.7, 42.0, 46.0, 51.4, 52.3, 52.8, 60.8, 60.9, 71.1, 71.4, 173.8, 173.9, 174.1, 174.2, 175.4, 175.5, 175.8. Missing 1 pepstatin CH_3, overlapped at 22.4 ppm.

3.4.12 BSA – poly(mannose) conjugate [33]

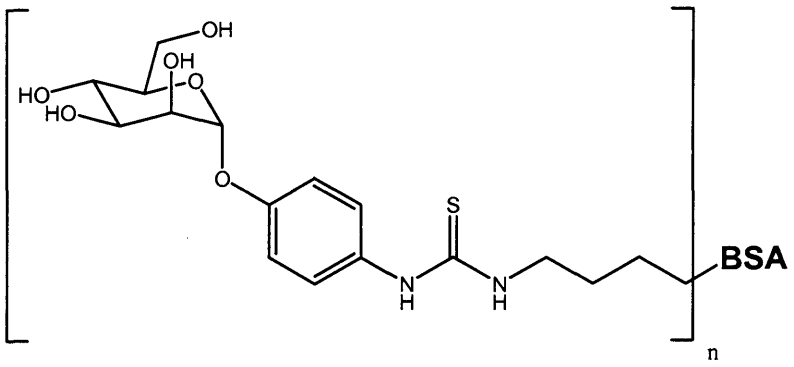

4-Isothiocyanatophenyl α-D-mannopyranoside **[11]** (43 mg, 0.14 mmol, approx. 60 equiv) and bovine serum albumin (153 mg, ~ 2.3 μmol, supplied by Sigma Aldrich) were dissolved in NaCl solution (0.15 M, 10 ml) in a 50 ml round-bottomed flask and stirred vigorously. The pH was adjusted to pH 9 (with the addition of 0.1M NaOH) and the reaction stirred continuously for 6 hours, maintaining the same pH by addition of NaOH. After this time the reaction mixture was stored overnight in a fridge. Next day the pH was adjusted to pH 7 and the reaction mixture dialysed with 0.15M NaCl solution (1L) for three days, changing the solution twice a day and stirring the dialysis solution continuously within a fridge. The dialysis tubing contents were further purified and de-salted using centrifugal filtration devices (Millipore) spun within a fixed 35° angle centrifuge at a relative centrifugal force (rcf) of 3000 for 90 mins, 21 °C (maximum 4 ml solution per device) before re-suspending the gelatinous product at the bottom of the device with water (4 ml).

This was repeated three times to maximise purification. Lyophilisation gave 126 mg (74 %) of a fine white powder.

m.p.: > 260 °C (decomposes).
MS (MALDI-TOF): MS peak range = 67,000 – 79,000. Top of peak for BSA ~ 66,430. Compound (35) ~ 74,032.
Difference = 7602, ∴~ 24.3 sugar units / BSA molecule.
Biochemical analysis: Analysis of free TNBS reactive amino groups[228] shows an approximate conjugation of 23 sugar units. Analysis of attached sugar units[229,230] shows an approximate conjugation of 22.5 sugar units.

3.4.13 Poly(mannosyl) BSA – pepstatin propane-1,3-diamine conjugate (MPC5) [34]

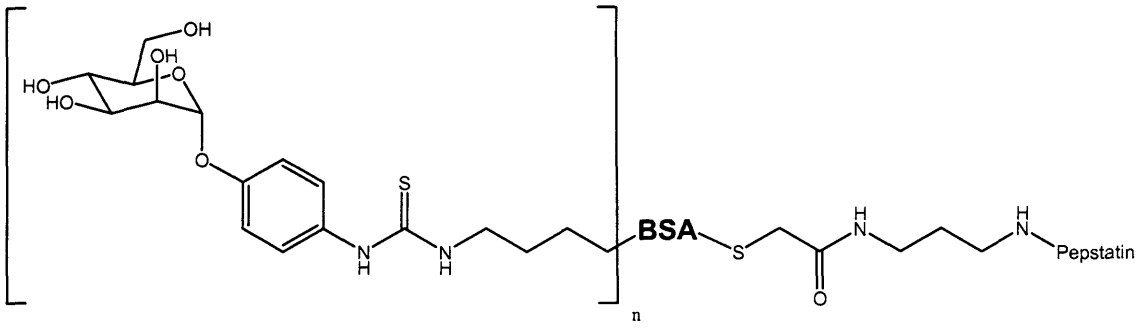

BSA – poly(mannose) conjugate **[33]** (30 mg, ~ 3.8 x 10^{-7} moles) was placed in a 25 ml round-bottomed flask and dissolved in 2 ml of phosphate buffer saline (PBS, 1M, pH 8.0) with stirring. To this was added iodoacetamide compound **[31]** (taken from 6 mg / ml stock in anhydrous DMF, 350 μg, 3.8 x 10^{-7} moles) and the reaction was stirred continuously overnight. The reaction mixture was dialysed once against 1M PBS solution (1L, pH 7.4) for 24h, changing the solution once and stirring the dialysis solution continuously within a fridge. Further purification and de-salting was achieved by using Millipore ultrafree-4 centrifugal filtration devices spun within a fixed 35° angle centrifuge at a rcf of 3000 for 90 mins, 21 °C (crude product made up to 4 ml with

water and total volume of 10 % DMSO). The gelatinous product at the bottom of the device was re-suspended in water (4 ml) and re-centrifuged in a new filtration device (3000 rcf, 90 mins) and repeated within the same device by re-suspending in water (4 ml). Lyophilisation gave 22 mg (73 %) of a fine white powder.

m.p.: > 260 °C (decomposes).
MS (MALDI-TOF): MS peak range = 67,500 – 80,000. Top of peak for compound **[33]** ~ 74,032, compound **[34]** ~ 74,093.
Difference = 61. MS appears to show a minimal increase in the value of the top peak, however a shift of an increase in the peak range of ~ 500 - 1,000 MW.

3.4.14 Poly(mannosyl) BSA – pepstatin cystamine conjugate (MPC6) [35]

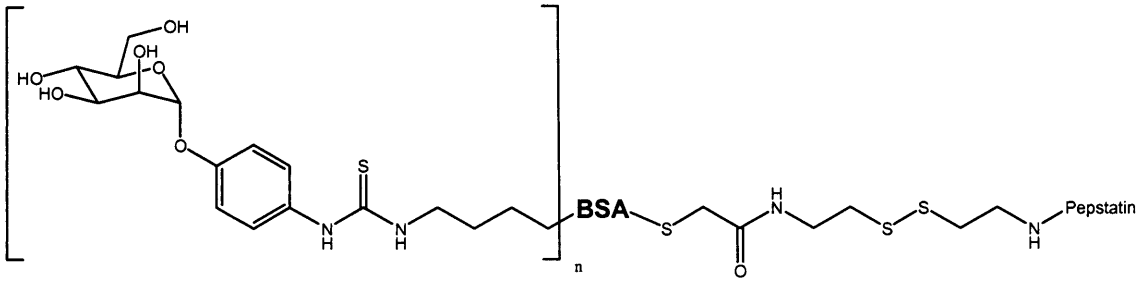

BSA – poly(mannose) conjugate **[33]** (30 mg, ~ 3.8 x 10^{-7} moles) was placed in a 25 ml round-bottomed flask and dissolved in 2 ml of phosphate buffer saline (PBS, 1M, pH 8.0) with stirring. To this was added iodoacetamide compound **[32]** (taken from 6 mg / ml stock in anhydrous DMF, 380 µg, 3.8 x 10^{-7} moles) and the reaction was stirred continuously overnight. The reaction mixture was dialysed once against 1M PBS solution (1L, pH 7.4) for 24h, changing the solution once and stirring the dialysis solution continuously within a fridge. Further purification and de-salting was achieved by using Millipore ultrafree-4 centrifugal filtration devices spun within a fixed 35° angle centrifuge at a rcf of 3000 for 90 mins, 21 °C (crude product made up to 4 ml with water and total volume of 10 % DMSO). The gelatinous product at the

bottom of the device was re-suspended in water (4 ml) and re-centrifuged in a new filtration device (3000 rcf, 90 mins) and repeated within the same device by re-suspending in water (4 ml). Lyophilisation gave 21 mg (70 %) of a fine white powder.

m.p.: > 260 °C (decomposes).
MS (MALDI-TOF): MS peak range = 69,000 – 81,500. Top of peak for compound **[33]** ~ 74,032, compound **[35]** ~ 75,163, difference = 1,131. Iodoacetamide compound **[32]** - iodine = 861.
MS shows at least the addition of one pepstatin derivative to BSA derivative, and a shift in the peak range.

3.5 Attempted synthesis of hexalysyl derivatives MPC3, MPC4

Peptides were made under standard peptide synthesis:
The resin (TGT Novasyn, pre-loaded with glycine; Calbiochem-Novabiochem UK Ltd., Nottingham, UK) was swelled in DMF (5 ml) for 20 min in a vial and then transferred to the synthesiser column (10 mm width). Fmoc deprotection was carried out using a 20 % piperidine solution in DMF for 5 minutes for standard Fmoc-protected amino acids and 10 minutes for the resin. The amino acid cycles included a 20 bubble-cycle activation of the residues with 0.6 M 1-hydroxybenzotriazole and 0.6 M diisopropyl carbodiimide solutions, both in DMF, followed by 15-minute coupling cycles for Fmoc-Lys (Boc)-OH or Fmoc-Lys (ivDde)-OH, carried out twice. Both the Fmoc deprotection and amino acid couplings were monitored quantitatively by measuring the U.V. absorbance (λ 365 nm). Each double-cycle was followed by a capping cycle using a 0.3 M solution of 1-acetylimidazole in DMF.

Several approaches towards MPC3 and MPC4 were attempted but were unsuccessful in the time available. Unfortunately, due to several unforeseen errors, some of the derivatives contained a mix of Dde and ivDde protecting groups. It was later noted that derivatives containing the Dde group with free lysine ε-amino groups nearby were conditions that allowed for the migration of the Dde group. As such, some compounds were made with two protecting groups attached with Dde being attached to any of the free ε-amino groups.

3.5.1 General method for cleavage of peptide from resin and purification

To a flask containing the resin (on average 1 g of resin was used) with attached synthesised peptide, was added acetic acid (1 ml), trifluoroethanol (1 ml) and CH_2Cl_2 (6 ml) and stirred continuously for 2 hours. The resin is filtered and washed with the peptide cleavage mixture. The solvent of the filtrate is removed *in vacuo* and the acetic acid removed *in vacuo* by azeotropic removal using hexane (5 x 30 ml). This left an orange oil that was purified by preparative HPLC using a MeOH / water gradient. For fully protected amino groups (Boc or Boc / Fmoc) this was typically a 50 % to 90 % MeOH in water gradient over 30 mins. For peptides with free amino groups, then a 20 % to 50 % MeOH in water gradient over 30 mins is used. Typical RT was from 15 mins (for free amino group peptides) to 30 mins (for fully protected peptides).

3.5.2 Automated peptide synthesis of hexalysyl (ivDde) peptide and subsequent Boc deprotection [36a]

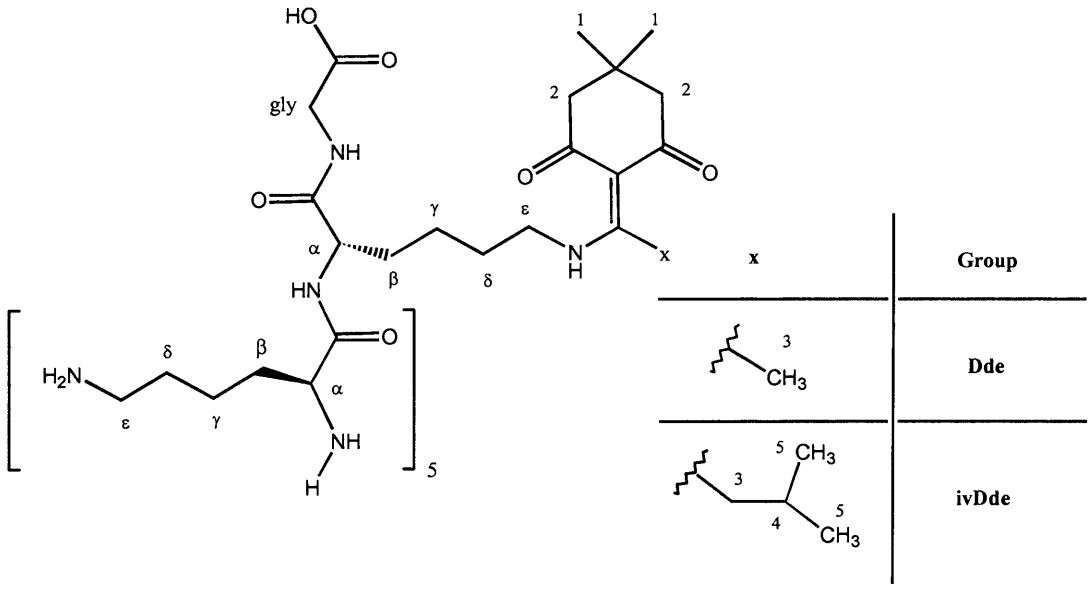

Figure 3.1: Hexalysyl (ivDde) peptide [36a]

The title compound (with Boc-protected lysines) was made using automated peptide synthesis under standard conditions with a final N-terminal Fmoc deprotection stage. The resin obtained from the peptide synthesiser (typically 1g of resin was used) was washed with DCM through a sinter to remove traces of DMF. The resin was transferred to a round-bottomed flask (250 ml) containing TFA (127.5 ml), thioanisole (7.5 ml, 63 μmol), phenol (8 mg, 85 μmol), TES (3.75 ml, 32.1 μmol) and H_2O (3.75 ml, 208 μmol). The resin mixture was stirred continuously for 4 hours under N_2 before being washed through a sinter with water (50 ml). All volatile solvents were removed from the filtrate *in vacuo* and the peptide precipitated on addition of ether to obtain a white solid. The solid was filtered, dissolved in 40 % AcOH / H_2O (50 ml) and lyophilised to obtain a crude white powder. Preparative HPLC (gradient, 10 % MeOH / H_2O to 40 % MeOH / H_2O over 25 mins, product RT = 5.3 mins), dissolving in 40 % AcOH / H_2O (20 ml) and lyophilisation gave a white powder of the titled peptide. On average, an included resin

quantity of 1 g (with a loading capacity of 0.22 meq / g) will give approximately 150 - 170 mg of final product.

R_f at baseline [1:4 methanol – $CHCl_3$, ninhydrin stain].
MS (ES+): *m/z* = 526 (100 %, *[{M + 3H}/2]*$^+$), 1051 (5.7%, *[M + 2H]*$^+$).
^{1}H NMR (CD_3OD, 400 MHz): δ 0.97 (6H, d, $J_{5,4}$ 6.7 Hz, H-5), 1.01 (6H, s, H-1), 1.50 (12H, m, 6 x H-γ), 1.60 – 1.90 (24H, m, 6 x H-β & 6 x H-δ), 2.36 (4H, s, H-2), 2.90 – 3.05 (12H, m, 5 x H-ε), 3.03 (2H, d, *J* 7.0 Hz, H-3), 3.53 – 3.56 (2H, m, H-ε*[ivDde]*), 3.86 – 3.98 (3H, m, gly & H-α*[ivDde]*), 4.34 (5H, m, H-α), 7.92 (3H, br, NH), 8.23 (1H, br, NH), 8.33 (1H, m, NH), 8.37 (1H, m, NH).
^{13}C NMR ($CDCl_3$, 100.6 MHz): δ 22.6, 22.78, 22.8, 23.5, 23.6, 23.7, 23.8, 23.9, 27.9, 28.3, 29.8, 30.2, 30.9, 32.0, 32.3, 32.6, 38.4, 40.2, 40.4, 53.6, 54.5, 107.89, 162.5, 162.9, 170.3, 172.9, 173.9, 173.94, 174.0, 174.1, 174.4, 178.3, 200.0. Missing multiple ^{13}C signals due to overlapping.

3.5.3 Hexalysyl peptide derivatives containing ivDde and Dde [36b]

Due to synthesis errors, some products contained both ivDde and Dde, synthesis and deprotection methods as above **[36a]**:

MS (ES+): *m/z* = 337.2 (100 %, *([M{Dde} + 2H]/3)*$^+$), 351.3 (65 %, *([M{ivDde} + 2H]/3)*$^+$), 505.6 (46 %, *([M{Dde} + 2H]/2)*$^+$), 526.6 (22 %, *([M{ivDde} + 2H]/2)*$^+$).
^{1}H NMR (CD_3OD, 400 MHz): δ 0.97 (6H, d, $J_{5,4}$ 6.7 Hz, H-5*[ivDde]*), 1.01 (6H, s, H-1*[Dde & ivDde]*), 1.47 – 1.52 (12H, m, 6 x H-γ), 1.68 – 1.73 & 1.82 – 1.89 (24H, m, 6 x H-β & 6 x H-δ), 2.36 (4H, s, H-2*[Dde & ivDde]*), 2.54 (3H, s, H-3*[Dde]*), 2.92 – 2.98 (10H, m, 6 x H-ε), 3.03 (2H, d, $J_{3,4}$ 6. 9 Hz, H-3*[ivDde]*), 3.48 – 3.51 (2H, m, H-ε), 3.88 (2H, d, *J* 3.4 Hz, gly), 3.96 (1H, t, $J_{\alpha,\beta}$ 6.4 Hz, H-α), 4.30 – 4.37 (5H, m, H-α).

^{13}C NMR (CD_3OD, 100.6 MHz): δ 18.5, 22.6, 23.5, 23.6, 23.7, 23.8, 27.9, 28.0, 28.1, 28.4, 29.5, 31.1, 31.9, 32.3, 40.2, 40.4, 53.4, 53.9, 71.3, 108.7, 162.9, 163.2, 170.3, 173.9, 173.94, 174.0, 174.1, 174.3, 175.5, 199.9. Missing multiple ^{13}C signals due to overlapping.

3.5.4 Boc protected hexalysyl (ivDde) peptide [37]

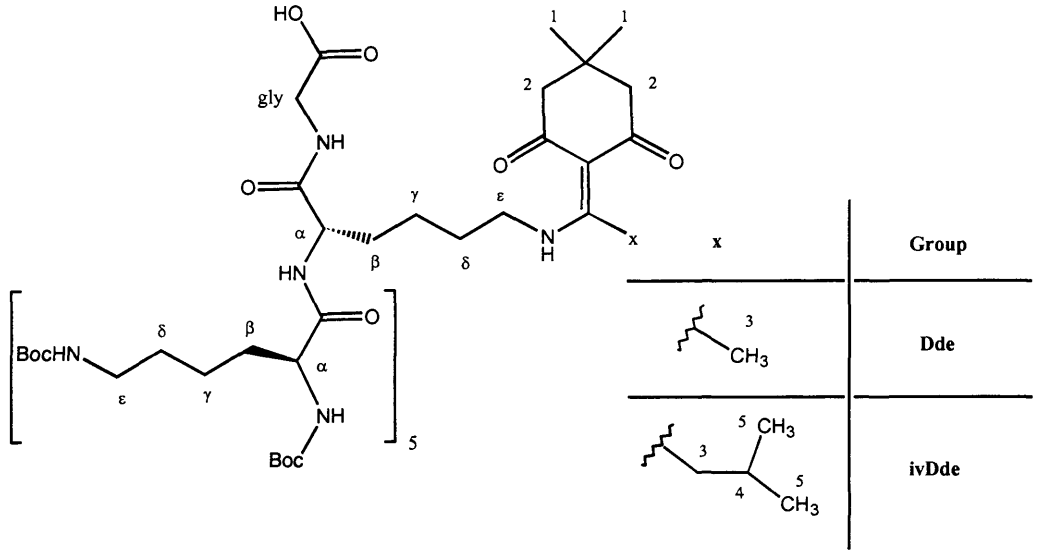

Figure 3.2: Boc-protected hexalysyl (ivDde) peptide [37]

Hexalysyl (ivDde/Dde) peptide [**36b**] (230 mg, 230 μmol) and anhydrous DMF (3 ml) were added to a flask and stirred. Di-*t*-butyl dicarbonate (262 μl, 233 mg, 1.07 mmol, 9 eq.) was dissolved into anhydrous DMF (1 ml) and added drop-wise to the flask followed by anhydrous TEA (1 ml). Stirring was continued overnight. T.l.c. showed the presence of a high proportion of product (R_f 0.8) and several other minor spots (1.5:8.5 methanol – CH_2Cl_2; R_f 0.7, 0.3 and at the baseline was some starting material). The solvent is removed *in vacuo*, re-dissolved in 15 % MeOH / 85 % CH_2Cl_2 and purified by flash chromatography (4 cm, gradient, 100 % CH_2Cl_2 to 50 % MeOH / CH_2Cl_2, 5 % increase in MeOH every 100 ml). Removal of the solvent *in vacuo* gave the title compound as an orange oil (323 mg, 202 μmol, 88 %).

R_f 0.6 [1:4 methanol – CH_2Cl_2; TFA pre-dipping then ninhydrin stain], compound **[36b]** at baseline.

MS (ES+): *m/z* = 1631.8 (70 %, *([M{Dde} + 1H + Na)*$^+$), 1673.8 (30 %, *([M{ivDde} + 1H + Na)*$^+$). Other peaks present with 2 x Dde & 2 x ivDde.

^{1}H NMR (CD_3OD, 400 MHz): δ 0.98 (6H, d, $J_{5,4}$ 6.7 Hz, H-5*[ivDde]*), 1.02 (6H, s, H-1*[Dde & ivDde]*), 1.42 – 1.91 (90H, m, *t*-butyl, 6 x H-γ, 6 x H-β & 6 x H-δ), 2.36 (4H, s, H-2*[Dde & ivDde]*), 2.55 (3H, s, H-3*[Dde]*), 2.96 – 3.04 (12H, m, 5 x H-ε & H-3*[ivDde]*), 3.48 – 3.51 (2H, t, $J_{\varepsilon,\gamma}$ 6.7 Hz, H-ε), 3.89 – 4.01 (2H, m, gly), 4.07 (1H, m, H-α), 4.30 – 4.40 (5H, m, H-α).

^{13}C NMR (CD_3OD, 100.6 MHz): δ 18.5, 22.9, 23.8, 24.2, 26.0, 26.7, 27.7, 28.1, 28.2, 28.4, 28.5, 28.6, 28.9 (*t*-butyl), 29.4, 30.5, 31.1, 31.7, 32.5, 34.7, 37.0, 41.2, 53.4, 71.1, 79.7, 108.6, 158.3, 158.5, 162.9, 163.3, 164.8, 175.4, 199.8. Missing multiple ^{13}C signals due to overlapping.

3.5.5 Attempted coupling of hexalysyl (ivDde) peptide [36a] and 4-isothiocyanatophenyl α-D-mannopyranoside [11]

4-Isothiocyanatophenyl α-D-mannopyranoside **[11]** (276 mg, 574 μmol, 15 eq.) was dissolved in anhydrous MeOH (2 ml), added to a round-bottomed flask containing anhydrous TEA (1 ml) and stirred. Hexalysyl (ivDde) peptide **[36a]** (40 mg, 38 μmol) was dissolved in anhydrous MeOH (3 ml) and slowly added to the flask and stirred continuously overnight. The reaction was monitored by t.l.c. (20 % MeOH / $CHCl_3$) such that the product had an R_f 0.45 (starting sugar R_f 0.6, hexalysyl [ivDde] peptide **[36a]** on baseline) and showed by UV and stained strongly by PMA but was not stained by ninhydrin. Purification by flash chromatography (4 cm, gradient, $CHCl_3$ to 30 % MeOH / $CHCl_3$) gave major fractions at 20 % MeOH / $CHCl_3$ and 30 % MeOH / $CHCl_3$. ^{1}H and

^{13}C NMR of both major products shows proton signals similar to compound **[11]** (or a derivative), however no signals for the hexalysyl (ivDde) compound **[36a]** were observed. This procedure was also attempted with the use of a 5:2 mix of MeOH:DCM (compound **[11]** is more soluble in DCM) but the desired product was not formed.

3.5.6 Coupling of hexalysyl (ivDde) peptide [36a] and 4-isothiocyanatophenyl α-D-mannopyranoside [11] to form compound [38]

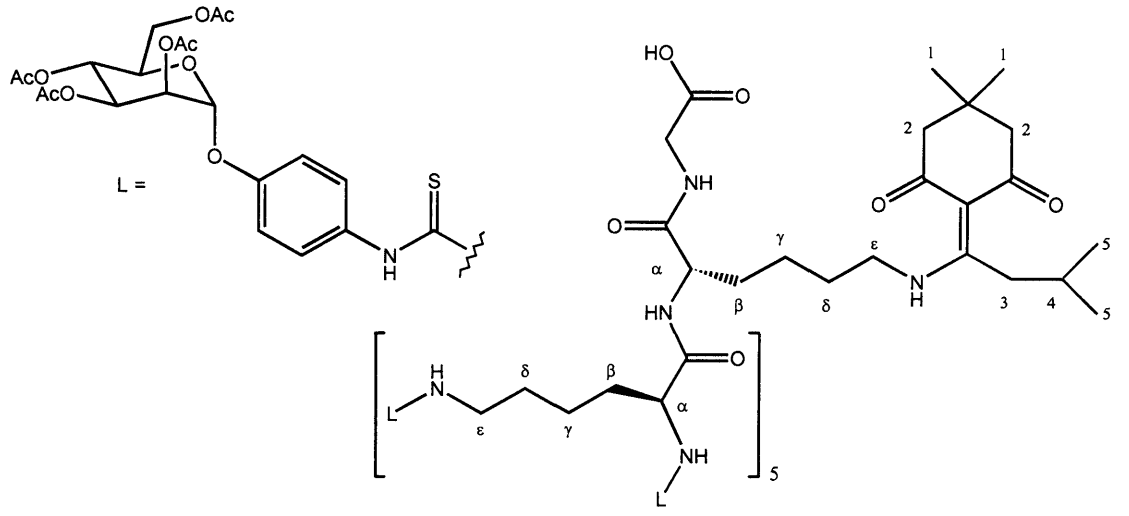

Figure 3.3: Hexalysyl (ivDde) peptide [38] coupled to 4-isothiocyanatophenyl α-D-mannopyranoside

4-Isothiocyanatophenyl α-D-mannopyranoside **[11]** (452 mg, 940 μmol, 10 eq.) and hexalysyl (ivDde) peptide **[36a]** (95 mg, 94 μmol) were added to a flask and dried *in vacuo*. Anhydrous THF (20 ml) and anhydrous DCM (10 ml) were added to the flask and stirred. Compound **[11]** dissolves well in this mixture, however the hexalysyl compound **[36a]** is only sparingly soluble. Anhydrous MeOH (10 ml) was added slowly to the flask to ensure the solubility of compound **[36]** without causing the crystallisation of the sugar compound **[11]**. The flask contents were stirred for 48 hours before the addition of anhydrous TEA (2 ml), and stirred for another 24 hours. The solvent was removed *in vacuo* and the flask contents dissolved in MeOH to crystallise sugar **[11]**.

The flask contents were filtered through Celite and the solvent removed *in vacuo*. T.l.c. of the filtrate (20 % MeOH / $CHCl_3$) shows the presence of four main products with PMA staining at R_f 0.8, R_f 0.7 (ninhydrin stain also), R_f 0.6 and R_f 0.3 – baseline. Flash chromatography (3 cm^3, gradient) involved the loading of the sample onto a $CHCl_3$ packed column, flushing through with $CHCl_3$ (200 ml) and then a gradient of 10 % MeOH / $CHCl_3$ to 35 % MeOH / $CHCl_3$ with 5 % increase in MeOH every 100 ml. At the end of the addition of 35 % MeOH / $CHCl_3$, any remaining sample was washed through with 50 % MeOH / $CHCl_3$. The column fractions containing the crude product (Rf 0.3 – baseline) were pooled and the solvent removed *in vacuo* to give 60 mg of a white powder. Attempts were made using various mass spectrometry methods (ES, MALDI-TOF, FAB), and NMR, to analyse the product, however these proved inconclusive.

3.5.7 Coupling of Boc protected hexalysyl peptide and pepstatin cystamine [39]

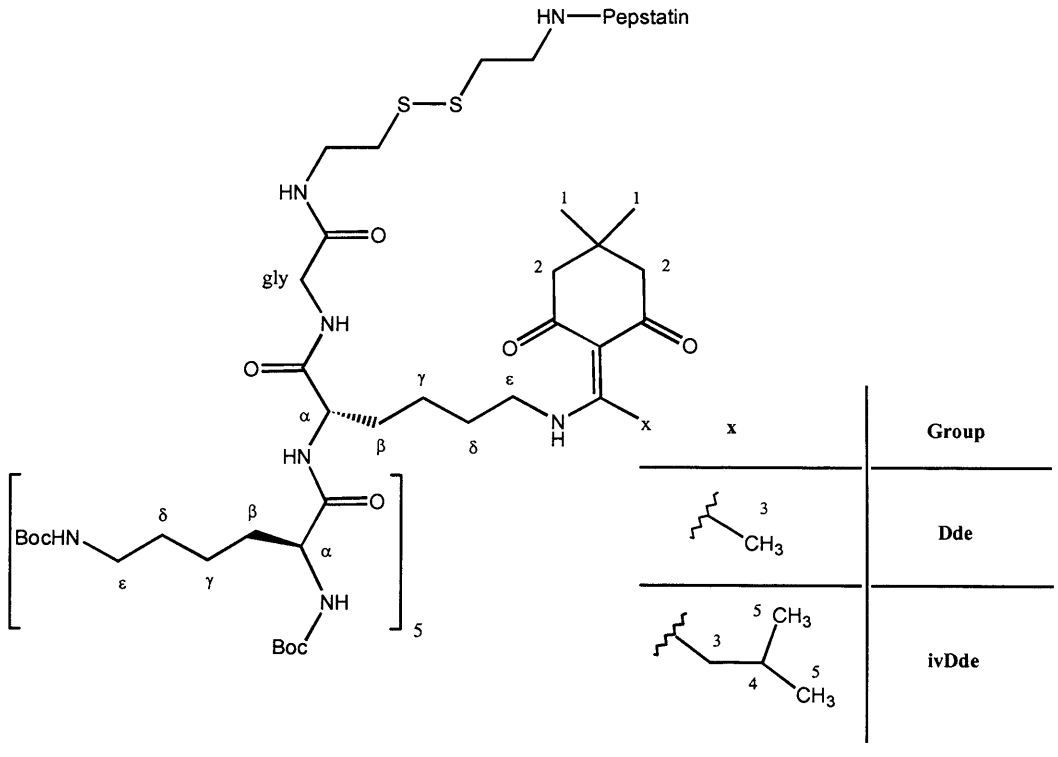

Figure 3.4: Boc protected hexalysyl peptide and pepstatin cystamine [39]

Boc protected hexalysyl peptide **[37]** (56mg, 35 μmol), NHS (40 mg, 350 μmol, 10 equiv.) and EDCI (33.4 mg, 175 μmol, 5 eq.) were added to a 10 ml round-bottomed flask, dissolved in anhydrous DMF (2 ml) and stirred continuously for 32 hours. The solvent was removed under high vacuum and the solid re-dissolved in CH_2Cl_2 20 ml). The organic layer was washed with 0.04M HCl solution (3 x 20 ml), dried over magnesium sulphate, filtered, and the solvent removed *in vacuo* to obtain 85 mg of the crude NHS ester. NMR did not give any additional information so the product was used as is in the coupling stage and assumed to be pure and quantitative yield.

The crude product (16.9 mg, 9.9 μmol, 1.02 equiv.) and pepstatin cystamine **[30]** (8 mg, 9.7 μmol) were added to a 10 ml round-bottomed flask, dissolved in anhydrous DMF (1 ml) and stirred for two days. The solvent was removed *in vacuo* and the crude product purified by preparative HPLC (10 % MeOH to 40 % MeOH in water over 30 mins). Four major products appeared with the largest at RT 36 – 39 min (HPLC run to 100% MeOH from 30 – 35 mins, then held for 2 mins at 100% before a gradient back to 10 % MeOH over 5 mins). The solvent from the product with RT 36 – 39 min was removed *in vacuo* and then remaining water was removed from the particulate matter by lyophilisation to obtain the title product as a white powder (14 mg, 5.8 μmol, 60 %).

R_f 0.4 [1:4 methanol – CH_2Cl_2; TFA pre-dipping then ninhydrin stain].
MS (ES+): *m/z* = 478.7 (100 %, *([M{Dde} – 5Boc + 10H)/4$^+$*), 494.3 (74 %, *([M{ivDde} – 5Boc + 9H + Na)/4$^+$*), 1055.5 (62 %, *([M{Dde} – 3Boc + 5H)/2$^+$*). Other peaks present with 2 x Dde.
^{1}H NMR (CD_3OD, 400 MHz): δ 0.86 – 1.01 (m), 1.27 – 1.82 (m), 2.04 – 2.13 (m), 2.13 (d, *J* 6.6 Hz), 2.29 – 2.36 (m), 2.45 (t, *J* 6.8 Hz), 2.55 (s), 2.79 – 2.85 (m), 2.95 – 3.03 (m), 3.43 – 3.56 (m), 3.60 – 3.63 (m), 3.94 – 4.00 (m), 4.09 – 4.15 (m), 4.24 – 4.26 (m), 4.93 (1H, s). Spectra assignment not possible due to broadness of spectrum.

Chapter 4

Chemical Synthesis Results and Discussion

The following chapter highlights in more detail some of the observations and conclusions of the synthetic work. The designs of the inhibitors were detailed in chapter 2 and shown in figures 2.7 and 2.8 (page 80), with detailed chemical structures of the final compounds shown in figure 2.14 (page 87).

4.1 Synthesis of mannose derivatives

4.1.1 Formation of per-*O*-acetylated 1,2,3,4,6-penta-*O*-acetyl-*α/β*-D-mannopyranose [1]

Complete acetylation of D-mannose[211] was accomplished by reacting D-mannose with 5 equivalents of acetic anhydride and the use of TEA as both solvent and base. The existence of an anomeric mixture is not a problem for further synthetic steps because of the influence of the anomeric effect and neighbouring group participation of the C-2 acetoxy group, which together help with the formation of the α-anomer at the C-1 position of mannose.

4.1.2 Synthesis of tetra-acetyl [2], acetimidate [3] and bromo [4] mannopyranosides

The selective de-acetylation of the anomeric position of 1,2,3,4,6-penta-*O*-acetyl-*α/β*-D-mannopyranose **[1]** to form the 2,3,4,6-tetra-*O*-acetyl-*α*-D-mannopyranose **[2]** (section 3.1.2) has been performed by several methods [215,231]. In our hands hydrazine acetate in anhydrous DMF[4,212,213] gave high yields of a single anomeric, crystalline product (77 % yield, 99 % α-anomer) (fig. 4.1).

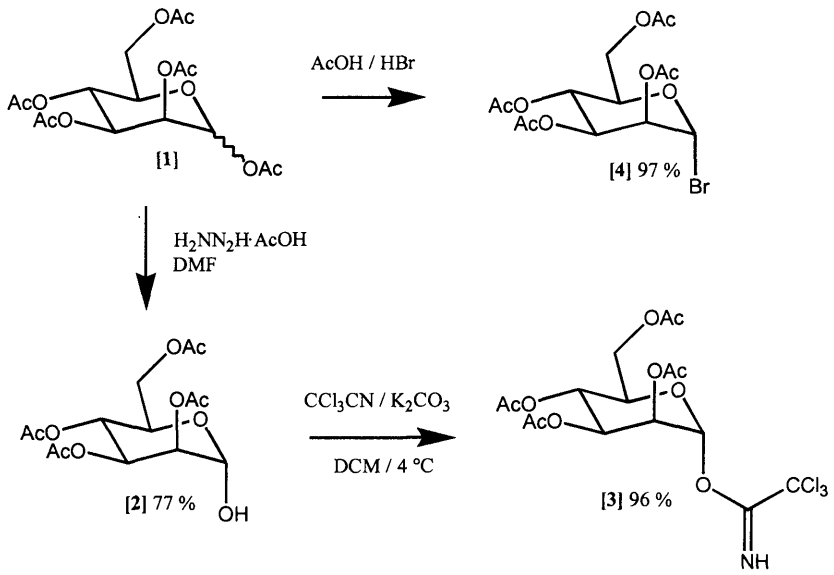

Figure 4.1: Synthesis of tetra-acetyl, bromo and acetimidate mannopyranosides

Formation of 2,3,4,6-tetra-*O*-acetyl-α-D-mannopyranosyl trichloro-acetimidate **[3]** from hemiacetal **[2]** is conventionally carried out with the use of trichloroacetonitrile in anhydrous DCM with base, to give the α-anomer. Potassium carbonate was chosen as an easily available mild base, giving a quantitative yield of a pure compound (fig. 4.1). The formation of mannosyl bromides[208,209] uses a mix of per-*O*-acetylated mannopyranose with acetic acid / hydrogen bromide at room temperature with complete formation of product within several hours. This procedure was followed (fig. 4.1) to give 2,3,4,6-tetra-*O*-acetyl-α-D-mannopyranosyl bromide **[4]** from the per-*O*-acetylated mannose **[1]** with a 97% yield.

4.1.3 Formation of 4-nitrophenyl 2,3,4,6-tetra-*O*-acetyl-β-D-manno-pyranose [5] and 4-nitrophenyl 2,3,4,6-tetra-*O*-acetyl-α-D-mannopyranose [6]

2,3,4,6-Tetra-*O*-acetyl-α-D-mannopyranosyl bromide **[4]** was reacted with 4-nitrophenol and tetramethylguanidine as base (section 3.1.5, page 95) giving exclusively the β-anomer **[5]**. The formation of the β-anomer

was verified by NOE to show correlations between the H-1, H-3 and H-5 protons. The formation of glycoside **[6]** used $BF_3.Et_2O$ (fig. 4.2)[232,233]. $BF_3.Et_2O$ was slowly added to a mixture of per-*O*-acetylated mannose and 4-nitrophenol at 0 °C in CH_2Cl_2 to obtain a high yield of crystalline product (89 %) after 24 hours. The suggested mechanism is shown in figure 4.2. The NOE shown in appendix II confirms the formation of this product. By addition of $BF_3.Et_2O$ to the β-anomer **[5],** it was possible to induced anomerisation to the more stable α-anomer **[6]**.

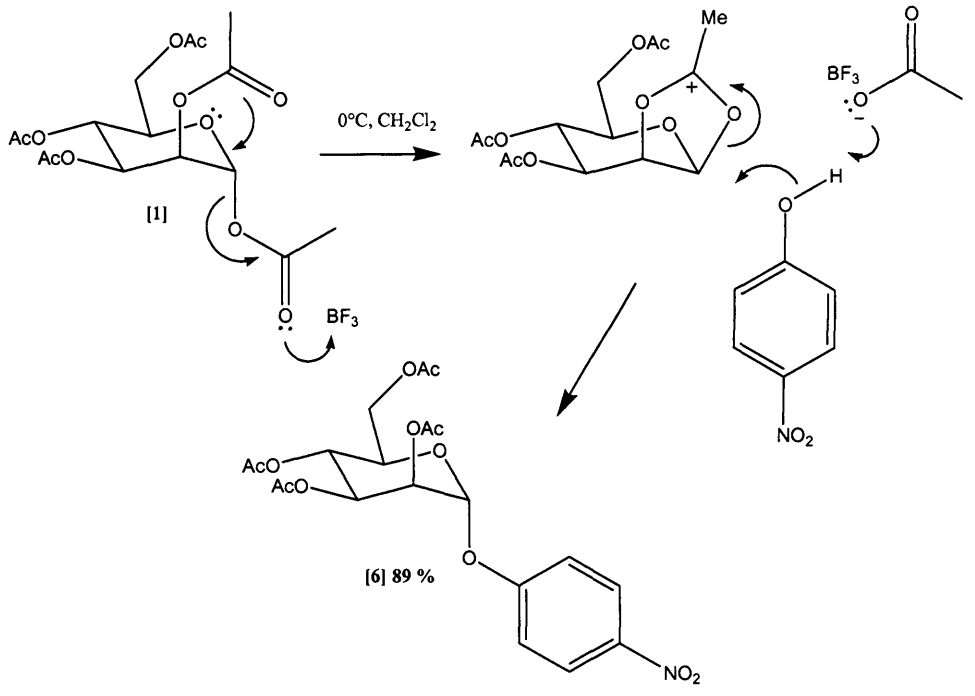

Figure 4.2: $BF_3.Et_2O$ catalysed formation of glycoside [6]

4.1.4 Acetyl deprotection of 4-nitrophenyl 2,3,4,6-tetra-*O*-acetyl-α-D-mannopyranose [6]

4-Nitrophenyl α-D-mannopyranoside **[9]** was used in the synthesis of MPC5 and MPC6. It is synthesised from 4-nitrophenyl 2,3,4,6-tetra-*O*-acetyl-α-D-mannopyranoside **[6]** by deacetylation using the addition of LiOH (1M) to pH 11, for several hours (fig. 4.3)[223].

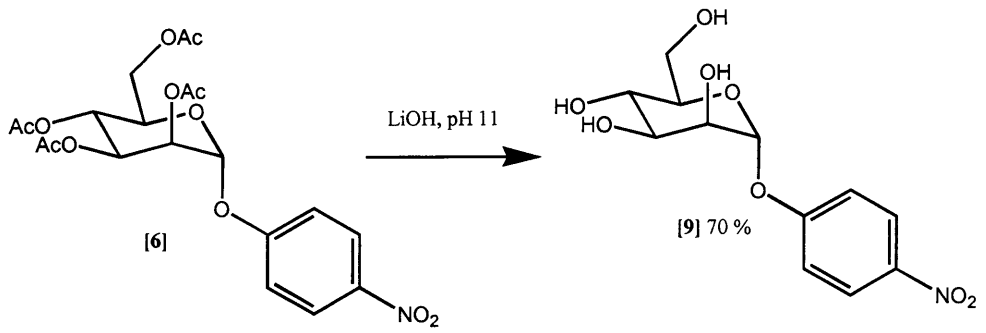

Figure 4.3: Formation of [9] by acetyl deprotection of [6]

4.1.5 Hydrogenation and formation of isothiocyanate derivatives from 4-nitrophenyl 2,3,4,6-tetra-*O*-acetyl-α-D-manno-pyranoside [6] and 4-nitrophenyl α-D-mannopyranoside [9]

The activation of acetyl-protected mannopyranoside **[6]** and deprotected mannopyranoside derivative **[9]** (fig. 4.4) requires the conversion of the nitro group to an isothiocyanate group. Reduction of the mannopyranosides **[6]** and **[9]** was by a routine atmospheric pressure hydrogenation at room temperature using 10 % Pd / C. Both reactions were complete within 4 hours, with high yields and easy purification by filtration through Celite.

The aromatic amines **[7]** and **[10]** were then treated with thiophosgene to convert them to the isothiocyanates (fig. 4.4)[201,234]. Although not as poisonous as the extremely dangerous phosgene, thiophosgene is toxic and requires careful handling (the exact precautions used are listed in the experimental in section 3.1.9, page 99). The usual method of addition of reagents is to add the amine slowly to a large excess of thiophosgene. This would reduce the possible reaction of isothiocyanate product with unreacted amine. This procedure was used in the formation of 4-isothiocyanatophenyl 2,3,4,6-tetra-*O*-acetyl-α-D-mannopyranoside **[8]**, using THF as solvent. However, addition of thiophosgene to amine **[10]** (but still with an excess of thiophosgene) in the synthesis of 4-

isothiocyanatophenyl α-D-mannopyranoside **[11]** also resulted in a high yield of product (97 %). The solvent was switched to EtOH / water as the solubility of compound **[10]** in THF was poor.

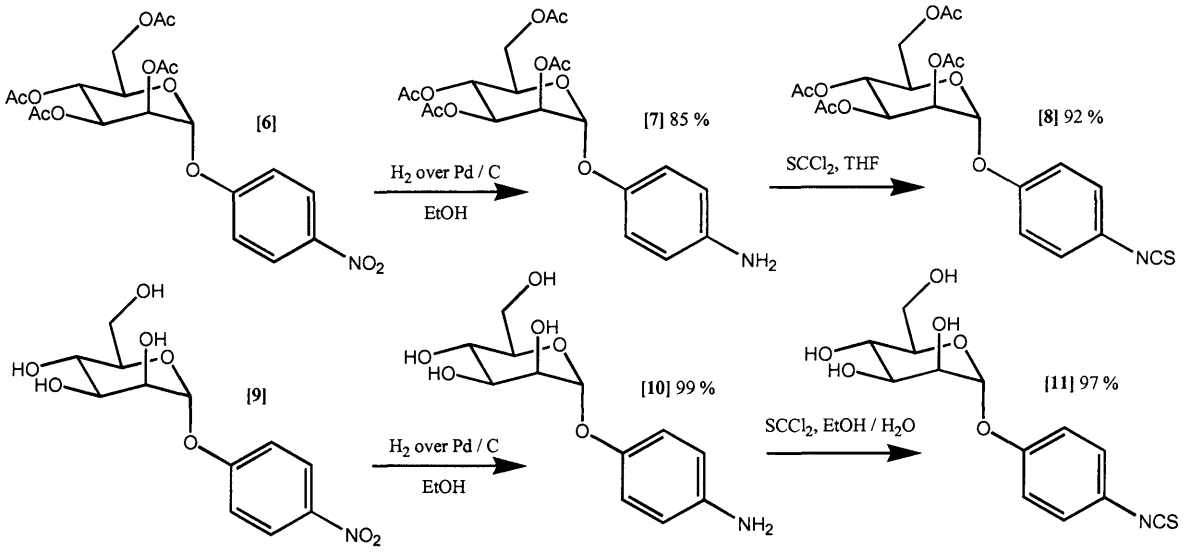

Figure 4.4: Formation of isothiocyanate derivatives [8] and [11]

4.2 Synthesis of benzyl 4-hydroxybutanoate and amine linkers

4.2.1 Benzyl 4-hydroxybutanoate [12]

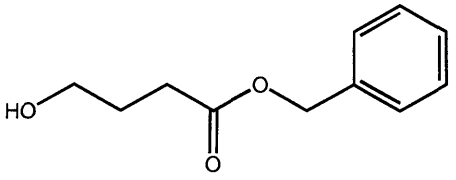

For the derivatives MPC1 and MPC2, benzyl 4-hydroxybutanoate spacer **[12]** is used. Several methods for its synthesis have been reported, including the method published by *Thaisrivongs et al* (a hydroboration – oxidation of benzyl 3-butenoate)[235], and *Toyokuni and Hakomori* (ring opening of 1,4-butyrolactone by benzyl alcohol)[4,236], however the procedure of *Weber et al*[226] was used here. The method involves the ring opening of 1,4-butyrolactone to form sodium 4-hydroxybutanoate,

followed by a phase-transfer catalysed reaction with benzyl bromide using tetrabutylammonium bromide as a phase transfer catalyst.

4.2.2 *N*-(*t*-Butyloxycarbonyl) propane-1,3-diamine [13] and *N*-(*t*-butyloxycarbonyl) cystamine [14]

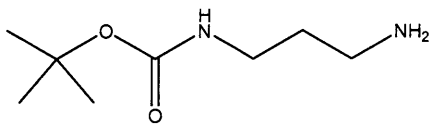

[13]

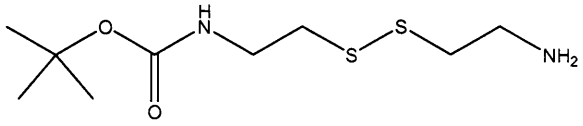

[14]

di-*t*-Butyl dicarbonate[227] was used in the mono-Boc protection of propane-1,3-diamine and cystamine. This proceedure gave high yields with a simple purification that required a series of aqueous workups. After reaction, removal of organic solvents *in vacuo* and then the dissolving of product **[13]** in slightly acidic aqueous solution (pH 6.5) allowed for the complete removal of di-protected 1,3-diamino propane (as a solid by filtration). Making the aqueous solution more ionic and basic (with brine / bicarbonate solution) and extraction of organics with $CHCl_3$ gives exclusively the desired product.

N-(*t*-Butyloxycarbonyl) cystamine **[14]** was prepared in much the same manner as above with the use of di-*t*-butyl dicarbonate with a few differences. As cystamine is supplied as the dihydrochloride, a base is needed (used sodium bicarbonate) to give the free amine. Solubility was an issue, and it was found that the best solvent mixture was a roughly equal mix of water and dioxane. It was essential to stir the mixture vigorously to avoid the production of mainly di-protected Boc-cystamine, due to the improved solubility of *N*-(*t*-butyloxycarbonyl) cystamine **[14]** and di-*t*-butyl dicarbonate within dioxane leading to di-substitution of Boc towards cystamine. As compound **[13]**, removal of organic solvent and dissolving of the product **[14]** in slightly acidic aqueous solution (pH 6.5) allowed for the removal of di-Boc-protected cystamine.

4.3 The synthesis of MPC1 / MPC2 precursors

The synthesis of intermediates leading to MPC1 / MPC2 (structures shown in figure 2.14, page 87) requires the formation of 3'-benzyloxycarbonylpropyl 2,3,4,6-tetra-*O*-acetyl-α-D-mannopyranose **[15]** (fig. 4.5), removal of the benzyl group and activation to an NHS ester (fig. 4.6), so that it may react with either *N*-(*t*-butyloxycarbonyl) propane-1,3-diamine (as used in MPC1) or *N*-(*t*-butyloxycarbonyl) cystamine (as used in MPC2).

4.3.1 Formation of 3'-benzyloxycarbonylpropyl 2,3,4,6-tetra-*O*-acetyl-α-D-mannopyranoside [15]

Initial attempts at the formation of the glycoside **[15]** used the trichloroacetimidate **[3]** with trimethylsilyl triflate (TMSOTf) as a catalyst. Multiple conditions were attempted, with the azeotropic removal of water, the addition of TMSOTf in different quantities (from 0.05 to 1.25 eq, relative to the alcohol) and reaction times (4 hours to 36 hours), however both yields and purity of final product were poor. The highest yield obtained was ~ 30 %, however the purity was insufficient as the multiple side products (up to six) could not be separated by flash chromatography. The reasons for the poor yield and multiple products are unclear, but side products derived from either the production of the acetoxonium intermediate or undesirable reactions of the triflate ion may be involved. This method (using TMSOTf) was used previously where yields were also low (24 %) which was thought to be due to the use of a secondary alcohol[216].

A second procedure was attempted using $BF_3.Et_2O$ as a Lewis acid under similar conditions as above with azeotropically dried reagents, CH_2Cl_2 as solvent and 1 to 1.25 equiv. of $BF_3.Et_2O$ (equivalent to alcohol). This immediately resulted in higher yields of up to 55 % after flash chromatography. The proposed mechanism for this reaction is shown in

figure 4.5. NMR of the product **[15]** showed that the alkyl chain attached at anomeric centre is diastereotopic. NOESY experiments (see appendix I) showed correlation between H-3 and H-5 and no correlation between H-5 and H-1, verifying the presence of the α-anomer.

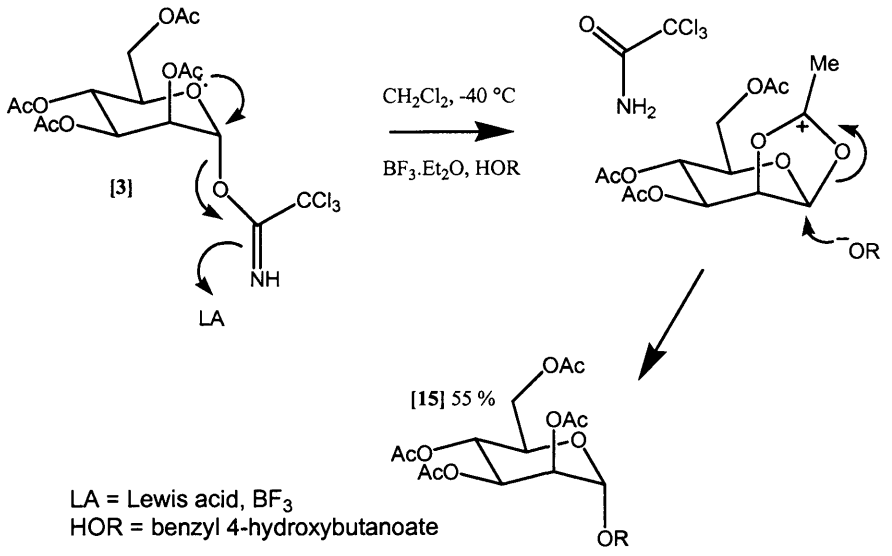

Figure 4.5: $BF_3.Et_2O$ catalysed formation of glycoside [15]

4.3.2 Mannose Spacer Linker conjugates of MPC1 and MPC2

Cleavage of the benzyl group requires hydrogenation with a palladium catalyst. This afforded an essentially quantitative yield of carboxylic acid **[16]** (fig. 4.6). For the synthesis of NHS ester **[17]**, it is important to perform the aqueous workup as soon as possible, and to dry the compound effectively. Long-term storage was not considered due to the compounds sensitivity to water, so the intermediate was used as soon as possible.

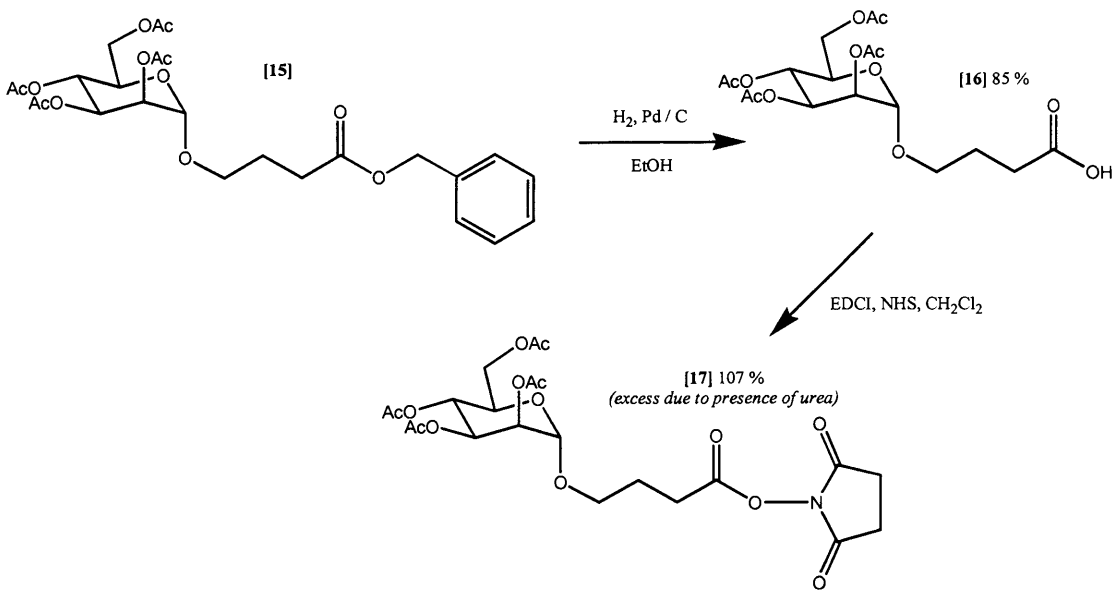

Figure 4.6: Formation of NHS ester [17]

The reaction of the NHS ester 3'-succinimidoxycarbonylpropyl 2,3,4,6-tetra-*O*-acetyl-α-D-mannopyranoside **[17]** with the relevant amine (fig. 4.7) required the mixing of NHS ester and amine in CH_2Cl_2 under anhydrous conditions. A few drops of TEA were added to ensure that the amine is deprotonated. The reaction was complete after 4 hours. Purification required flash chromatography and yields were high (65 – 82 %). The final step was the removal of the Boc group (fig. 4.7). Although the removal of Boc group with trifluoroacetic acid (TFA) is usually performed with the use of scavengers (as for synthesis of amines **[29]** and **[30]**), this was not used for the derivatives of MPC1 and MPC2 due to purification difficulties in the removal of the scavengers. The free amines needed to be reacted with pepstatin – NHS as soon as possible in order to avoid degradation. NMR spectra had poorly resolved signals.

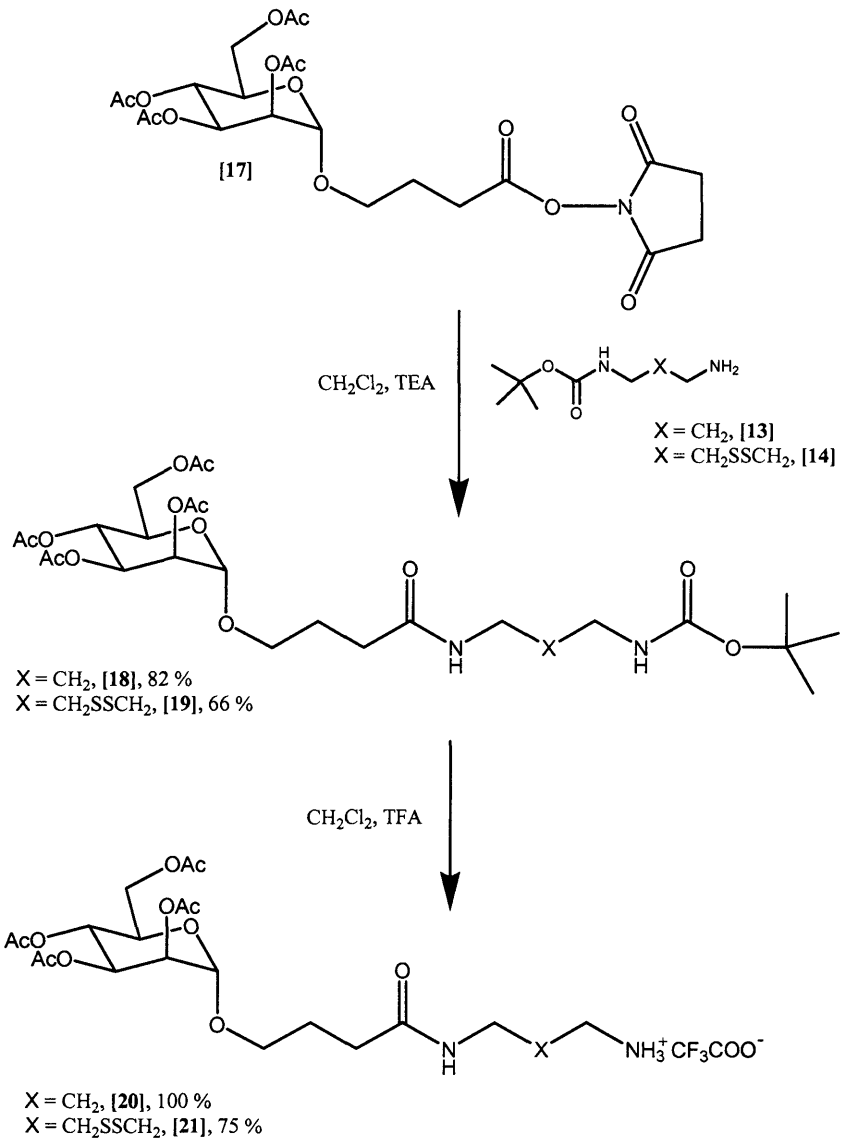

Figure 4.7: Formation of TFA salt derivatives [20] and [21]

4.4 Synthesis of MPC1, MPC2 and other pepstatin analogues

Given the expense of pepstatin and the limited quantities available for use, only small-scale reactions were feasible. The insolubility of pepstatin in most solvents was an advantage with respect to purification. The most useful analysis for the determination of products and reaction completion was mass spectroscopy, in particular electrospray mass spectroscopy (ES MS), which always gave positive results for product ions. NMR was not always useful until final purification of known products was achieved, due to the difficulty of interpreting the data. In some situations, the insolubility of pepstatin analogues made obtaining NMR data difficult. Some pepstatin derivatives were also difficult to visualise by t.l.c., making the progress of reactions difficult to follow.

4.4.1 Pepstatin – NHS

The free carboxylic acid of pepstatin may be activated by NHS ester formation (fig. 4.8). Reaction of EDCI, NHS and pepstatin in anhydrous, distilled DMF and vigorous stirring overnight gave high yields of pepstatin – NHS. A white suspension of insoluble pepstatin is present at the beginning of the reaction but dissolves over 4 hours. It was not possible to distinguish pepstatin from product by t.l.c., so at least 16 hours was allowed for the reaction. The most successful purification of compound **[22]** was to remove of the DMF in high *vacuo* followed by several washes of the solid with water (containing a few drops of 0.1M HCl), a wash with ether and drying for 24 hours under vacuum over anhydrous phosphorus pentoxide. The obtained product yield of 93 % is of mass recovery, as no indication of purity was possible by analytical methods.

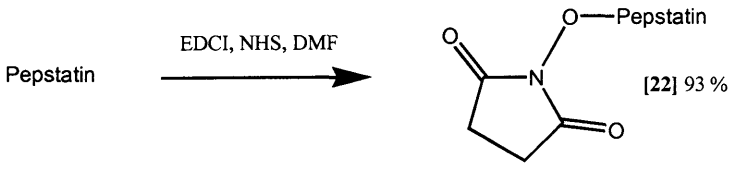

Figure 4.8: Formation of pepstatin NHS [22]

4.4.2 MPC1, MPC2 and their pepstatin precursors

The final four steps in the micro scale (typically between 20 – 40 mg) synthesis of MPC1 or MPC2 required the coupling of pepstatin NHS **[22]** to *N*-(3-(2,3,4,6-tetra-*O*-acetyl-α-D-mannopyranosyloxy)propylcarbonyl) ,*N*'-(trifluoroacetyl) propane-1,3-diamine **[20]**, or *N*-(3-(2,3,4,6-tetra-*O*-acetyl-α-D-mannopyranosyloxy)propylcarbonyl),*N*'-(trifluoroacetyl) cystamine **[21]**, followed by the removal of the acetyl groups on mannose to give fully deprotected mannose (fig. 4.9).

Coupling of pepstatin – NHS **[22]** was performed by the combination of both NHS ester **[22]** and either of the amines **[20]** or **[21]** in DMF containing a large excess of TEA to liberate the free amine from the TFA salt. As mentioned above, freshly distilled DMF is needed for synthesis. Initial efforts to synthesise **[23]** and **[24]** gave lower yields than expected due to the presence of pepstatin dimethylamide. At least five equivalents of the amine derivatives **[20]** or **[21]** compared to pepstatin NHS **[22]** were used. Purification by reverse-phase preparative HPLC (gradient, 60 % MeOH / water to 95 % MeOH / water over 25 mins) allowed easy seperation of the products **[23]** and **[24]** from starting materials due to the significant differences in solubility and thus large differences in HPLC retention times.

The final step in the synthesis of MPC1 and MPC2 involved the removal of the mannose acetyl protecting groups from **[23]** and **[24]** (fig. 4.9). The method chosen[223] was the addition of LiOH solution (1M) to pH 11 and stirring for several hours. Purification by reverse-phase preparative HPLC (gradient, 20 % MeCN / water to 60 % MeCN / water over 25

mins) allowed easy seperation of the more hydrophilic compounds MPC1 **[25]** and MPC2 **[26]** from their precursors **[23]** and **[24]**.

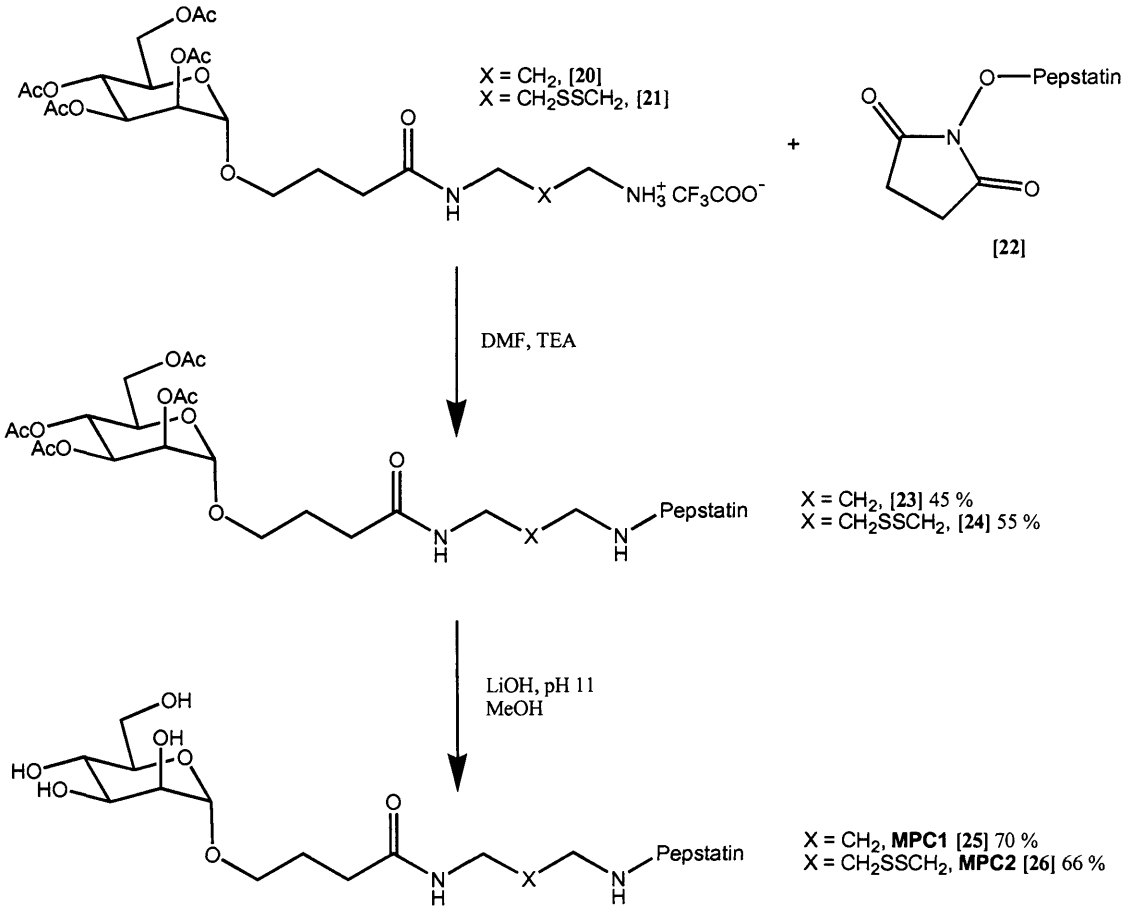

Figure 4.9: Formation of MPC1 and its precursor

4.4.3 Mass Spectroscopy / NMR assignment of pepstatin analogues

MPC1 precursor **[23]** has complete NMR assignments based on ^{1}H and ^{13}C NMR, DEPT135, COSY and HSQC NMR experiments, as shown in appendices III – VII, respectively. MPC1 and MPC2 (fig. 2.14, page 87), and the two immediate precursors, are the most complex and largest pepstatin analogues upon which reasonable NMR assignment is possible. It was essential to ensure that NMR assignment was possible for these analogues and that these assignments were consistent with other

pepstatin analogues, and as such the NMR numerical assignment of the carbon and proton nuclei within the pepstatin molecule follow that of the largest pepstatin derivative molecule, that being the acetyl-mannoside derivative **[26]**.

4.4.4 Pepstatin – linker conjugates

N-(*t*-Butyloxycarbonyl),*N*'-(pepstatinyl) propane-1,3-diamine **[27]** and *N*-(*t*-butyloxycarbonyl), *N*'-(pepstatinyl) cystamine **[28]** were both synthesised by the coupling of the respective amine derivatives **[13]** and **[14]** with pepstatin – NHS (fig. 4.10). Removal of the Boc group with TFA in the presence of scavengers (fig. 4.10) was followed by t.l.c., the reactions were complete in 4 hours. Solubility in MeOH or MeCN was sufficient to allow preparative reverse-phase HPLC purification of *N*-(pepstatinyl) propane-1,3-diamine **[29]** (50 % MeOH / water to 100 % MeOH over 25 mins) and *N*-(Pepstatinyl) cystamine **[30]** (40 % MeCN / water to 80 % MeCN over 30 mins) to obtain pure, high yielding compounds (60 – 90%).

The final step to synthesise *N*-(iodoacetyl),*N*'-(pepstatinyl) propane-1,3-diamine **[31]** and *N*-(iodoacetyl),*N*'-(pepstatinyl) cystamine **[32]** was effected by the addition of iodoacetic anhydride to the respective free amines (fig. 4.10). Reactions were fast (as measured by t.l.c., visualised by ninhydrin stain) and 2 hours was sufficient time for the reaction. Initial purification was by an aqueous wash with KI solution included (to stop the possibility of iodine exchange with other halogens), however in one instance purification was attempted with washing in ethyl acetate alone. This method appeared to both crystallise the product more effectively and improve the purity, as shown by improved NMR data. Yields were in the 50 - 83% range.

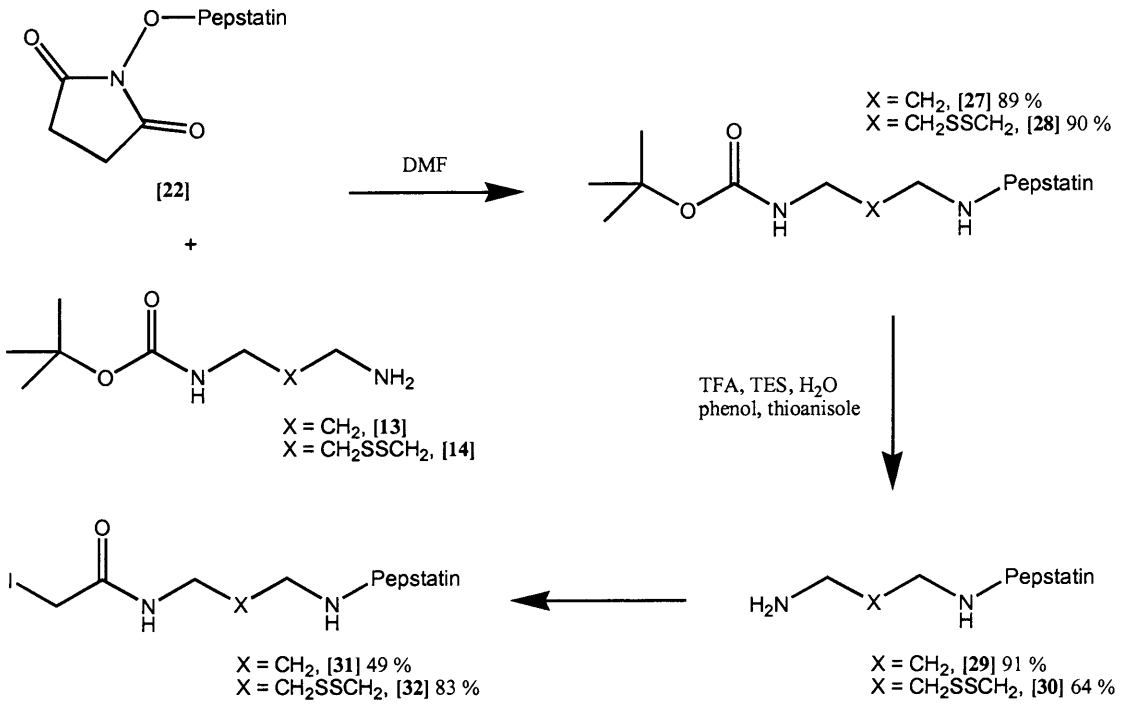

Figure 4.10: Formation of iodoacetamides [31] and [32]

4.5 BSA – conjugate, MPC5 and MPC6

The use of the carrier Bovine Serum Albumin (BSA) in MPC5 **[34]** and MPC6 **[35]** meant a different approach was needed for synthesis, aqueous reaction conditions were needed[185].

4.5.1 BSA – mannose conjugate [33]

4-Isothiocyanatophenyl α-D-mannopyranoside **[11]** was coupled to BSA in 0.15M NaCl to give **[33]** (fig. 4.11)[201]. BSA contains a total of 59 lysine ε-amine groups[185], and it was anticipated from previous mannose receptor binding studies that conjugation of at least 10 mannose units would allow for significant binding to the mannose receptor to allow uptake by the receptor[2,237]. Dialysis and further purification with the use of centrifugal filtration devices (with 12,000 molecular weight cut-off)

was considered sufficient to remove free mannosyl derivatives and salts. Analysis was primarily by the use of matrix-assisted laser desorption time-of-flight mass spectroscopy (MALDI-TOF MS), which showed that approximately 23 mannosyl units were attached to each BSA (section 6.3.1, page 203 and appendix VIII, page 258). Biochemical analysis to assess the average number of free lysine residues per BSA molecule, and the average number of attached sugar derivatives per BSA molecule, showed a good correlation with the MS data (section 6.3.1, page 205).

4.5.2 MPC5 and MPC6 synthesis

Synthesis of MPC5 and MPC6 was achieved by the formation of a thioether bond between a cysteine sulfhydryl with either iodoacetamide derivatives of pepstatin propane-1,3-diamine **[31]** or of pepstatin cystamine **[32]** (fig. 4.11). 1M PBS solution was used as the buffer, and a maximum of 20 % DMF was used to solubilise the added iodoacetamide derivatives and to not precipitate the protein (which precipitates at approximately 30 % DMF). Protein denaturing, if it occurs under these conditions, was not considered a problem for the task of the protein being a carrier or as a delivery mechanism towards the mannose receptor. Vigorous stirring was required to ensure adequate mixing of the reagents. Dialysis and centrifugal filtration devices were again used to remove free mannosyl derivatives and salts. Quoted yields (fig. 4.11) are of mass recovery. Determination of sulfhydryl content using Ellman's reagent[238] with BSA and compounds **[33]** – **[35]** to assess the amount of conjugated pepstatin derivative to each BSA molecule did not prove successful. MALDI-TOF MS showed with MPC6 an increase in molecular weight (measured at the top of the peak obtained) of at least 1000 M_r (appendix IX). MS was not so successful with MPC5, which showed little increase in peak M_r, but a total peak shift of between 500 – 1000 M_r.

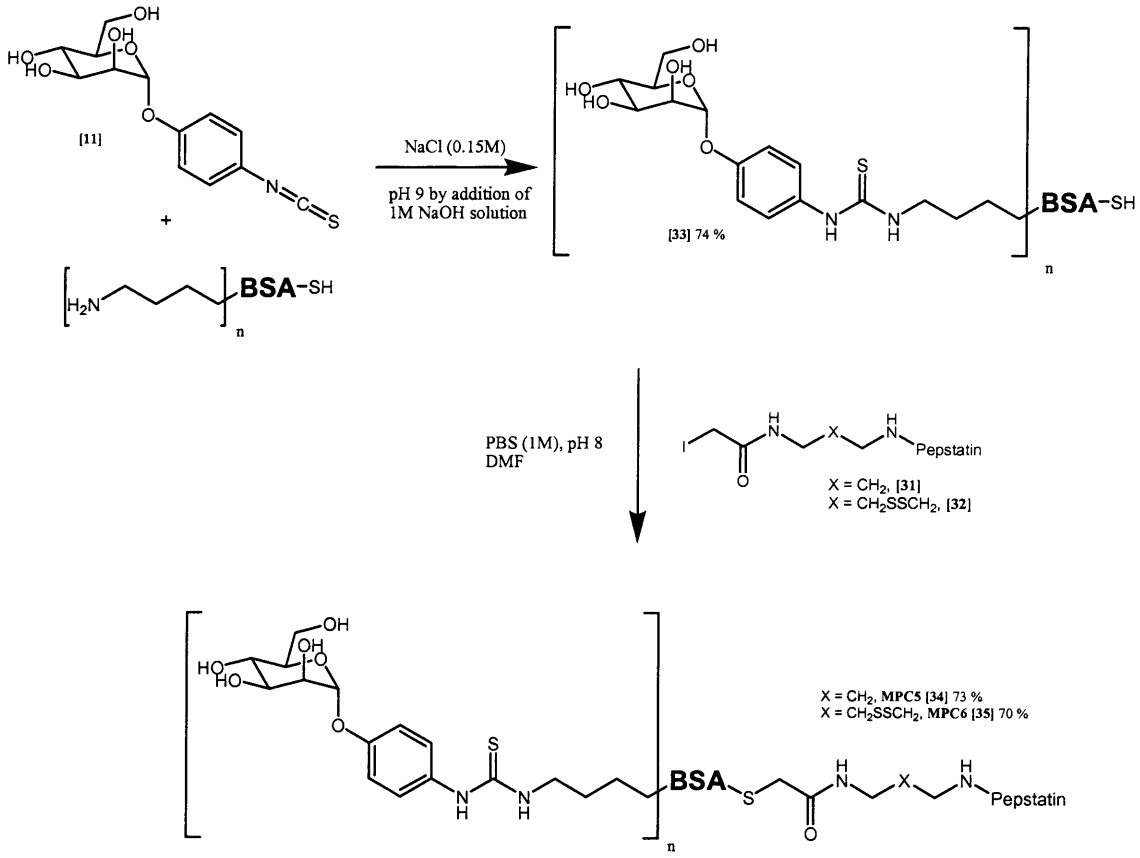

Figure 4.11: Formation of MPC5 [34] and MPC6 [35]

4.6 Attempted synthesis of hexalysyl derivatives MPC3 and MPC4

MPC3 and MPC4 are based on a hexalysyl backbone, with six mannosyl units attached to five lysine ε-amino groups and one α-amino N-terminal lysine, with another lysine containing an ivDde protecting group, the non-cleavable (MPC3) or cleavable (MPC4) inhibitor moieties being attached to the C-terminus of the peptide (fig. 4.12).

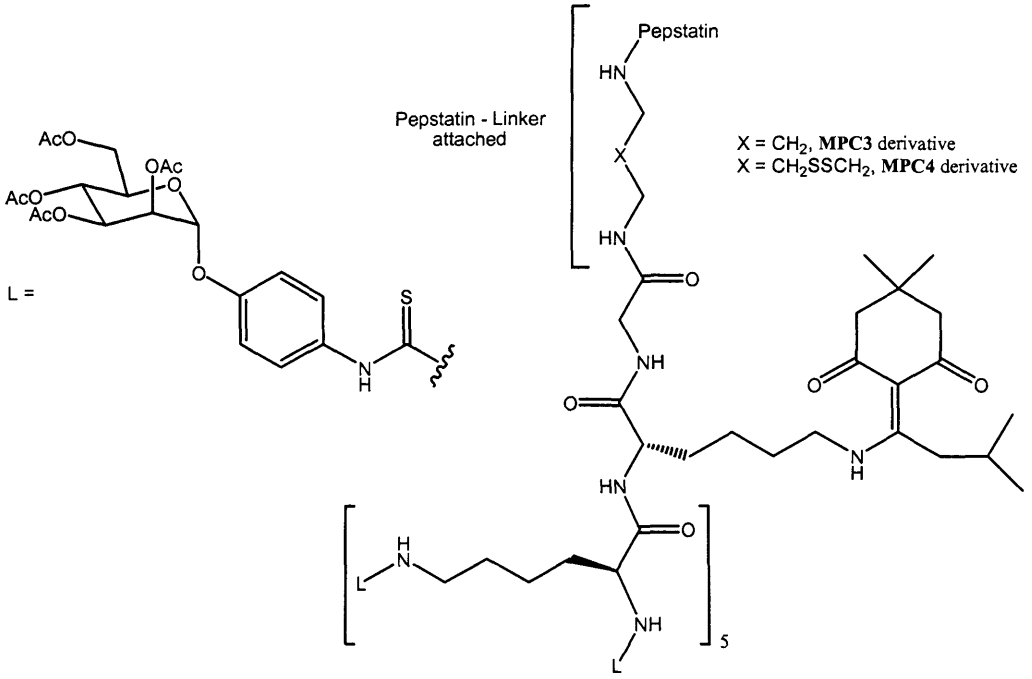

Figure 4.12: Structure of MPC3 / MPC4 inhibitors

4.6.1 Peptide synthesis

The initial strategy was to synthesise a hexalysyl carrier on a peptide synthesiser, H-(Lys(Boc))$_5$Lys(ivDde)-Gly-OH. Cleavage from the resin and removal of the attached Boc groups would thus give a linear peptide containing six free amine groups to which it would be possible to attach the mannosyl units. Cleavage from the resin and removal of the Boc groups was done in one step in the presence of TFA plus scavengers. Vigorous stirring for 4 hours was sufficient to remove the peptide from

the resin and deprotection of the Boc groups. For all peptides, removal of all solvent, precipitation with ether, and purification by preparative HPLC gave the required peptide as a crystalline white solid.

The experimental procedures in section 3.5 (page 133) give examples of the peptides upon which the most accurate analytical data was obtained at that time. These peptides (the free amino hexalysyl **[36a]** and **[36b]** and the fully Boc-protected hexalysyl **[37]**) were those chosen for subsequent steps in the synthesis. **[36a]** and **[37]** were peptides with mixed Dde / ivDde protecting groups, visible by NMR. In general, analysis to show the presence of products was difficult due to the size of compounds. NMR peaks were often very broad, allowing only a tentative assignment. Equally, ES MS was often insufficient due to the size of ions being too large for the detectors. Only multiply charged ions (i.e. from peptides containing free amino groups) gave obvious ion traces.

It was noted later on that derivatives containing the Dde group with free lysine ε-amino groups allowed migration of the Dde group to occur[239]. As such, some compounds were made with two protecting groups attached with an extra Dde being attached to any of the free ε-amino groups. This served to complicate the analysis of product formation.

4.6.2 Coupling of mannosyl units to hexalysyl peptide

The coupling of the isothiocyanatophenyl derivatives **[11]** to the hexalysyl peptide **[36a]** (i.e. that with free lysine amino groups) was attempted several times, initially with no success. It became clear that initial problems were solubility issues. The mannosyl derivative **[11]** is readily soluble in CH_2Cl_2, but crystallised in MeOH. The reverse was seen with the peptide. Inclusion of THF to a mixture of the two solvents increased the solubility of both reagents, and the reaction proceeded, although yields were low. An alternative solvent such as DMF might

have proved more successful. Figure 4.13 shows the structure of the product **[38]**.

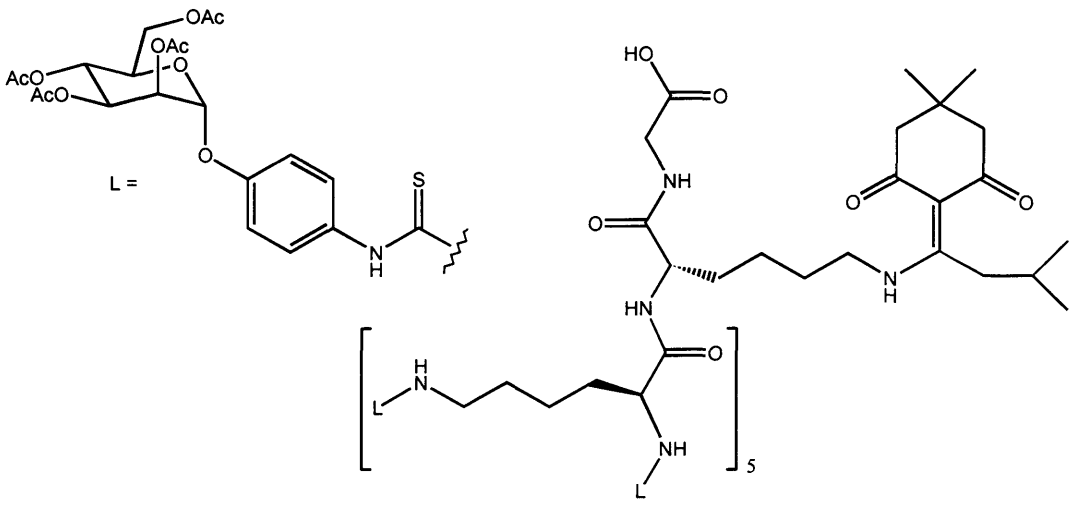

Figure 4.13: Structure of [38]

Two problems existed. Firstly, the large size and complexity of the product made it impossible to accurately assign the NMR chemical shifts, due to significant broadening of the spectral peaks. In addition, ES MS was unable to observe an ion trace as the size was too large, and no sufficiently ionisable groups were present to allow multiply charged ions. At the time, confirmation of the presence of product was only possible with the rough assignment of chemical shifts characteristic to each half of the reaction (i.e. observable proton signals for the lysine CH_2 protons, and observable benzyl signals). Attempts were made to couple this with pepstatin derivatives, however the difficulty in observing product formation and the likelihood that product formation may be difficult (no evidence showed coupling of pepstatin derivatives to the mannosyl – peptide **[38]**) due to steric interactions, suggested that an alternative approach for the synthesis of MPC3 / MPC4 would be desirable.

4.6.3 Coupling of pepstatin cystamine derivative [30] to hexalysyl peptide [37]

Given the problems with synthesis caused by attaching the mannosyl derivatives first, a different approach, coupling pepstatin – linker derivatives to Boc protected hexalysyl peptide **[37]** was sought. The first step was the coupling of pepstatin cystamine **[30]** to form compound **[39]** (fig. 4.14).

The NHS ester of the hexalysyl peptide **[37]** was formed by reaction with of EDCI and NHS for 32 hours. An aqueous workup (which was mildly acidic to reduce the chance of hydrolysis) was used. NMR of the crude NHS ester was ambiguous, so the intermediate was used directly. A slight excess of pepstatin cystamine **[30]** was added (DMF solvent) and the reaction stirred for 2 days. Purification gave a major product (60 % yield). Initially due to a lack of an MS ion, (even for MS samples treated with TFA to remove the Boc groups) it was felt that the isolated product was a mixture of starting materials. However, a more careful examination of the ES MS spectra (once considering the mixed Dde / ivDde situation) shows that the product may have actually been present. NMR signals were poorly resolved, but like mannosyl – peptide **[38]**, there were characteristic peaks of each of the coupled halves of the product **[39]**.

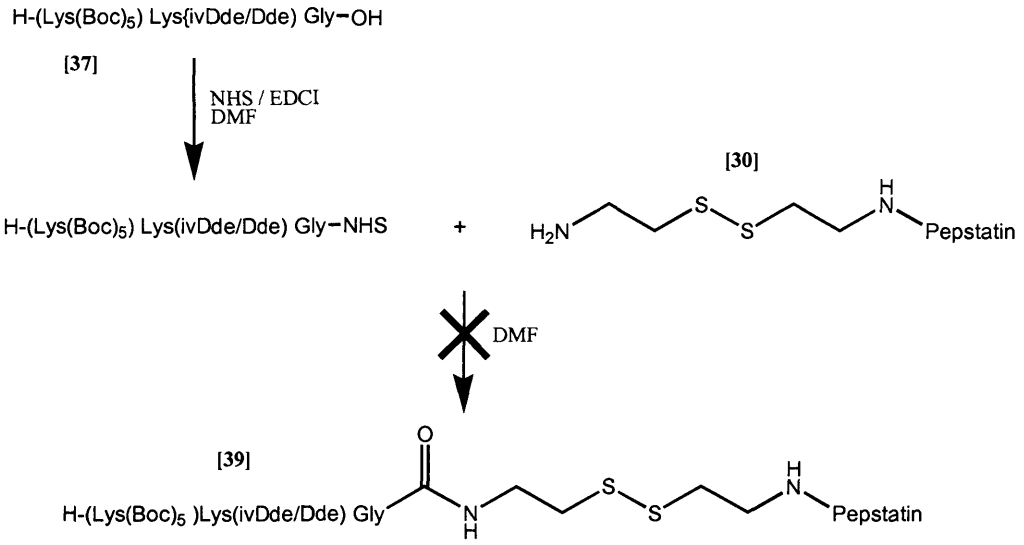

Figure 4.14: Attempted coupling of pepstatin - cystamine [30] to Boc-hexalysyl derivative [37]

Other attempts at coupling pepstatin – linker derivatives to carrier peptides (pepstatin propane-1,3-diamine **[29]** and pepstatin cystamine **[30]**) were unsuccessful for several of the previously mentioned difficulties. With limited time and resources available it was not possible to complete the synthesis of MPC3 and MPC4, however, several factors became apparent from the attempts in synthesis of these compounds that will become useful in future attempts.

Chapter 5

Methods for Biological Study

5.1 Tissue culture media and buffers

All cells were incubated at 37 °C, 5% CO_2 unless stated otherwise.

Complete RPMI 1640 medium

RPMI 1640 with L-Glutamine (Gibco, Paisley, UK)

10% Fetal Calf Serum (FCS; PAA Laboratories, Linz, Austria)

100U/ml Penicillin, 100µg/ml Streptomycin (both from Clare Hall Laboratories, ICRF, London, UK)

50µM 2-Mercaptoethanol (2-ME; Gibco)

Complete E4 medium

E4 low bicarbonate (ICRF)

5% FCS, 1% L-Glutamine (2mM, ICRF), 50µM 2-ME

100U/ml Penicillin, 100µg/ml Streptomycin

Complete Iscove's medium

Iscove's Modified Dulbecco's Medium (Gibco)

10% FCS, 1% L-Glutamine, 50µM 2-ME

100U/ml Penicillin, 100µg/ml Streptomycin

MEM

Modified Eagle Medium with HEPES (ICRF) and 2% FCS

Hanks buffered saline solution (HBSS) staining buffer

HBSS (Gibco), 10% rabbit serum

0.1% sodium azide (Sigma-Aldrich, Poole, UK)

IL-2 ELISA wash buffer

9.0g NaCl, 1ml Tween 20 (Sigma-Aldrich), H_2O to 1L, pH 7.4

IL-2 ELISA diluent buffer

PBS, 0.5% BSA (w/v; Sigma-Aldrich), 0.1% Tween 20, pH 7.4

5 x TBE buffer (per 400ml)

21.6g Tris base, 11g boric acid, 40ml 0.1M EDTA (all from Sigma-Aldrich)

5.2 Cells and tissue culture

A20 cell line

A20 is a murine B-cell lymphoma-derived cell line expressing I-A^d and I-E^d MHC class-II. A20 has been shown to express both cathepsin E (CE) and cathepsin D (CD), approximately 80% of the aspartic proteinase activity can be attributed to CE[112]. Cells were cultured in complete E4 medium. Cells were passaged every 2-3 days and maintained at a density of between 2 x 10^5/ml and 5 x 10^5 cells/ml.

DO11-10

DO11-10 is a T-cell hybridoma with I-A^d class II restriction and with specificity for the dominant epitope from chicken egg OVA (p323-p339). Cells were cultured in complete E4 medium. Cells were passaged every

2-3 days and maintained at a density of between 2 x 10^5/ml and 5 x 10^5cells/ml.

CTLL-2

CTLL-2 (a kind gift from Dr. B. Stockinger, NIMR, London, UK) is an IL-2-dependent CTL-derived human T-cell line. Cells were cultured in complete RPMI 1640 medium without PS and grown in flasks upright to maximise cell-cell contact. Cell were maintained at a density of 1 x 10^4 cells/ml and passaged every 3-4 days or when density reached 5 x 10^5 cells/ml.

X63

X63 (a kind gift from Dr. B. Stockinger, London), is a murine myeloma cell line continually secreting murine GM-CSF from an episomal vector carrying the neomycin resistance gene. Cells were cultured in complete Iscove's medium and passaged every 3-4 days. X63 were cultured with 1mg/ml G418 Sulphate (Gibco) to prevent loss of vector. To obtain medium containing granulocyte-macrophage colony-stimulating factor (GM-CSF), cells were washed three times in culture medium to remove traces of G418, and then cultured at 3 x 10^5 cells/ml for 24-36 hours. The supernatant (s/n) was frozen for long-term storage. For DC cultures, 10% of the s/n was added to the culture medium.

FSDC

FSDC, a kind gift from Dr. P. Castiglioni (Milan), is a transformed immature DC cell line. Cells were cultured in Iscove's complete medium and passaged at 3-4 day intervals by vigorous agitation or mild trypsinisation with 0.25% trypsin in versene.

Generation of murine bone-marrow derived DC

DCs were grown from murine femur bone marrow from F^4-F^8 mice generated by backcrossing cathepsin D +/– heterozygotes expressing I-A^b (a kind gift from Dr. C. Pieters[110]) with Balb/c mice expressing I-A^d. These mice (named B112 for convenience) were homozygous, heterozygous or wild type for cathepsin D, with low expression of I-A^k and high expression of I-A^d.

Murine femurs were removed and the bone marrow flushed out with MEM using a fine-gauge needle. The red blood cells were removed by re-suspending cells in 3ml of red blood lysing buffer (Gibco) for three mins and washing three times in MEM. Cells were cultured at 3-4 x 10^5/ml (10ml per flask) in complete Iscove's medium containing 10% GM-CSF s/n from X63 cell culture and 20mM HEPES. On day three, 8ml of the medium was removed (slowly with flask at an angle to avoid removing DC clusters), 5ml of MEM added slowly and the cells washed by gentle agitation. 5ml of the s/n containing non-adherent T-cells were removed and 8ml of fresh complete Iscove's medium (with GM-CSF and HEPES) added. On day five the cells were removed by slightly vigorous pipetting and placed into fresh Iscove's complete medium. The cells were ready for use on day six or seven, and were harvested by gentle pipetting to remove only non-adherent or slightly adherent T-cells. This cell population is defined as immature dendritic cells.

5.3 Antigen processing – method of study

The majority of the biological work presented is based upon a cellular antigen presentation assay. This assay studies the intracellular processing of antigen by aspartic proteinases. The study of cathepsin E within the lympoblastoid B-cell line A20 has been described previously. The majority (approximately 80%) of the aspartic protease activity within A20 cells is attributable to cathepsin E[112].

Figure 5.1 shows a diagrammatic representation of the antigen presentation assay. In brief, OVA antigen is added to A20 cells that take up and then degrade the protein into short peptides, a proportion of which are loaded onto class II MHC molecules. One of these peptides, the p323 peptide (known to be produced by cathepsin E), is loaded onto the I-A^d MHC class-II molecule. The T-cell hybridoma DO11-10 expresses a T-cell receptor that recognises this p323 peptide/I-A^d complex. Recognition stimulates the production of the cytokine IL-2. The presence of proteolytic inhibitors such as pepstatin leads to the inhibition of OVA processing, and thus p323 peptide production, leading to reduced IL-2 production. Secreted IL-2 in the cultures is measured either by ELISA or by ^3H thymidine incorporation in the indicator CTLL-2 cytotoxic T-cell line (T-cells that rapidly proliferate in the presence of IL-2).

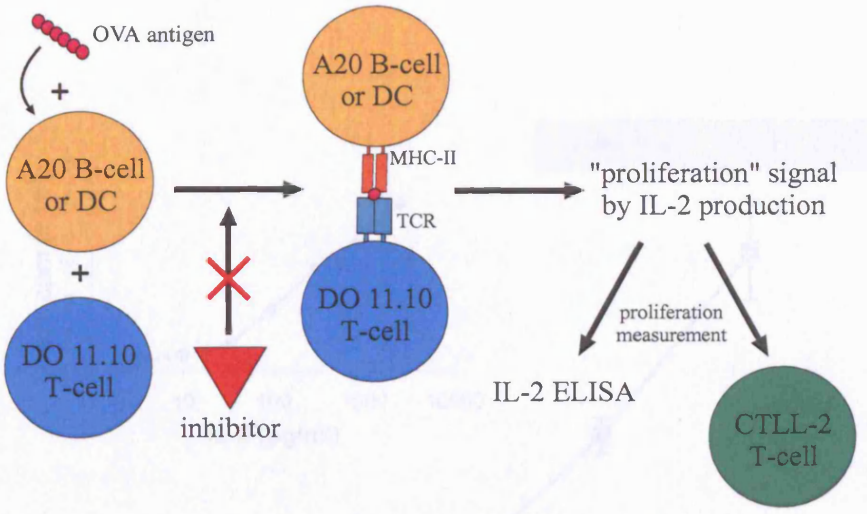

Figure 5.1: Schematic of antigen presentation assay used to measure cellular aspartic proteinase activity

A representative example showing OVA and p323 titrations using this standard assay is shown in figure 5.2. The minimum concentration of ovalbumin protein required to provide a sufficient quantity of processed antigen for MHC-II presentation is 0.5 mg/ml (approximately 10 μM). The amount of p323 peptide required however is significantly lower than that for OVA protein (less than 0.1μg/ml, 0.1μM), presumably because p323 peptide does not need uptake or processing, but can bind directly to the peptide-binding site of the MHC class-II molecule. Subsequent sections of this chapter describe the methods outlined above.

(a)

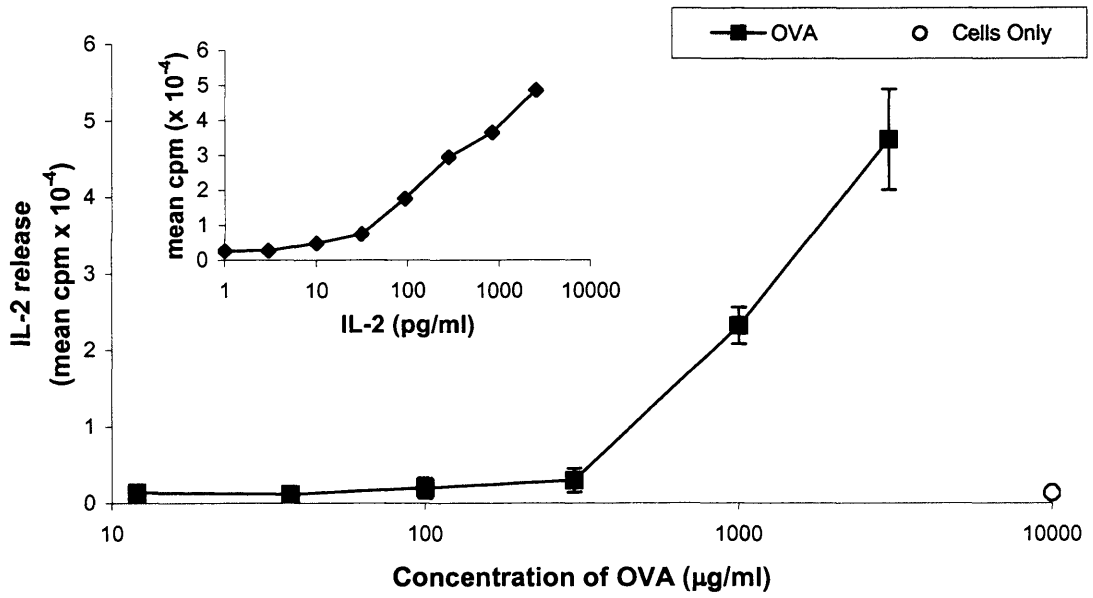

(b)

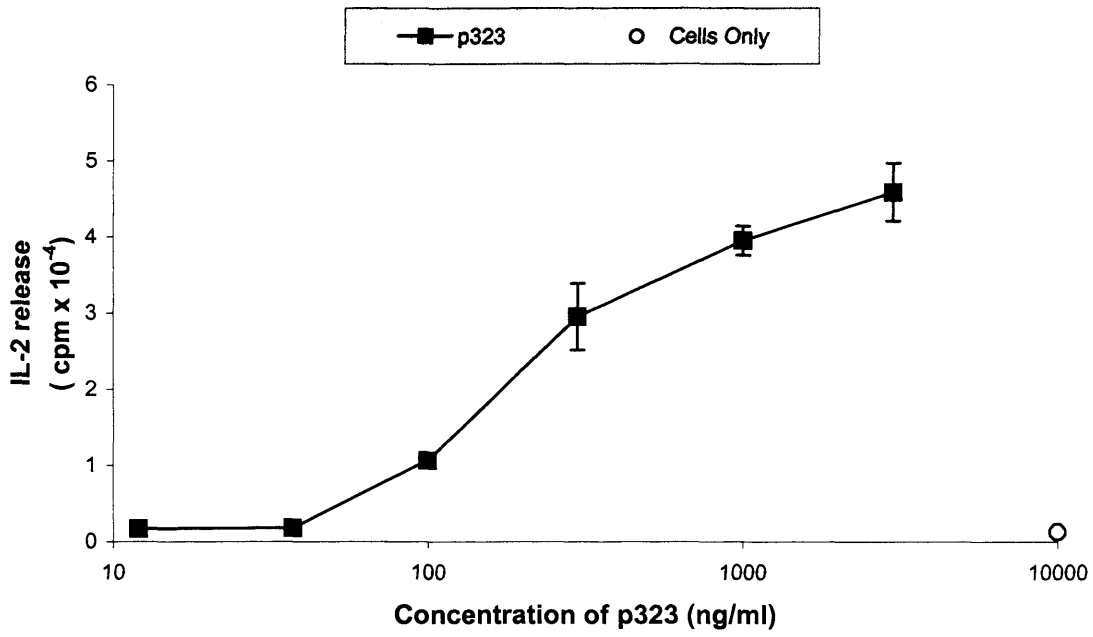

Figure 5.2: Response of DO11-10 cells to a) OVA and b) p323 peptide, presented by A20 B-cells. DO11-10 hybridoma T-cells (10^5) and A20 lymphoblastoid B-cells (10^5) were co-cultured together in the presence of a range of antigen concentrations for 24 hours and IL-2 release was measured by CTLL assay. Results are expressed as the mean ^{3}H-thymidine incorporation from triplicate cultures and are representative of four separate experiments. Graph a) shows the IL-2 standard curve

5.4 OVA and p323 peptide presentation assay

In order to determine the capacity of the APC used throughout the following studies to present processed whole antigen or synthetic antigenic peptides, IL-2 production was determined following the co-culture of murine DCs or A20, with DO11-10 cells in the presence of OVA or p323 peptide. All cells were washed in MEM before use. A20 or DO11-10 cells were added at a concentration of 5 x 10^4 cells/well in 50µl. DCs were used at 2.5 x 10^4 cells/well in 50µl. Antigen (ag) was included in a volume of 50µl, inhibitor solutions in 50µl, giving a total volume of 200µl for each assay. If A20 cells were used then complete E4 medium was used for all assay components. If DCs were used then complete RPMI 1640 medium was used as the medium.

All assays were performed in sterile, 96 well, flat bottomed tissue culture plates, and each condition was repeated in triplicate wells. In assays where the cell number was constant, either a range of ag doses or inhibitor concentrations were tested. OVA was dissolved in medium immediately before use to give a stock concentration of 20mg/ml, diluted further in medium to give the concentration required. OVA-peptide was dissolved in H_2O to give a stock concentration of 1mg/ml, and diluted in medium to give the concentration required. Inhibitor and inhibitor control solutions were used at varied concentrations from 216µM with threefold serial dilutions down to 800nM, or constant at several concentrations within this range. Inhibitors were added to DO11-10 & APC 30 mins prior to adding OVA or p323 peptide.

Triplicate wells containing only APC and DO11-10 but no ag were included as a negative control in order to determine the 'background' IL-2 levels, and included on all appropriate graphs as the 'Cells only' control. APC, DO11-10 & Ag, in the absence of inhibitor, defined the

positive control of maximum IL-2 production, and included on appropriate graphs as 'p323' or 'OVA' control. For inhibitors that included DMSO, a control of just DMSO only was used to assess the effect of DMSO on the assay. For MPC5 and MPC6, BSA – conjugate **[33]** was used as the control (see sections 3.4.12, page 130 and 4.5.1, page 156, for BSA – conjugate **[33]** description).

Cells, Ag and inhibitor were co-cultured for 24 hours at 37°C in 5% CO_2. Cells were briefly centrifuged, and 50µl of s/n from each well was removed and transferred to a new sterile, round-bottomed, 96 well tissue culture plate and stored at –20°C until use. Assay plates containing cells and extra s/n were also frozen and stored, allowing the IL-2 measurements to be repeated if necessary.
If a toxicity assay was performed then 100µl of the cells and supernatant were kept (thus 100µl removed from assay plate for IL-2 measurements) and used as for the procedure in section 5.7.

5.5 MPC inhibitor concentrations and controls

Pepstatin A (BaChem, Meyerside, UK), DMSO (Sigma-Aldrich) and all synthesised inhibitors (refer to chapter 3 for chemistry experimental procedures) were stored lyophilised, but stock concentrations were prepared in different solutions. Pepstatin A was stored frozen at –20 °C within DMSO, and diluted into distilled H_2O for use. Stock solutions of MPC1 and MPC2 were made up with a small amount of DMSO (as % required for experiment) before addition of distilled H_2O. MPC5 and MPC6 were dissolved in distilled H_2O. Table 5.1 shows the MW and calculated stock concentration of inhibitors used within assays.

Inhibitor	MW	Stock concentration
Pepstatin	686	$^{1}/_{75}$ of 16.2mg/ml = 216μM
MPC1	990	0.64mg/ml = 216μM
MPC2	1068	0.69mg/ml = 216μM
MPC5	~75,000	16.2mg/ml = 72μM
MPC6	~75,000	16.2mg/ml = 72μM
BSA – conjugate **[33]**	~74,000	16.2mg/ml = 72μM

Table 5.1: Inhibitor stock concentrations as used for assays

5.6 Quantification of IL-2 release with CTLL-2

In order to remove any exogenous IL-2, CTLL-2 cells were washed three times in MEM, rested at 37°C in full medium for 90 mins and washed a further two times. 50µl of complete medium containing 5 x 10^3 CTLL-2 cells were then added to each 50µl of supernatant from OVA / OVA-peptide presentation assay (see section 5.3). To quantify the amount of IL-2 produced within a presentation assay, a series of three-fold dilutions of IL-2 standard (from 2.5ng/ml) were included, again at 50µl/well. The assay was incubated at 37°C in 5% CO_2 for 24 hours. Cells were then incubated for a further 16 hours in the presence of 3.7 x 10^{-2} MBq ^{3}H-thymidine/well. Cells were then harvested and thymidine incorporation determined using the LKB Wallac-Rack beta liquid scintillation counter.

In some assays CTLL-2 proliferation / viability was measured using the MTT assay, rather than ^{3}H thymidine incorporation. 20µl per well of MTT (5mg/ml, Sigma-Aldrich) was added to cell cultures for the last 4 hours of 28 hours culture. Viable cells reduce the yellow MTT to a dark blue formazan. Cells were lysed by the addition of 100µl of 10% SDS/0.01M HCl and incubated at 37°C overnight. The optical density (OD) at 570nm ($OD_{570-630}$) was determined using a Dynax MRX_{TC} Revelation plate reader (Middlesex, UK).

5.7 Quantification of IL-2 release with IL-2 ELISA

96-well, Maxisorp, Nunc-Immuno plates (Merch Eurolab, Lutterworth, UK) were prepared by coating 100µl/well of mouse IL-2 capture antibody (0.5mg/ml, eBioscience, London, UK) diluted 1/400 with PBS, pH 7.4. ELISA plates were covered with cling film and kept overnight for 12-18 hours at 2-8°C. The plates were washed three times with wash buffer and 300µl/well of diluent buffer was added for two hours at room temperature. If the plates were not used immediately then they were stored for up to five days at 4°C. The plates were washed three times with wash buffer and 50µl of supernatant (or diluted supernatant) from OVA / OVA-peptide presentation assay (section 5.3, page 168) was added per well. Only duplicates of each condition of presentation assay were done. For negative control wells (i.e. cells only, medium only) 50µl of supernatant was added per well. For wells containing OVA / OVA – peptide then 50µl of two dilutions of 1/4 and 1/10 of supernatant in diluent buffer were used. A series of three-fold dilutions were also included of IL-2 from 1ng/ml. ELISA Plates were incubated at 37°C for 1½ hours.

The plates were washed three times with wash buffer and 100µl/well of a biotinylated anti-murine IL-2 antibody (0.5mg/ml; eBioscience) diluted 1/2,000 to 250ng/ml in diluent buffer was added and incubated at 37°C for 1 hour. The plates were then washed four times with wash buffer and 100µl/well of streptavadin-horse radish peroxidase (1mg/ml, eBioscience) diluted 1/13,3000 to 75ng/ml in diluent buffer was added and incubated at 37°C for 45 minutes. Plates were washed three times in wash buffer and then 100µl/well of TMB solution (Pharmingen, San Diego, USA) was added. After 10-15 mins was added 100µl/well of 1.8N H_2SO_4 to stop development of the blue colour. The OD was read at 450nm using a Dynax MRX_{TC} Revelation plate reader.

5.8 Measurement of cell viability within presentation assay

To determine the toxicity of reagents included in the OVA / OVA-peptide presentation assay (section 5.3, page 168) cell viability by MTT assay was used. 20µl per well of MTT (5mg/ml) was added to cell cultures for 4 hours after 24 hours of co-culture. Cells were lysed by the addition of 100µl of 10% SDS/0.01M HCl and incubated at 37°C overnight. The OD was determined at 570nm ($OD_{570-630}$) using a Dynax MRX_{TC} Revelation plate reader.

5.9 Measurement of cell viability of CTLL-2 cells

In order to remove any exogenous IL-2 prior to inclusion in any assay, CTLL-2 were washed three times in MEM, rested at 37°C in complete RPMI 1640 medium for 90 mins and washed a further two times and suspended in complete RPMI 1640 medium at 10^5/ml. 100µl/well of cell suspension was then added to a sterile, 96 well flat bottomed plate, to which was added 50µl of 50 Units/ml IL-2. 50µl of inhibitor and inhibitor control solutions were used at varied concentrations from 216µM with threefold serial dilutions down to 8µM. In all cases, the effective concentration of inhibitors was a quarter on addition to the other 150µl of assay. Triplicate wells containing CTLL-2 with or without IL-2, but no inhibitor, were included as controls. Cell viability was measured by using a standard MTT assay as described in section 5.6.

5.10 Determination of cellular endocytosis

FSDC or murine bone marrow-derived DC cells were washed in MEM before use. Cells were suspended in complete RPMI 1640 medium at 1 x 10^6 cells/ml. 50µl/well of cell suspension was added to sterile, 96 well round bottomed plates. For assays with BSA – conjugate or MPC5/6 addition, cells were pelleted and re-suspended in inhibitor solution in complete RPMI 1640 medium and pre-incubated for 15 mins at 37°C, 5% CO_2. For assays with cytochalasin D (Sigma-Aldrich), cells were pelleted and re-suspended in the appropriate cytochalasin D concentration in complete RPMI 1640 medium and pre-incubated for 30 mins at 37°C, 5% CO_2. 50µl/well of the yellow dyes fluorescein-dextran (FITC-DX; Sigma-Aldrich) or Lucifer Yellow (LY; Sigma-Aldrich) were added either at the fixed concentration of 2mg/ml or a three-fold dilution over a range of concentrations from 6mg/ml (3mg/ml in assay) and incubated at 37°C, 5% CO_2 for 1 hour. Background uptake was assessed by incubation of cells with dye at 4°C for 30 mins on ice. Uptake of all dyes was stopped by adding 100µl/well of cold PBS, 1% FCS, 0.1% azide. Cells were washed three times in cold PBS, 1% FCS, 0.1% azide and then re-suspended in cold PBS, 1% FCS, 0.1% azide, cell fluorescence was analysed by flow cytometry using a FACScan (Becton Dickinson, Twickenham, UK).

5.11 Flow cytometric analysis of DC phenotype

Expression of CD11c, CD86, DEC-205 and MHC class-II ($I\text{-}A^{d/b}$) on murine DC was analysed by flow cytometry. Murine bone marrow-derived DCs were washed and re-suspended at $5x10^5$/ml in HBSS staining buffer for 15 mins. Primary antibody was added for 30 mins. The cells were washed three times with staining buffer and incubated in FITC-conjugated rabbit anti-rat IgG antibody (1:50; DAKO A/S, Denmark) (or buffer only if using a directly conjugated primary antibody) and kept covered from light on ice for 30 mins. The cells were washed three times with staining buffer and re-suspended in 150µl of 2.5% formaldehyde in PBS and analysed by flow cytometry using a FACScan (Becton Dickinson).

5.12 Inhibition of cathepsin D / E – enzymatic studies

A fluorogenic substrate for cathepsin D and cathepsin E has previously been described as part of a sensitive assay for the detection of these enzymes. The substrate MOCAc-Gly-Lys-Pro-Ile-Leu-Phe-Phe-Arg-Leu-Lys(Dnp)γ-NH_2 is designed specifically to be cleaved by both of these enzymes. Under the supervision of Prof. T. Kageyama (Kyoto University, Japan) this peptide substrate was used in enzymatic competition assays to test the activity of pepstatin A and the modified MPC inhibitors[127]. Figure 5.3 shows in diagrammatic form how this assay works.

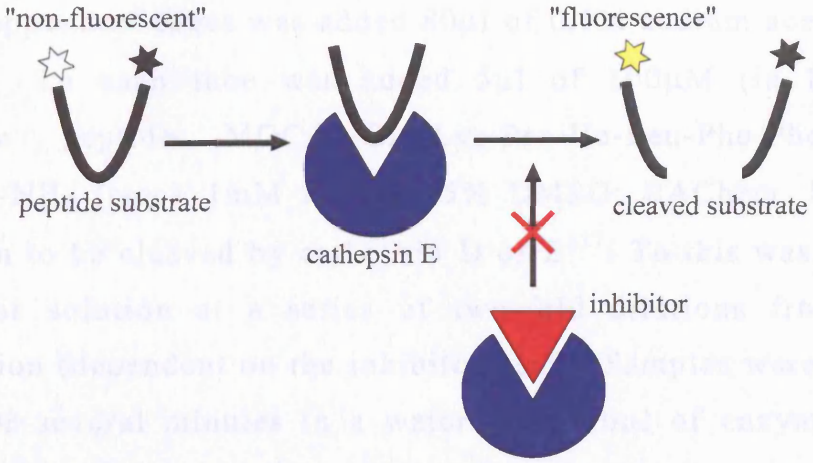

Figure 5.3: Schematic representation of the enzymatic competition assay used for test of the effect of inhibitors on cathepsin E

Initial tests used a variable quantity of fluorogenic substrate with a fixed quantity of enzyme and inhibitor to obtain data able to fit into a Lineweaver-Burk plot (data not shown). However, the data from this assay were highly variable between different experiments. An alternative method proposed by Dixon whereby the inhibitor concentration is changed and enzyme and substrate concentrations kept constant proved more successful[240]. Using the Dixon method it is possible to acquire data that follows the general equation shown in figure 5.4, and from a graph of % activatity vs. inhibitor concentration, approximate inhibitor IC_{50} values are obtainable.

$$\% \text{ activation} = \frac{F_s - C}{F_m} \times 100$$

F_m = maximum fluorescence (i.e. max. substrate, no inhibitor)

C = fluorescence of maximum substrate concentration alone

F_s = fluorescence at inhibitor concentration

Figure 5.4: Definition of % activation

Rat and monkey Cathepsin D / E was a kind gift of Prof. T. Kageyama (Kyoto University, Japan). Stocks are stored in 0.05M sodium acetate buffer, 50% glycerol, 0.25M NaCl, at –20°C.

To 0.5ml eppendorf tubes was added 80µl of 0.1M sodium acetate buffer (pH 4.0). To each tube was added 5µl of 100µM (in H_2O) of a fluorogenic peptide MOCAc-Gly-Lys-Pro-Ile-Leu-Phe-Phe-Arg-Leu-Lys(Dnp)γ-NH_2 (stock 1mM in H_2O, 5% DMSO; BAChem, Meyerside, UK) known to be cleaved by cathepsin D or E[127]. To this was added 5µl of inhibitor solution at a series of two-fold dilutions from various concentration (dependent on the inhibitor used). Samples were incubated at 37°C for several minutes in a water bath. 10µl of enzyme solution (0.01M sodium acetate buffer, pH 5.5) at 0.5µg/ml was added to each sample, and the reaction was allowed to continue at 37°C for 30 mins before adding 200µl of 5% trichloroacetic acid to precipitate the enzymes. Negative / positive controls were included as a sample without enzyme, or contained no inhibitor, respectively. Samples were centrifuged at 13,000rpm for a few seconds before reading OD (excitation 328nm, emission 393nm) using a Hitachi fluorescence spectrophotometer (Hitachi, Japan).
Data were analysed by the Dixon method[240] plotted as fluorescence (converted to % activity) vs. inhibitor concentration to obtain the IC_{50} value for the appropriate inhibitor.

5.13 Assessment of cellular mycoplasma levels by PCR and gel electrophoresis

This protocol is based on the Stratagene Mycoplasma PCR test (Amsterdam, the Netherlands) for the detection of most Mycoplasma infections. Cells were assessed for mycoplasma infection every 4-6 months. To external DNA contamination, all solutions were UV irradiated. PCR were run with and without an internal control to approximate the level of Mycoplasma infection, the control giving a single band at 420-bp. A positive control (*Mycoplasma orale*) was also

used. Supernatant from confluent grown cell cultures grown in the absence of antibiotic were used.

100µl of s/n was boiled for 5 mins before cleaning the DNA using Strataclean Resin (Stratagene) to prepare a template for PCR (as described in stratagene instructions). Templates can be stored at –20°C for several days if not used immediately. The following stock was prepared for PCR; the total volume needed being twice the number of templates (with / without internal control) plus three (positive / negative / internal controls only):

27.2µl H_20, 0.4µl dNTP (25mM stock; Sigma-Aldrich)

0.4µl Taq DNA polymerase (2.5U/µl stock; Promega, Wisconsin, U.S.A.)

5µl 10x Buffer, 3µl of 25mM $MgCl_2$ (both provided with Taq DNA polymerase)

2µl Primers (5µM of each primer, provided with stratagene mycoplasma PCR set)

The stock was divided into controls and two sets per sample to be tested. For the Internal control set, 2µl of internal control (provided with Stratagene Mycoplasma PCR set) was added, otherwise 2µl of water was added. For the positive / negative control set, 10µl of positive control / water was added to the appropriate reaction tube, respectively. 10µl of template was added to each sample, and all samples covered with a drop of mineral oil, and run using a Perkin Elmer Cetus DNA thermal cycler (refer to Stratagene Mycoplasma protocol). PCR samples were mixed with loading buffer and run on a 3% agarose gel at 100mV for ~30mins in TBE buffer. The first and last lanes contained 100bp DNA molecular marker set (Promega).

5.14 Screening of mouse cathepsin D genotype by PCR

DNA was prepared from B112 mouse (see section 6.5.1, page 213) tail snips as follows. Tail snips were placed into Eppendorf tubes containing 500µl of 0.2% SDS, 0.1M Tris pH 8.5, 5mM EDTA, 200mM NaCl in H_2O, and 5µl proteinase K solution (10mg/ml Proteinase K in H_2O). The tubes were agitated for 3-4 hours at 55°C, after which they were centrifuged for 10 secs at 13,000RPM, and the s/n was tipped into 500µl of propan-2-ol. The solution was mixed by inversion until DNA precipitation occurred. The DNA was removed with the tip of a micropipette and added to 200µl H_2O and incubated at 37°C for 2hrs. 2µl of each DNA sample were added to a PCR mixture [0.3µl Taq DNA polymerase, 2.5µl 10x buffer, 3µl $MgCl_2$ (all three from promega), 1.2µl dNTP (10mM; Sigma-Aldrich), 0.5µl each of Primer 1 and 2 (CatD forward = TTGGAGAGTTAGCCTGAGCTACTG, CatD reverse = CCTCAGCTGTAGTTGCTCACATGA, Sigma-Aldrich) and 12µl of purified H_2O]. PCR reaction was run using a Perkin Elmer Cetus DNA thermal cycler with a hot start at 95°C and 35 cycles (1min @ 95°C, 2min @ 58°C, 3min @ 72°C) and analysed on a 1% agarose / 0.5 M TBE gel.

Using the above primers, disrupted cathepsin D genes (that contain a neomycin cassette, and present in heterozygous or homozygous cathepsin D mice) gave a PCR amplification product with DNA bands of ~1.5 Kb in size (see figure 5.5 for gene map). These bands are stronger in homozygous mice. Wild-type cathepsin D gene gives a ~280 bp band in either heterozygous or wild-type cathepsin D mice (stronger band in wild-type mice).

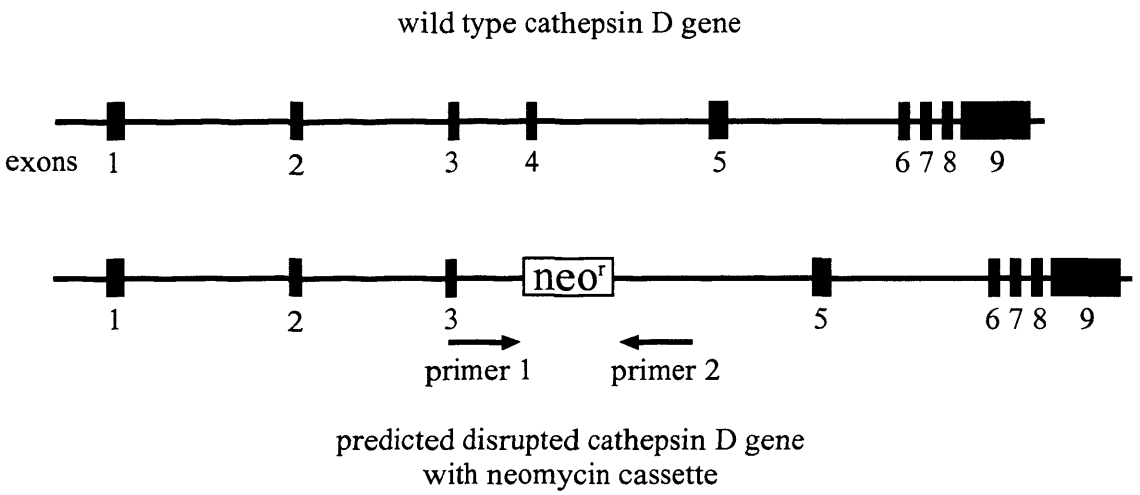

Figure 5.5: Map of wild type and disrupted cathepsin D gene

Chapter 6

The Use of pepstatin inhibitors in dissecting the role of cathepsin E

6.1 Pepstatin A as an inhibitor of the aspartic protease cathepsin E

The use of pepstatin as a potent inhibitor is restricted because of inadequate solubility, poor cell permeability, lack of specificity for either cell or protease, and at high concentrations, toxicity. The effect of pepstatin A upon antigen processing and presentation within the models used in this thesis (section 5.3, page 168) is used as the standard for comparison with other modified pepstatin A inhibitors.

6.1.1 The inhibitor pepstatin A is able to inhibit the enzymatic cleavage of a peptide substrate for rat cathepsin E

Figure 6.1 shows the inhibition of rat cathepsin E (50 ng/ml) activity by variable concentrations of pepstatin A (from 30 – 240 pM). An IC_{50} of 77 ± 4 pM is obtained for pepstatin A based on the results of three experiments.

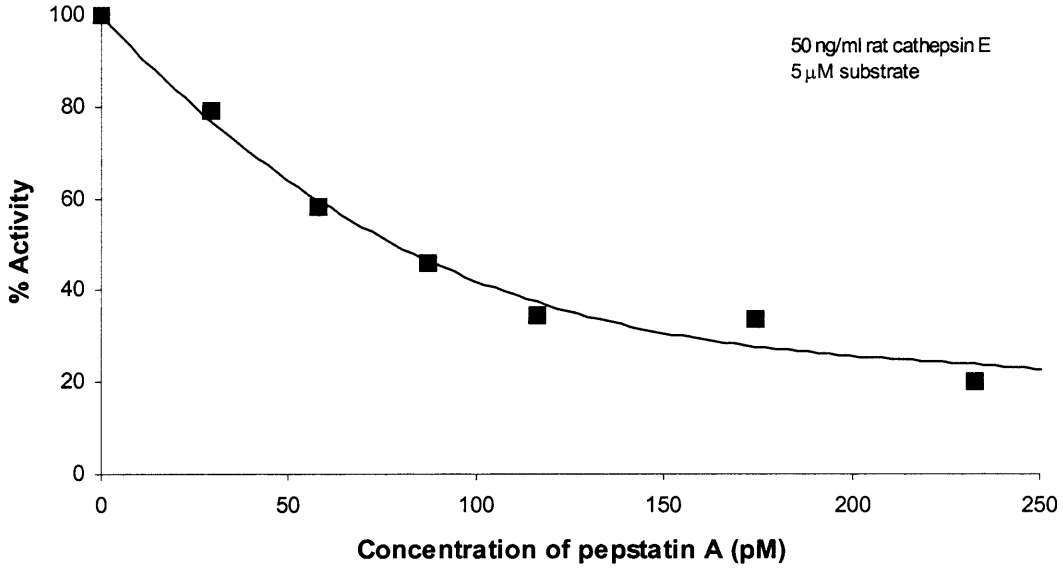

Figure 6.1: Inhibition by pepstatin A of the enzymatic cleavage of fluorogenic substrate MOCAc-Gly-Lys-Pro-Ile-Leu-Phe-Phe-Arg-Leu-Lys(Dnp)γ-NH_2 (5 ng/ml) by rat cathepsin E (50 ng/ml). Details of the assay method are listed in section 5.12. Results are representative of three experiments and expressed as % activity *vs* pepstatin A concentration

6.1.2 Pepstatin A can inhibit DO11-10 response to OVA but not OVA peptide p323 when presented by A20 cells

A representative example of the effect of pepstatin A on IL-2 release from DO11-10 cells upon incubation with A20 cells and either OVA or OVA peptide p323 is shown in figures 6.2, 6.3 and 6.4. Pepstatin A inhibits IL-2 release by DO11-10 cells in a dose dependent manner when in the presence of OVA antigen and A20 cells (fig. 6.2a). 54μM of pepstatin A almost completely inhibits IL-2 release. Some of this effect, however, is due to the presence of DMSO, its effect also being dose dependent (fig. 6.2a). The difference between the effect of Pepstatin / DMSO and DMSO alone is statistically significant (fig. 6.4a). At this high concentration of pepstatin (54 μM), there is also a major effect of pepstatin on the presentation of p323 peptide (fig. 6.2b), a process that does not require antigen processing. Much of this effect is due to the presence of DMSO (fig. 6.2b).

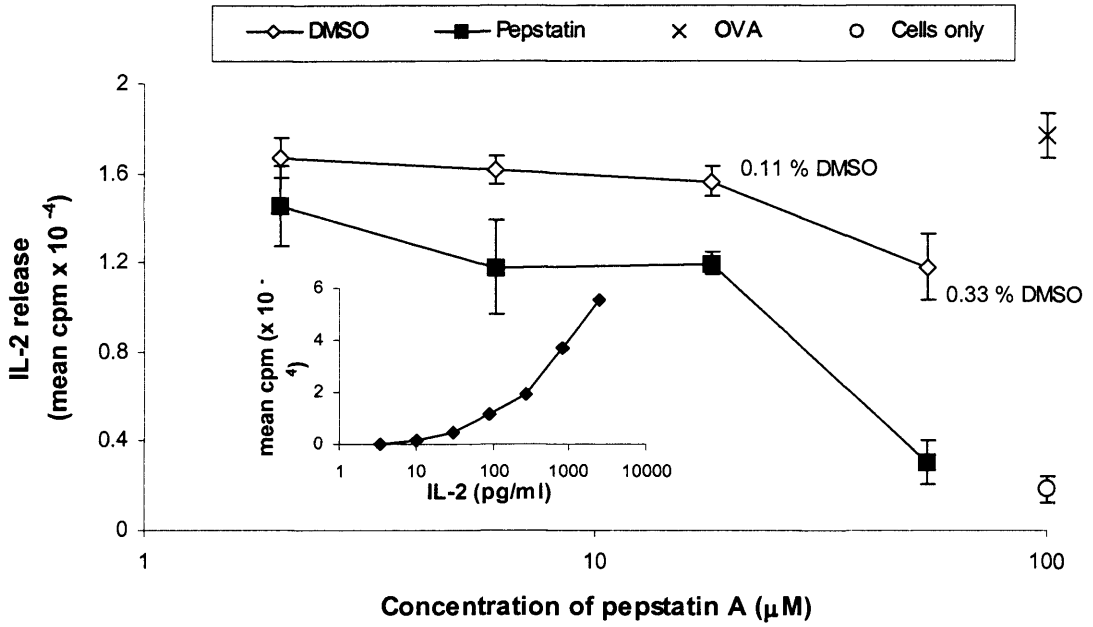

Figure 6.2a: Response of DO11-10 cells to OVA (0.5mg/ml), presented by A20 cells with varied concentrations of pepstatin A / DMSO or DMSO alone. IL-2 release measured by CTLL assay. Results are expressed as the mean ^{3}H-thymidine incorporation from triplicate cultures and are representative of six different experiments. Graph includes the IL-2 control for graphs shown in figure 6.2a and figure 6.2b. The OVA positive control is cells and OVA protein.

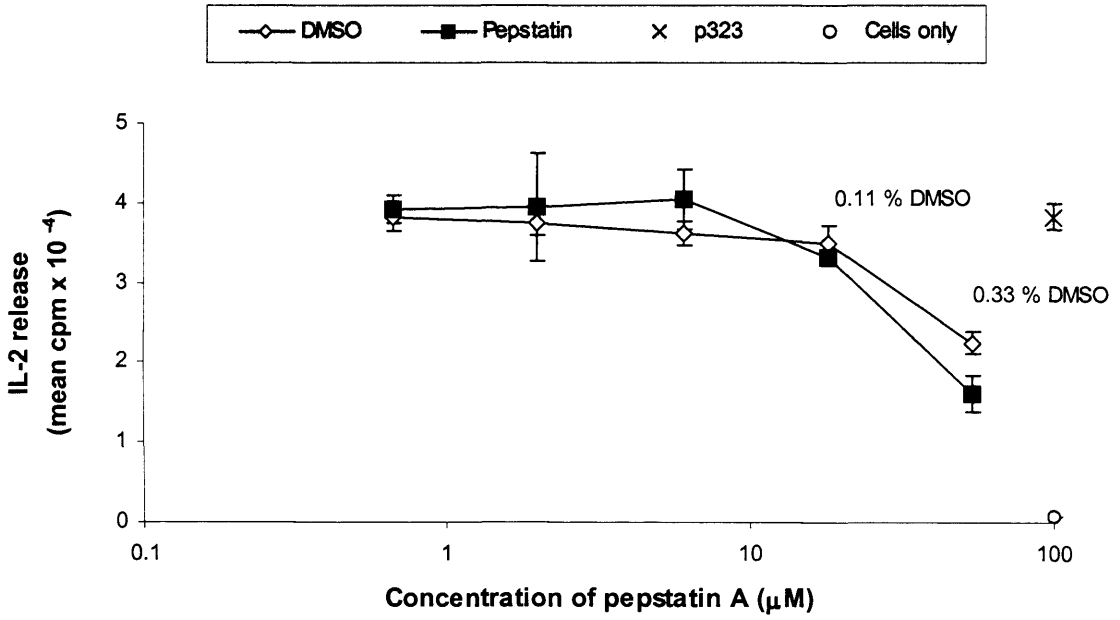

Figure 6.2b: Response of DO11-10 cells to p323 peptide (0.05μg/ml), presented by A20 cells with varied concentrations of pepstatin A / DMSO or DMSO alone. IL-2 release measured by CTLL assay. Results are expressed as the mean ^{3}H-thymidine incorporation from triplicate cultures and are representative of six different experiments. The p323 positive control is cells and p323 peptide.

Figure 6.3 shows the effect of Pepstatin and DMSO on viability of OVA-treated and p323-treated A20 cells. Pepstatin / DMSO or DMSO alone are slightly toxic at the highest concentrations used (0.33 %, figure 6.3). There is an observed cell death of up to 30 % with pepstatin / DMSO, and slightly lower for DMSO (fig. 6.4b). Taken together, these data suggest that pepstatin has a significant inhibitory effect on antigen processing. However, some of this effect is due to DMSO-related inhibition, and non-antigen processing inhibition or cellular toxicity of pepstatin and DMSO. It was not possible to decrease the amount of DMSO present by increasing the concentration of pepstatin A in the stock DMSO solution further, since this resulted in the appearance of crystalline insoluble pepstatin aggregates in the cultures. The toxicity of DMSO is substantially reduced at 0.11 % while pepstatin A (18 μM) inhibits by 50 – 60 % (fig. 6.4a). At this concentration, the effect on p323 presentation to DO11-10 cells (fig. 6.4a) and the % assay cell death (fig. 6.4b) is minimal

(a)

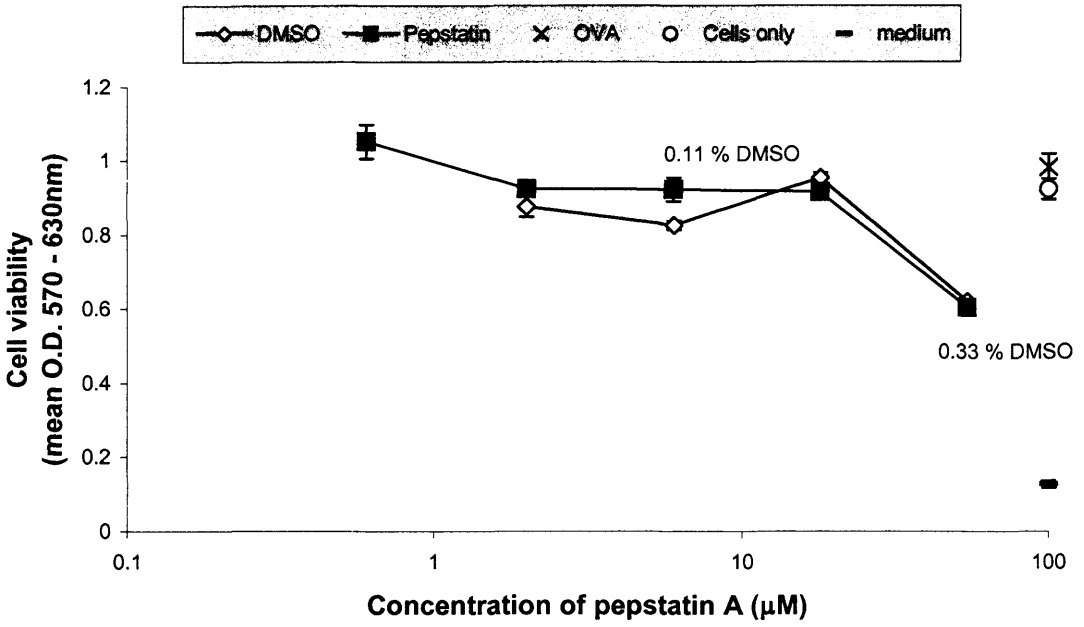

(b)

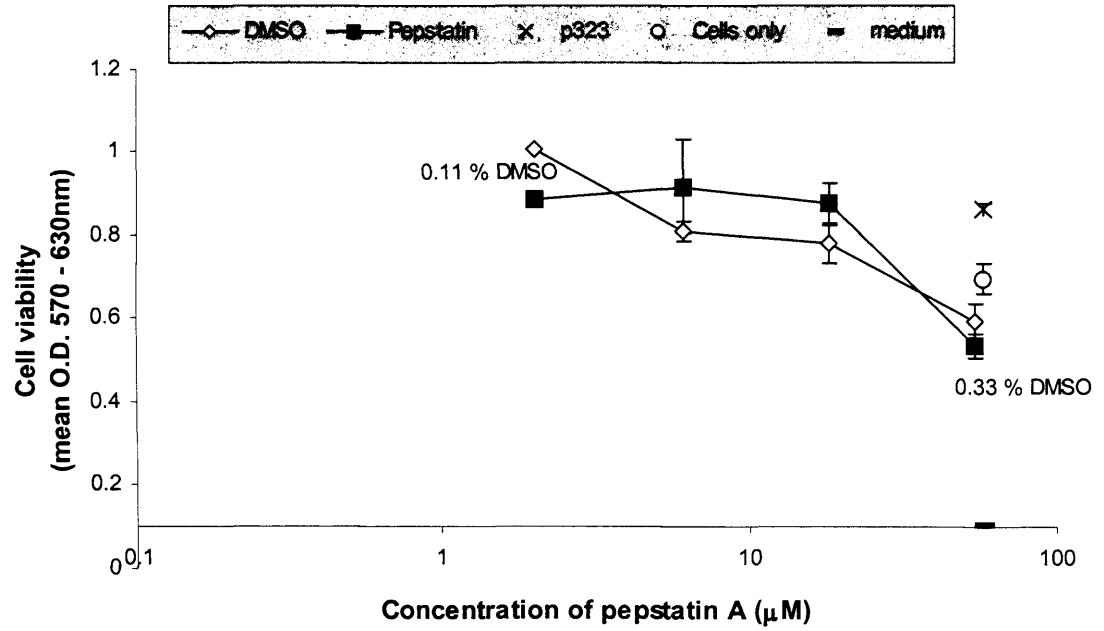

Figure 6.3: Cell viability of cells in antigen presentation assay (shown in figure 6.2): response of DO11-10 cells to a) OVA (0.5mg/ml) and b) p323 peptide (0.05μg/ml), presented by A20 cells with varied concentrations of pepstatin A and DMSO. Cell viability measured by MTT incorporation and expressed as the mean O.D. (570 – 630 nm) from duplicate cultures. Results are representative of six different experiments. The p323 / OVA, cells only and medium only controls are also included

(a)

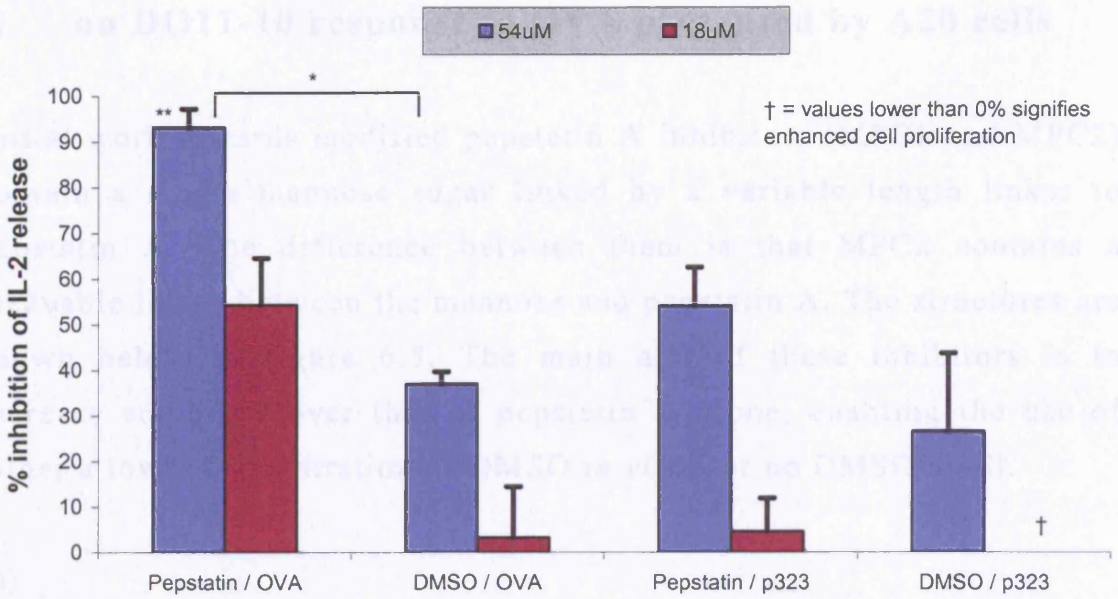

(b)

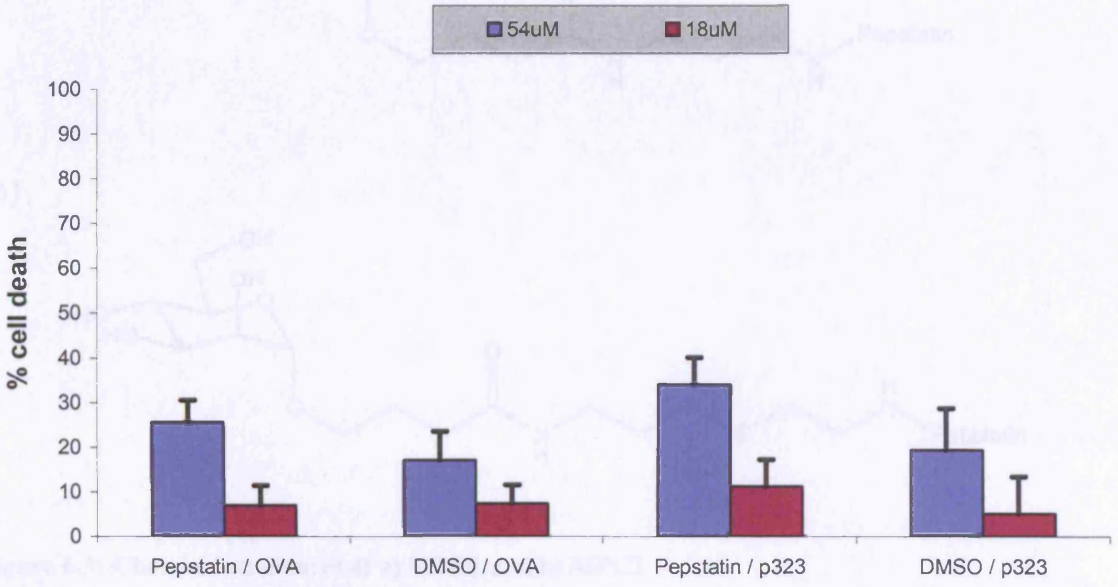

Figure 6.4: The effect of Pepstatin on a) OVA or p323 presentation by A20 cells and b) cell viability. Both graphs show the results with 54μM Pepstatin and its equivalent DMSO concentration (0.33%), and 18μM Pepstatin and its equivalent DMSO concentration (0.11%).

% inhibition of IL-2 release calculated for experimental point as 100 – [(IL-2 production in presence of inhibitor / IL-2 production in absence of inhibitor) x 100]. Background IL-2 in absence of antigen was subtracted from all values before the calculations. % cell death was calculated as 100 – [(viability in presence of inhibitor / viability in absence of inhibitor) x 100]. Results show the mean +/- SEM of at least four separate experiments. * $p < 0.05$ *versus* OVA/DMSO control, ** $p < 0.01$ *versus* OVA/medium control

6.2 MPC1 / MPC2 aspartic protease inhibitors and effect on DO11-10 response to OVA presented by A20 cells

Initial work towards modified pepstatin A inhibitors (MPC1 and MPC2) contain a single mannose sugar linked by a variable length linker to pepstatin A. The difference between them is that MPC2 contains a cleavable linker between the mannose and pepstatin A. The structures are shown below in figure 6.5. The main aim of these inhibitors is to increase solubility over that of pepstatin A alone, enabling the use of either a lower concentration of DMSO *in vitro*, or no DMSO at all.

(a)

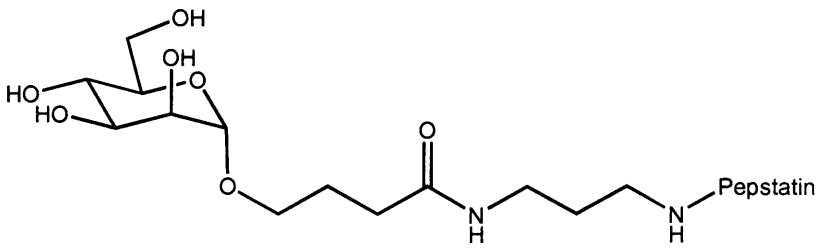

(b)

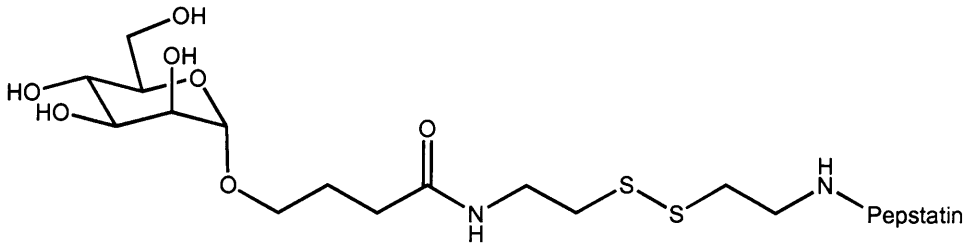

Figure 6.5: Chemical structures of a) MPC1 and b) MPC2

6.2.1 MPC1 and MPC2 inhibit the enzymatic cleavage of a peptide substrate for rat cathepsin E, at a similar level to pepstatin A

Using the Dixon method[240], data for the inhibition of cleavage of fluorogenic substrate by rat cathepsin E was obtained. Figures 6.6 and 6.7 show a representative plot of this data for MPC1 and MPC2 respectively.

IC_{50} values are in the picomolar range, and similar to that of pepstatin. MPC1 (n = 3), IC_{50} = 133 ± 23 pM. MPC2 (n = 4), IC_{50} = 86 ± 47 pM. This data shows that the attachment of a small linker and sugar unit does not cause any reduction in the inhibitory effects of pepstatin A.

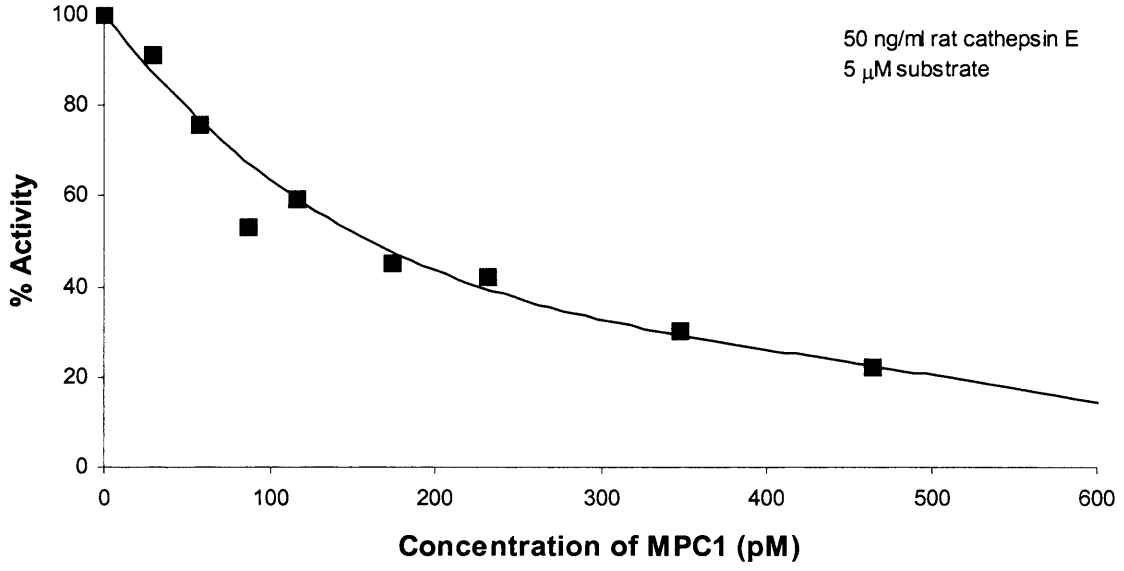

Figure 6.6: Inhibition by MPC1 of the enzymatic cleavage of fluorogenic substrate by rat cathepsin E. Results are representative of three experiments and expressed as % activity against MPC1 concentration

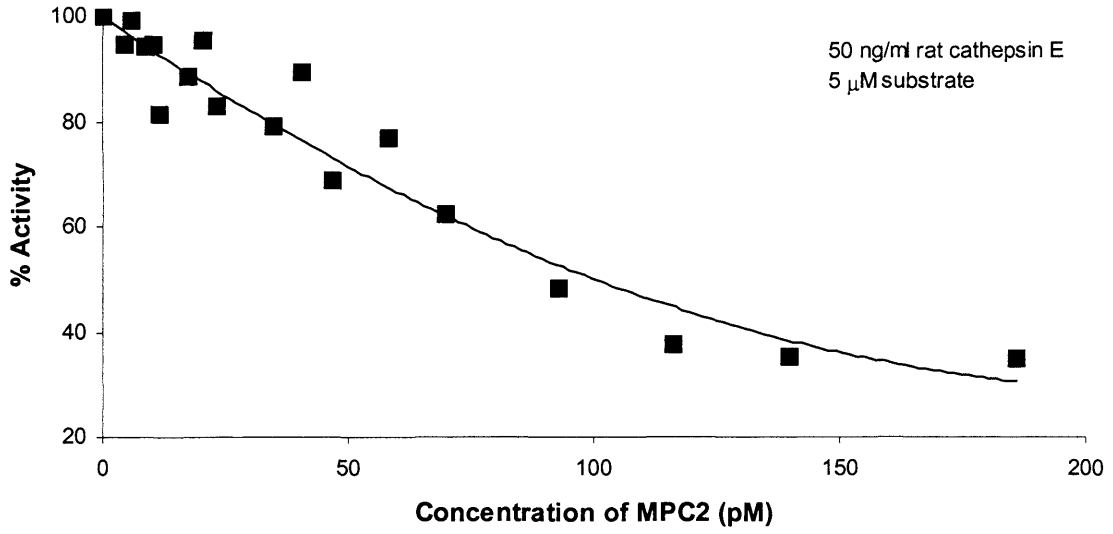

Figure 6.7: Inhibition by MPC2 of the enzymatic cleavage of fluorogenic substrate by rat cathepsin E. Results are representative of four experiments and expressed as % activity against MPC2 concentration

6.2.2 The effect of MPC1 dissolved in water on the DO11-10 response to A20 cells pulsed with OVA antigen

It was evident during synthesis of MPC1 that its solubility was considerably greater than that of pepstatin A alone. MPC1 had excellent solubility in organic solvents, especially methanol. The solubility in water was much higher than that of pepstatin. At high concentrations of MPC1 (> 0.5 mM) a slight cloudiness was visible, but at the lower concentrations used in assays (<54 μM) the compound appeared to be completely water soluble.

Figure 6.8a shows the effect of MPC1 (stock solution in water) on IL-2 release by DO11-10 T-cells upon incubation with A20 cells and OVA antigen. Cell viability for this assay is shown in figure 6.8b. The almost complete inhibition of IL-2 release observed in figure 6.8a at higher concentrations of MPC1 (54 μM) is mainly attributed to cellular toxicity,

as shown by figure 6.8b. Observation of the wells of the assay containing higher concentrations of MPC1 showed the presence of a crystalline material (fig. 6.9). The serial dilution of MPC1 directly in the culture wells of an assay or separately before adding to each well did not change the outcome. MPC2 was also tried in a limited number of experiments with similar results.

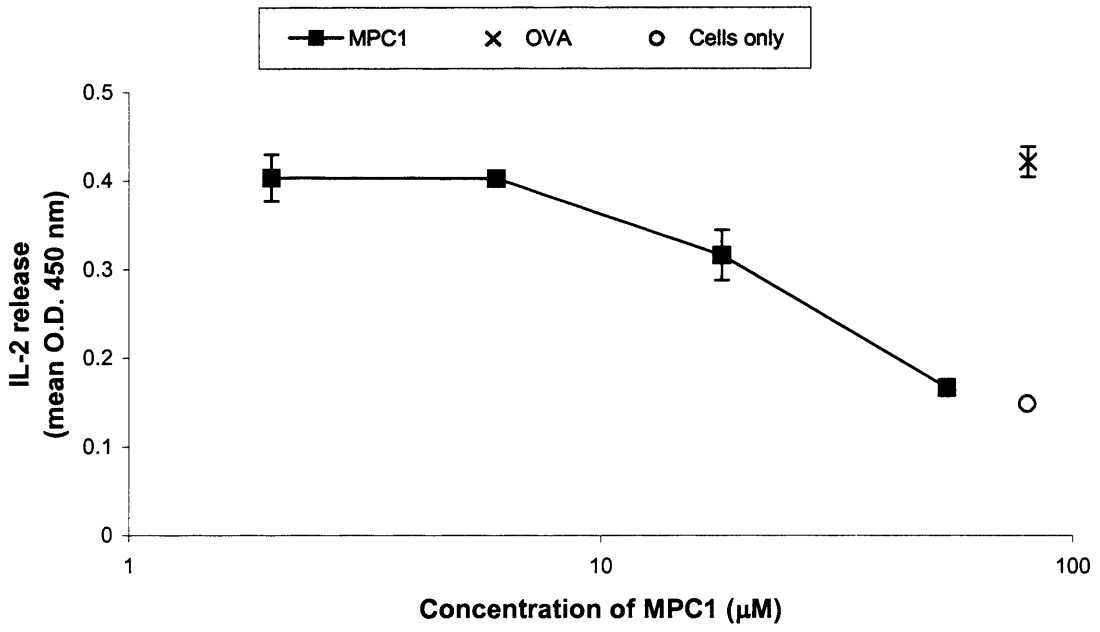

Figure 6.8a: Response of DO11-10 cells to OVA presented by A20 cells: varied concentrations of MPC1 (dissolved in water). IL-2 release by DO11-10 cells, measured by IL-2 ELISA and expressed as the mean O.D. (450 nm) from duplicate cultures. Results are representative of six separate experiments. Experiment uses 1mg/ml OVA

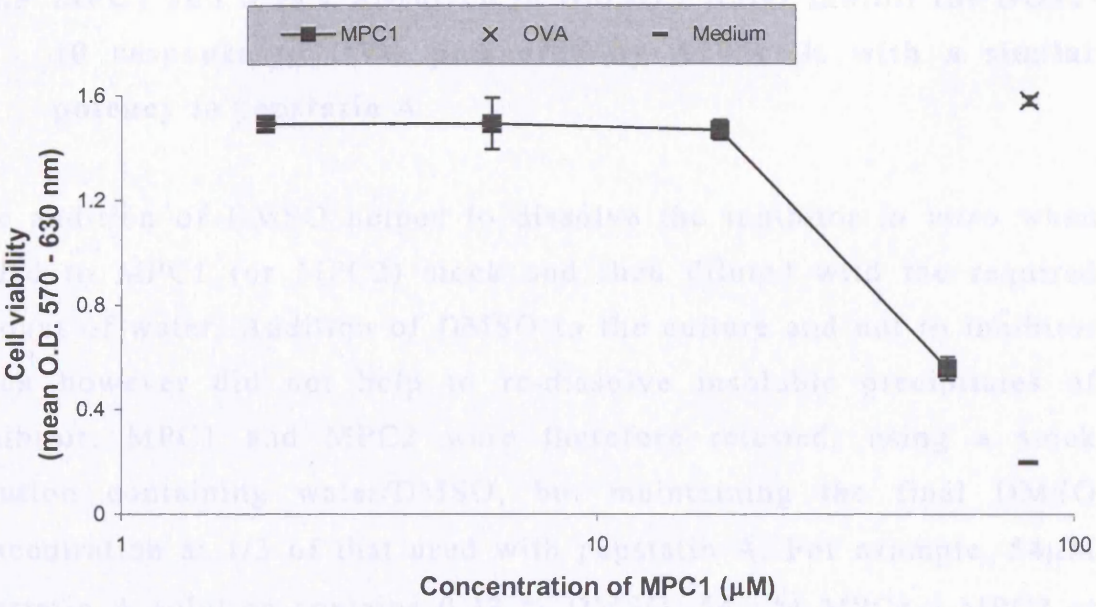

Figure 6.8b: Cell viability of assay shown in figure 6.8a. measured by MTT incorporation and expressed as the mean O.D. (570 – 630 nm) from triplicate cultures. Results are representative of six separate experiments

(a) (b)

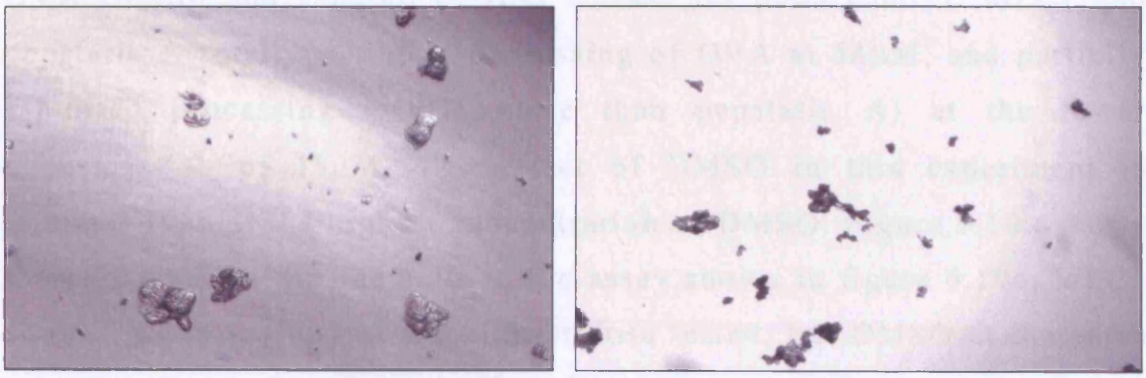

Figure 6.9: Light microscope pictures at 4,000 x magnification of MPC1 and MPC2 dissolved in water (25 %) and E4 culture medium (75 %). a) MPC1, b) MPC2. The solubility of MPC1 / MPC2 was much reduced in culture medium (containing salts, proteins etc.) compared to its solubility in water (not shown) causing dissolved inhibitor to crystallise out of solution in the culture wells

6.2.3 MPC1 and MPC2 dissolved in DMSO / water inhibit the DO11-10 response to OVA presented by A20 cells with a similar potency to pepstatin A

The addition of DMSO helped to dissolve the inhibitor *in vitro* when added to MPC1 (or MPC2) stock and then diluted with the required amount of water. Addition of DMSO to the culture and not to inhibitor stock however did not help to re-dissolve insoluble precipitates of inhibitor. MPC1 and MPC2 were therefore retested, using a stock solution containing water/DMSO, but maintaining the final DMSO concentration at 1/3 of that used with pepstatin A. For example, 54μM pepstatin A solution contains 0.33 % DMSO. 54 μM MPC1 / MPC2 at 54μM would therefore contain 0.11 % DMSO.

Figure 6.10a shows the effect of MPC1, pepstatin A and DMSO on the response of DO11-10 cells to OVA presented by A20 cells. IL-2 control is not shown for brevity, but IL-2 release was at levels similar to previous experiments with approximately 400 pg/ml of IL-2 release for OVA control and 1 ng/ml of IL-2 release for p323 control. MPC1 and pepstatin A totally inhibited processing of OVA at 54μM, and partially inhibited processing (MPC1 more than pepstatin A) at the lower concentration of 18μM. The effect of DMSO in this experiment is minimal even at the highest concentration of DMSO. Figure 6.10b shows the cell viability for the cells in the assay shown in figure 6.10a. MPC1 showed some toxicity at the highest dose tested, but DMSO at the same concentration had a minimal effect. The difference between pepstatin and MPC1 in their effect to decrease IL-2 release is likely to be due to differences in cell viability, as shown by comparing figure 6.10a to figure 6.10b.

(a)

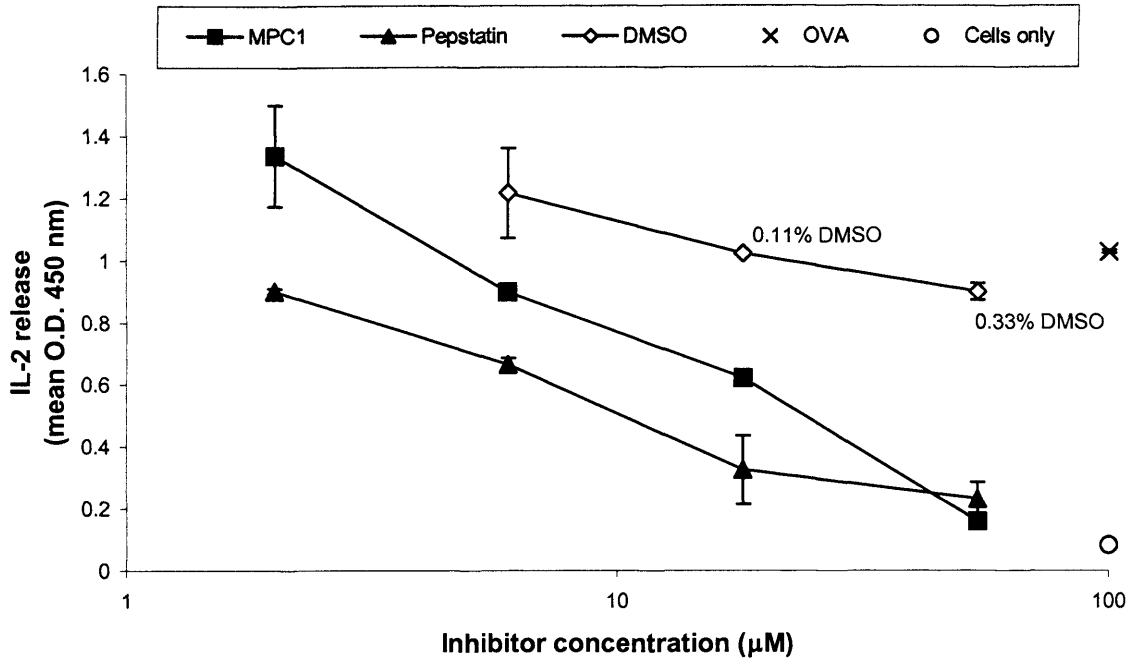

(b)

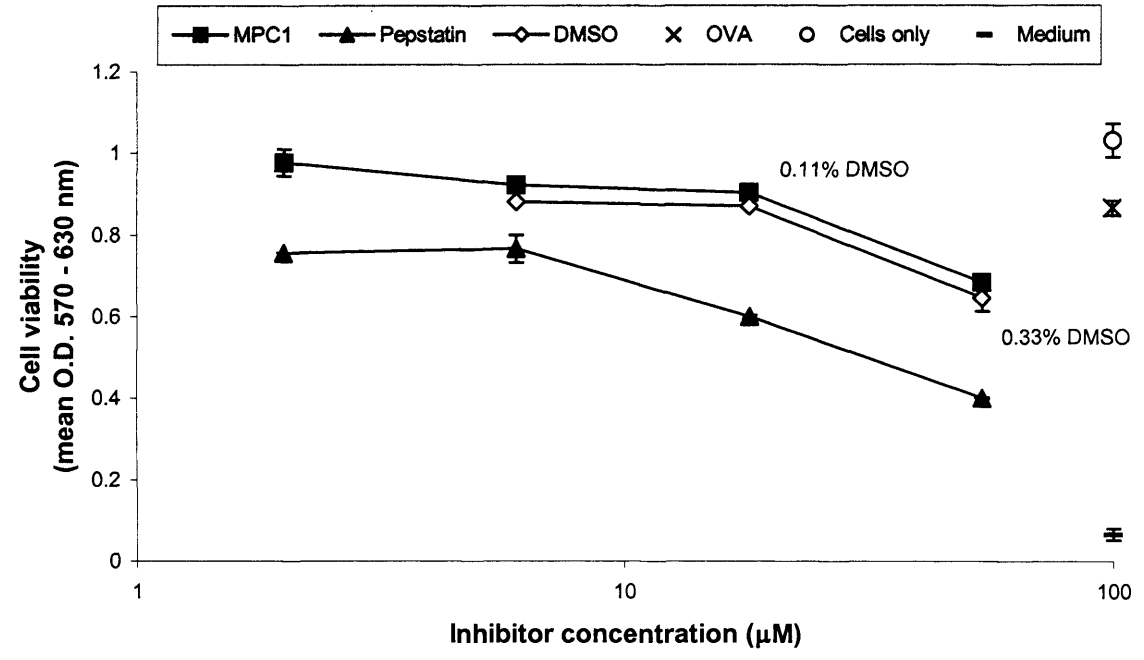

Figure 6.10: Response of DO11-10 cells to OVA presented by A20 cells in the presence of varied concentrations of MPC1, pepstatin A and DMSO. a) IL-2 release by DO11-10 cells, measured by IL-2 ELISA and expressed as the mean O.D. (450 nm) from duplicate cultures. b) Cell viability measured by MTT incorporation and expressed as the mean O.D. (570 – 630 nm) from triplicate cultures. Results for both graphs are representative of four separate experiments. Experiment uses 3mg/ml OVA, 0.33% DMSO at 54μM pepstatin A, and 0.11% DMSO for MPC1 at 54μM

Figure 6.11a shows the effect of MPC2 and pepstatin A on inhibition of IL-2 release by DO11-10 cells. The data shows a similar trend of MPC2 as MPC1, i.e. complete inhibition of OVA processing within A20 cells at the higher concentration of 54μM but less than pepstatin A at lower concentrations, and an effect that is dose dependent.

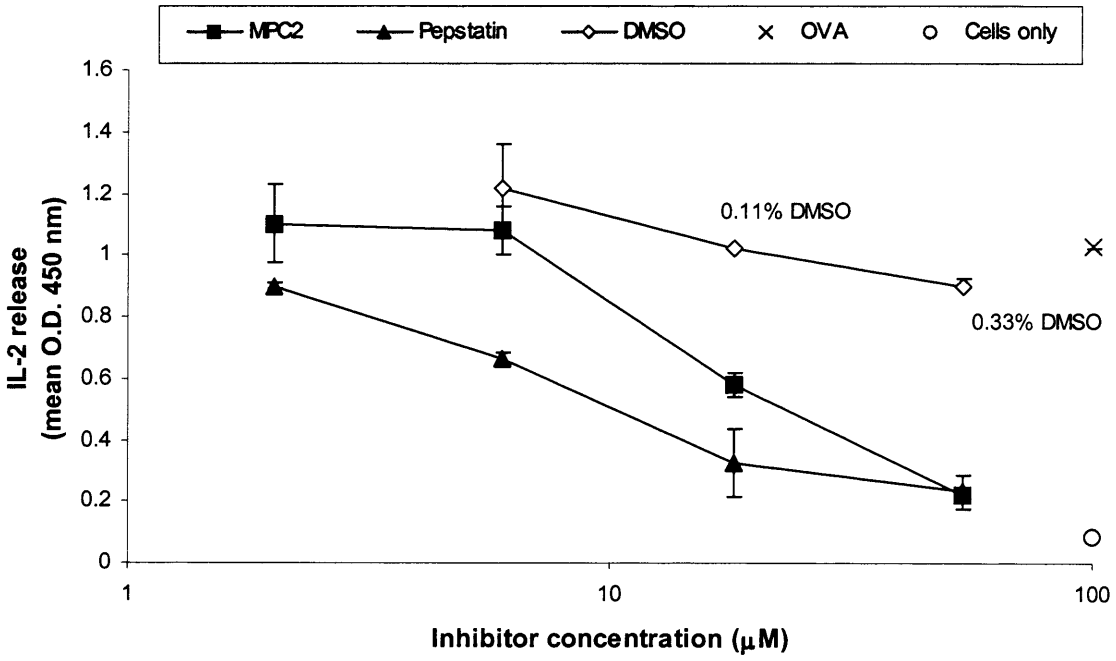

Figure 6.11a: Response of DO11-10 cells to OVA presented by A20 cells in the presence of varied concentrations of MPC2, pepstatin A and DMSO. IL-2 release by DO11-10 cells, measured by IL-2 ELISA and expressed as the mean O.D. (450 nm) from duplicate cultures. Results are representative of four separate experiments. Experiment uses 3mg/ml OVA, 0.33% DMSO at 54μM pepstatin A, and 0.11% DMSO for MPC2 at 54μM

Figure 6.11b shows a higher cell viability with MPC2 compared with that of pepstatin A, this trend being similar to MPC1. Like MPC1, the difference in inhibitor effect between MPC2 and pepstatin upon IL-2 release is possibly due to the difference in cell viability.

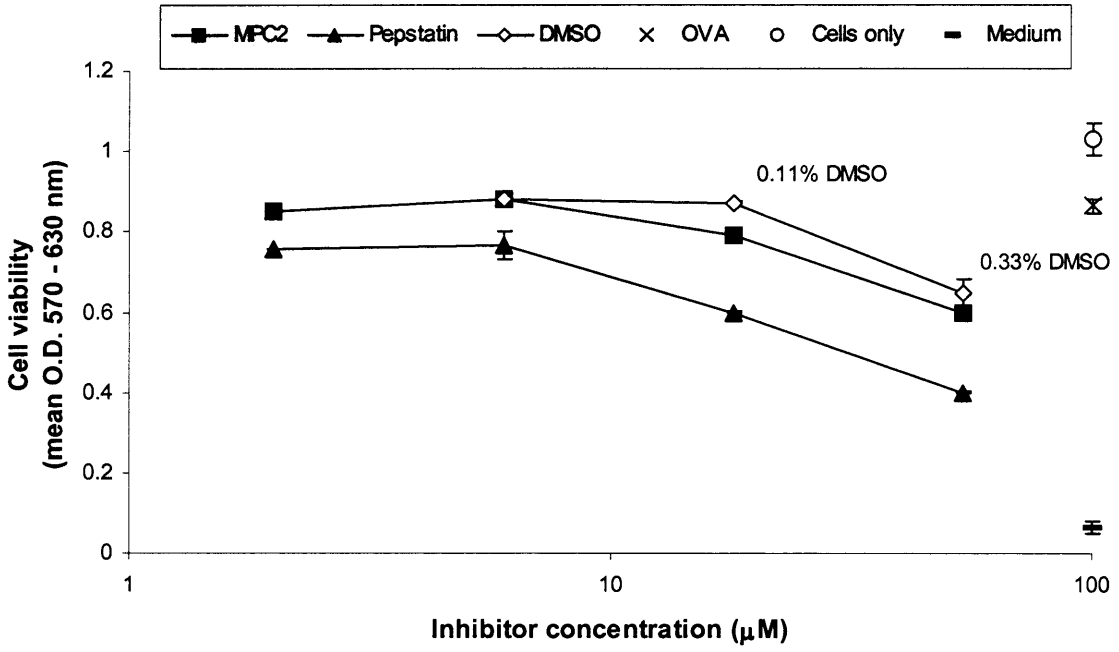

Figure 6.11b: Cell viability of experiment presented in figure 6.11a, measured by MTT incorporation and expressed as the mean O.D. (570 – 630 nm) from triplicate cultures. Results are representative of four separate experiments.

A summary of the % inhibition of release of IL-2 and % assay cell death for MPC1, MPC2 and DMSO, at 54μM and 18μM is shown in figure 6.12a and 6.12b respectively. Figure 6.12a clearly shows that the total inhibition observed with MPC1 and MPC2 at 54μM is due to inhibition of proteolytic activity and only partly due to an effect on cell viability. This inhibition is statistically significant.

(a)

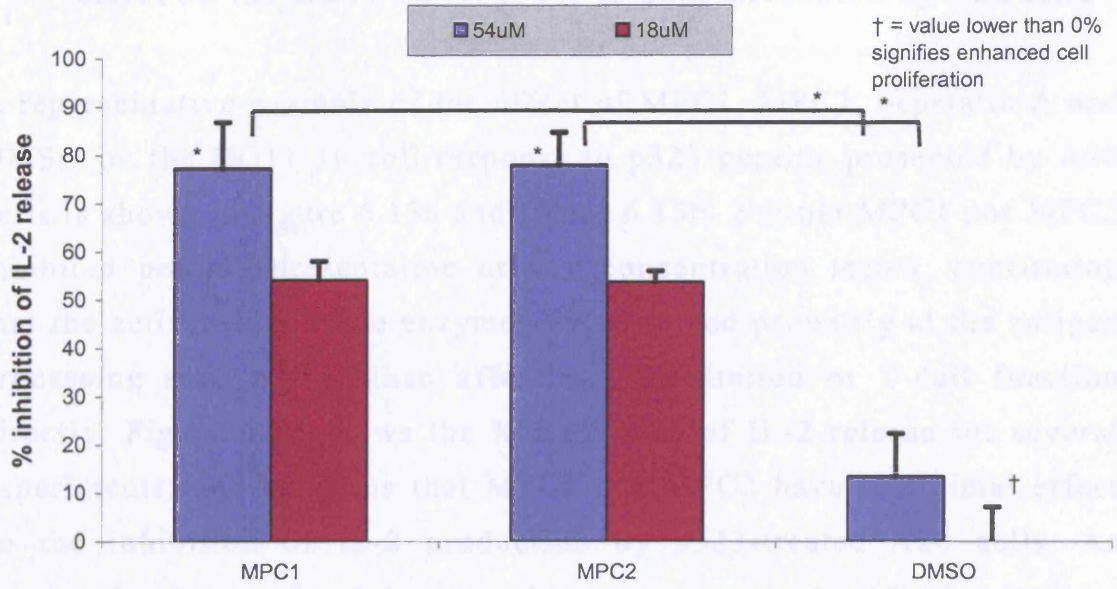

(b)

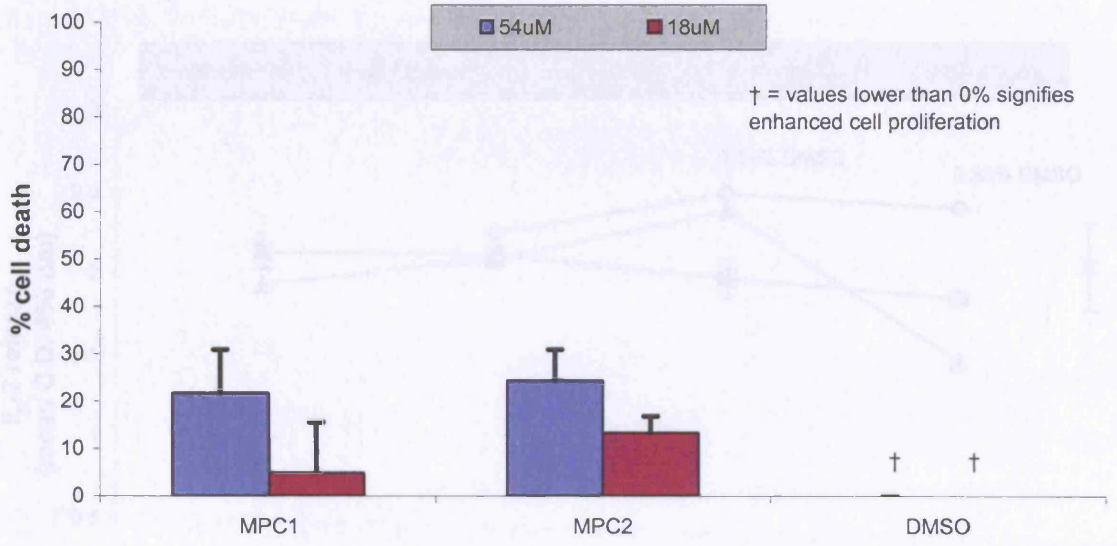

Figure 6.12: The effect of MPC1 / MPC2 on a) OVA presentation by A20 cells and b) cell viability. Both graphs show the results with 54μM MPC1 / MPC2 and its equivalent DMSO concentration (0.11%), and 18μM MPC1 / MPC2 and its equivalent DMSO concentration (0.037%).

Results show the mean +/- SEM of four separate experiments. * $p < 0.05$ *versus* OVA/medium control, or where specified, OVA/DMSO control. % inhibition of IL-2 release and % cell death calculated as described in legend to fig 4.4.

6.2.4 MPC1 and MPC2 when dissolved with DMSO have minimal effect on the DO11-10 response to p323 presented by A20 cells

A representative example of the effect of MPC1, MPC2, pepstatin A and DMSO on the DO11-10 cell response to p323 peptide presented by A20 cells is shown in figure 6.13a and figure 6.13b. Neither MPC1 nor MPC2 inhibited peptide presentation at any concentration tested, confirming that the activities of these enzymes was directed primarily at the antigen processing step, rather than affecting presentation or T-cell function directly. Figure 6.14 shows the % inhibition of IL-2 release for several experiments, and confirms that MPC1 and MPC2 have a minimal effect on the inhibition of IL-2 production by p323-treated A20 cells. As previously shown (fig. 6.4, page 189), pepstatin A (54μM) also inhibits the presentation of p323 to DO11-10 cells and reduces cell viability.

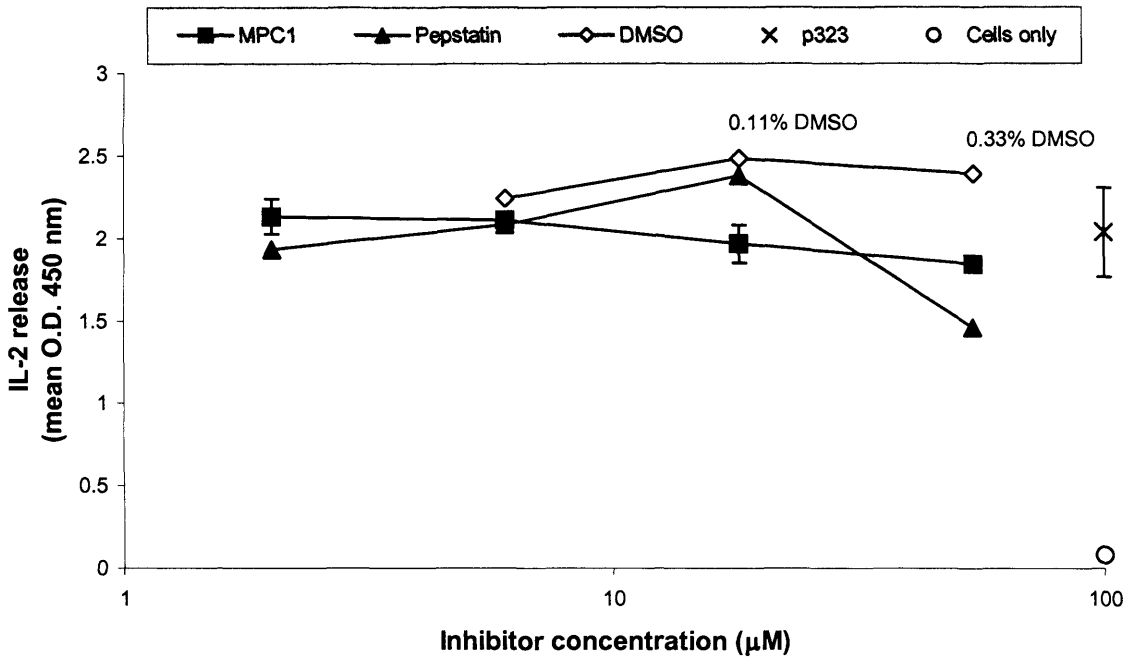

Figure 6.13a: Response of DO11-10 cells to p323 peptide presented by A20 cells in the presence of varied concentrations of MPC1, pepstatin A and DMSO. IL-2 release by DO11-10 cells, measured by IL-2 ELISA and expressed as the mean O.D. (450 nm) from duplicate cultures. Results are representative of four separate experiments. Experiment uses 0.1μg/ml p323 peptide, 0.33% DMSO at 54μM pepstatin A, and 0.11% DMSO for MPC1 at 54μM

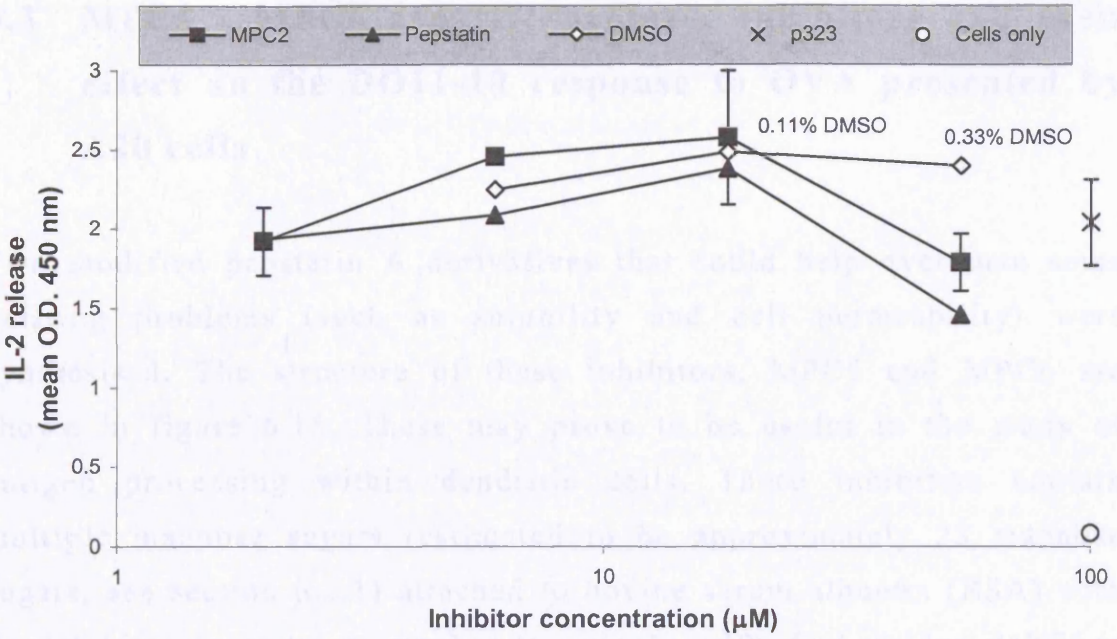

Figure 6.13b: Response of DO11-10 cells to p323 peptide presented by A20 cells in the presence of varied concentrations of MPC2, pepstatin A and DMSO. IL-2 release by DO11-10 cells, measured by IL-2 ELISA and expressed as the mean O.D. (450 nm) from duplicate cultures. Results are representative of four separate experiments. Experiment uses 0.1μg/ml p323 peptide, 0.33% DMSO at 54μM pepstatin A, and 0.11% DMSO for MPC2 at 54μM

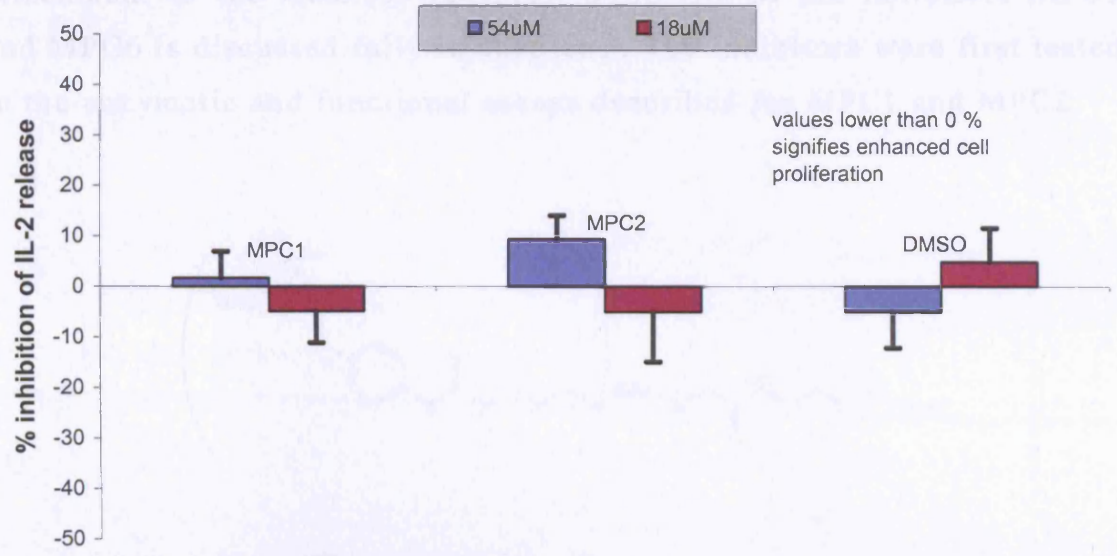

Figure 6.14: The effect of MPC1 / MPC2 on the presentation of p323 by A20 cells. Graph shows the effects caused by 54μM of MPC1 / MPC2 and its equivalent DMSO concentration (0.11%), and 18μM of MPC1 / MPC2 and its equivalent DMSO concentration (0.037%). Results show the mean +/- SEM of four separate experiments. % inhibition of IL-2 release calculated for each experiment as the % difference in IL-2 production between the p323 control (0 % inhibition of IL-2 production) and cells only control (baseline or no IL-2 production, thus 100 % inhibition).

6.3 MPC5 / MPC6 aspartic protease inhibitors and their effect on the DO11-10 response to OVA presented by A20 cells

Two modified pepstatin A derivatives that could help overcome some existing problems (such as solubility and cell permeability) were synthesised. The structure of these inhibitors, MPC5 and MPC6 are shown in figure 6.15. These may prove to be useful in the study of antigen processing within dendritic cells. These inhibitors contain multiple mannose sugars (estimated to be approximately 23 mannose sugars, see section 6.3.1) attached to bovine serum albumin (BSA) with the inhibitor pepstatin A attached to a single sulfhydryl residue. MPC6 is a cleavable version of MPC5, containing a disulphide linkage. As discussed in chapter 2, it was predicted that these inhibitors would show better solubility over MPC1 and MPC2, and introduce a targeting element by allowing increased endocytosis into dendritic cells by attachment to the mannose receptor. Synthesis of the inhibitors MPC5 and MPC6 is discussed fully in chapter 3. The inhibitors were first tested in the enzymatic and functional assays described for MPC1 and MPC2.

(a)

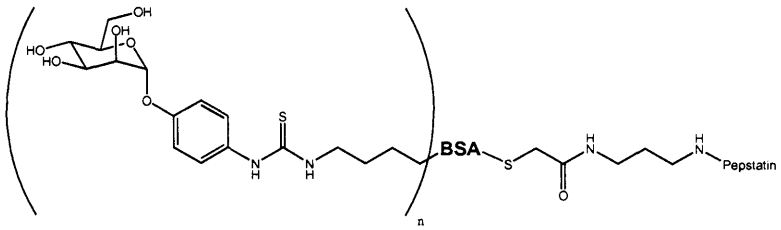

(b)

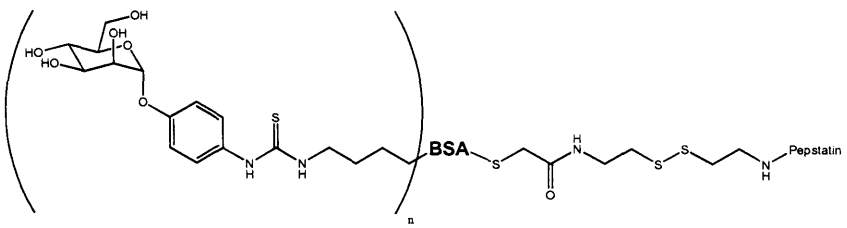

Figure 6.15: The chemical structures of a) MPC5 and b) MPC6

6.3.1 The MPC5 and MPC6 precursor BSA conjugate [33] contains approximately 23 conjugated mannose sugars

Determination of the average amount of conjugation of isothiocyanatomannosyl sugar derivatives attached to the BSA conjugate **[33]** (**[33]** refers to the numbered synthesis compound listed within chapter 3) is done by three methods, mass spectrometry (MALDI-TOF), biochemical analysis for total mannose content and free amino groups. The first method using MALDI-TOF mass spectrometry gave a detectable average mass for BSA with a peak at 66,430 (appendix VIII). The mass of BSA conjugate **[33]** gave a peak at 74,030 with a peak range between 67,000 – 79,000 (appendix VIII). This range is expected due to the varied number of conjugated mannosyl compounds, with the median mass at 74,030. The difference between BSA and BSA conjugate **[33]** equates to approximately 24.3 mannose units / BSA molecule.

Biochemical analysis for the presence of sugars is possible by using the phenol – sulphuric acid method[229,230]. A graph of concentration of the compound 4-aminophenyl α-D-mannopyranoside **[10]** *vs* absorption (fig. 6.16) is used as a reference for determining the amount of mannose sugars attached to the mannosylated BSA conjugate **[33]**. Table 6.1 shows the absorbance values obtained for BSA conjugate **[33]** (three different experiments, two concentrations per experiment) from which an estimated number of mannosyl units per BSA are calculated by using the linear equation from figure 6.16. The mean of these gives a value of 23.1 +/– 2.5 mannosyl units per BSA for BSA conjugate **[33]**.

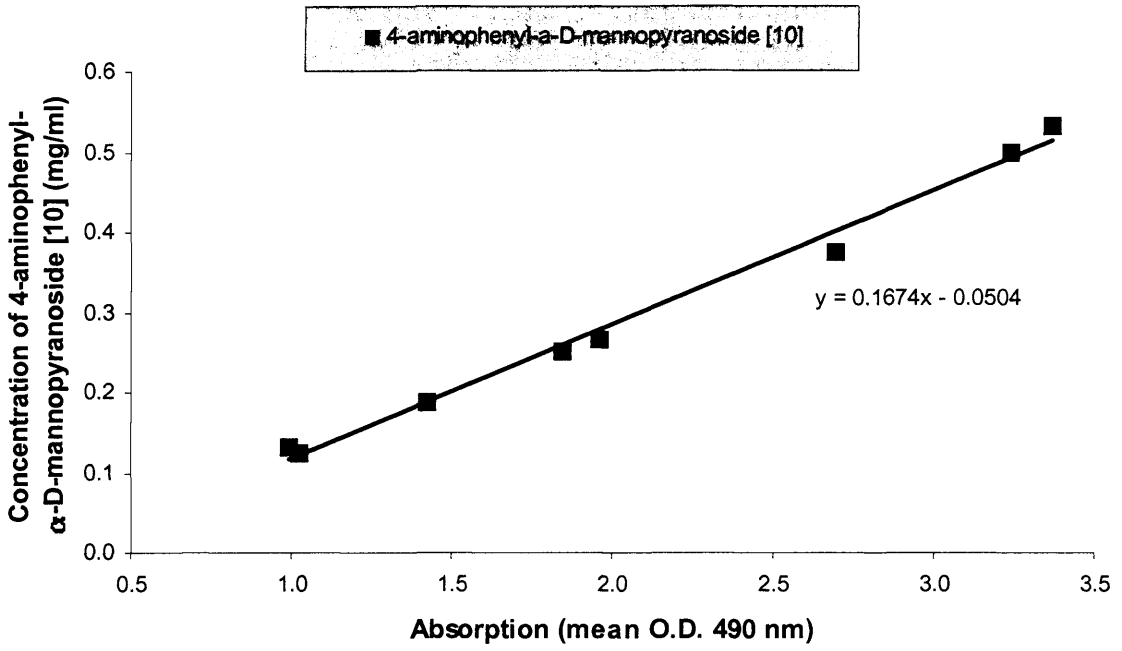

Figure 6.16: Selected data from a standard curve of 4-aminophenyl α-D-mannopyranoside [10]. Each data point is the mean of three separate experiments, each experiment being run in triplicate, and selected as all the data with absorbance between approx 1.0 and 3.5. This selected range fits a linear equation, the plot of which is used to help calculate the number of mannose units per BSA conjugate [33]

BSA conjugate [33] (mg/ml)	3.6	1.8	3.6	1.8	3.6	1.8
Absorbance (mean O.D. 490 nm)	2.15	1.18	1.79	1.35	2.19	1.22
Estimated number mannoses / BSA	23.52	22.31	18.89	26.62	23.97	23.24

Average	S.D.
23.1	2.5

Table 6.1: Estimated number of mannosyl sugar units per BSA molecule on BSA conjugate [33]. Absorptions of three separate tests of two different concentrations were run as triplicates, and from the absorption observed, the mean number of mannosyl sugars per BSA of BSA conjugate [33] was calculated from the equation listed in figure 6.16. The mean and standard deviation of these six values is calculated as 23.1 +/- 2.5

Biochemical analysis for amino groups, such as the number of free lysine amino acids on BSA conjugate **[33],** is possible by using the trinitrobenzenesulfonic acid (TNBS) method[228,241]. A standard curve of BSA and BSA conjugate **[33]** (fig. 4.17) is obtained by 1 in 2 dilutions from 10 mg/ml and 20 mg/ml of BSA and BSA conjugate **[33]** respectively. These plots give a correlation that fits an quadratic equation (fig. 6.17). From this equation it is calculated that an absorbance = 1.0 is equivalent to 5.80 mg/ml (87.1 μM) of BSA and 10.44 mg/ml (141 μM) of BSA conjugate **[33]**.

To determine if all of the amino groups on BSA are able to react with TNBS, a test of the absorbance of BSA and BSA under denaturing conditions (addition of 10% of 2% w/v SDS) with a longer duration for TNBS reaction (30 mins compared with 5 mins normally) was performed with / without a change of pH to neutrality after reaction (sometimes required to ensure non-reversible addition of TNBS addition by sulfite displacement). The results (not shown) showed a limited difference in the value obtained for the absorption. It was assumed that all of the amino groups of BSA were reactable towards TNBS (i.e. 60 including a terminal NH_2). As such, it was calculated:

Free amino groups per BSA = 60

87.1μM BSA x 60 amino groups = 5.23mM free amino groups per BSA

∴ 5.23mM / 141 μM BSA conjugate **[33]** concentration =
37 amino groups per BSA conjugate **[33]**

∴ 60 – 37 = <u>23 attached mannosyl units per BSA conjugate **[33]**</u>

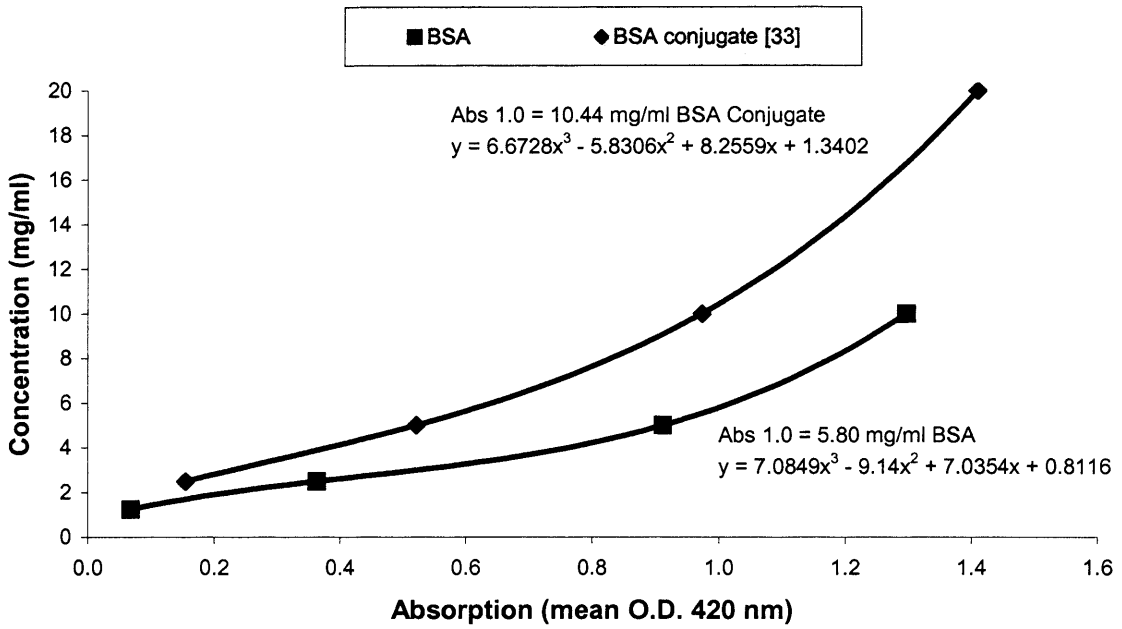

Figure 6.17: Standard curve of BSA and BSA Conjugate [33]. Each data point is the mean of three separate experiments, each experiment being run in triplicate. Quadratic equations are included for each correlation, from which the number of free lysine amino groups on BSA Conjugate [33] is calculated.

6.3.2 Mass spectrometry suggests that MPC6 contains a single attached pepstatin A

Determination of protein sulfhydryl groups on proteins is traditionally accomplished by the use of Ellman's reagent[238]. However for unknown reasons this method did not give reproducible results. Alternatively, the use of MALDI-TOF mass spectrometry and enzymological data (section 6.3.3) help to confirm the presence of a single pepstatin A molecule attached to BSA conjugate **[33]** within MPC5 and MPC6.

MPC6 shows a peak range = 69,000 – 81,500, with the median peak for MPC6 being ~ 75,163 (appendix IX). This is both an increase in median peak value over BSA conjugate **[33]** of 1,131 (pepstatin A analogue MW = 861) and a peak range increase in mass of at least 2,000 MW, both factors indicate the presence of an extra molecule. Unfortunately, the mass spectrometry data for MPC5 does not show this and on its own

would suggest no change between MPC5 and BSA conjugate **[33]**. With MPC5 there is at most a slight skew in the peak of MPC5 towards a higher mass but not significantly to clearly suggest the inclusion of a pepstatin analogue like that of MPC6 (appendix IX). Although the MS data and the enzymological data (next section) suggest the inclusion of a pepstatin molecule onto at least MPC6, there is no concrete evidence without an analysis of the free sulfhydryl on BSA, and as such, no accurate measurement of the percentage of pepstatin conjugated via a disulphide of MPC5 / MPC6 is known. This is discussed further in the conclusion.

6.3.3 MPC5 and MPC6, but not BSA-conjugate, inhibit the enzymatic cleavage of a peptide substrate for rat cathepsin E

Using the Dixon method described in chapter 5[240], data for the inhibition of cleavage of fluorogenic substrate by rat cathepsin E was obtained for MPC5, MPC6 and the precursor BSA conjugate **[33]**. Figure 6.18 shows plots of data for BSA conjugate **[33]**, MPC5 and MPC6. An accurate trend-line could not be applied to the graph of BSA conjugate **[33]**, although the data suggested an approx. IC_{50} value in the 0.5 – 2 μM range. This is many orders of magnitude higher than the values for pepstatin A and MPC1 / MPC2, which have values in the picomolar range. Any inhibition that may be occurring from BSA conjugate **[33]** is likely to be due to competition for cleavage by cathepsin E enzyme as BSA and mannosylated BSA have been shown to be cleaved by a cathepsin D-like enzyme most likely to be cathepsin E[242,243].

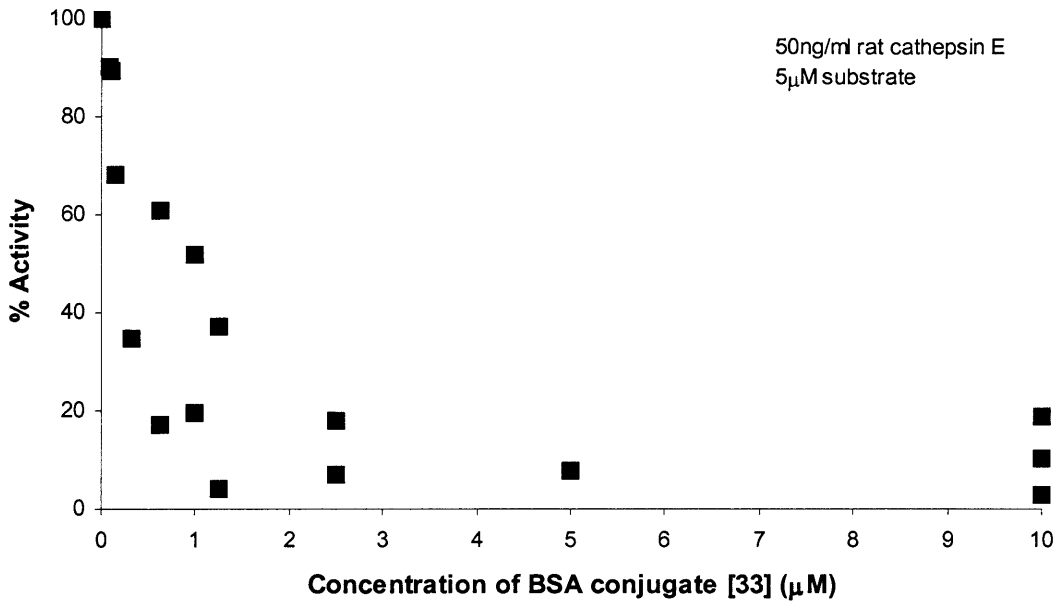

Figure 6.18: Inhibition by BSA conjugate [33] of the enzymatic cleavage of fluorogenic substrate by rat cathepsin E. Results are the combination of four separate experiments and expressed as % activity against BSA conjugate [33] concentration

MPC5 and MPC6 however showed much more potent inhibition of substrate cleavage (fig. 6.19), in the low nM range. Although the IC_{50} values are still an order of magnitude higher than pepstatin A, the difference in IC_{50} between BSA-conjugate **[33]** and MPC5 / MPC6 suggests the presence of pepstatin A in the inhibitors. The purification procedure used for MPC5 and MPC6 makes it unlikely that any free pepstatin is present in the MPC5 or MPC6 solutions, it is thus unlikely that the inhibition of fluorogenic compound by MPC5 / MPC6 over that of BSA-conjugate **[33]** is due to free pepstatin. The higher IC_{50} values for MPC5 / MPC6 compared with pepstatin A may suggest that steric factors play a role in reducing the potency of pepstatin A when conjugated to BSA. An alternative explanation is that the percentage of conjugated pepstatin molecules per BSA-conjugate **[33]** is low. This issue is discussed further in the conclusion.

(a)

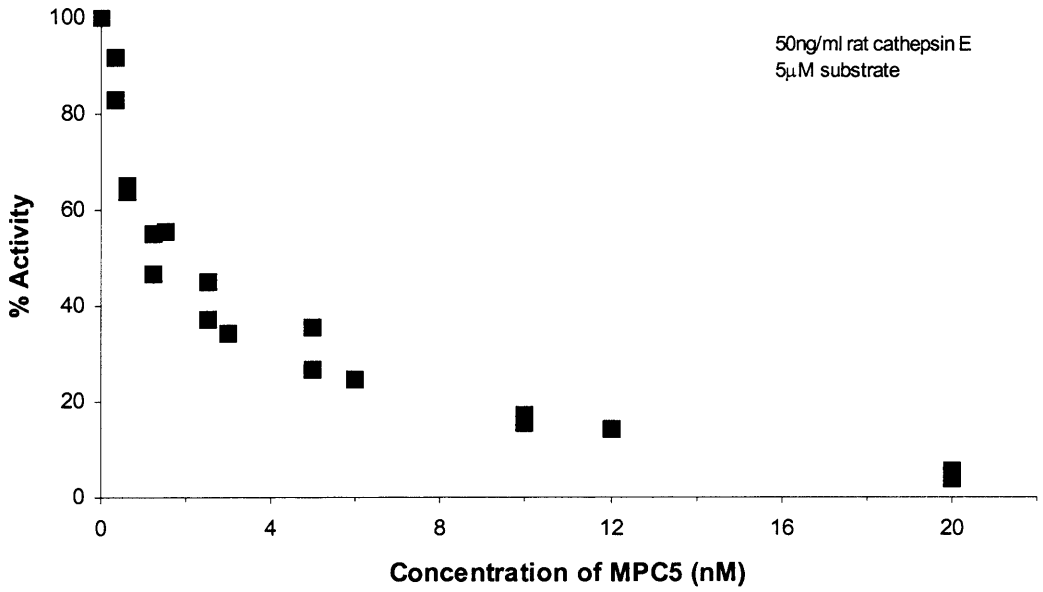

(b)

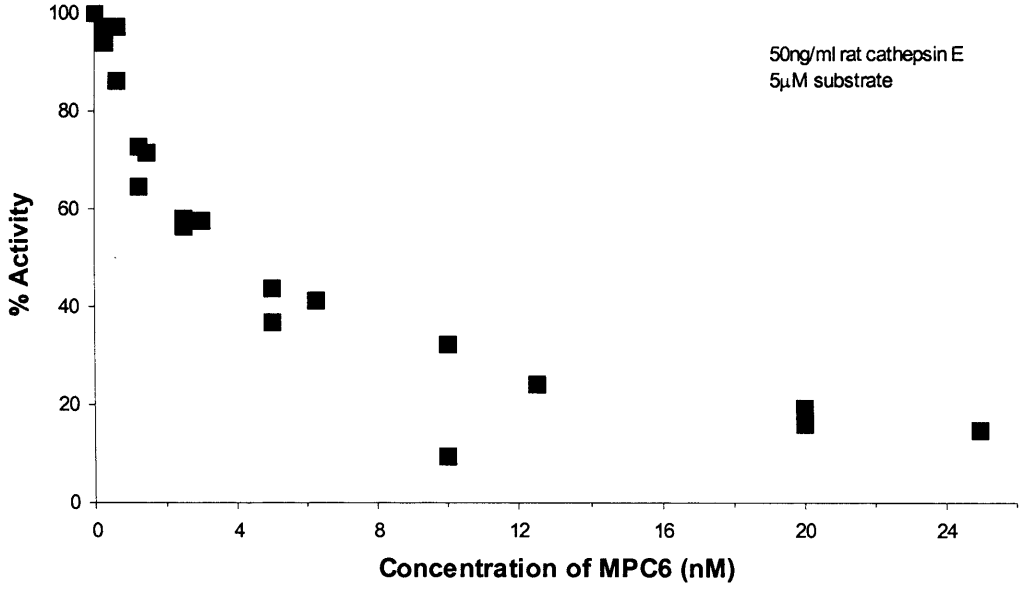

Figure 6.19: Inhibition by a) MPC5 and b) MPC6 of the enzymatic cleavage of fluorogenic substrate by rat cathepsin E. Results are the combination of three separate experiments and expressed as % activity against inhibitor concentration

6.3.4 MPC5 and MPC6 do not inhibit the DO11-10 response to OVA presented by A20 cells

A representative example of the inhibition of IL-2 release from DO11-10 cells in the presence of OVA-treated A20 cells, with varied concentration of MPC5, MPC6, and mannose-BSA conjugate **[33]**, is shown in figure 6.20. A summary of % inhibition of IL-2 release by DO11-10 cells, and % assay cell death is shown in figures 6.21a and 6.21b, respectively. There is no significant inhibition of IL-2 release in the presence of MPC5 or MPC6, in fact, MPC5 seemed to cause a proliferative response (fig. 6.21a). However, mannose-BSA conjugate **[33]** seemed to cause significant inhibition of IL-2 release at the 54μM concentration. The reason for this discrepancy is unknown, however may be the result of competition for antigen, and is discussed in the conclusion. The discrepancy between these compounds is not understood. Interestingly, the % assay cell death (fig. 6.21b) for all three compounds seems to be similar, with a low effect on cell death.

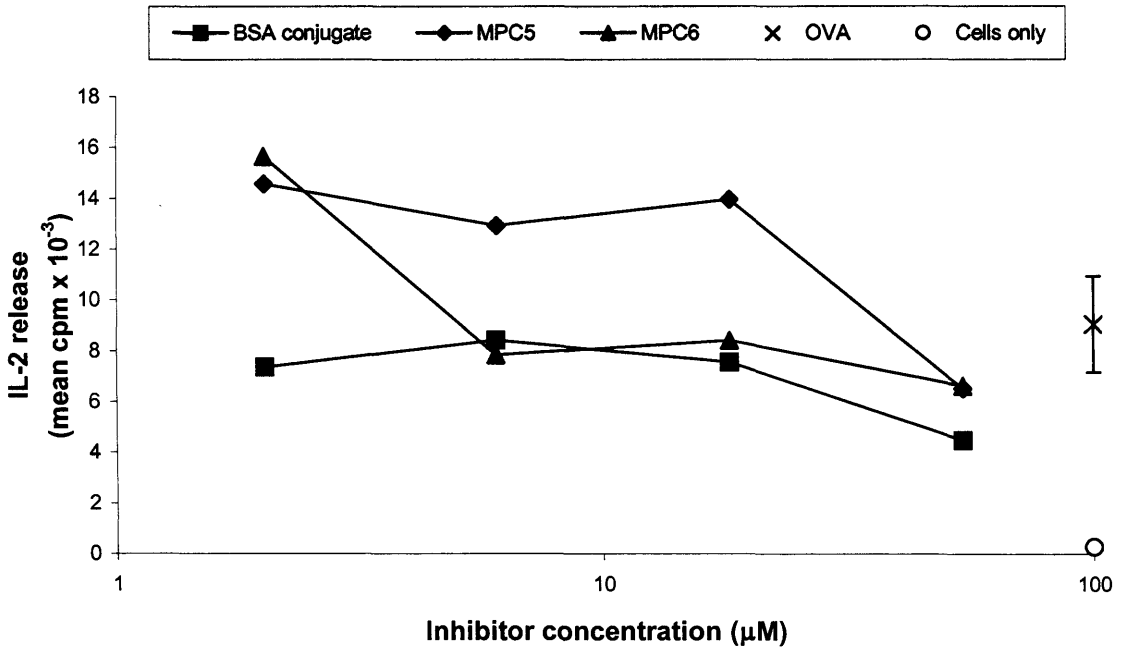

Figure 6.20: Response of DO11-10 cells to A20 cells presenting OVA antigen (0.5 mg/ml) with varied concentration of BSA conjugate [33], MPC5 and MPC6. IL-2 release measured by ^{3}H-thymidine incorporation, and results expressed as the mean from triplicate cultures. Data is representative of three different experiments

(a)

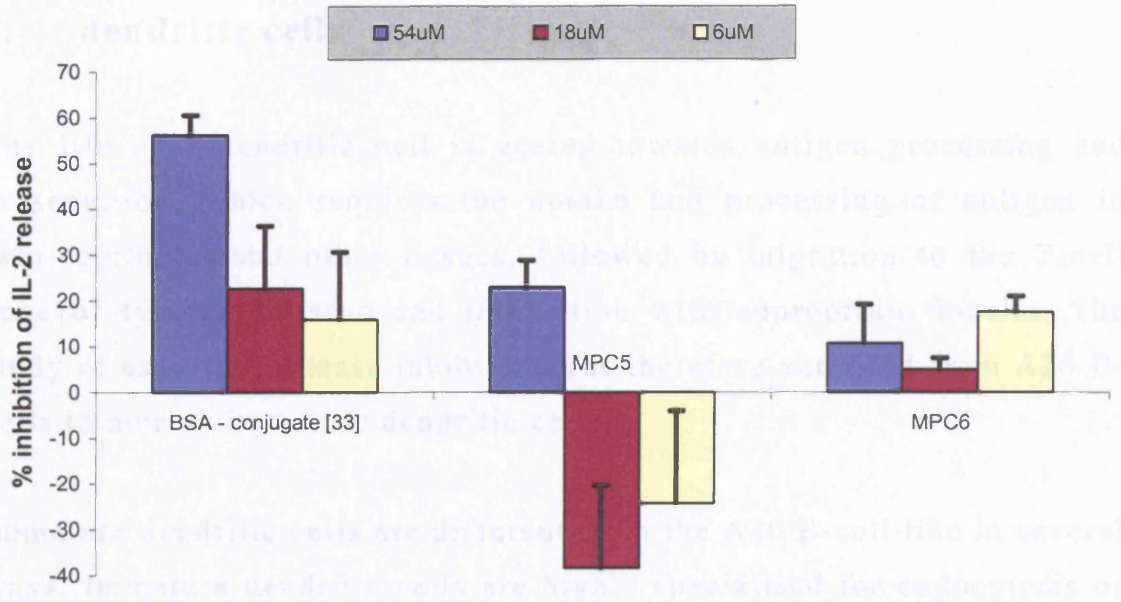

(b)

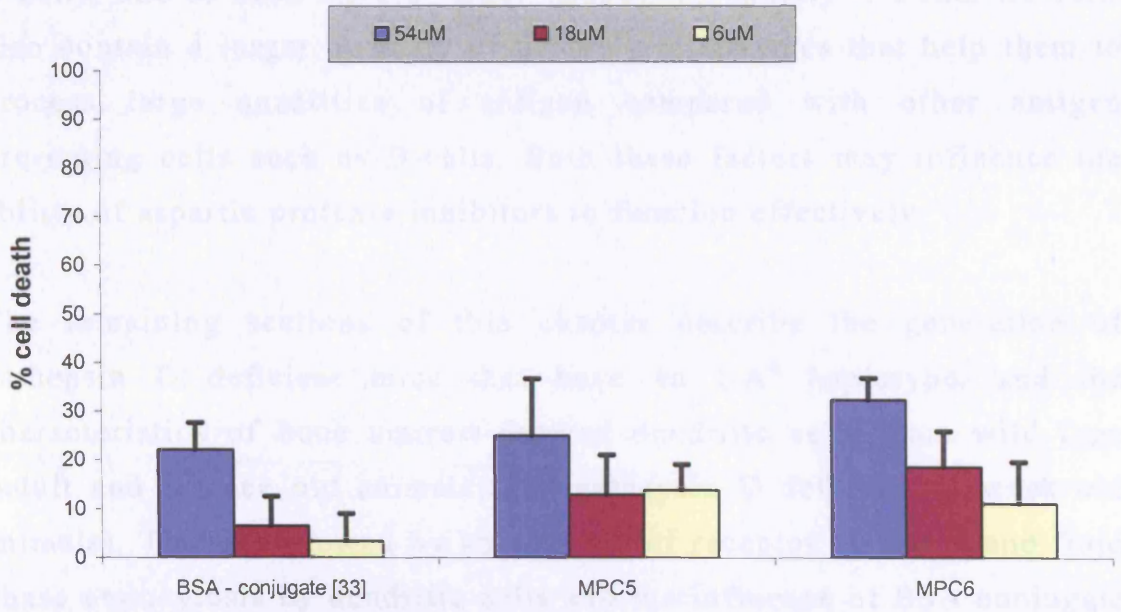

Figure 6.21: The effect of MPC5 / MPC6 and BSA – conjugate [33] within OVA-treated A20 cells on a) the % inhibition of IL-2 production by DO11-10 T-cells and on b) assay cell death. Both graphs show the effects caused by 54μM, 18μM and 6μM of the MPC5 / MPC6 inhibitors and their control. Results show the mean +/- SEM of three separate experiments. % inhibition of IL-2 release calculated for each experiment as the % difference in IL-2 production between the OVA control (0 % inhibition of IL-2 production) and cells only control (baseline or no IL-2 production, thus 100 % inhibition). % assay cell death calculated for each experiment as the % difference in cell viability between the OVA control (0 % assay cell death) and Medium only control (no cells represents 100 % assay cell death).

6.4 Aspartic proteases and antigen processing by mouse dendritic cells

The life of a dendritic cell is geared towards antigen processing and presentation, which requires the uptake and processing of antigen in skin, epithelia and other tissues, followed by migration to the T-cell zone of lymphoid tissue and interaction with appropriate T-cells. The study of aspartic protease inhibitors was therefore extended from A20 B-cells to murine immature dendritic cells.

Immature dendritic cells are different from the A20 B-cell line in several ways. Immature dendritic cells are highly specialised for endocytosis of antigen, either *via* fluid phase (macropinocytosis) or by receptor mediated uptake. In theory, this should equate into a larger uptake of antigen. However A20 cells are considerably larger than murine *ex vivo* B-cells, and as such have a larger endocytic capacity[12]. Dendritic cells also contain a larger quantity of proteolytic enzymes that help them to process large quantities of antigen compared with other antigen presenting cells such as B-cells. Both these factors may influence the ability of aspartic protease inhibitors to function effectively.

The remaining sections of this chapter describe the generation of cathepsin D deficient mice that have an I-A^d haplotype, and the characteristics of bone marrow-derived dendritic cells from wild type (adult and 3 week old animals) and cathepsin D deficient (3 week old animals). This is followed by an analysis of receptor mediated and fluid phase endocytosis by dendritic cells and the influence of BSA conjugate **[33]** on this uptake, and finally some effects of aspartic proteinase inhibitors MPC1, 2, 5 and 6 on processing and presentation of ovalbumin and ovalbumin peptide p323.

6.5 Generation of Cathepsin D deficient mice and immature dendritic cells

Cathepsin D deficient mice were obtained as a kind gift from the laboratory of Dr. C. Pieters[110]. The line was maintained as a heterozygote colony in the Biological Services at UCL. The mice were derived from 129 SvJ strain, and expressed MHC of H-2^b haplotype. It was necessary to introduce the H-2^d MHC haplotype, so the antigen presenting cells could be used in combination with the DO11-10 T-cell model as described previously.

6.5.1 Cathepsin D +/- heterozygous mice with I-A^d haplotype

Female 129Sv/J heterozygous mice carrying the inactivated cathepsin D gene were backcrossed with male Balb/c mice for four generations. Heterozygote breeders from each generation were selected by PCR genotyping (section 5.14, page 182) of tail DNA. Forward and reverse primers of DNA were situated between exons 3 and 5 of the cathepsin D gene (fig. 5.5, page 183). Disrupted cathepsin D gene contained a neomycin cassette, and PCR amplification produced an ~1.5Kb band in heterozygous or homozygous mice and an ~280bp band in either heterozygous or wild-type mice (fig. 6.22). Like the parental strain[110], cathepsin D homozygous, F^4 generation mice (from here onwards termed B112 mice) died after three to four weeks. Homozygotes were smaller than normal mice and showed reduced mobility by three weeks. 100% of the mice selected as homozygotes for dendritic cell preparation based upon physical appearance were confirmed homozygous by PCR. As expected for the mouse population, almost 25 % (32 homozygous from a total population of 133 mice) were homozygous.

Figure 6.22: Example agarose gel of genotyping of mice expressing wild-type or disrupted cathepsin D gene

F^4 generation, female B112 mice were used to determine the MHC haplotype. Tail bleeds were used to provide blood cells for phenotypic analysis of the expression of MHC class-II I-A^d or I-A^b. Antibodies HB3 (anti-mouse I-A^d) and 3TP (anti-mouse I-A^b) were used for phenotyping. Figure 6.23 shows an example of a fluorescence histogram analysis and dot plot for typical I-A^b or I-A^d expression from whole blood of either Balb/c (fig. 6.23a) or 129/SvJ (fig. 6.23b) mice. Mice selected for further generation of B112 populations were selected from litters based upon the high expression of paternal I-A^d and no expression of I-A^b. An example histogram and dot plot of a B112 mouse that was I-A^b –ve and I-A^d +ve is shown in figure 6.23c. Of 15 F^4 generation mice tested, 8 fit the required haplotype and were selected for further breeding.

(a)

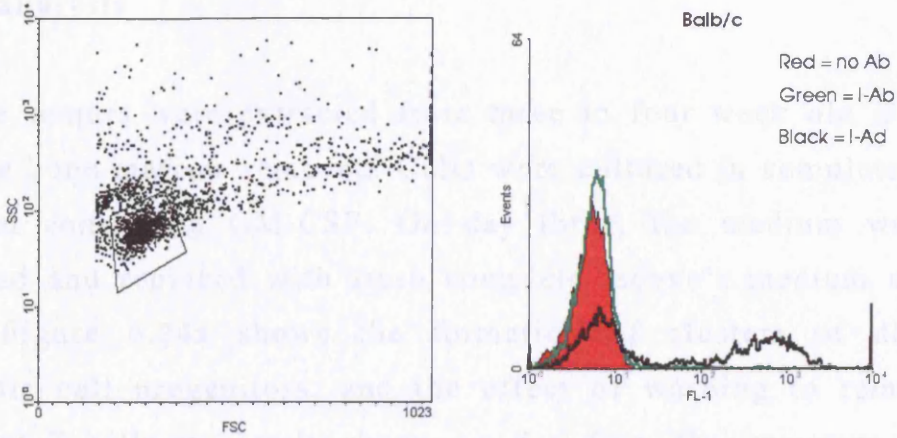

(b)

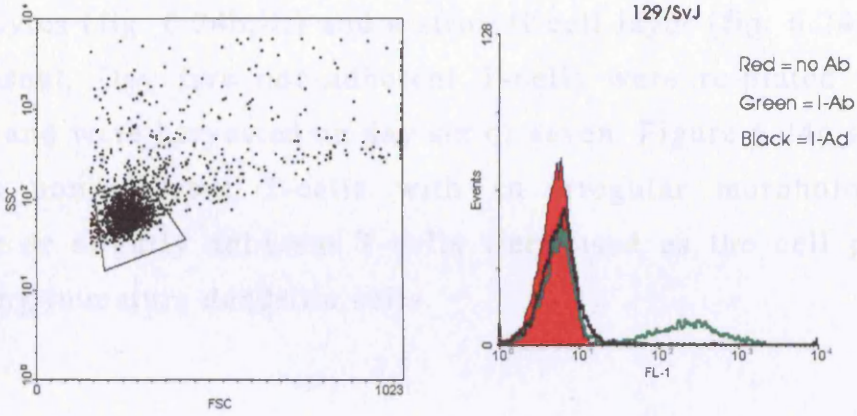

(c)

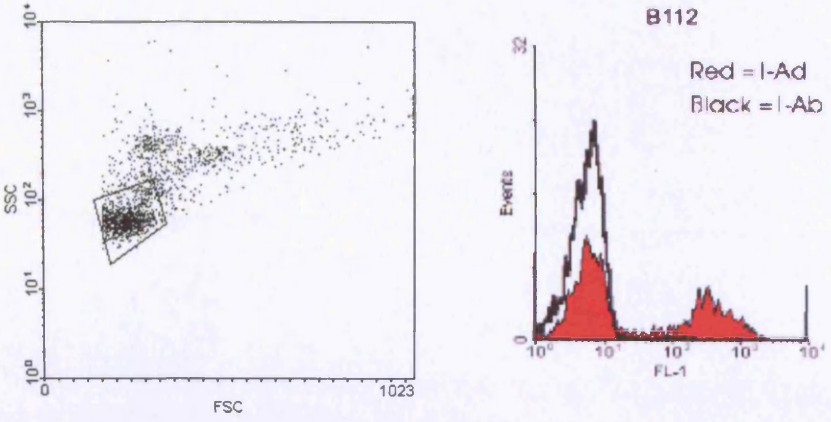

Figure 6.23: Fluorescence dot plot and histogram analysis of I-A^b or I-A^d expression within (a) Balb/c mouse whole blood, (b) 129/SvJ mouse whole blood and (c) B112 mouse tail bleed. Antibodies used were 1/50 concentration of HB3 (I-A^d) and 1/50 concentration of 3TP (I-A^b)

6.5.2 Generation of B112 mouse dendritic cells and phenotypic analysis

Murine femurs were extracted from three to four week old B112 mice and the bone marrow removed. Cells were cultured in complete Iscove's medium containing GM-CSF. On day three, the medium was gently removed and replaced with fresh complete Iscove's medium with GM-CSF. Figure 6.24a shows the formation of clusters of developing dendritic cell progenitors, and the effect of washing to remove non-adherent T-cells is clearly shown on day five, the immature dendritic cells detach from the clusters (fig. 6.24b,ii). Other cells, possibly granulocytes (fig. 6.24b,iii) and a stromal cell layer (fig. 6.24b,iv) were also present. Day five non-adherent T-cells were re-plated into fresh medium and were harvested on day six or seven. Figure 6.24c show these cells as non-adherent T-cells with an irregular morphology. Non-adherent or slightly adherent T-cells were used as the cell population containing immature dendritic cells.

(a)

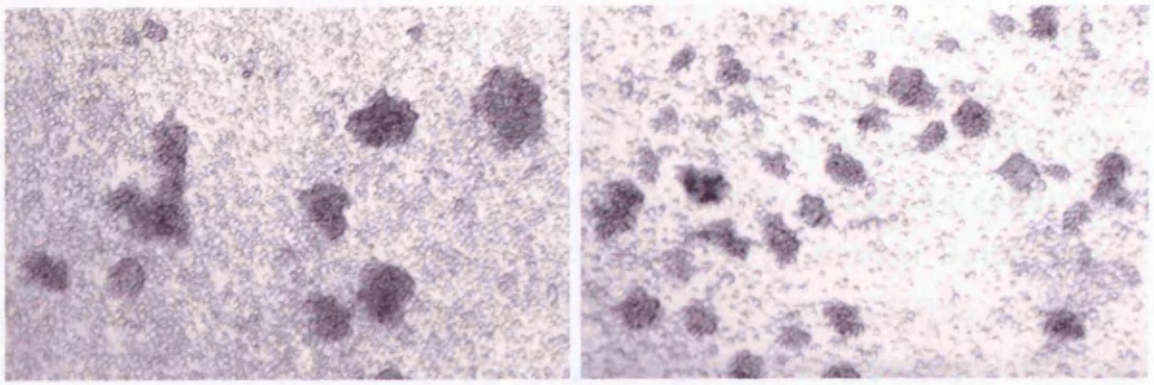

(b)

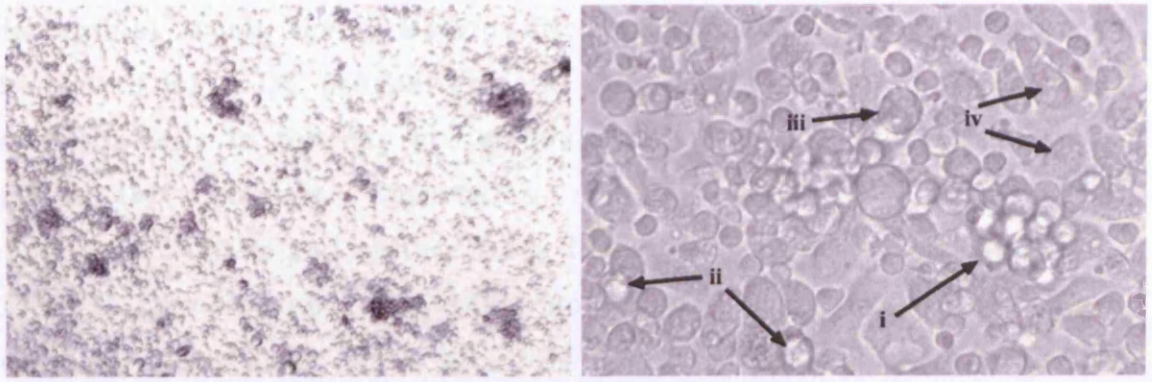

(c)

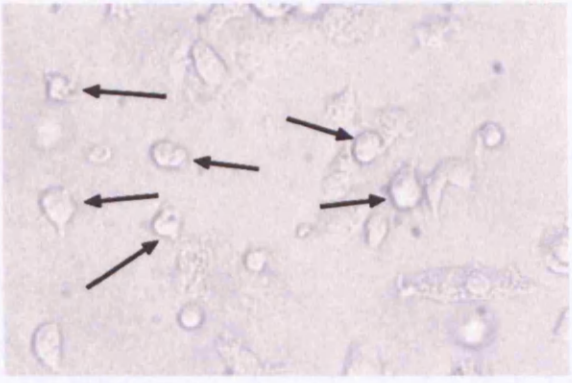

Figure 6.24: Light-microscope image of developing dendritic cells from murine femur bone marrow. a) Day three cells showing clusters of dendritic cell progenitors. Pictures taken before and after washing show the reduced number of non-adherent, non-clustered cells after washing. Magnification = 4000. b) Day five cells at 4000 magnification and 16,000 magnification respectively. These two figures show a decreased amount and density of dendritic cell clusters (i). Immature dendritic cells and progenitors are present in culture (ii), along with other larger cells, possibly granulocytes (iii). This view also shows clearly the developing stromal/fibroblast T-cell layer (iv). c) Day six re-plated cells clearly showing non-adherent immature dendritic cells (arrows)

Flow cytometry was used to identify cell surface markers on dendritic cells cultured from normal Balb/c mice, +/+ or +/- B112 mice (wild-type, WT), or -/- cathepsin D knockout B112 mice. Figure 6.25 shows representative fluorescence histograms for MHC class-II, CD11c (DC integrin), CD86 (co-stimulation marker on antigen presenting cells) and DEC-205 (C-type lectin found on DCs). In general, normal Balb/c mice showed much higher expression of MHC class-II, CD11c, CD86 and DEC 205 than B112 mouse cells, suggesting a larger percentage population of dendritic cells compared with the B112 mice. B112 mice were used at three to four weeks of age, and as such were significantly smaller that the normal week seven Balb/c mice. There were fewer developing clusters of B112 DC progenitor cells and as such, overall population of dendritic cells in the day six or seven cultures of B112 cells may be considerably smaller. Maturation of these cells by addition of lipopolysaccharide and culture for a further 3 days increased expression of MHC class-II and CD86 (data not shown) as expected for mature dendritic cells. Later work by Prof. B. Chain showed that culture of these cells from these young mice for a total of 14 – 20 days further increased the yield of immature DCs.

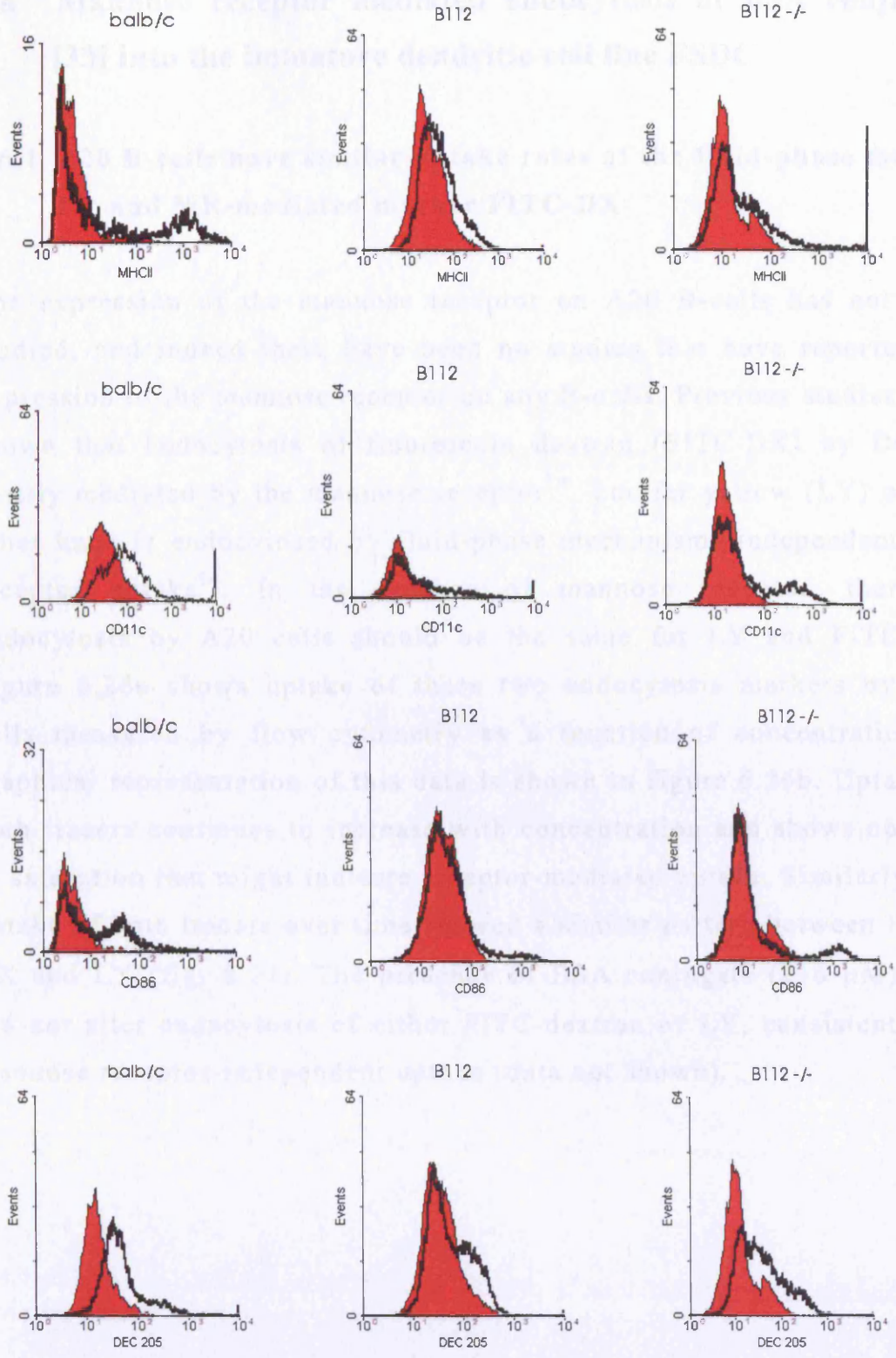

Figure 6.25: Flow cytometric analysis of bone marrow cultures from Balb/c, B112 and B112 -/- mice. Representative histograms of MHC class-II, CD11c, CD86 and DEC 205 expression. Filled histograms show appropriate isotype control or no antibody, while the thick black line shows the antibody staining for the particular protein of interest.

6.6 Mannose receptor mediated endocytosis of BSA conjugate [33] into the immature dendritic cell line FSDC

6.6.1 A20 B-cells have similar uptake rates of the fluid-phase marker LY and MR-mediated marker FITC-DX

The expression of the mannose receptor on A20 B-cells has not been studied, and indeed there have been no studies that have reported the expression of the mannose receptor on any B-cells. Previous studies have shown that endocytosis of fluorescein dextran (FITC-DX) by DCs is mostly mediated by the mannose receptor[14]. Lucifer yellow (LY) on the other hand is endocytosed by fluid-phase mechanisms independently of receptor uptake[14]. In the absence of mannose receptor, therefore endocytosis by A20 cells should be the same for LY and FITC-DX. Figure 6.26a shows uptake of these two endocytosis markers by A20 cells measured by flow cytometry as a function of concentration. A graphical representation of this data is shown in figure 6.26b. Uptake of both tracers continues to increase with concentration and shows no sign of saturation that might indicate receptor-mediated uptake. Similarly, the uptake of both tracers over time showed a similar pattern between FITC-DX and LY (fig. 6.27). The presence of BSA conjugate (216 μM) **[33]** did not alter endocytosis of either FITC-dextran or LY, consistent with mannose receptor-independent uptake (data not shown).

(a)

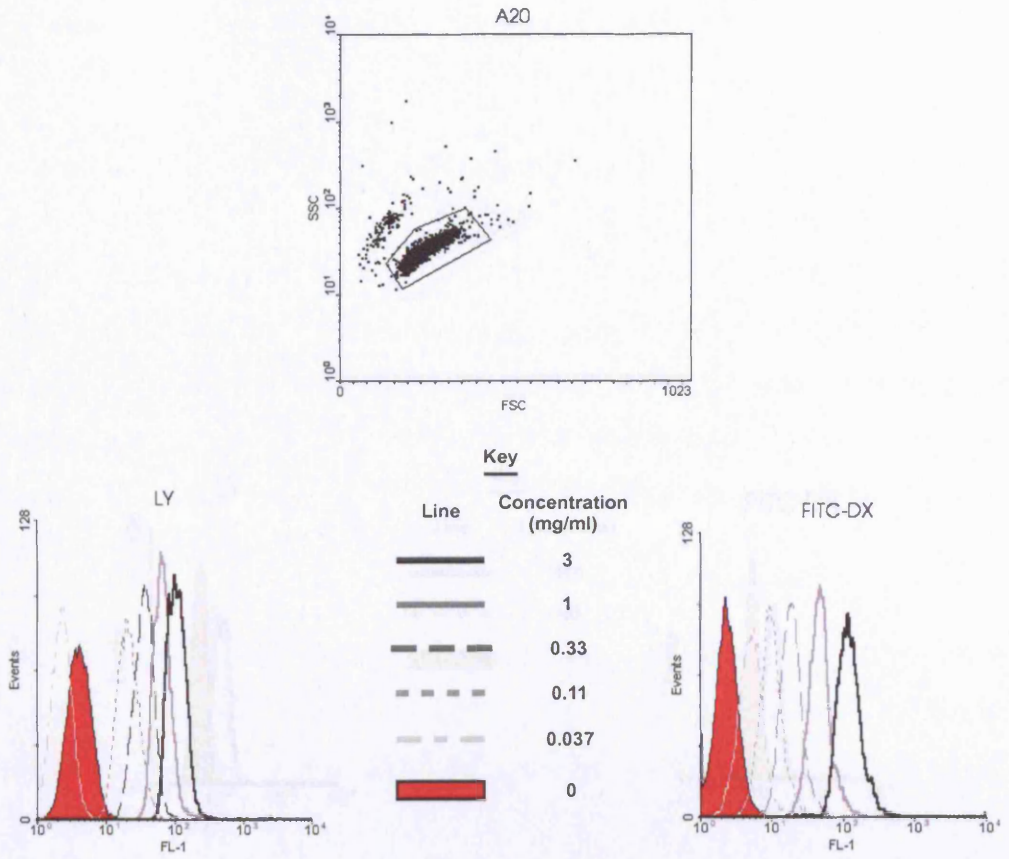

(b)

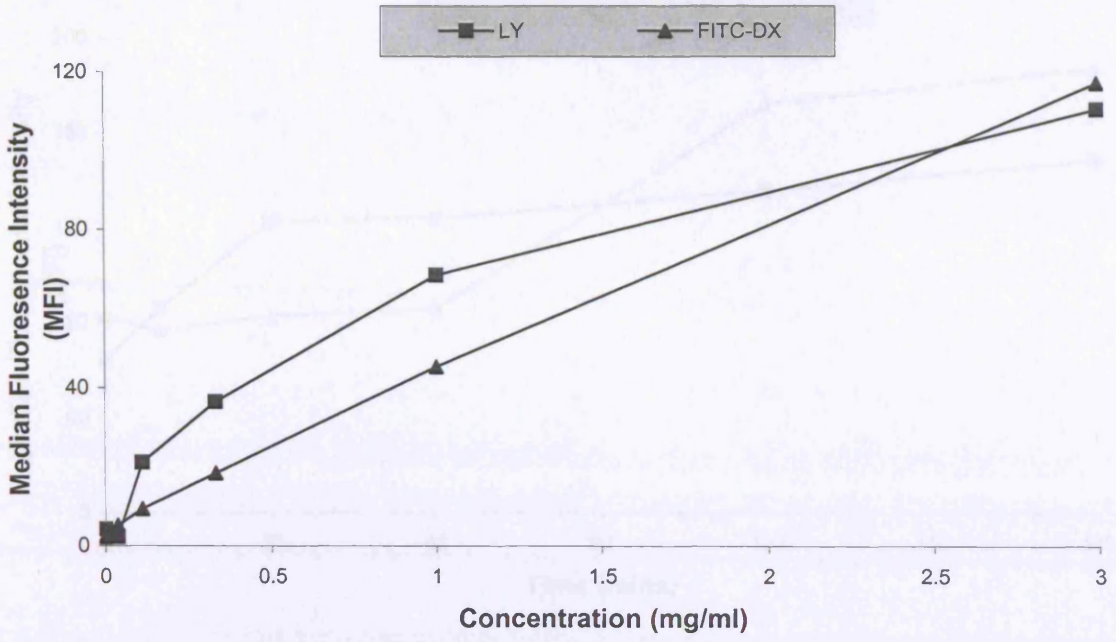

Figure 6.26: (a) Top panel: forward scatter / side scatter plot of A20 cells. Bottom panels: FL1 histogram of A20 cells incubated in the presence of various concentrations of LY and FITC-DX for 1 hour. (b) Median FL1 taken from histogram plots shown in a) as a function of concentration of LY and FITC-DX. Data is a representative example of at least three experiments

(a)

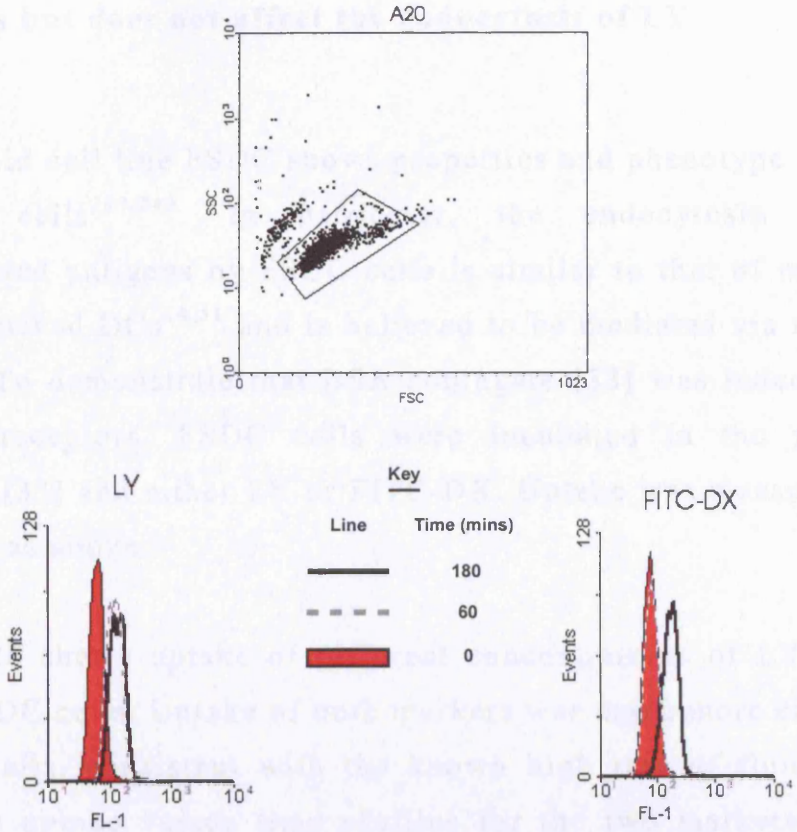

(b)

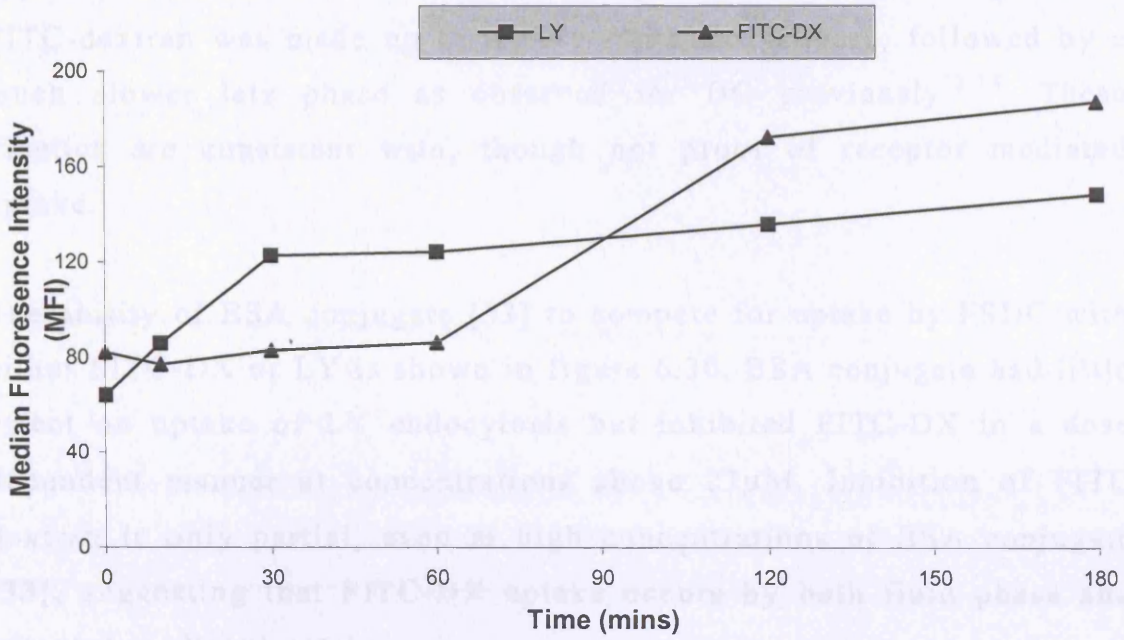

Figure 6.27: (a) Top panel: forward scatter / side scatter plot of A20 cells. Bottom panel: FL1 histogram of A20 cells incubated in the presence of 1 mg/ml LY or FITC-DX for various times. (b) Median FL1 taken from histogram plots shown in a) as a function of time of uptake. Data is a representative example of at least three experiments

6.6.2 BSA conjugate [33] inhibits the uptake of FITC-DX into FSDC cells but does not affect the endocytosis of LY

The myeloid cell line FSDC shows properties and phenotype of immature dendritic cells[244,245]. In particular, the endocytosis of soluble mannosylated antigens by FSDC cells is similar to that of murine bone-marrow-derived DCs[14,51] and is believed to be mediated via the mannose receptor. To demonstrate that BSA conjugate **[33]** was indeed bound by mannose receptors, FSDC cells were incubated in the presence of conjugate **[33]** and either LY or FITC-DX. Uptake was measured by flow cytometry as above.

Figure 6.28 shows uptake of different concentrations of LY and FITC-DX by FSDC cells. Uptake of both markers was much more efficient than for A20 cells, consistent with the known high rate of fluid uptake by DC[12]. The uptake versus time profiles for the two markers were quite different however (fig. 6.29). Uptake of Lucifer yellow was approximately linear for a three-hour period. In contrast, uptake of FITC-dextran was made up of a very rapid early phase, followed by a much slower late phase as observed for DC previously[12,14]. These kinetics are consistent with, though not proof of receptor mediated uptake.

The ability of BSA conjugate **[33]** to compete for uptake by FSDC with either FITC-DX or LY is shown in figure 6.30. BSA conjugate had little effect on uptake of LY endocytosis but inhibited FITC-DX in a dose dependent manner at concentrations above 27μM. Inhibition of FITC dextran is only partial, even at high concentrations of BSA conjugate **[33]**, suggesting that FITC-DX uptake occurs by both fluid phase and receptor-mediated uptake.

(a)

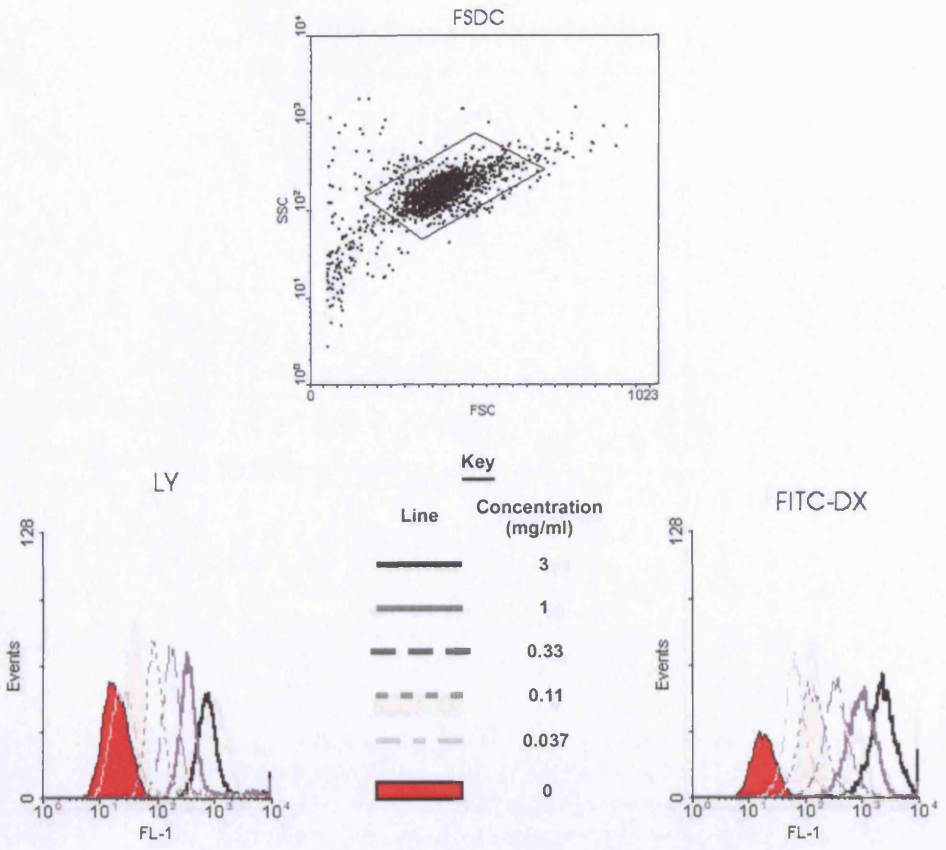

(b)

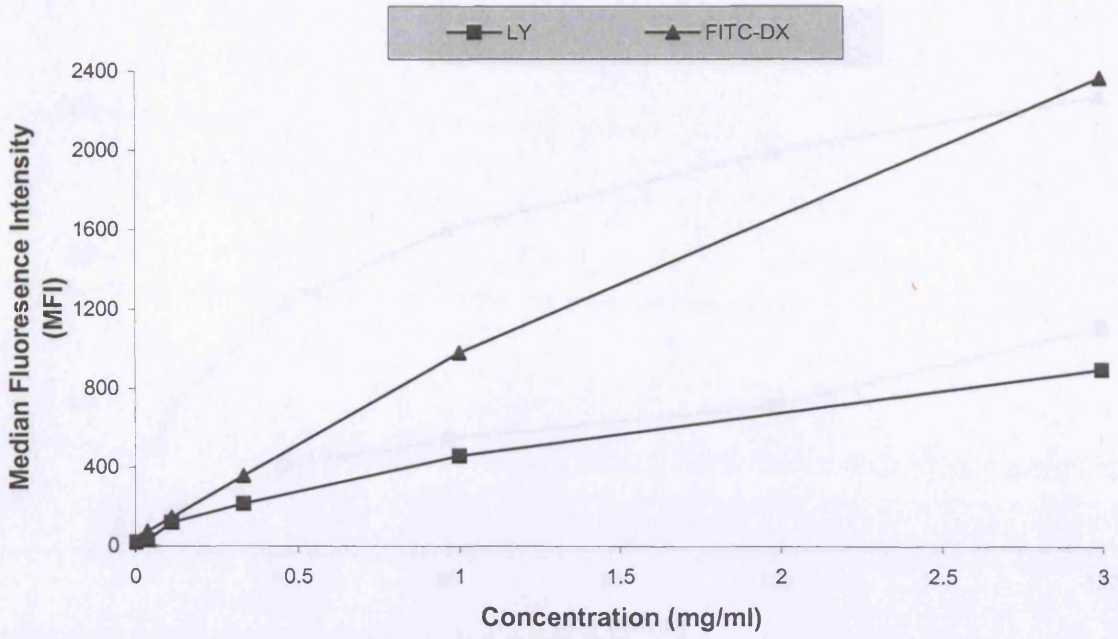

Figure 6.28: (a) Top panel: forward scatter / side scatter plot of FSDC cells. Bottom panels: FL1 histogram of FSDC cells incubated in the presence of various concentrations of LY and FITC-DX for 1 hour. (b) Median FL1 taken from histogram plots shown in a) as a function of concentration of LY and FITC-DX. Data is a representative example of at least three experiments

(a)

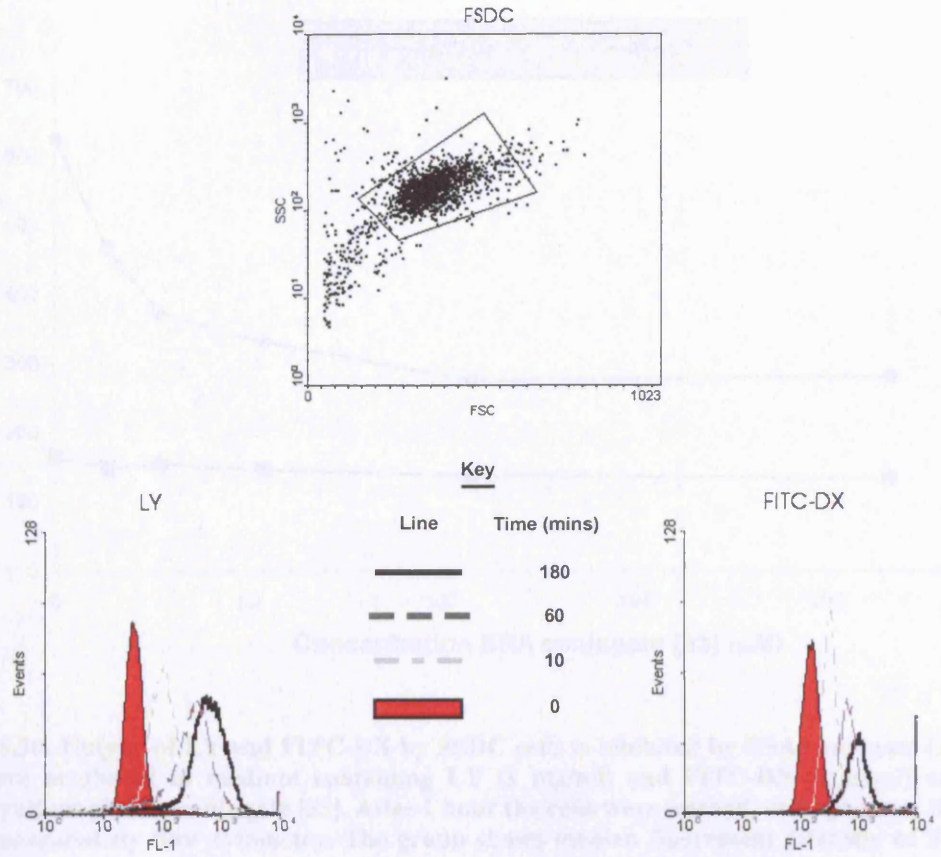

(b)

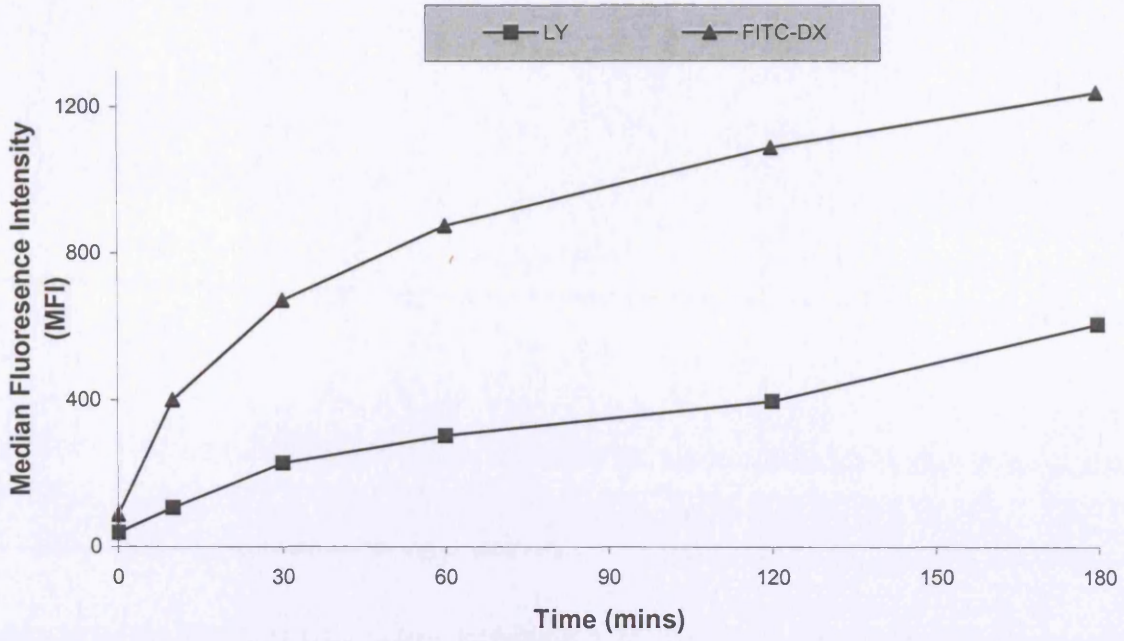

Figure 6.29: (a) Top panel: forward scatter / side scatter plot of FSDC cells. Bottom panel: FL1 histogram of FSDC cells incubated in the presence of 1 mg/ml LY or FITC-DX for various times. (b) Median FL1 taken from histogram plots shown in a) as a function of time of uptake. Data is a representative example of at least three experiments

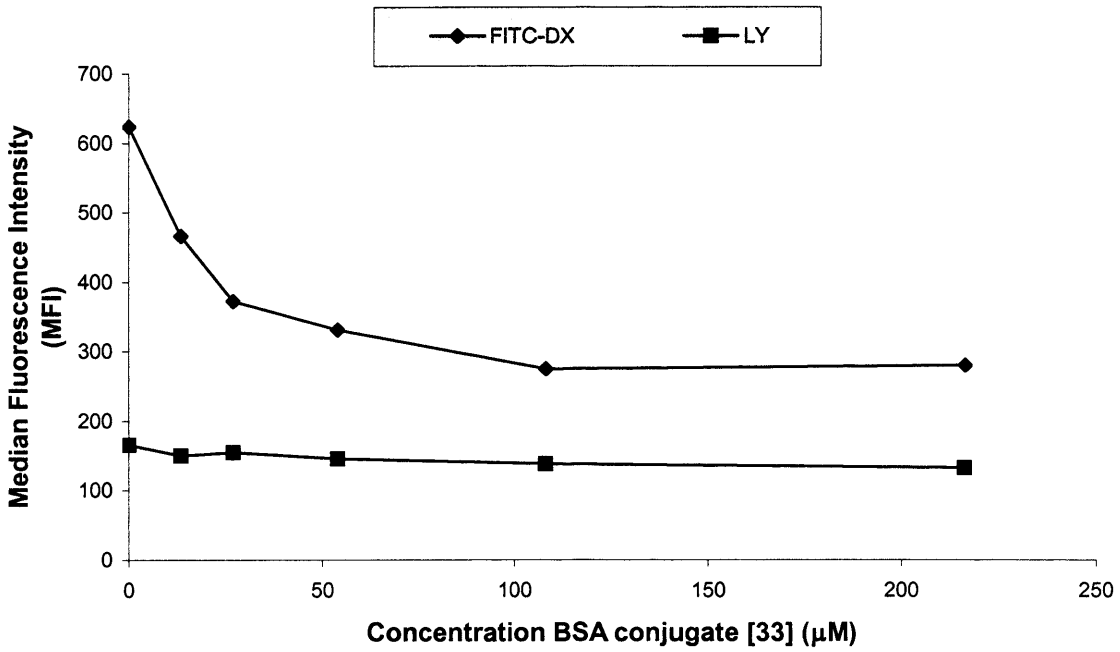

Figure 6.30: Uptake of LY and FITC-DX by FSDC cells is inhibited by BSA conjugate [33]. FSDC cells were incubated in medium containing LY (1 mg/ml) and FITC-DX (1mg/ml) and varied concentrations of BSA conjugate [33]. After 1 hour the cells were washed, and uptake of fluorescent probe measured by flow cytometry. The graph shows median fluorescent intensity of FSDC cells *versus* concentration of BSA conjugate. Data is a representative example of three experiments

6.7 Processing and presentation of ovalbumin and peptide p323 by murine bone marrow DC

A representative example of OVA and p323 peptide presentation by adult Balb/c DC to DO11-10 cells is shown in figure 6.31. The amount of ovalbumin protein and p323 peptide required to produce a detectable response is in the range of 0.5 – 1 mg/ml OVA (11 – 23 μM) and less than 0.1μg/ml (60 nM) p323 peptide. Similar levels of IL-2 release can be achieved as A20 cells but at lower numbers of DCs. This suggests that the processing and presentation capacity of DCs is greater than that of A20 cells under similar conditions. Bone marrow cell concentrations of 2 x 10^5 cells / ml or 5 x 10^5 cells / ml were commonly used. Of this population, the total number of immature DCs present ranged from 30 % to 60 %. Ideally, a purer population of DCs would provide more reproducible results. However, such an option was not available for this initial study.

(a)

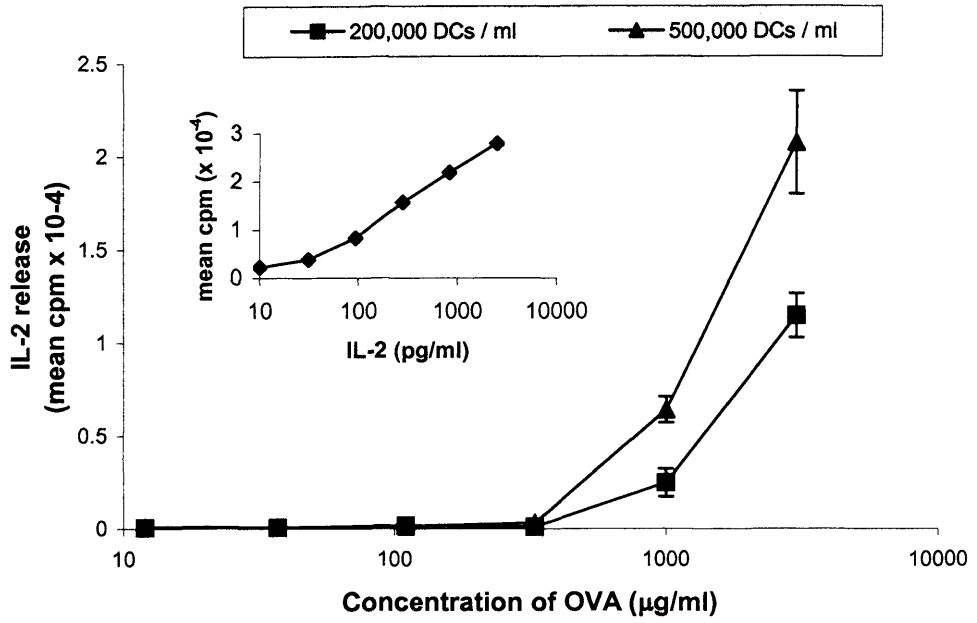

(b)

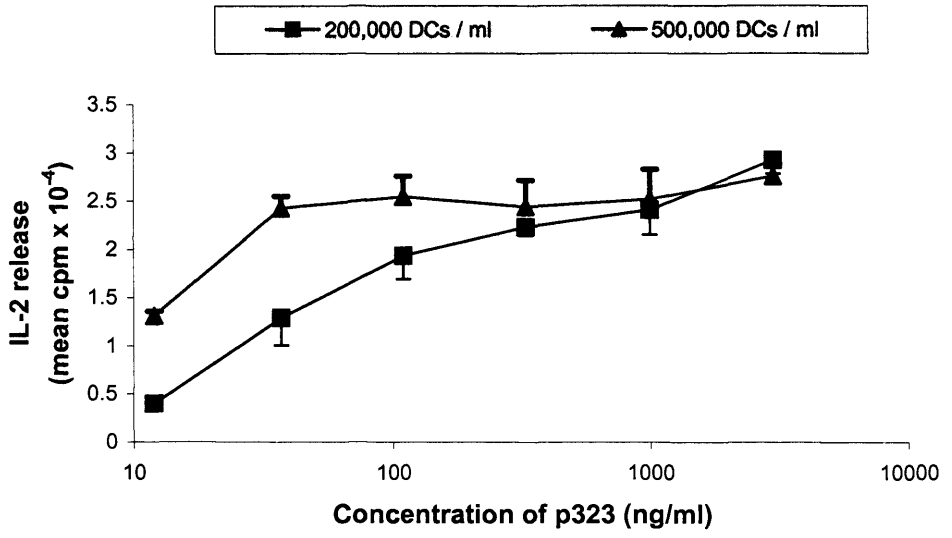

Figure 6.31: Response of DO11-10 cells to a) OVA and b) p323 peptide, presented by dendritic cells. DO11-10 hybridoma T-cells (10^6/ml) and adult Balb/c DCs (2 x 10^5/ml and 5 x 10^5/ml) were co-cultured together in the presence of a range of antigen concentrations for 24 hours. IL-2 release was determined by CTLL assay. Results are expressed as the mean ^{3}H-thymidine incorporation from triplicate cultures and are representative of three separate experiments. Graph a) shows the IL-2 control for the data of both graphs

6.7.1 Pepstatin A inhibits DO11-10 response to OVA but not OVA peptide p323 when presented by Balb/c DCs

The observed effect of pepstatin A upon inhibition of A20 cell processing of OVA protein is well characterised (section 6.1.2, page 185). Using the same model, pepstatin A also inhibited processing/presentation by bone marrow derived immature DCs (fig. 6.32 – 6.34). Figure 6.32a shows that at 54μM of pepstatin A (0.33 % DMSO) the inhibition of IL-2 release is substantial (approximately 80 %) (fig. 6.34). DMSO at the same concentration had a more limited effect on processing. There is also a limited toxicity effect of either pepstatin A or DMSO at these same concentrations (fig. 6.32b), and importantly, no effect upon p323 presentation (fig. 6.33). Figure 6.34 shows the percentage inhibition of IL-2 release and percentage toxicity.

Apart from the number of DCs used, all other variables in the antigen presentation assay are the same as for the use of A20 cells. DCs *in vivo* have a larger capacity of antigen uptake than B-cells *in vivo*, due to both the smaller size of these B-cells and the extra mechanisms used by DCs to endocytose. This may not translate into A20 B-cells, which are larger than *ex vivo* murine B-cells, and as such may have similar levels of antigen / inhibitor uptake to murine bone marrow derived DCs. As there is no efficient T-cell targeting design incorporated into MPC1 or MPC2, and given the size of the A20 cells compared to normal B-cells, it is possible that the effects observed with pepstatin A could be comparable between A20 cells and DCs.

(a)

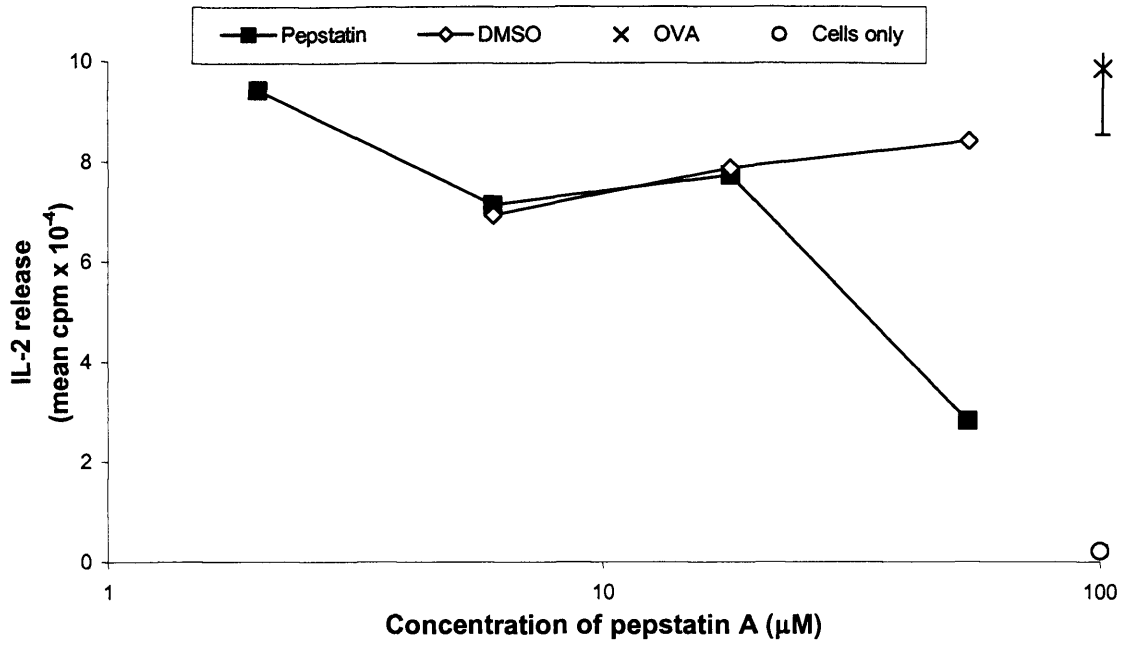

(b)

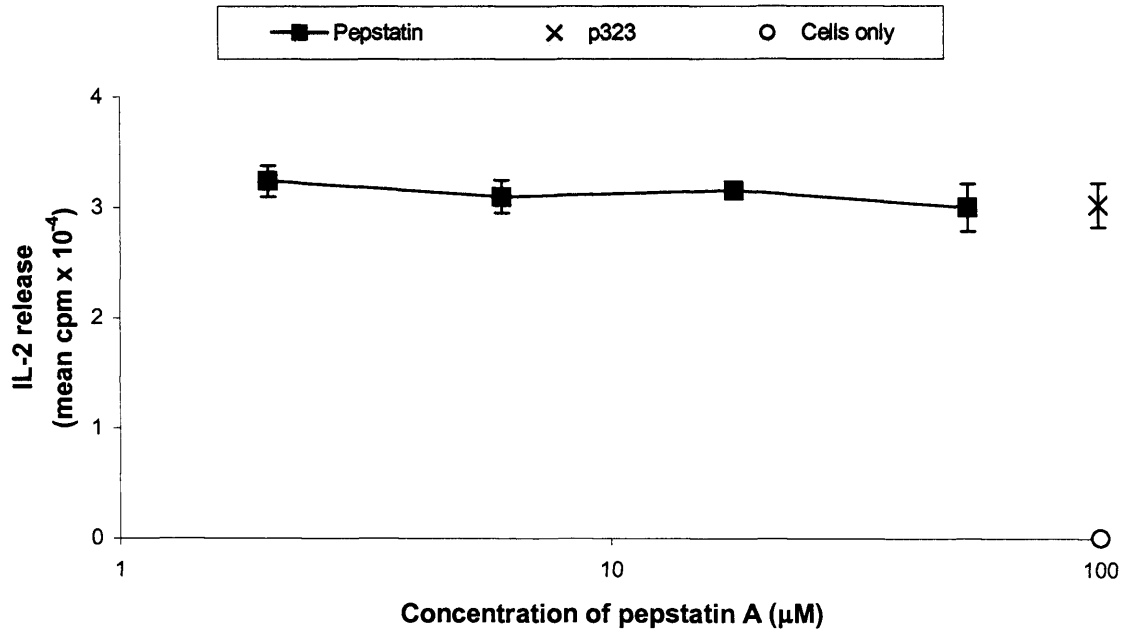

Figure 6.32: Response of DO11-10 cells to a) OVA (3mg/ml) and b) p323 peptide (0.1μg/ml), presented by DCs with varied concentrations of pepstatin A / DMSO and DMSO alone. IL-2 release measured by CTLL assay. Results are expressed as the mean ^{3}H-thymidine incorporation from triplicate cultures and are representative of three separate experiments.

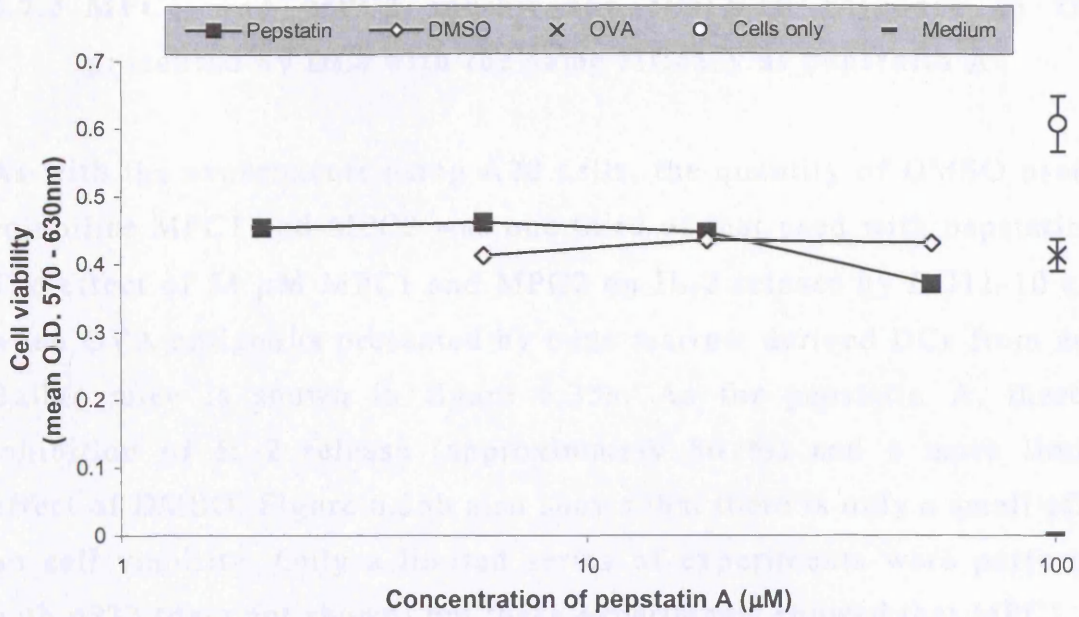

Figure 6.33: Cell viability of antigen presentation assay (shown in figure 4.32a): response of DO11-10 cells to OVA (3mg/ml) presented by Balb/c DCs: with varied concentrations of pepstatin A and DMSO. Cell viability measured by MTT incorporation and expressed as the mean O. D. (570 – 630nm) from triplicate cultures and are representative of three different experiments

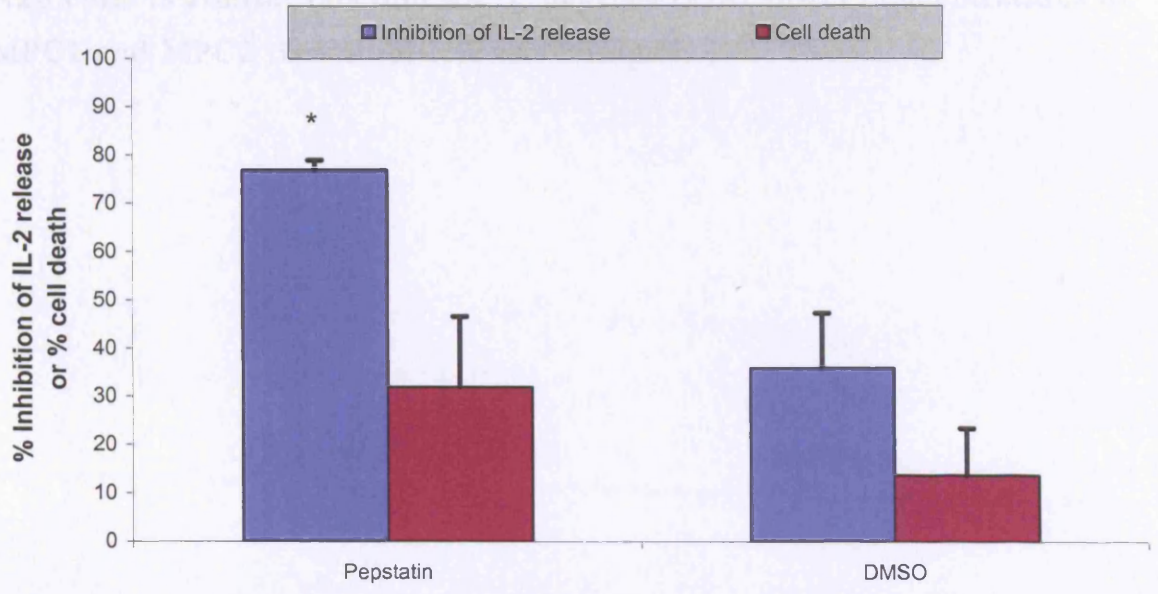

Figure 6.34: The effect of Pepstatin / DMSO and DMSO alone on the OVA presentation by Balb/c DCs and cell viability. Graph shows the results with 54μM of Pepstatin along with its equivalent DMSO concentration (0.33 %). Results show the mean +/– SEM of three separate experiments. * $p < 0.01$ *versus* OVA control. % inhibition of IL-2 release and % cell death calculated as described in legend to fig. 6.4

6.7.2 MPC1 and MPC2 inhibit the DO11-10 response to OVA presented by DCs with the same efficacy as pepstatin A

As with the experiments using A20 cells, the quantity of DMSO used to solubilise MPC1 and MPC2 was one third of that used with pepstatin A. The effect of 54 μM MPC1 and MPC2 on IL-2 release by DO11-10 cells when OVA antigen is presented by bone marrow derived DCs from adult Balb/c mice is shown in figure 6.35a. As for pepstatin A, there is inhibition of IL-2 release (approximately 80 %) and a more limited effect of DMSO. Figure 6.35b also shows that there is only a small effect on cell viability. Only a limited series of experiments were performed with p323 (data not shown) but these experiments showed that MPC1 and MPC2 do not inhibit the presentation of p323 peptide to DO11-10 cells. A summary of data obtained for MPC1 and MPC2 at 54μM is shown in figure 6.36. In general the effects observed with MPC1 / MPC2 within A20 cells is similar (section 6.2.3, page 195). At lower concentrations of MPC1 and MPC2 the inhibition was minimal.

(a)

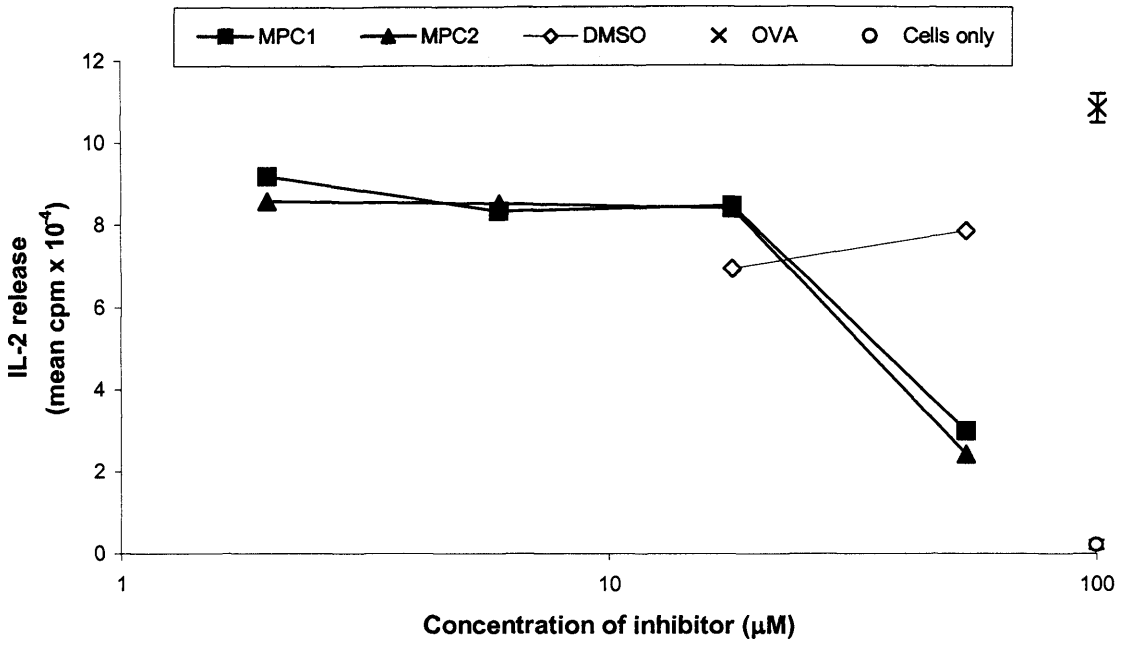

(b)

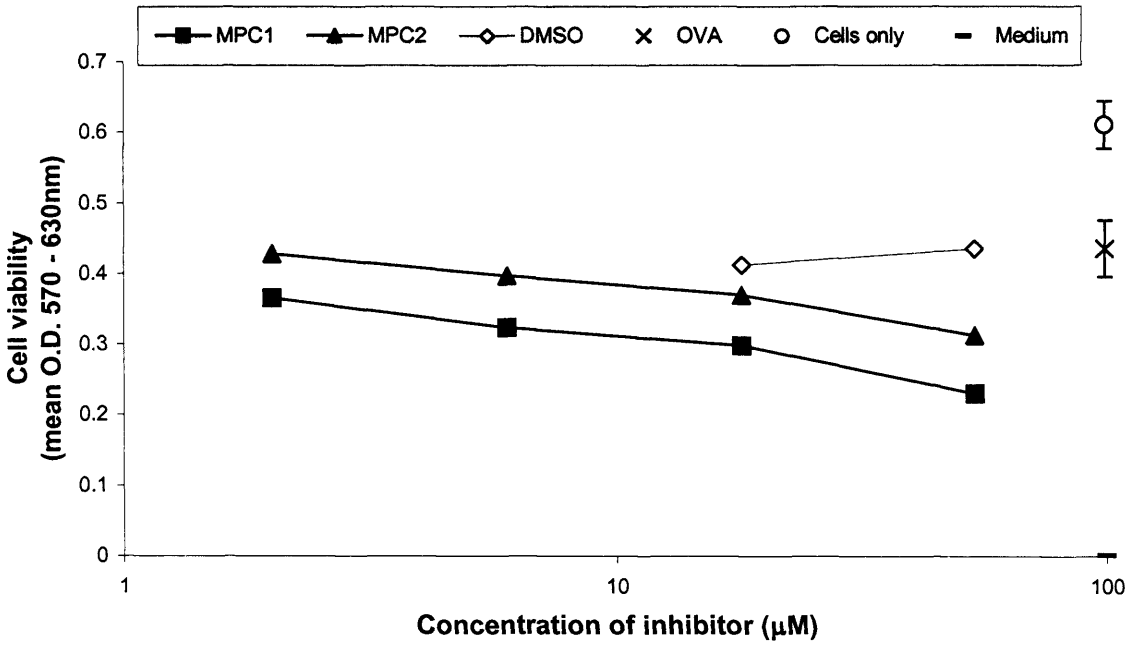

Figure 6.35: Response of DO11-10 cells to OVA presented by Balb/c DCs: varied concentrations of MPC1, MPC2 and DMSO added. a) IL-2 release by DO11-10 cells, measured CTLL assay. Results are expressed as the mean ^{3}H-thymidine incorporation from triplicate cultures. b) Cell viability measured by MTT incorporation and expressed as the mean O. D. (570 – 630nm) from triplicate cultures and are representative of three different experiments. Results for both graphs are representative of at least three separate experiments. Experiment uses 5 x 10^{5} DCs/ml, 3mg/ml OVA and 0.11% DMSO at 54μM MPC1 or MPC2

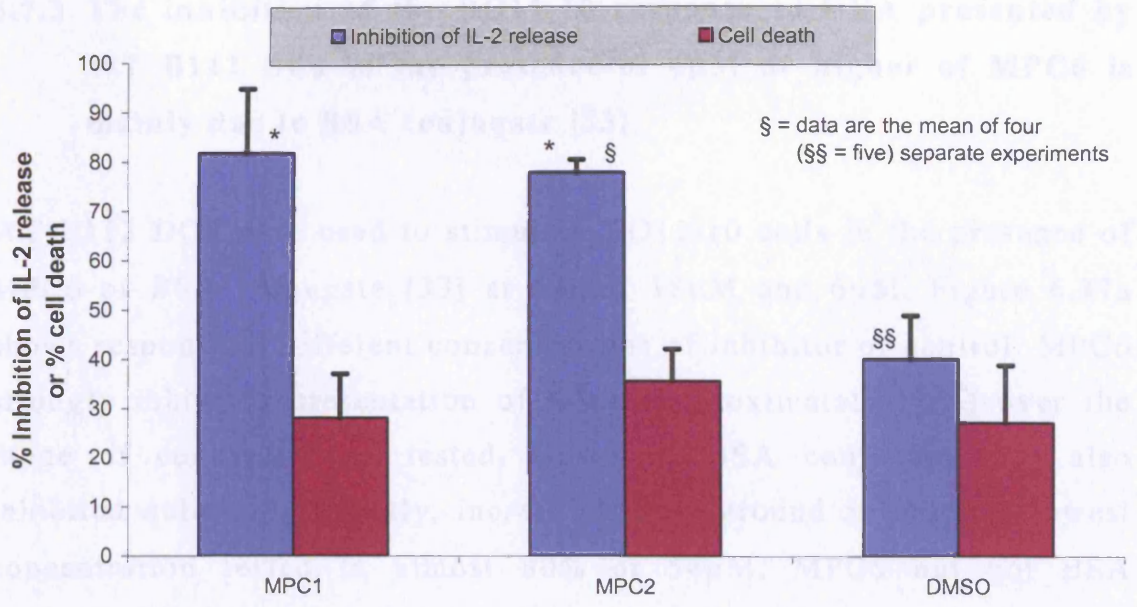

Figure 6.36: The effect of MPC1, MPC2 (both including DMSO) and DMSO alone on the OVA presentation by Balb/c DCs and cell viability. Graph shows the results with 54μM of MPC1 and MPC2 along with its equivalent DMSO concentration (0.11 %). Results show the mean +/– SEM of three separate experiments, unless otherwise stated. * $p < 0.01$ *versus* OVA control. % inhibition of IL-2 release and % cell death calculated as described in legend to fig. 6.4

6.7.3 The inhibition of the DO11-10 response to OVA presented by WT B112 DCs in the presence of 6μM or higher of MPC6 is mainly due to BSA conjugate [33]

WT B112 DCs were used to stimulate DO11-10 cells in the presence of MPC6 or BSA conjugate **[33]** at 54μM, 18μM and 6μM. Figure 6.37a shows response at different concentrations of inhibitor or control. MPC6 strongly inhibited presentation of OVA (approximately 80%) over the range of concentrations tested. However, BSA conjugate **[33]** also inhibited quite significantly, increasing from around 50% at the lowest concentration tested to almost 80% at 54μM. MPC6 but not BSA mannose **[33]** had much less effect on p323 peptide presentation except at the highest concentration of 54μM). A more limited set of experiments with MPC5 (data not shown) did not display any inhibition above or beyond that of BSA conjugate **[33]**.

(a)

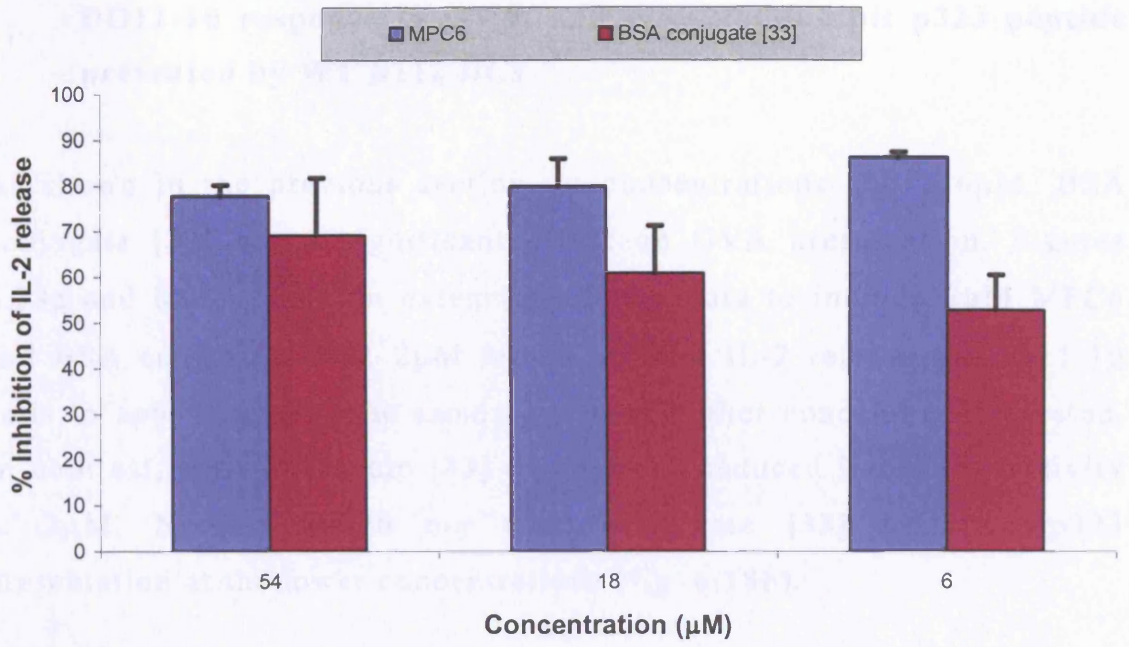

(b)

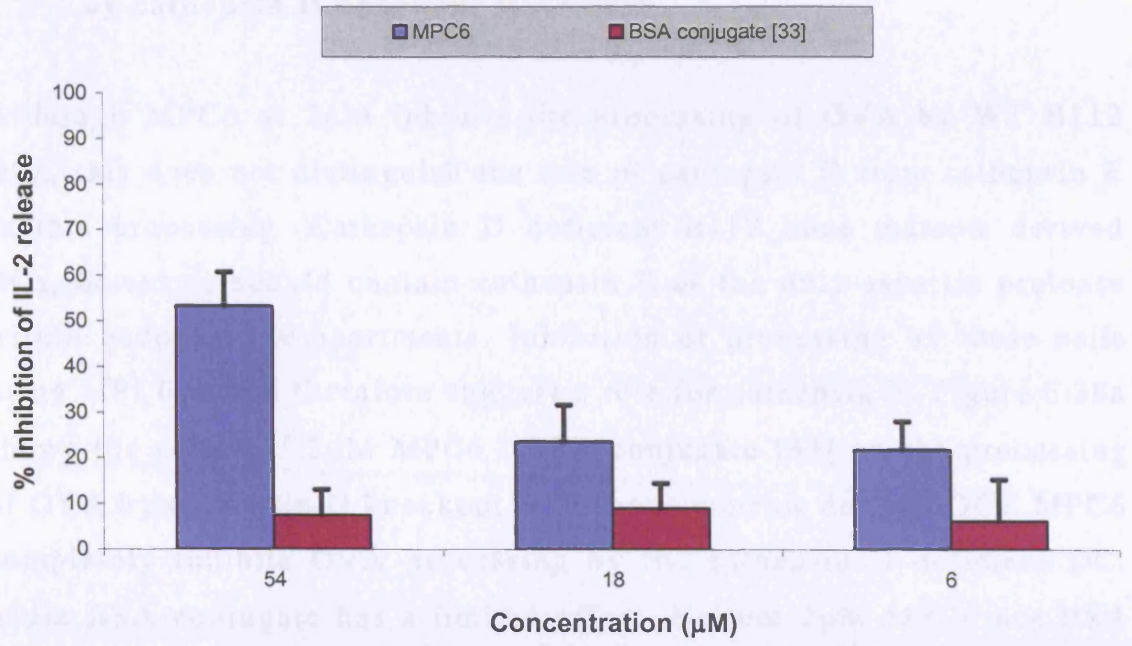

Figure 6.37: The effect of varied concentrations of MPC6 on a) OVA (1mg/ml) presentation by WT B112 DCs, and b) p323 (0.1µg/ml) presentation by WT B112 DCs. Results show the mean +/– SEM of three separate experiments. % inhibition of IL-2 release calculated as described in legend to fig. 6.4. IL-2 release was measured for each experiment by ^{3}H-thymidine incorporation in triplicate cultures.

6.7.4 MPC6 (2μM) but not BSA conjugate [33] (2μM) inhibit the DO11-10 response to OVA, and does not inhibit p323 peptide presented by WT B112 DCs

As shown in the previous section, at concentrations above 6μM, BSA conjugate **[33]** has a significant effect on OVA presentation. Figures 6.38a and 6.38b show an extension of this data to include 2μM MPC6 and BSA conjugate **[33]**. 2μM MPC6 inhibits IL-2 release by DO11-10 cells to approximately the same degree as higher concentrations tested. In contrast, BSA conjugate **[33]** has a much-reduced inhibitory activity at 2μM. Neither MCP6 nor BSA conjugate **[33]** inhibited p323 presentation at the lower concentrations (fig. 6.38b).

6.7.5 MPC6 but not BSA conjugate [33] (2μM) inhibit the DO11-10 response to OVA, and does not inhibit p323 peptide presented by cathepsin D knockout B112 DCs

Although MPC6 at 2μM inhibits the processing of OVA by WT B112 DCs, this does not distinguish the role of cathepsin D from cathepsin E in this processing. Cathepsin D deficient B112 bone marrow derived DCs, however, should contain cathepsin E as the only aspartic protease within endocytic compartments. Inhibition of processing by these cells using MPC6 would therefore suggest a role for cathepsin E. Figure 6.38a shows the effect of 2μM MPC6 / BSA conjugate **[33]** on the processing of OVA by cathepsin D knockout B112 bone marrow derived DCs. MPC6 completely inhibits OVA processing by the cathepsin D deficient DC, while BSA conjugate has a limited effect. Neither 2μM MPC6 nor BSA conjugate inhibit p323 presentation.

(a)

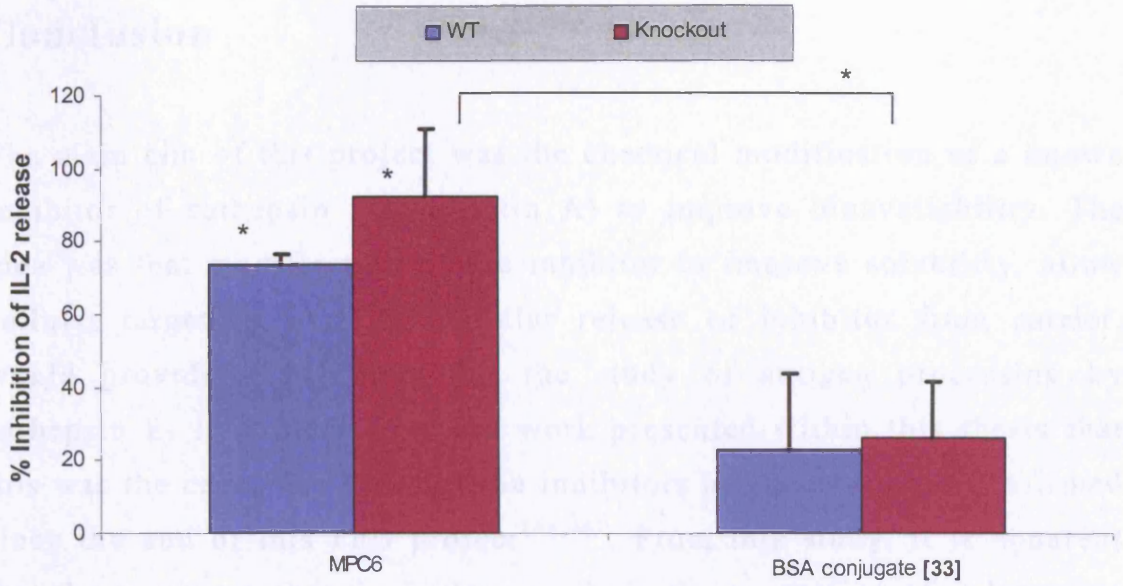

(b)

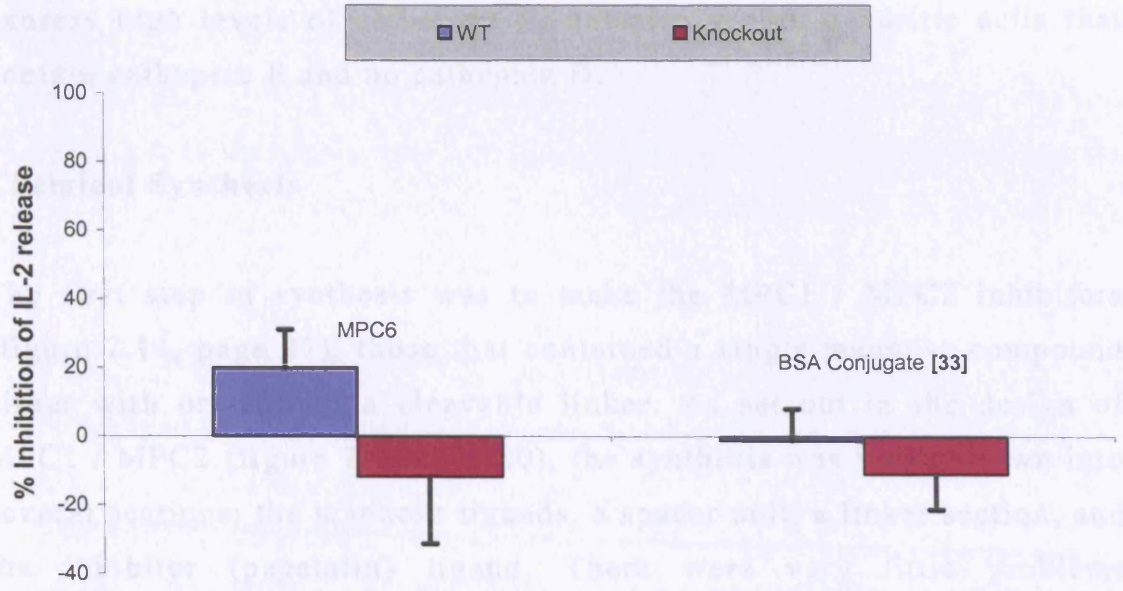

Figure 6.38: The effect MPC6 (2 μM) and BSA conjugate [33] (2 μM) on a) OVA (1mg/ml) presentation by WT B112 DCs and cathepsin D deficient B112 DCs, and b) p323 (0.1μg/ml) presentation by WT B112 DCs and cathepsin D deficient B112 DCs. Results show the mean +/– SEM of three separate experiments. * $p < 0.01$ *versus* OVA control, or where specified *versus* BSA conjugate [33] control. % inhibition of IL-2 release calculated as described in legend to fig. 6.4. IL-2 release was measured for each experiment by ^{3}H-thymidine incorporation in duplicate cultures.

Conclusion

The main aim of this project was the chemical modification of a known inhibitor of cathepsin E (pepstatin A) to improve bioavailability. The idea was that modification of the inhibitor to improve solubility, allow cellular targeting, and intracellular release of inhibitor from carrier, would provide a new tool for the study of antigen processing by cathepsin E. It is clear from the work presented within this thesis that this was the case. The value of the inhibitors has been further confirmed since the end of this PhD project[246,247]. From this study, it is apparent that the enzyme cathepsin E plays a role in the processing of at least one antigen, in this case the generation of a dominant immunogenic peptide from OVA protein. Not only has this been shown in A20 B-cells, that express high levels of cathepsin E, but also within dendritic cells that contain cathepsin E and no cathepsin D.

Chemical Synthesis

The first step in synthesis was to make the MPC1 / MPC2 inhibitors (figure 2.14, page 87), those that contained a single mannose compound either with or without a cleavable linker. As set out in the design of MPC1 / MPC2 (figure 2.7, page 80), the synthesis was broken down into several sections; the mannose ligands, a spacer unit, a linker section, and the inhibitor (pepstatin) ligand. There were very little problems encountered in the synthesis of each of these sections, with most reactions allowing for the isolation of pure high yielding compounds. The coupling chemistry used to join these sections was also successful in terms of yield and obtaining pure compounds. The first route for the formation of 3'-benzyloxycarbonylpropyl 2,3,4,6-tetra-*O*-acetyl-α-D-mannopyranoside **[15]** resulted in slightly impure material, however the reaction of 2,3,4,6-tetra-*O*-acetyl-α-D-mannopyranosyl trichloro-

acetimidate **[3]** with benzyl 4-hydroxy-butanoate **[12]** using $BF_3.Et_2O$ was both selective for the α-anomer and provided moderately high yields with little impurities. The final stages of coupling pepstatin to the rest of the MPC1 / MPC2 framework provided some interesting insights into the physical properties of pepstatin. Pepstatin analogues were both crystalline and easy to handle in purification procedures.

For MPC5 and MPC6 (figure 2.8, page 80), a different synthetic strategy was used to include an alternative aromatic spacer moiety, based upon other studies[3] that showed improved affinity for the mannose receptor. The synthesis of the mannose – spacer ligand 4-nitrophenyl 2,3,4,6-tetra-*O*-acetyl-α-D-mannopyranoside **[6]** (section 3.1.6, page 96) was improved over the methods used for MPC1 / MPC2, with a shorter synthetic pathway to give a higher yielding crystalline material. Unlike MPC1 / MPC2, pepstatin – linker analogues were synthesised first, and were then coupled to the mannosylated BSA carrier. It was felt this approach would be better for both the synthesis, purification and analysis of compounds, especially considering the physical properties learnt about pepstatin that showed pepstatin analogues to be potentially easy to purify.

One key point regarding the coupling efficiency of the pepstatin inhibitor within compound MPC6 was not addressed. Specifically, there is no quantitative data which analyses the stoichiometry of the pepstatin/BSA conjugate for either MPC5 or in particular MPC6. However, considerable efforts (both by dialysis and gel chromatography purification) were made to remove free pepstatin, making it unlikely that free pepstatin had a role in the inhibition effects observed with MPC6. Attempts were made to measure the conjugation efficiency of pepstatin to BSA by using Ellman's test for the presence of free sulfhydryl groups on the BSA, however with little success. This problem needs to be looked at again in the future.

The synthesis of MPC3 / MPC4 was not completed. The unfortunate mixing of Dde and ivDde protected lysine and the synthesis of hexalysyl compounds containing both of these groups made it difficult to analyse mass spectral data. Although it was felt that the coupling of 4-isothiocyanatophenyl α-D-mannopyranoside **[11]** to the hexalysyl carrier (starting at section 3.5.5, page 138) was successful due to the disappearance of ninhydrin staining (an indication of no free amino groups being present), both mass spectra and NMR data were inconclusive, a problem that also occurred in other attempted synthesis steps. One of the problems with the synthesis mentioned above was solubility, an issue that may be overcome with the use of an alternative solvent such as DMF. Several alternative approaches may help in the synthesis of these compounds (see future work, page 248).

Enzymology

Inhibition by pepstatin A of the enzymatic cleavage of a fluorogenic substrate by rat cathepsin E showed an IC_{50} value within the pM range (fig. 6.1, page 185). The IC_{50} values for MPC1 / MPC2 are also in the picomolar range, similar to that of pepstatin, suggesting that the attached ligands do not interfer significantly with the binding of pepstatin to cathepsin E.

MPC5 and MPC6 have an IC_{50} within the nM range (fig. 6.19, page 209). This much higher value does suggest an interference in the binding of MPC5 / MPC6 to cathepsin E compared with pepstatin alone. This difference is likely to be due to steric interference by the BSA carrier or the spacer/linker . However, BSA – conjugate **[33]** without the addition of pepstatin has an approx. IC_{50} value of inhibition of rat cathepsin E in the 0.5 – 2 μM range. This large difference in the IC_{50} values of MPC5 / MPC6 compared with BSA – conjugate **[33]** is most likely due to the attachment of pepstatin. It has been shown that the cellular degradation

of BSA and mannosylated BSA is inhibited by the presence of pepstatin A[242,243] suggesting an involvement of aspartic proteinases in their catabolism. This could explain why BSA – conjugate has some inhibitory effect by itself being a target for catabolism by cathepsin E (as opposed to the fluorogenic substrate). This may also be a factor for MPC5 / MPC6.

Solubility

DMSO is required to solubilise pepstatin before it is used *in vitro*. This introduces toxicity effects on a cell assay. The use of DMSO is also required to avoid crystallisation of the inhibitors MPC1 / MPC2. The amount required for MPC1 and MPC2, however, is lower than that required by pepstatin A, such that toxicity is greatly reduced. The attachment of multiple mannose units to BSA to form the backbone of the MPC5 / MPC6 inhibitors (figure 2.14, page 87) greatly improves their solubility in water, such that no DMSO is required. The drawback to this is that the size of a protein carrier does introduce its own problems, for example, the fact that the protein carrier itself was able to inhibit at higher concentrations. The eventual synthesis of the MPC3 / 4 type of inhibitors (i.e. those with a poly-lysine backbone) may overcome this type of problem.

Targeting – the effect of inhibitors on A20 cells

As reported previously, Pepstatin A is a potent inhibitor of the processing of OVA antigen within the A20 cell line[112]. MPC1 and MPC2 are able to completely abolish the response (i.e. IL-2 release) of DO11-10 cells to OVA presented by A20 cells. As shown in figures 6.10 to 6.14 (page 196 – 201), this effect is due to the inhibitors themselves and only a minimal effect is due to DMSO, cell viability, or other cellular effects that could cause inhibition of p323 presentation.

Unlike the inhibition of IL-2 release when using A20 cells and pepstatin, MPC1 or MPC2 inhibitors, there is a varied effect of MPC5 and MPC6 on A20 cell processing that shows only a partial inhibition of IL-2 or in some circumstances an increase in IL-2 production, as shown for MPC5 in figure 6.21a (page 211). The reason for this varied effect is unknown. One possibility for their poor inhibition may be linked to the difference in IC_{50} between pepstatin A and that of MPC5 and MPC6. Pepstatin A has an IC_{50} on rat cathepsin E within the pM range (fig. 6.1, page 185). This translates into inhibition of A20 cell processing at approximately 54μM. In contrast, MPC5 and MPC6 have an IC_{50} on cathepsin E within the nM range (fig. 6.19, page 209). Without any means of selective uptake of MPC5 or MPC6 into A20 cells over that of pepstatin A, there may be a requirement to use over 0.5mM of MPC5 or MPC6 to inhibit A20 cell processing. Such concentrations would not be possible with the MPC5 and MPC6 inhibitors.

Another possibility for poor inhibition may be due to the dynamics of protein movement and degradation within the A20 B-cell that leads to the shuttling of MPC5 and MPC6 to lysosomes before either MPC5 or MPC6 can inhibit OVA cleavage by its attached pepstatin, or cleavage of a pepstatin A analogue from MPC6. This idea is based upon several facts on the way BSA and mannosylated BSA is degraded in antigen presenting cell endosomes. The A20 B-cell contains endosomal compartments similar to other antigen presenting cells[48], i.e. endosomes that have a decreased pH gradient towards lysosomal like vesicles along which antigen may travel. The process of antigen movement towards the lysosome can be slower than the speed at which antigen can be cleaved in endosomes to allow binding of antigenic peptides to MHC-II molecules, and as such antigen can be cleaved along any part of the endosome / lysosome vesicular pathway. Mannosylated BSA has been shown to be degraded in early lysosomes[248] and is transported to lysosomes when in the presence of pepstatin A[242].

This suggests that MPC5 and MPC6 may be able to inhibit their own catabolism , the net effect being the transport of MPC5 and MPC6 to the lysosome with no inhibition of antigen processing being observed. To investigate this hypothesis will need more study, outside the scope of this project.

Targeting – the effect of inhibitors on DCs

Immature dendritic cells are different from the A20 B-cell line in several ways. Immature dendritic cells are highly specialised in endocytosis, either *via* fluid phase or receptor mediated pathways. In theory this should equate into a larger uptake of antigen. In addition, DC, but not B cells or A20 cells express members of the mannose-binding receptor family, and can therefore take up mannosylated analogues of pepstatin via receptor mediated endocytosis. These two factors may impact on the ability of aspartic protease inhibitors to function effectively.
The development of the B112 mice population (see section 6.5, 213) made it possible to study the effect of aspartic proteinases inhibitors on wild type and cathepsin D deficient DCs. It was not felt that the inhibitors MPC1 and MPC2 would be valuable inhibitors for the study of these cells. Unfortunately, the limitations with cell numbers and project duration meant that only a limited set of MPC5 and MPC6 experiments were performed, and in all cases there were no significant inhibition effects observed with MPC5 compared to its control BSA conjugate **[33]**. It would not be unreasonable to assume that MPC6 would be more potent than MPC5 because of its ability to be enzymatically cleaved intracellularly by thiol reductases to release an unencumbered pepstatin A analogue. The lack of MPC5 effect may be an indication of this, or as mentioned previously, some type of shuttling of MPC5 into lysosomes where it could be easily destroyed by the proteolytic environment. It is likely this could happen to MPC6 also, however cleavage of the linker in

MPC6 may allow for it to inhibit aspartic proteinase function. More work would be needed to assess the value of the cleavable linker.

The effects of pepstatin, MPC1 and MPC2 upon antigen processing using murine derived bone marrow DCs (section 6.7.1, page 229 and section 6.7.2, page 232) are similar to the effects seen within A20 cells (sections 6.1, page 184 and section 6.2, page 190). At lower concentrations of inhibitor (below 54μM), the effect of pepstatin / MPC1 / MPC2 was minimal compared with that observed using A20 cells. This may be explained by the increased proteolytic ability of DCs over that of A20 cells such that at 18μM of inhibitor enough OVA protein is processed to provide a sufficient amount of p323 peptide for antigen response by DO11-10 cells. Very small amounts of antigen are required to provide a sufficient T-cell response, as is evident for the difference of dose response seen between p323 peptide and OVA protein. It should also be pointed out that the MPC1 and MPC2 inhibitors only contain a single mannose sugar, and as such are unlikely to have a high affinity for the mannose receptor to aid in endocytosis.

There were no specific inhibition effect observed when using high concentrations of MPC6 (i.e. 6μM or above) (section 6.7.3, 235), a possible explanation of this is as follows. It has been previously shown that BSA and mannosylated BSA are both cleaved by aspartic proteases[242,243], and it would not be unreasonable to assume that BSA should therefore act as a competitive inhibitor due to the high concentration of BSA conjugate **[33]** or MPC6 used, an idea mentioned previously. A difference here with the use of DCs is that BSA conjugate **[33]** displays a reduced inhibition at 6μM, while MPC6 maintains a high inhibition (approximately 80 %). MPC6 (or even MPC5), containing an inhibitory pepstatin molecule, may inhibit cathepsin D / E by either BSA catabolism or pepstatin binding.

The effect of MPC6 (2μM) on B112 WT and cathepsin D deficient DCs was also investigated. Interestingly, the effect of the control BSA – conjugate **[33]** at 2μM is greatly reduced. In consequence, figure 6.38 (page 238) shows that both B112 murine WT and cathepsin D deficient DCs show a statistically significant greater inhibition of OVA processing by MPC6 over that of BSA – conjugate **[33]**. Importantly, both MPC6 and BSA – conjugate **[33]** did not inhibit the presentation of p323 peptide to DO11-10 T-cells. The fact that cathepsin D deficient DCs are also significantly inhibited in their ability to process OVA antigen has important implications for the role of cathepsin E within the processing of OVA. Some experiments that used cathepsin D deficient DCs actually showed inhibition greater that 100 % (fig. 6.38a, page 238). Such inhibition above that of the cells only control could possibly be an indication of cell death or anergy, maybe due to other important effects of cathepsin E.

Although data was limited, there was an indication that the levels of IL-2 release observed with B112 cathepsin D knockout DCs is generally lower than that of WT B112 DCs. This may be an indication that cathepsin D participates in the processing of OVA antigen within DCs. Antigen that enters lysosomes would be efficiently cleaved by cathepsin D and may re-enter the endosomal pathway for binding onto MHC-II molecules.

Proteolysis and antigen processing

It is clear from recent literature, that there is still a lot of information to be gained for the role of proteolytic enzymes within antigen processing. It can be generally concluded that at present proteolytic enzymes such as those mentioned in section 1.7 (starting at page 46) have varied functions in antigen presenting cells. Although they are all involved in the processing of antigen or important cellular molecules, it is clear that the exact environment that the enzymes are located, as well as the type

of antigen that they encounter, plays a changing role upon the functions of each of these proteolytic enzymes. The field is continually evolving to highlight the contributions that individual enzymes play in different aspects of antigen processing.

It is traditionally thought that aspartic proteinase function is not essential for the generation of antigens within mice. However, our own work, and that by others (section 1.7.4, page 51) has shown that *in vitro* aspartic proteinase activity may be important. This is extended by the work presented in this thesis and that has been published[247], showing that cathepsin E has an important role in the proteolysis of OVA antigen within DCs. Watts *et al* showed that the presentation of myoglobin antigen to T-cells by DCs lacking CD was surprisingly enhanced, and that this effect was pepstatin-sensitive[249]. The conclusion from this work indicated opposing functions of aspartyl proteinases in antigen processing, whereby cathepsin E may be the important enzyme involved in the processing of myoglobin antigen at optimal levels within DCs, whereas cathepsin D may exert destructive effects upon myoglobin, and thus reduce the efficiency of processing.

In this research, we show that at least in the case of OVA antigen when processed either by A20 B-cells, or by DCs, there is non-redundancy for the role of aspartic proteinases in the generation of the p323 fragment (amino acids 323 – 339) from OVA protein. Many other studies, however, show redundancy in proteolytic enzyme function, and this may also be true for the aspartic proteinases. Specific non-redundant functions, however, have also been demonstrated for AEP by Watts *et al*[77], whereby AEP can destroy a potentially important T-cell epitope, the HLA-DR2-restricted encephalito-genic MBP epitope (MBP 85-99), which contains an AEP cleavable site (Asn-94). The fact that AEP and aspartic proteinases are able to direct the immune response of specific antigen

processing models may suggest that other proteinases may also have such selective activity patterns.

The difference between these two studies and the general consensus may lie in the complexity of the antigen processing pathway. We have shown that with the use of a selective, soluble, cell and vesicular targeted inhibitor of aspartic proteinases, the recognition of the p323 fragment of OVA is completely abolished. It may be that future work in the field of antigen processing requires to take into consideration the factors that guide antigen into a cell through to its eventual antigenic peptide. Carefully planned experiments that target proteolytic inhibitors into various intracellular compartments may hold the key to unravelling the role of proteolytic enzymes on particular antigens or within particular intracellular vesicles.

Future work

There are several areas of the synthesis that need to be improved for future work. A method to detect the coupling efficiency of pepstatin to BSA – conjugate **[33]** or other MPC inhibitors needs to be addressed. One alternative to the Ellman's test for measuring free sulfhydryl content would be to use an improved marker for sulfhydryls, such as an iodoacetyl analogue of a fluorophore, and use to examine the difference in its reaction with BSA – conjugate **[33]** and MPC5 or MPC6. Alterntively, partial tryptic digestion of MPC6 followed by HPLC-mass spectroscopy, could be used to assay the degree of conjugation.

An important area that was very much missed in this report was the completion of the MPC3 / MPC4 inhibitors. Given the increased affinity of such multivalent ligands for the mannose receptor, and the likelihood that they would be much more potent and less toxic that the inhibitors tested, the future synthesis and testing of such ligands is very exciting.

Several lessons were learnt from the attempted synthesis of MPC3 / MPC4. The analysis of products was difficult, and this needs to be addressed. The coupling of the sugar units to the hexalysyl backbone had the additional problem of reactant solubility. An alternative approach might be to attach the Lysyl (ivDde) – linker – pepstatin units separately from the then pentalysyl and sugar units. Existing chemistry could be used to obtain a linker – pepstatin molecule; attachment of an ivDde protected lysine molecule to pepstatin should be easy, with purification and analysis not being a major problem. Subsequent attachment of this to a Boc-protected pentalysyl framework may aid in the analysis (no complex sugar signals found in NMR spectra) and in purification (HPLC would be ideal to separate the product). Deprotection of Boc groups should proceed without problem, leaving attachment of the sugar units as the last step, with analysis by MALDI-TOF MS being possible with such a large compound.

Unfortunately, time limitations at the end of this project restricted the experiments performed. However, it is clear from this study that within DCs, cathepsin E plays a role in the antigen processing of OVA. My own data showed that even at concentrations of MPC6 below 2μM, significant inhibition was still observed. There are several areas of research that would have significantly improved this report. More data using the B112 mice would allow a more detailed and accurate analysis of both the role of cathepsin E and the effect of MPC6. A major limitation was the number of cells obtainable from the B112 mice at the early stage of life that they were being used. Another problem was the purity of the DC population, at most this was ~ 60 %, but it was common to obtain populations as low as 30 %. A more accurate analysis of the DC populations obtainable from B112 cells may have helped to explain the low yields of DCs. Recent work by Prof. B. Chain has improved the yields of cells obtained by extending the culture duration[247]. With the additional use of FACS cell sorting, Prof B. Chain has been able to

obtain high yields of purer DC populations. The data obtained from these cells extends the work presented here[247].

The results presented naturally lead to a whole range of possible future approaches to study the role of cathepsin E. Without a doubt, the use of other antigens would be important to show if cathepsin E has an effect on other antigens too. The selective targeting of particular vesicles is also possible. As previously mentioned, the DEC-205 molecule when bound by antigen (or antibody) is able to target to late endosomal / lysosomal vesicles[34]. The improvements in cell culture of human DCs over the last decade means that the role of cathepsin E within human DCs could be explored. The possibility of targeting DCs *in vivo* is also a possibility. Although it has been suggested that it would be difficult to synthesis a cathepsin E-specific inhibitor[126], this is still an option that could be explored. In fact, some of the already synthesised cathepsin D inhibitors (see section 1.7.5, page 59) may distinguish between these two enzymes, and would be a good starting point.

In conclusion, the work presented in this thesis suggests that further interdisciplinary collaborations between chemists and immunologists will provide a fruitful avenue to approach the molecular dissection of antigen processing pathways. In turn, this will lead not only to improved understanding of the generation of the immunological repertoire, but possible new approaches to therapeutic intervention for the control of cancer, autoimmune disease or other immune-mediated pathologies.

Appendix I: NOE of 3-benzyloxycarbonylpropyl 2,3,4,6-tetra-*O*-acetyl-α-D-mannopyranoside **[15]**

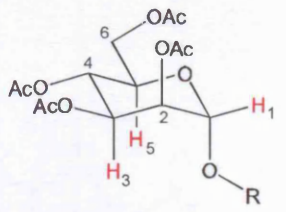

R =

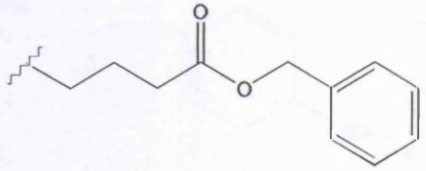

Large H-3 / H-5 NOE

Minimal H-1 / H-3 or
H-1 / H-5 NOE

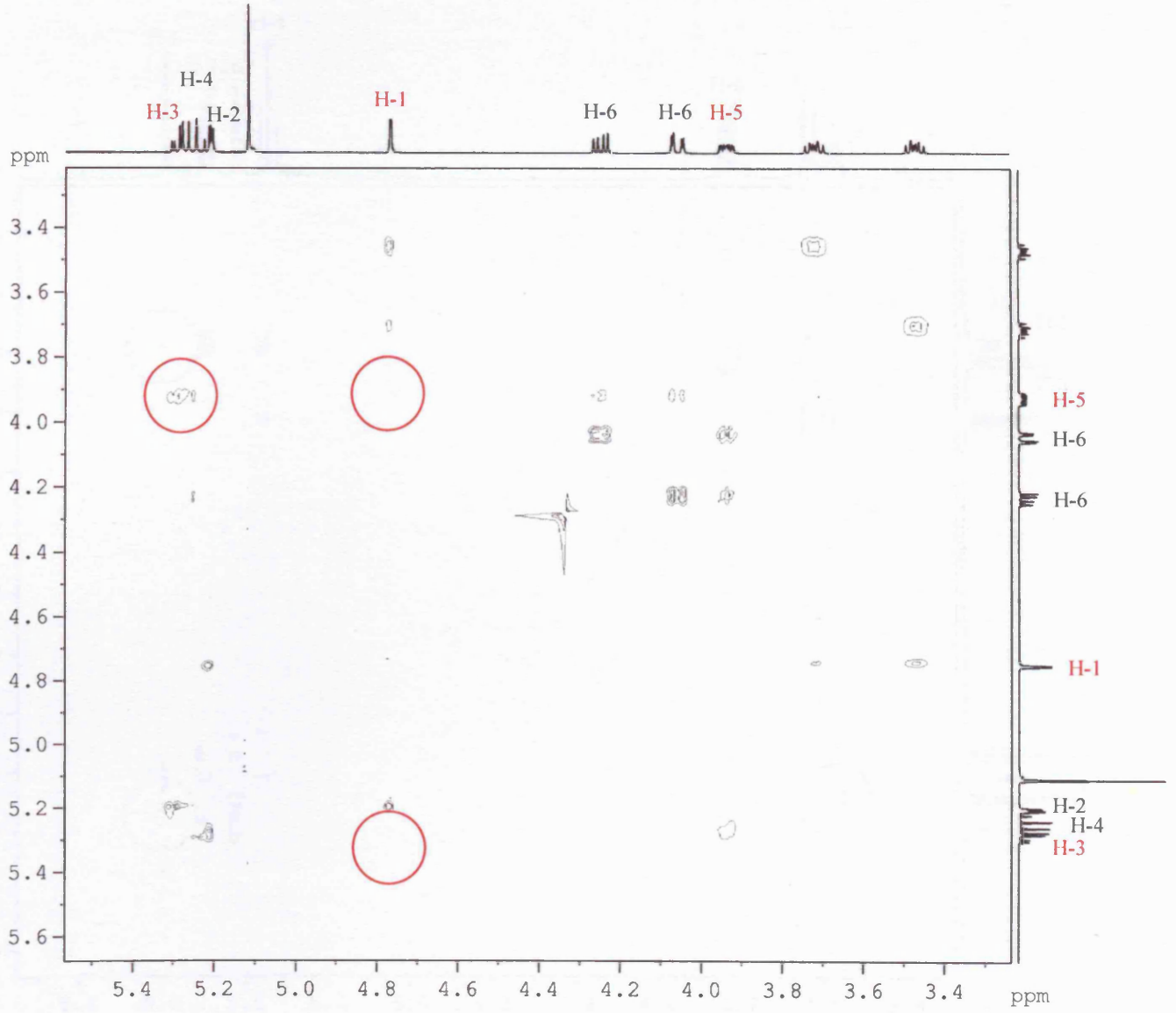

Appendix II: NOE of 4-nitrophenyl 2,3,4,6-tetra-*O*-acetyl-α-D-mannopyranoside **[6]**

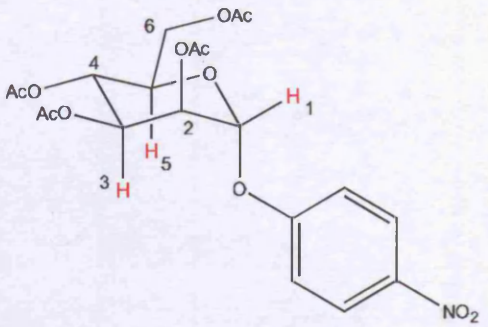

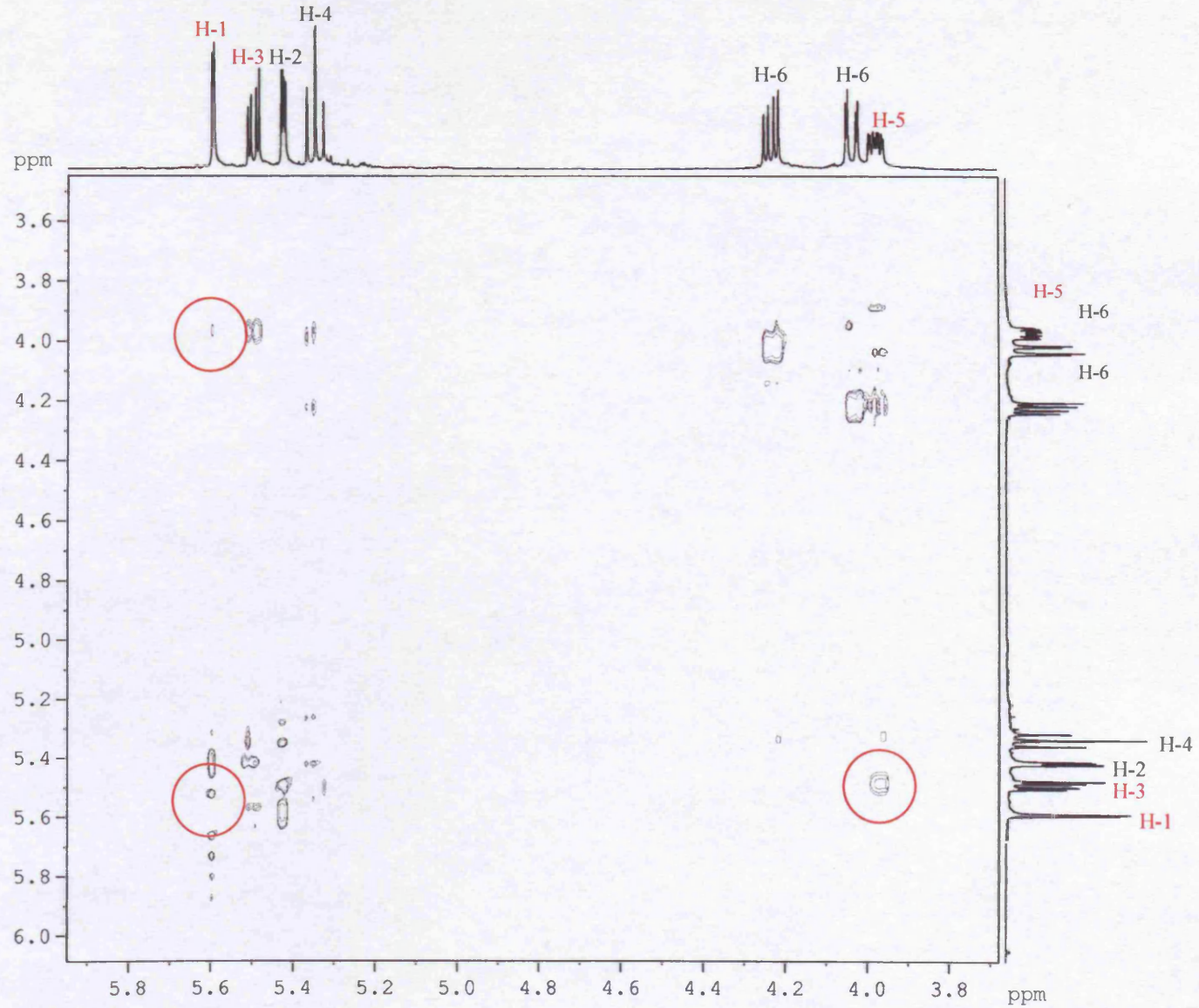

Large H-3 / H-5 NOE

Minimal H-1 / H-3 or
H-1 / H-5 NOE

Appendix III: ^{1}H NMR of acetylated MPC1

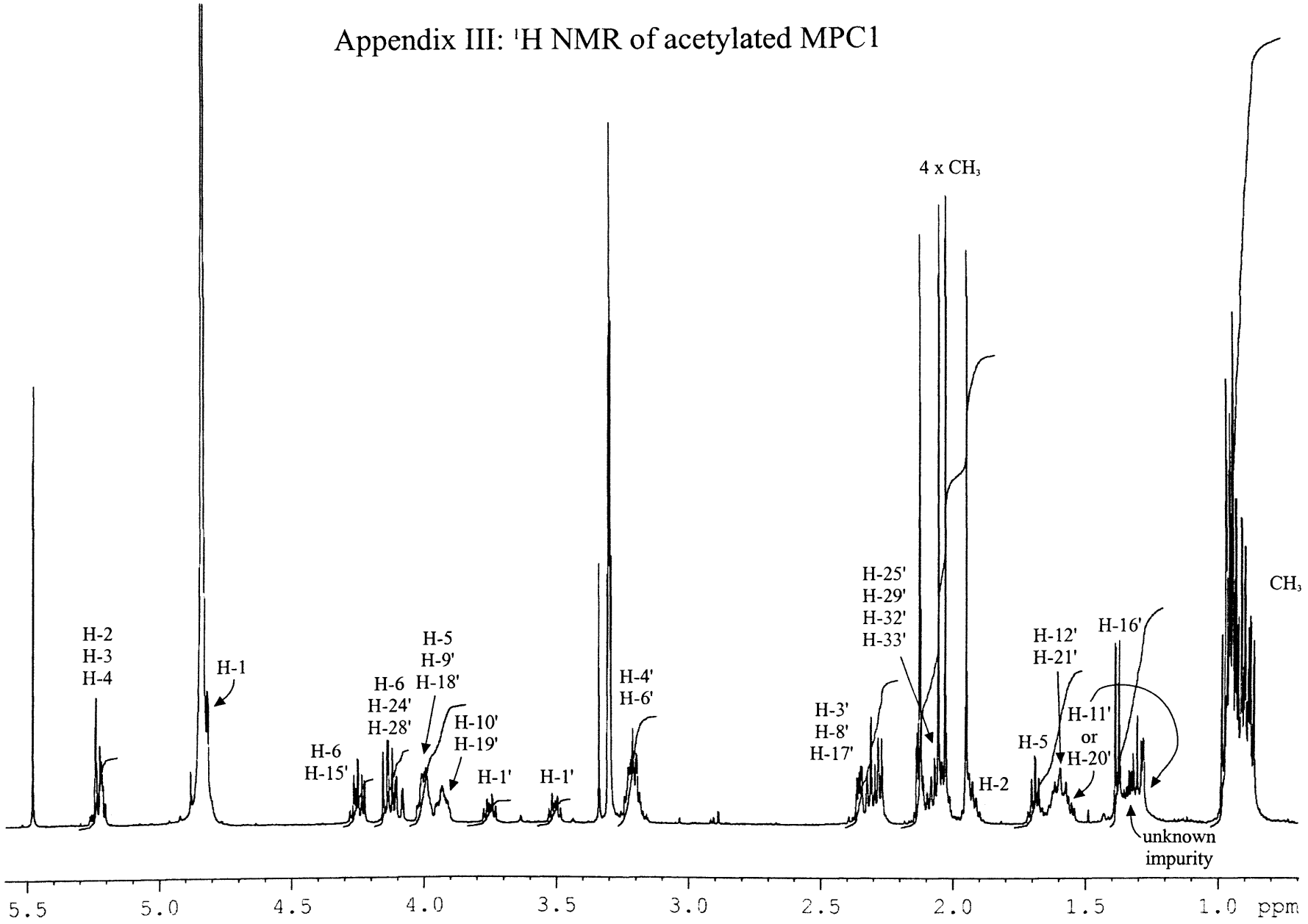

Appendix IV: ^{13}C NMR of acetylated MPC1

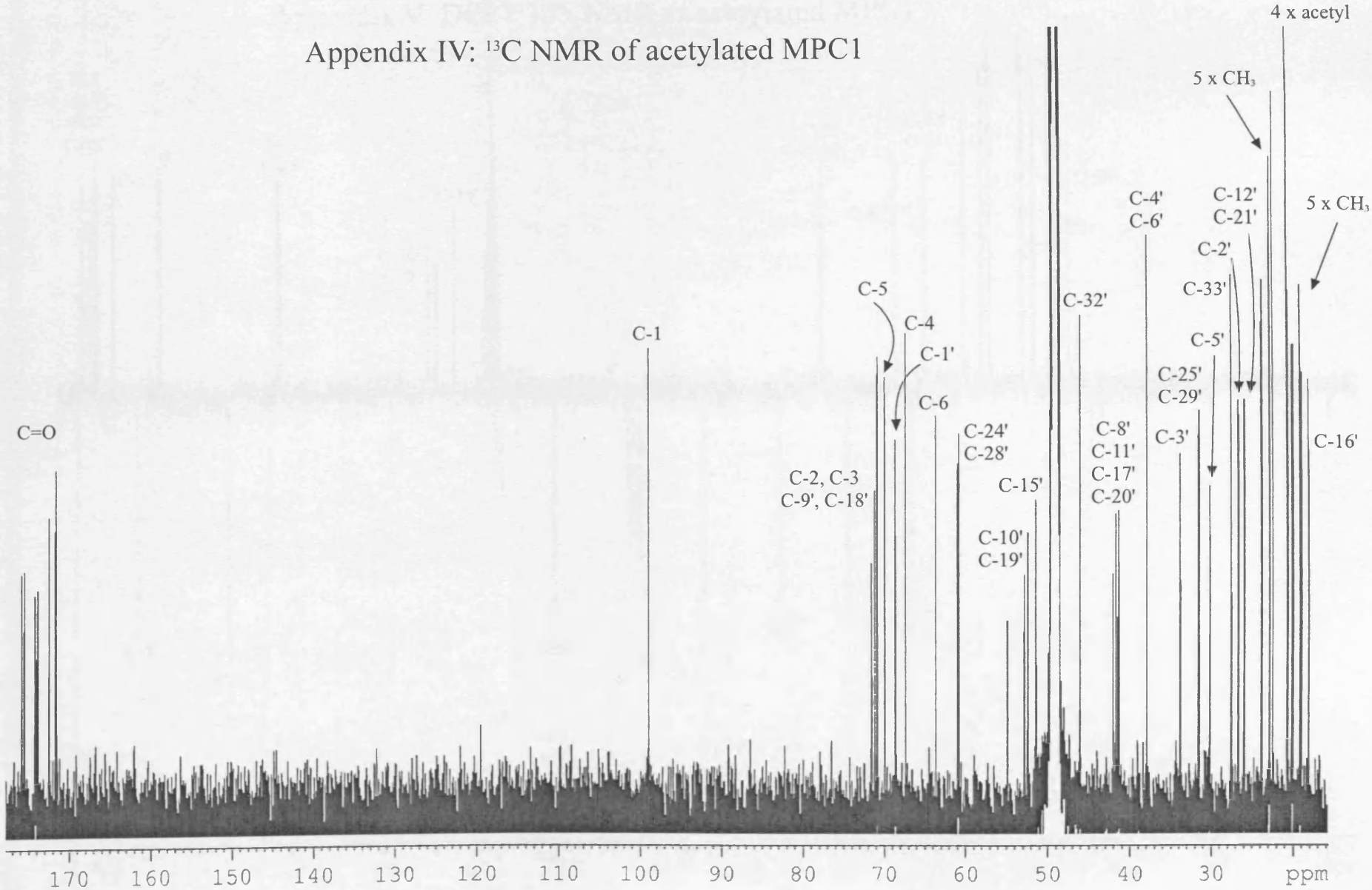

Appendix V: DEPT 135 NMR of acetylated MPC1

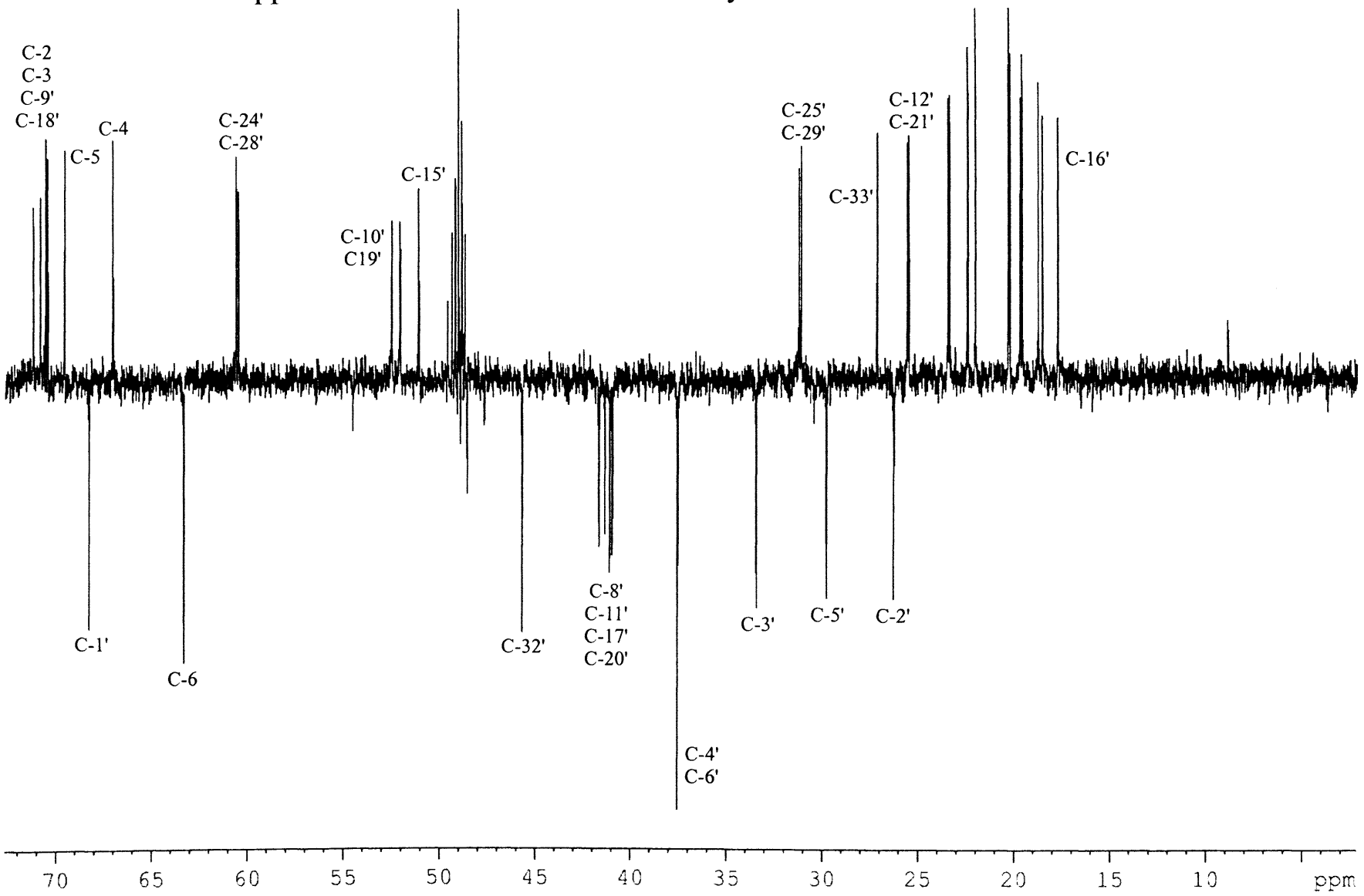

Appendix VI: COSY NMR of acetylated MPC1

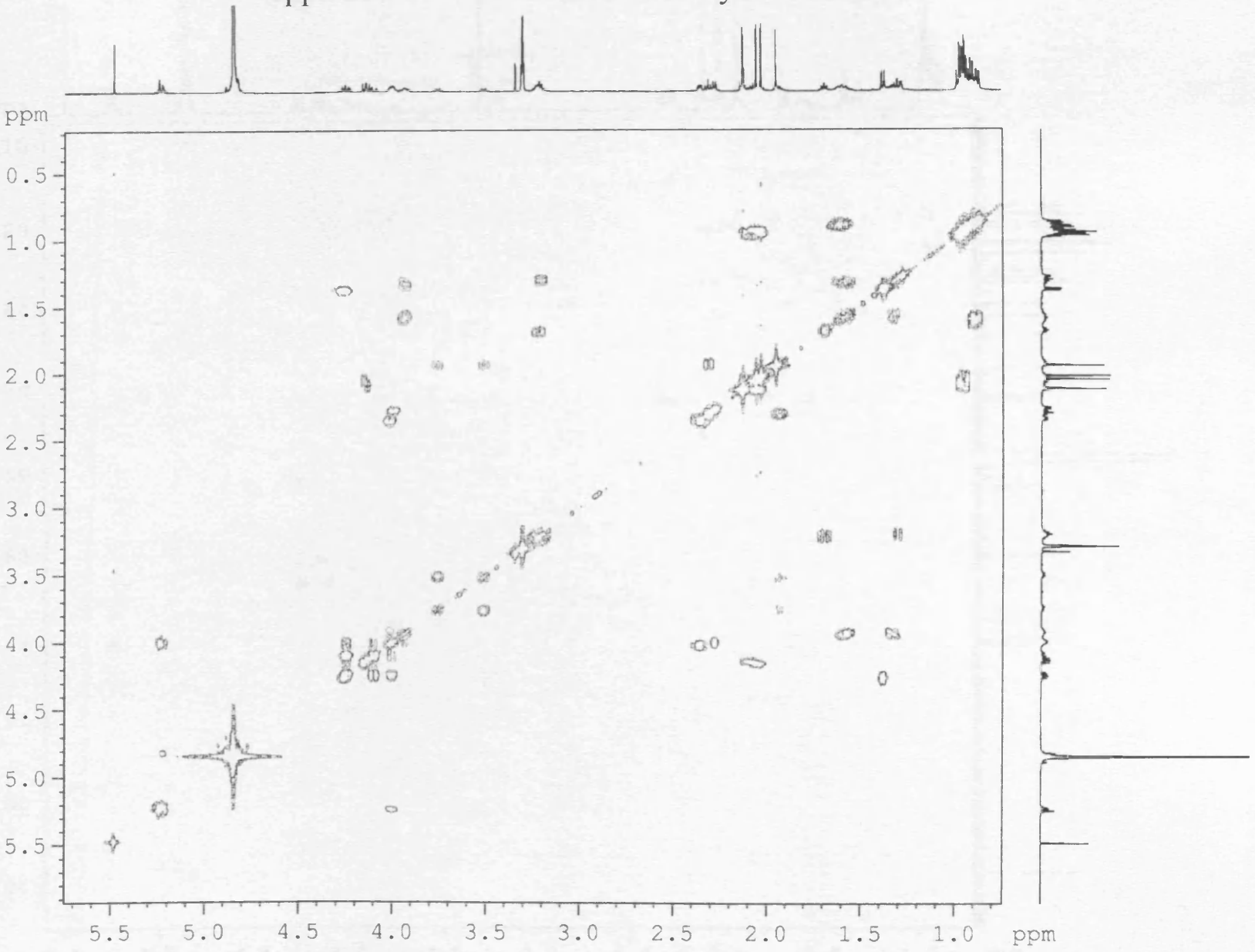

Appendix VII: HSQC NMR of acetylated MPC1

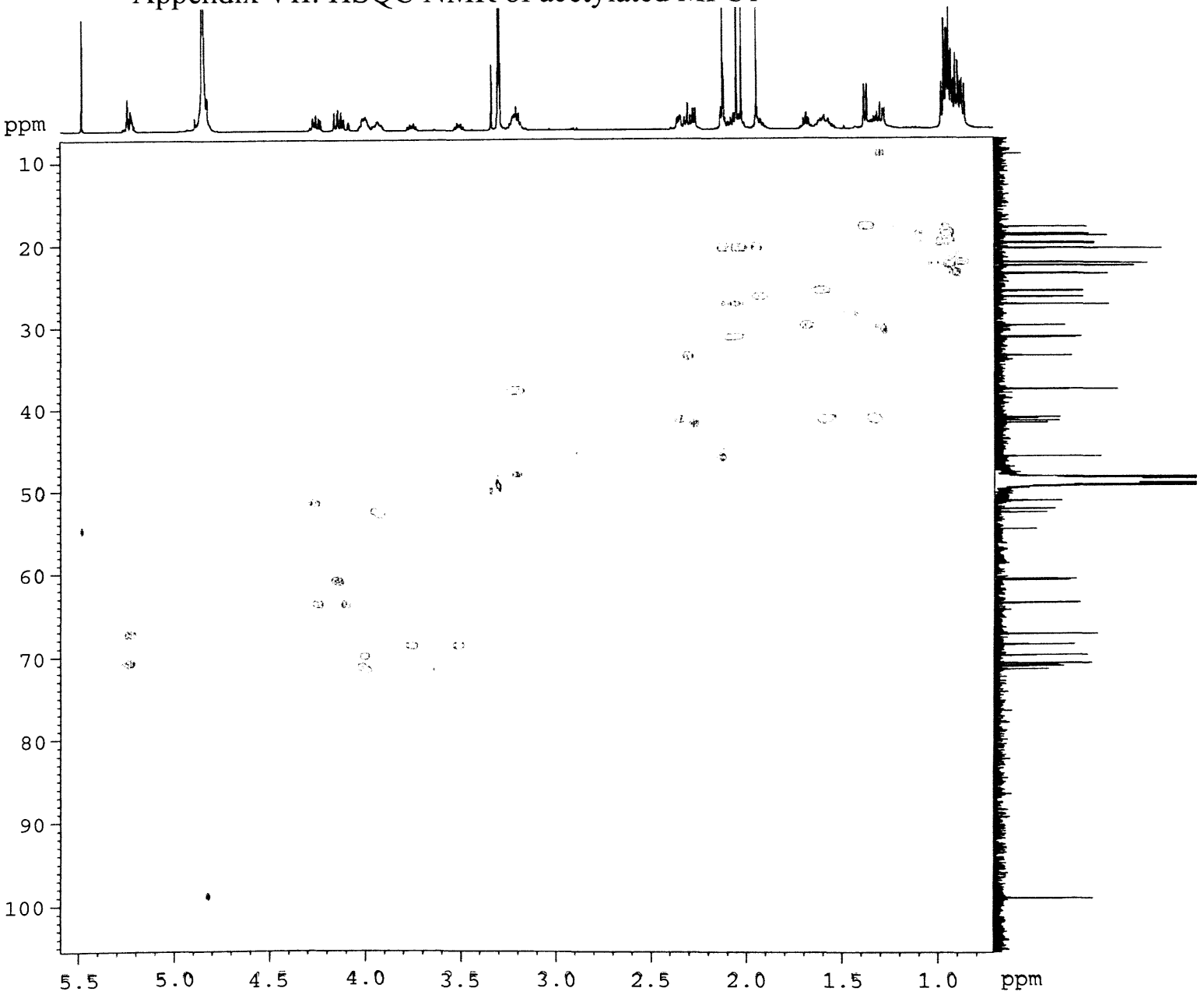

Appendix VIII: MALDI-TOF MS of BSA and BSA conjugate **[33]**

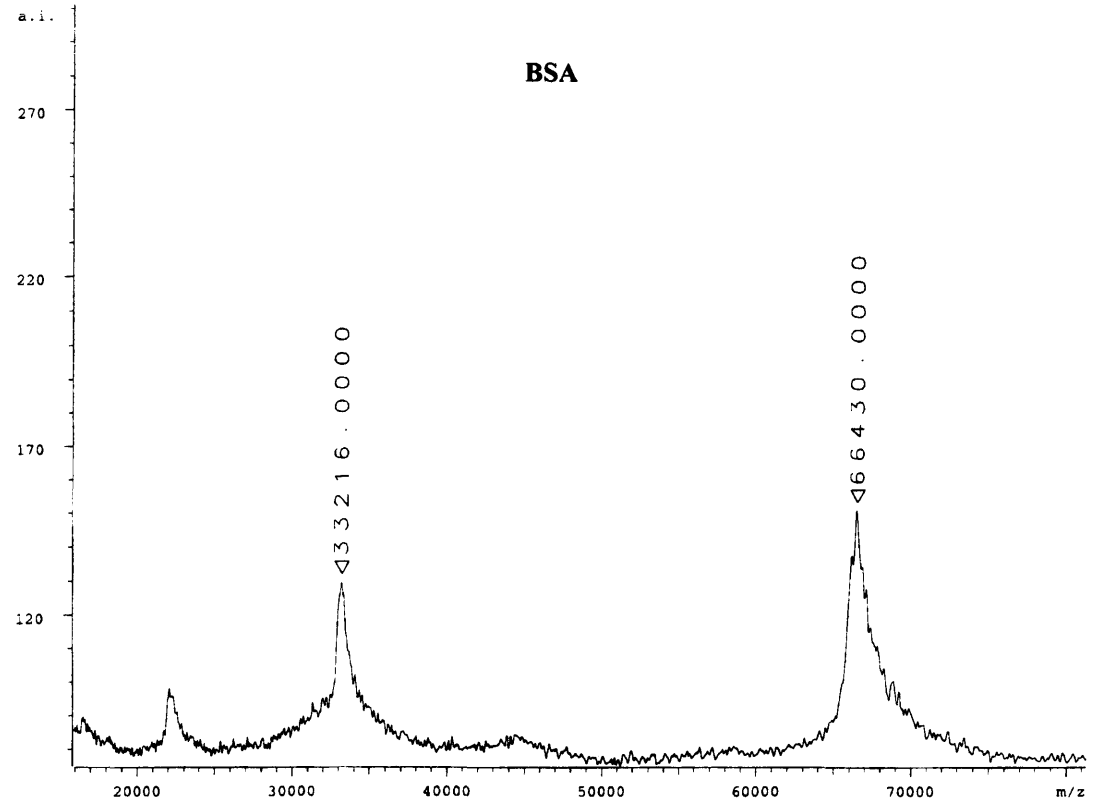

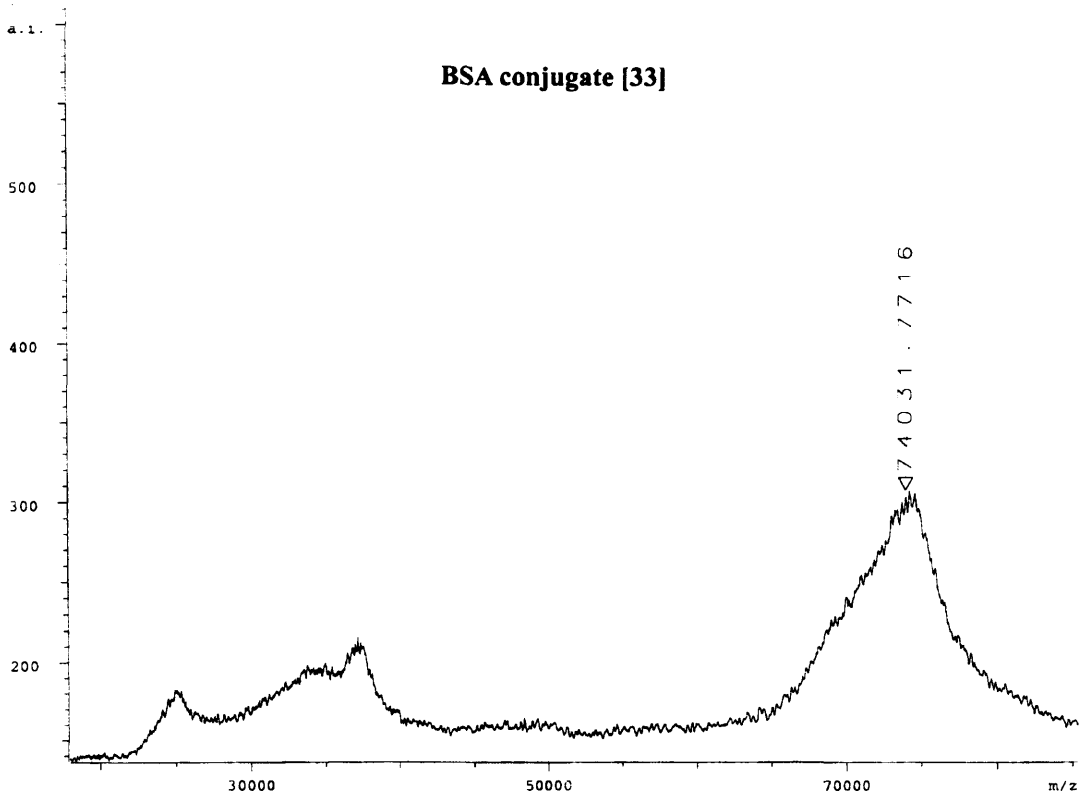

Appendix IX: MALDI-TOF MS of MPC5 and MPC6

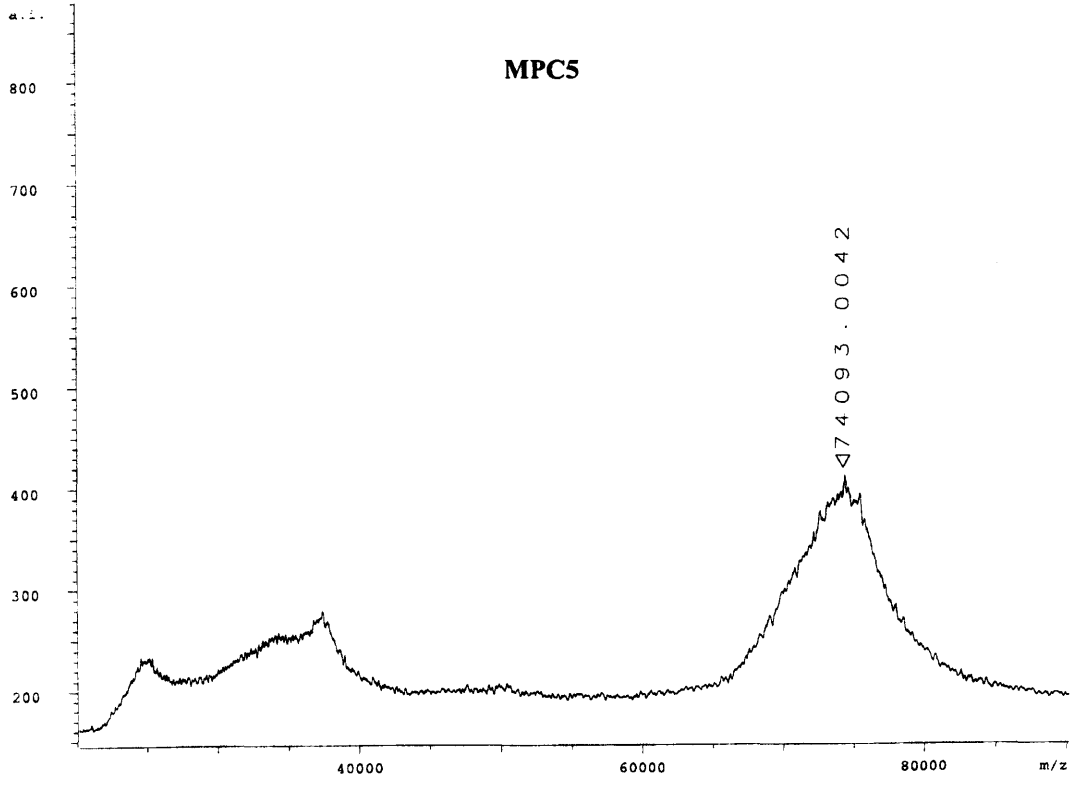

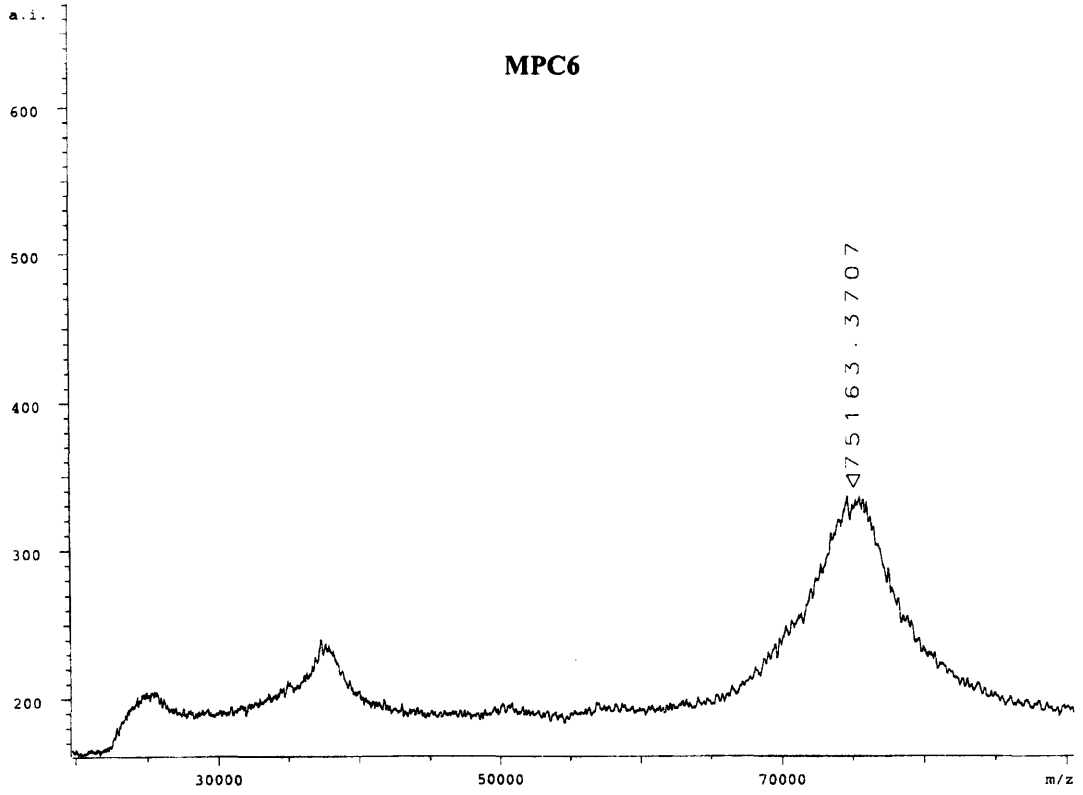

References

1. Robbins, J. C., Hanh Lam, M., Tripp, C. S., Bugianesi, R. L., Ponpipom, M. M., and Shen, T. Y., *Proc. Natl. Acad. Sci. USA*, **1981**, 78, 7294-7298.

2. Ponpipom, M. M., Bugianesi, R. L., Robbins, J. C., Doebber, T. W., and Shen, T. Y., *J. Med. Chem.*, **1981**, 24, 1388-1395.

3. Biessen, E. A. L., Noorman, F., van Teijlingen, M. E., Kuiper, J., Barrett-Bergshoeff, M., Bijsterbosch, M. K., Rijken, D. C., and van Berkel, T. J. C., *J. Biol. Chem.*, **1996**, 271, 28024-28030.

4. Toyokuni, T. and Hakomori, S.-I., *Methods Enzymol.*, **1994**, 247, 325-341.

5. Bonifaz, L. C., Bonnyay, D. P., Charalambous, A., Darguste, D. I., Fujii, S.-I., Soares, H., Brimnes, M. K., Moltedo, B., Moran, T. M., and Steinman, R. M., *J. Exp. Med.*, **2004**, 199, 815-824.

6. Harding, C. V., Ramachandra, L., and Wick, M. J., *Curr. Opin. Immunol.*, **2003**, 15, 112-119.

7. Barois, N., de Saint-Vis, B., Lebecque, S., Geuze, H. J., and Kleijmeer, M. J., *Traffic*, **2002**, 3, 894-905.

8. Kleijmeer, M. J., Ramm, G., Schuurhuis, D., Griffith, J., Rescigno, M., Ricciardi-Castagnoli, P., Rudensky, A. Y., Ossendorp, F., Melief, C. J. M., Stoorvogel, W., and Geuze, H. J., *J. Cell. Biol.*, **2001**, 155, 53-63.

9. Akira, S., *Curr. Opin. Immunol.*, **2003**, 15, 5-11.

10. Villadangos, J. A. and Heath, W. R., *Sem. Immunol.*, **2005**., 17, 262-272.

11. Banchereau, J., Briere, F., Caux, C., Davoust, J., Lebecque, S., Liu, Y.-J., Pulendran, B., and Palucka, K., *Annu. Rev. Immunol.*, **2000**, 18, 767-811.

12. Levine, T. P. and Chain, B. M., *Proc. Natl. Acad. Sci. USA*, **1992**, 89, 8342-8346.

13. Steinman, R. M. and Swanson, J. A., *J. Exp. Med.*, **1995**, 182, 283-288.

14. Sallusto, F., Cella, M., Danieli, C., and Lanzavecchia, A., *J. Exp. Med.*, **1995**, 182, 389-400.

15. Underhill, D. M. and Ozinsky, A., *Curr. Opin. Immunol.*, **2002**, 14, 103-110.

16. Steinman, R. M., *Annu. Rev. Immunol.*, **1991**, 9, 271-296.

17. West, M. A., Wallin, R. P. A., Matthews, S. P., Svensson, H. G., Zaru, R., Ljunggren, H.-G., Prescott, A. R., and Watts, C., *Science*, **2004**, 305, 1153-1157.

18. Watts, C., *Science*, **2004**, 304, 976-977.

19. Blander, J. M. and Medzhitov, Ruslan., *Nature*, Feb 19, **2006**.

20. Syme, R. M., Spurrell, J. C. L., Amankwah, E. K., Green, F. H. Y., and Mody, C. H., *Infect. Immunity*, **2002**, 5972-5981.

21. Bozza, S., Gaziano, R., Spreca, A., Bacci, A., Montagnoli, C., Francesco, P. d., and Romani, L., *J. Immunol.*, **2002**, 168, 1371.

22. Inaba, K., Inaba, M., Naito, M., and Steinman, R. M., *J. Exp. Med.*, **1993**, 178, 479-488.

23. Mousavi, S. A., MalerØd, L., Berg, T., and Kjeken, R., *Biochem. J.*, **2004**., 377, 1-16.

24. Harris, J., Werling, D., Hope, J. C., Taylor, G., and Howard, C. J., *Trends Immunol.*, **2002**, 23, 158-164.

25. Lamaze, C. and Schmid, S. L., *Curr. Opin. Cell. Biol.*, **1995**, 7, 573-580.

26. Pontow, S. E., Blum, J. S., and Stahl, P. D., *J. Biol. Chem.*, **1996**, 271, 30736-30740.

27. Prigozy, T. I., Sieling, P. A., Clemens, D., Stewert, P. L., Beher, S. M., Porcelli, S. A., Brenner, M. B., Modlin, R. L., and Kronenborg, M., *Immunity*, **1997**, 6, 187-197.

28. Mullin, N. P., Hitchen, P. G., and Taylor, M. E., *J. Biol. Chem.*, **1997**, 272, 5668-5681.

29. Stahl, P. D., Schlesinger, L. S., Sigardson, E., Rodmann, J. S., and Lee, Y. C., *Cell*, **1980**, 19, 207-215.

30. Engering, A. J., Cell, M., Fluitsma, D., Brockhaus, M., Hoefsmit, E. C. M., Lanzavecchia, A., and Pieters, J., *Eur. J. Immunol.*, **1997**, 27, 2417-2425.

31. Tan, M. C. A. A., Mommaas, A. M., Drijfhout, J. W., Jordens, R., Onderwater, J. J. M., Verwoerd, D., Mulder, A. A., van der Heiden, A. N., Scheidegger, D., Oomen, L. C. J. M., Ottenhoff, T. H. M., Tulp, A., Neefjes, J. J., and Koning, F., *Eur. J. Immunol.*, **1997**, 27, 2426-2435.

32. Jiang, W., Swiggard, W. J., Heufler, C., Peng, M., Mirza, A., Steinman, R. M., and Nussenzweig, M. C., *Nature*, **1995**, 375, 151-155.

33. Kato, M., Neil, T. K., Fearnley, D. B., McLennan, A. D., Vuckovic, S., and Hart, D. N. J., *Int. Immunol.*, **2000**, 12, 1511-1519.

34. Mahnke, K., Guo, M., Lee, S., Sepulveda, H., Swain, S. L., Nussenzweig, M. C., and Steinman, R. M., *J. Cell. Biol.*, **2000**, 151, 673-683.

35. Cambi, A., Gijzen, K., de Vries, J. M., Torensma, R., Joosten, B., Adema, G. J., Netea, M. G., Kullberg, B. J., Romani, L., and Figdor, C. G., *Eur. J. Immunol.*, **2003**, 33, 532-538.

36. Figdor, C. G., van Kooyk, Y., and Adema, G. J., *Nature Rev. Immunol.*, **2002**, 2, 77-84.

37. Engering, A. J., Geijtenbeek, T. B. H., and van Kooyk, Y., *Trends Immunol.*, **2002**, 23, 480-485.

38. Geijtenbeek, T. B. H., van Vliet, S. J., Engering, A. J., 't Hart, B. A., and van Kooyk, Y., *Annu. Rev. Immunol.*, **2004**, 22, 33-54.

39. Taylor, M. E., BezouŠka, K., and Drickamer, K., *J. Biol. Chem.*, **1992**, 267, 1719-1726.

40. Taylor, M. E. and Drickamer, K., *J. Biol. Chem.*, **1993**, 268, 399-404.

41. Taylor, M. E., *Biochem. Soc. Trans.*, **1993**, 21, 468-473.

42. Maxfield, F. R. and McGraw, T. E., *Nature Rev. Mol. Cell Biol.*, **2004**, 5, 121-132.

43. Neefjes, J. J., *Eur. J. Immunol.*, **1999**, 29, 1421-1425.

44. Hiltbold, E. M. and Roche, P. A., *Curr. Opin. Immunol.*, **2002**, 14, 30-35.

45. Murk, J.-L., Stoorvogel, W., Kleijmeer, M. J., and Geuze, H. J., *Sem. Cell. Develop. Biol.*, **2002**, 13, 303-311.

46. Lutz, M. B., Rovere, P., Kleijmeer, M. J., Assmann, C. U., Oorschot, V. M., Rescigno, M., Geuze, H. J., Davoust, J., and Ricciardi-Castagnoli, P., *Adv. Exp. Med. Biol.*, **1997**, 417, 167-169.

47. Weaver Jr, D. J. and Voss Jr, E. W., *Immunology*, **1999**, 96, 557-568.

48. Kleijmeer, M. J., Morkowski, S., Griffith, J. M., Rudensky, A. Y., and Geuze, H. J., *J. Cell. Biol.*, **1997**, 139, 639-649.

49. West, M. A., Lucocq, J. M., and Watts, C., *Nature*, **1994**, 369, 147-151.

50. Kleijmeer, M. J., Ossevoort, M. A., van Veen, C. J. H., van Hellemond, J. J., Neefjes, J. J., Kast, W. M., Melief, C. J. M., and Geuze, H. J., *J. Immunol.*, **1995**, 154, 5715-5724.

51. Lutz, M. B., Rovere, P., Kleijmeer, M. J., Rescigno, M., Assmann, C. U., Oorschot, V. M., Geuze, H. J., Trucy, J., Demandolx, D., and Davoust, J., *J Immunol*, **1997**, 159, 3707-3716.

52. Delamerre, L., Pack, M., Chang, H., Mellman, I., and Trombetta, E. S., *Science*, **2005**, 307, 1630-1634.

53. Villadangos, J. A., Schnorrer, P., and Wilson, N. S., *Immunol. Rev.*, **2005**, 207, 191-205.

54. Li, P., Gregg, J. L., Wang, N., Zhou, D., O'Donnell, P., Blum, J. S., and Crotzer, V. L., *Immunol. Rev.*, **2005**, 207, 206-217.

55. Brown, J. H., Jardetzky, T. S., and Saper, M. A., *Nature*, **1993**, 364, 33-39.

56. Chicz, R. M., Urban, R. G., and Lane, W. S., *Nature*, **1992**, 358, 764-768.

57. Sercarz, E. E. and Maverakis, E., *Nature Rev. Immunol.*, **2003**, 3, 621-629.

58. Scott, C. A., Peterson, P. A., Teyton, L., and Wilson, I. A., *Immunity*, **1998**, 8, 319-329.

59. Cresswell, P., *Annu. Rev. Immunol.*, **1994**, 12, 259-293.

60. Matza, D., Kerem, A., and Shacher, I., *Trends Immunol.*, **2003**, 24, 264-268.

61. Blum, J. S. and Cresswell, P., *Proc. Natl. Acad. Sci. USA*, **1988**, 85, 3975-3979.

62. Maric, M. A., Taylor, M. D., and Blum, J. S., *Proc. Natl. Acad. Sci. USA*, **1994**, 91, 2171-2175.

63. Villadangos, J. A., Riese, R. J., Peters, C., Chapman, H. A., and Ploegh, H. L., *J. Exp. Med.*, **1997**, 186, 549-560.

64. Nakagawa, T., Roth, W., Wong, P., Nelson, A., Farr, A., Deussing, J., Villadangos, J. A., Ploegh, H. L., Peters, C., and Rudensky, A. Y., *Science*, **1998**, 280, 450-453.

65. Busch, R., Doebele, R. C., Patil, N. S., Pashine, A., and Mellins, E. D., *Curr. Opin. Immunol.*, **2000**, 12, 99-106.

66. Nanda, N. K. and Sant, A. J., *J. Exp. Med.*, **2000**, 192, 781-788.

67. Kaye, P. M., Chain, B. M., and Feldmann, M., *J. Immunol.*, **1985**, 134, 1930-1934.

68. Santambrogio, L., Sato, A. K., Carven, G. J., Beljanskaya, S. L., Strominger, J. L., and Stern, L. J., *Proc. Natl. Acad. Sci. USA*, **1999**, 96, 15056-15061.

69. Watts, C., *Curr. Opin. Immunol.*, **2001**, 13, 26-31.

70. Riese, R. J. and Chapman, H. A., *Curr. Opin. Immunol.*, **2000**, 12, 107-113.

71. Neefjes, J. J. and Dantuma, N. P., *Nature Rev. Drug Disc.*, **2004**, 3, 58-68.

72. Collins, D. S., Unanue, E. R., and Harding, C. V., *J. Immunol.*, **1991**, 147, 4054-4059.

73. Kang, H. K., Mikszta, J. A., Deng, H., Sercarz, E. E., Jensen, P. E., and Kim, B. S., *J. Immunol.*, **2000**, 164, 1775-1782.

74. Phan, U. T., Arunachalam, B., and Cresswell, P., *J. Biol. Chem.*, **2000**, 275, 25907-25914.

75. Phan, U. T., Lackman, R. L., and Cresswell, P., *Proc. Natl. Acad. Sci. USA*, **2002**, 99, 12298-12303.

76. Maric, M., Arunachalam, B., Phan, U. T., Dong, C., Garrett, W. S., Cannon, K. S., Alfonso, C., Karlsson, L., Flavell, R. A., and Cresswell, P., *Science*, **2001**, 294, 1361-1365.

77. Antonious, A. N., Blackwood, S.-L., Mazzeo, D., and Watts, C., *Immunity*, **2000**, 12, 391-398.

78. Manoury, B., Mazzeo, D., Fugger, L., Viner, N., Ponsford, M., Streeter, H., Mazza, G., Wraith, D. C., and Watts, C., *Nature Immunol.*, **2002**, 3, 169-174.

79. Maehr, R., Hang, H. C., Mintern, J. D., Kim, Y.-M., Cuvillier, A., Nishimura, M., Yamada, K., Shirahama-Noda, K., Hara-Nishimura, I., and Ploegh, H. L., *J. Immunol.*, **2005**, 174, 7066-7074.

80. Manoury, B., Mazzeo, D., Li, D. N., Billson, J., Loak, K., Benaroch, P., and Watts, C., *Immunity*, **2003**, 18, 489-498.

81. Watts, C., Matthews, S. P., Mazzeo, D., Manoury, B., and Moss, C. X., *Immunol. Rev.*, **2005**, 207, 218-228.

82. Turk, V., Turk, B., and Turk, D., *EMBO J.*, **2001**, 20, 4629-4633.

83. Bohley, P. and Seglen, P. O., *Experientia*, **1992**, 48, 151-157.

84. Katunuma, N., Matsunaga, Y., Himeno, K., and Hayashi, Y., *J. Biol. Chem.*, **2003**, 384, 883-890.

85. Deussing, J., Roth, W., Saftig, P., Peters, C., Ploegh, H. L., and Villadangos, J. A., *Proc. Natl. Acad. Sci. USA*, **1998**, 95, 4516-4521.

86. Bevec, T., Stoka, V., Pungercic, G., Dolenc, I., and Turk, V., *J. Exp. Med.*, **1996**, 183, 1331-1338.

87. Hsieh, C.-S., deRoos, P., Honey, K., Beers, C., and Rudensky, A. Y., *J. Immunol.*, **2002**, 168, 2618-2625.

88. Nakagawa, T., Brissette, W. H., Lira, P. D., Griffiths, R. J., Petrushova, N., Stock, J., McNeish, J. D., Eastman, S. E., Howard, S. E., and Clarke, S. R., *Immunity*, **1999**, 10, 207-217.

89. Bania, J., Gatti, E., Lelouard, H., David, A., Cappello, F., Weber, E., Camosseto, V., and Pierre, P., *Proc. Natl. Acad. Sci. USA*, **2003**, 100, 6664-6669.

90. Beck, H., Schwarz, G., Schröter, C. J., Deeg, M., Baier, D., Stevanovic, S., Weber, E., Driessen, C., and Kalbacher, H., *Eur. J. Immunol.*, **2001**, 31, 3726-3736.

91. Shi, G. P., Bryant, R. A., Riese, R. J., Verhelst, S., Driessen, C., Li, Z., Bromme, D., Ploegh, H. L., and Chapman, H. A., *J. Exp. Med.*, **2000**, 191, 1177-1185.

92. Dunn, B. M., *Chem. Rev.*, **2002**, 102, 4431-4458.

93. Cooper, J. B., *Curr. Drug. Targ.*, **2002**, 3, 155-173.

94. Dash, C., Kulkarni, A., Dunn, B. M., and Rao, M., *Crit. Rev. Biochem. Mol. Biol.*, **2003**, 38, 89-119.

95. Tatnell, P., Powell, D. J., Hill, J., Smith, T. S., Tew, D. G., and Kay, J., *FEBS Lett.*, **1998**, 441, 43-48.

96. Grüninger-Leitch, F., Schlatter, D., Küng, E., Nelböck, P., and Döbeli, H., *J. Biol. Chem.*, **2002**, 277, 4687-4693.

97. Zhang, T., Maekawa, Y., Yasutomo, K., Ishikawa, H., Nashed, B. F., Dainichi, T., Hisaeda, H., Sakai, T., Kasai, M., Mizuochi, T., Asao, T., Katunuma, N., and Himeno, K., *Biochem. Biophys. Res. Comm.*, **2000**, 276, 693-701.

98. Medd, P. G. and Chain, B. M., *Sem. Cell. Develop. Biol.*, **2000**, 11, 203-210.

99. Tsukuba, T., Okamoto, K., Yoshizaki, H., Morikawa, W., Nakanishi, H., and Yamamoto, K., *Mol. Cell.*, **2000**, 10, 601-611.

100. Diment, S., Leech, M. S., and Stahl, P. D., *J. Biol. Chem.*, **1988**, 263, 6901-6907.

101. *"Proteinases in mammalian cells and tissues"*, Barrett, A. J. ed., North-Holland Publishing Co., Amsterdam., **1977**.

102. Kageyama, T., Tatematsu, M., Ichinose, M., Yahagi, N., Miki, K., Moriyama, A., and Yonezawa, S., *Zool. Sci.*, **1998**, 15, 517-523.

103. Metcalf, P. and Furek, M., *EMBO J.*, **1993**, 12, 1293-1302.

104. Godbold, G. D., K. Ahn, S. Yeyeodu, L.-F. Lee, J. P. Y. Ting, and A. H. Erickson., *"Aspartic Proteinases"*, James, ed., Plenum Press, New York, **1998**, pp. 153-162.

105. Baldwin, E. T., Bhat, T. N., Gulnik, S., Hosur, M. V., Sowder, R. C., Cachau, R. E., Collins, J., Silva, A. M., and Erickson, J. W., *Proc. Natl. Acad. Sci. USA*, **1993**, 90, 6796-6800.

106. Helsleth, D. L. Jr. and Veis, A., *Proc. Natl. Acad. Sci. USA*, **1984**, 81, 3302-3306.

107. Ladror, U. S., Snyder, S. W., Wang, G. T., Holzman, T. F., and Krafft, G. A., *J. Biol. Chem.*, **1994**, 269, 18422-18428.

108. Deiss, L. P., Galinka, H., Berissi, H., Cohen, O., and Kimchi, A., *EMBO J.*, **1996**, 15, 3861-3870.

109. Heinrich, M., Wickel, M., Schneider-Brachert, W., Gahr, J., Schwandner, R., Weber, T., Brunner, J., Krönke, M., and Schütze, S., *EMBO J.*, **1999**, 18, 5252-5263.

110. Saftig, P., Hetman, M., Schmahl, W., Weber, K., Heine, L., Mossmann, H., Köster, A., Hess, B., Evers, M., Figura, K. v., and Peters, C., *EMBO J.*, **1995**, 14, 3599-3608.

111. Moss, C. X., Villadangos, J. A., and Watts, C., *Eur. J. Immunol.*, **2005**, 35, 3442-3451.

112. Bennett, K., Levine, T., Ellis, J. S., Peanasky, R. J., Samloff, I. M., Kay, J., and Chain, B. M., *Eur. J. Immunol.*, **1992**, 22, 1519-1524.

113. Sastradipura, D. F., Nakanishi, H., Tsukuba, T., Nishishita, K., Sakai, H., Kato, Y., Gotow, T., Uchiyama, Y., and Yamamoto, K., *J. Neurochem.*, **1998**, 70, 2045-2056.

114. Finzi, G., Cornaggia, M., Capella, C., Fiocca, R., Bosi, F., Solcia, E., and Samloff, I. M., *Histochem.*, **1993**, 99, 201-211.

115. Solcia, E., Paulli, M., Silini, E., Fiocca, R., Finzi, G., Kindl, G., Boveri, E., Bosi, F., Cornaggia, M., Capella, C., and Samloff, I. M., *Eur. J. Histochem.*, **1993**, 37, 19-26.

116. Sealy, L. C., Mota, F., Rayment, N., Tatnell, P., Kay, J., and Chain, B. M., *Eur. J. Immunol.*, **1996**, 26, 1838-1843.

117. Cook, M., Caswell, R. C., Richards, R. J., Kay, J., and Tatnell, P., *Eur. J. Biochem.*, **2001**, 268, 2658-2668.

118. Okamoto, K., Yu, H., Misumi, Y., Ikehara, Y., and Yamamoto, K., *Arch. Biochem. Biophys.*, **1995**, 322, 103-111.

119. Tatnell, P., Lees, W. E., and Kay, J., *FEBS Lett.*, **1997**., 408, 62-66.

120. Kageyama, T., *Eur. J. Biochem.*, **1993**, 216, 717-728.

121. Finley, E. M. and Kornfeld, S., *J. Biol. Chem.*, **1994**, 269, 31259-31266.

122. Tatnell, P., S. D. Fowler, D. Bur, W. E. Lees, and J. Kay., *"Aspartic Proteinases"*, James, ed., Plenum Press, New York, **1998**, pp. 147-152.

123. Fowler, S. D., Kay, J., Dunn, B. M., and Tatnell, P., *FEBS Lett.*, **1995**, 366, 72-74.

124. Thomas, D. J., Richards, A. D., Jupp, R. A., Ueno, E., Yamamoto, K., Samloff, I. M., Dunn, B. M., and Kay, J., *FEBS Lett.*, **1989**, 243, 145-148.

125. Yasuda, Y., Ikeda, S., Sakai, H., Tsukuba, T., Okamoto, K., Nishishita, K., Akamine, A., Kato, Y., and Yamamoto, K., *Eur. J. Biochem.*, **1999**, 266, 383-391.

126. Ostermann, N., Gerhartz, B., Worpenberg, S., Trappe, J., and Eder, J., *J. Mol. Biol.*, **2004**, 342, 889-899.

127. Yasuda, Y., Kageyama, T., Akamine, A., Shibata, M., Kominami, E., Uchiyama, Y., and Yamamoto, K., *J. Biochem.*, **1999**, 125, 1143.

128. Shibata, M., Sakai, H., Sakai, E., Okamoto, K., Nishishita, K., Yasuda, Y., Kato, Y., and Yamamoto, K., *Eur. J. Biochem.*, **2003**, 270, 1189-1198.

129. Kageyama, T., Ichinose, M., and Yonezawa, S., *J. Biol. Chem.*, **1995**, 270, 19135-19140.

130. Kageyama, T., *Methods Enzymol.*, **1995**, 248, 120-136.

131. Athauda, S. B. P., Takahashi, T., Inoue, H., Ichinose, M., and Takahashi, K., *FEBS Lett.*, **1991**, 292, 53-56.

132. Lees, W. E., Kalinka, S., Meech, J., Capper, S. J., Cook, N. D., and Kay, J., *FEBS Lett.*, **1990**, 273, 99-102.

133. Kageyama, T., Yonezawa, S., Ichinose, M., Miki, K., and Moriyama, A., *Biochem. Biophys. Res. Comm.*, **1996**, 223, 549-553.

134. Rao-Naik, C., Guruprasad, K., Batley, B., Rapundalo, S., Hill, J., Blundell, T. L., Kay, J., and Dunn, B. M., *Proteins: Struct. Funct. Genet.*, **1995**, 22, 168-181.

135. Arnold, D., Keilholz, W., Schild, H., Dumrese, T., Stevanovic, S., and Rammensee, H.-G., *J. Biol. Chem.*, **1997**, 378, 883-891.

136. Liu, J., Tsukuba, T., Okamoto, K., Ohishi, M., and Yamamoto, K., *J. Biochem.*, **2002**, 132, 493-499.

137. Tsukuba, T., Okamoto, K., Okamoto, Y., Yanagawa, M., Kohmura, K., Yasuda, Y., Uchi, H., Nakahara, T., Furue, M., Nakayama, K., Kadowaki, T., Yamamoto, K., and Nakayama, K., *J. Biochem.*, **2003**, 134, 893-902.

138. Mowat, A. M., *Nature Rev. Immunol.*, **2003**, 3, 331-341.

139. Sealy, L. C., *PhD Thesis, University of London*, **1996**.

140. Siegrist, C. A., Martinez Soria, E., Kern, I., and Mach, B., *J. Exp. Med.*, **1995**, 182, 1793-1799.

141. Yee, C. S. K., Yao, Y., Li, P., Klemsz, M. J., Blum, J. S., and Chang, C.-H., *J. Immunol.*, **2004**, 172, 5528-5534.

142. Nishioku, T., Hashimoto, K., Yamashita, K., Liou, S.-Y., Kagamiishi, Y., Maegawa, H., Katsube, N., Peters, C., Figura, K. v., Saftig, P., Katanuma, N., Yamamoto, K., and Nakanishi, H., *J. Biol. Chem.*, **2002**, 277, 4816-4822.

143. Hewitt, E. W., Treumann, A., Morrice, N., Tatnell, P., Kay, J., and Watts, C., *J. Immunol.*, **1997**, 159, 4693-4699.

144. Diment, S., *J. Immunol.*, **1990**, 145, 417-422.

145. O'Neil, D. A., "The enzymology of antigen processing", *PhD Thesis, University of London*, **1997**.

146. Zhang, T., Maekawa, Y., Hanba, J., Dainichi, T., Nashed, B. F., Hisaeda, H., Sakai, T., Asao, T., Himeno, K., Good, R. A., and Katunuma, N., *Immunology*, **2000**, 100, 13-20.

147. Riese, R. J., Wolf, P. R., Bromme, D., Natkin, L. R., Villadangos, J. A., Ploegh, H. L., and Chapman, H. A., *Immunity*, **1996**, 4, 357-366.

148. Umezawa, H., *Methods Enzymol.*, **1976**, 45, 678-695.

149. Marciniszyn, J., Hartsuck, J. A., and Tang, J., *J. Biol. Chem.*, **1976**, 251, 7088-7094.

150. Marciniszyn, J., Hartsuck, J. A., and Tang, J., *Adv. Exp. Med. Biol.*, **1977**, 95, 199-210.

151. Majer, P., Collins, J. R., Gulnik, S. V., and Erickson, J. W., *Prot. Sci.*, **1997**, 6, 1458-1466.

152. Bott, R., Subramanian, E., and Davies, D. R., *Biochemistry*, **1982**, 21, 6956-6962.

153. Hamdaoui, B., Dewynter, G., Capony, F., Montero, J.-L., Toiron, C., Hnach, M., and Rochefort, H., *Bull. Soc. Chim. Fr.*, **1994**, 131, 854-864.

154. Brygier, J., Vincentelli, J., Nijs, M., Guermant, C., Paul, C., Baeyensvolant, D., and Looze, Y., *Appl. Biochem. Biotech.*, **1994**, 47, 1-10.

155. Campbell, P., Glover, G. I., and Gunn, J. M., *Arch. Biochem. Biophys.*, **1980**, 203, 676-680.

156. Knight, C. G., Hornebeck, W., Matthews, I. T., Hembry, R. M., and Dingle, J. T., *Biochem. J.*, **1980**, 191, 835-843.

157. Matthews, I. T., Decker, R. S., and Knight, C. G., *Biochem. J.*, **1981**, 199, 611-617.

158. Dahlgren, A., Kvarnstrom, I., Vrang, L., Hamelink, E., Hallberg, A., Rosenquist, A., and Samuelsson, B., *Bioorg. Med. Chem.*, **2003**, 11, 3423-3437.

159. Hu, J., Cwi, C. L., Smiley, D. L., Timm, D., Erickson, J. A., McGee, J. E., Yang, H. C., Mendel, D., May, P. C., Shapiro, M., and McCarthy, J. R., *Bioorg. Med. Chem. Lett.*, **2003**, 13, 4335-4339.

160. Bessodes, M., Antonakis, K., Herscovici, J., Garcia, M., Rochefort, H., Capony, F., Lelièvre, Y., and Scherman, D., *Biochem. Pharm.*, **1999**, 58, 329-333.

161. Carroll, C. D., Johnson, T. O., Tao, S., Lauri, G., Orlowski, M., Gluzman, I. Y., Goldberg, D. E., and Dolle, R. E., *Bioorg. Med. Chem. Lett.*, **1998**, 8, 3203-3206.

162. Bi, X., Haque, T. S., Zhou, J., Skillman, A. G., Lin, B., Lee, C. E., Kuntz, I. D., Ellman, J. A., and Lynch, G., *J. Neurochem.*, **2000**, 74, 1469-1477.

163. Lee, C. E., Kick, E. K., and Ellman, J. A., *J. Am. Chem. Soc.*, **1998**, 120, 9735-9747.

164. Cappiello, M. G., Wu, Z., Scott, B. B., McGeehan, G. M., and Harrison, R. K., *Protein Exp. Purif.*, **2004**, 37, 53-60.

165. Binkert, C., Frigerio, M., Jones, A., Meyer, S., Pesenti, C., Prade, L., Viani, F., and Zanda, M., *ChemBioChem*, **2006**, 7, 181-186.

166. Kageyama, T., *Eur. J. Biochem.*, **1998**, 253, 804-809.

167. Ng, K. K. S., Peterson, J. F. W., Cherney, M. M., Garen, C., Zalatoris, J. J., Rao-Naik, C., Dunn, B. M., Martzen, M. R., Peanasky, R. J., and James, M. N. G., *Nature Struct. Biol.*, **2000**, 7, 653-657.

168. Grant, D. A., Ford, T. F., and McCulloch, R. J., *Biochem. &. Pharm.*, **1982**, 31, 2302-2305.

169. corbell, J. B., Lundquist, J. J., and Toone, E. J., *Tetrahedron Asymm.*, **2000**., 11, 95-111.

170. Lundquist, J. J. and Toone, E. J., *Chem. Rev.*, **2002**, 102, 555-578.

171. Kéry, V., Krepinskí, J. J. F., Warren, C. D., Capek, P., and Stahl, P. D., *Arch. Biochem. Biophys.*, **1992**, 298, 49-55.

172. Maródi, L., Korchak, H. M., and Johnston, R. B., *J. Immunol.*, **1991**, 146, 2783-2789.

173. Nigou, J., Zelle-Rieser, C., Gilleron, M., Thurnher, M., and Puzo, G., *J. Immunol.*, **2001**, 166, 7477-7485.

174. Ley, S. V., Baeschlin, D. K., Dixon, D. J., Foster, A. C., Ince, S. J., Priepke, H. W. M., and Reynolds, D. J., *Chem. Rev.*, **2001**, 101, 53-80.

175. Grice, P., Ley, S. V., Pietruszka, J., Osborn, H. M. I., Priepke, H. W. M., and Warriner, S. L., *Chem. -Eur. J.*, **1997**, 3, 431-440.

176. Matsuo, I., Miyazaki, T., Isomura, M., Sakakibara, T., and Ajisaka, K., *J. Carbohydr. Chem.*, **1998**, 17, 1249-1258.

177. Merritt, J. R., Naisang, E., and Fraser-Reid, B., *J. Org. Chem.*, **1994**, 59, 4443.

178. Heng, L., Ning, J., and Kong, F., *Carbohydr. Res.*, **2001**, 331, 431-437.

179. Danishefsky, S. J., Hu, S., Cirillo, P. F., Eckhardt, M., and Seeberger, P. H., *Chem. -Eur. J.*, **1997**, 3, 1617-1628.

180. Ohsumi, Y., Hoppe, C. A., Ogawa, T., and Lee, Y. C., *Arch. Biochem. Biophys.*, **1988**, 260, 241-249.

181. Perkins, S. J. and Dwek, R. A., *Biochemistry*, **1980**, 19, 245-258.

182. Mullin, N. P., Hall, K. T., and Taylor, M. E., *J. Biol. Chem.*, **1994**, 269, 28405-28413.

183. Jansen, R. W., Molema, G., Ching, T. L., Oosting, R., Harms, G., Moolenaar, F., Hardonk, M. J., and Meijer, D. K. F., *J. Biol. Chem.*, **1991**, 266, 3343-3348.

184. Hoppe, C. A. and Lee, Y. C., *Biochemistry*, **1984**, 23, 1723-1730.

185. *"Bioconjugate Techniques"*, Hermanson, G. T., ed., Academic Press, **1996**.

186. Lemieux, R. U., Bundle, D. R., and Baker, D. A., *J. Am. Chem. Soc.*, **1975**, 97, 4076.

187. Shin, J., Shum, P., and Thompson, D. H., *J. Control. Rel.*, **2003**, 91, 187-200.

188. Lee, S., Greenwald, R. B., McGuire, J., Yang, K., and Shi, C., *Bioconj. J.*, **2001**, 12, 163-169.

189. Rodrigues, P. C. A., Scheuermann, K., Stockmar, C., Maier, G., Fiebig, H. H., Unger, C., Mülhaupt, R., and Kratz, F., *Bioorg. Med. Chem. Lett.*, **2003**., 13, 355-360.

190. Yoo, H. S., Lee, E. A., and Park, T. G., *J. Control. Rel.*, **2002**, 82, 17-27.

191. Mercadel, M., Domingo, J. C., Petriz, J., Garcia, J., and de Madariaga, M. A., *Biochim. Biophys. Acta.*, **2000**, 1509, 299-310.

192. Kirpotin, D., Hong, K., Mullah, N., Papahadjopoulos, D., and Zalipsky, S., *FEBS Lett.*, **1996**, 388, 115-118.

193. Feener, E. P., Shen, W.-C., and Ryser, H. J. P., *J. Biol. Chem.*, **1990**, 265, 18780-18785.

194. Jensen, P. E., *J. Exp. Med.*, **1991**, 174, 1121-1130.

195. Phan, U. T., Maric, M., Dick, T. P., and Cresswell, P., *Immunogenetics*, **2001**, 53, 342-346.

196. Saito, G., Swanson, J. A., and Lee, K.-D., *Adv. Drug. Del. Rev.*, **2003**, 55, 199-215.

197. Chhabra, S. R., Hothi, B., Evans, D. J., White, P. D., Bycroft, B. W., and Chan, W. C., *Tetrahedron Lett.*, **1998**, 39, 1603-1606.

198. Jones, J., *"Amino Acid and Peptide Synthesis"*, S. G. Davies, ed., Oxford University Press, **1994**, pp. 25-41.

199. *"An Introduction to Peptide Chemistry"*, Bailey, P. D., ed., John Wiley & Sons Ltd, **1997**, pp. 114-151.

200. Shapiro, G., Büchler, D., Dalvit, C., Frey, P., del Carmen Fernández, M., Gomez-Lor, B., Pombo-Villar, E., Stauss, U., Swoboda, R., and Waridel, C., *Bioorg. Med. Chem.*, **1997**, 5, 147-156.

201. McBroom, C. R., Samanen, C. H., and Goldstein, I. J., *Methods Enzymol.*, **1972**, 28, 212-219.

202. Mukerjee, A. K. and Ashare, R., *Chem. Rev.*, **1991**, 91, 1-24.

203. Kryczka, K., Lewandowski, M., Kazimierczak, J., and Bombinska, D., *Organika*, **2001**, 65-72.

204. Schropl, E. and Pohloudek-Fabini, R., *Pharmazie*, **1968**, 23, 484-490.

205. Lemieux, R. U. and Chü, N. J., *Abstr. Pap. Am. Chem. Soc.*, **1958**, 133, 31N.

206. *"Stereoelectronic Effects in Organic Chemistry"*, Deslongchamps, P., ed., Pergamon, Oxford., **1983**.

207. *"Monosaccharides: Their Chemistry and Their Roles in Natural Products"*, Collins, P. and R. Ferrier., ed., John Wiley & Sons Ltd., Chichester, **1995**.

208. Michael, A., *Am. Chem. J.*, **1879**, 1, 305-316.

209. Koenigs, W. and Knorr, E., *Ber. Dtsch. Chem. Ges.*, **1901**, 34, 957-981.

210. Schmidt, R. R. and Michel, J., *Angew. Chem. Int. Ed.*, **1980**, 19, 731-732.

211. Goux, W. J. and Unkefer, C. J., *Carbohydr. Res.*, **1987**, 159, 191-210.

212. Mori, M., Ito, Y., and Ogawa, T., *Carbohydr. Res.*, **1990**, 195, 199-224.

213. Utille, J.-P. and Priem, B., *Carbohydr. Res.*, **2000**, 329, 431-439.

214. Franzyk, H., Meldel, M., Paulsen, H., and Bock, K., *J. Chem. Soc., Perkin. Trans. 1.*, **1995**, 2883-2898.

215. Mikamo, M., *Carbohydr. Res.*, **1989**, 191, 150-153.

216. Boger, D. L., Teramoto, S., and Zhou, J., *J. Am. Chem. Soc.*, **1995**, 117, 7344-7356.

217. Abbott, S. D., Gasnon, L., Lagraoui, M., Kadhim, S., Attardo, G., Zacharie, B., and Penney, C. L., *J. Med. Chem.*, **1998**, 41, 1909-1926.

218. Ademark, P., Lundquist, J. J., Hagglund, P., Tenkanen, M., Torto, N., Tjerneld, F., and Stalbrand, H., *J. Biotech.*, **1999**, 75, 281-289.

219. Nagase, T., Shinkai, S., and Hamachi, I., *Chem. Comm.*, **2001**, 229-230.

220. Winum, J.-Y., Leydet, A., Seman, M., and Montero, J.-L., *Farmaco*, **2001**, 56, 319-324.

221. Pagé, D., Zanini, D., and Roy, R., *Bioorg. Med. Chem.*, **1996**, 4, 1949-1961.

222. Monsigny, M., Roche, A. C., and Midoux, P., *Biol. Cell.*, **1984**, 51, 187.

223. Rosenfeld, L., *Carbohydr. Res.*, **1976**, 155.

224. Amaike, M., Kobayashi, H., and Shinkai, S., *Bull. Chem. Soc. Japan.*, **2000**, 73, 2553-2558.

225. Smith, D. F., Zopf, D., and Ginsburg, V., *Methods Enzymol.*, **1978**, 50, 163-175.

226. Weber, A. E., Halgren, T. A., Doyle, J. J., Lynch, R. J., Siegl, P. K. S., Parsons, W. H., Greenlee, W. J., and Patchett, A. A., *J. Med. Chem.*, **1991**, 34, 2692-2701.

227. Wang, Q. X. and Phanstiel IV, O., *J. Org. Chem.*, **1998**, 63, 1491-1495.

228. Fields, R., *Methods Enzymol.*, **1972**, 25, 464-469.

229. Lowry, O. H., Resebrough, N. J., Farr, A. L., and Randell, R. J., *J. Biol. Chem.*, **1951**, 193, 350-356.

230. Dubois, M., Gilles, K. A., Hamilton, J. K., Rebers, P. A., and Smith, F., *Anal. Chem.*, **1956**, 28, 350-356.

231. Hashimoto, S., Honda, T., and Ikegami, S. J., *J. Chem. Soc., Chem. Comm.*, **1989**, 685.

232. Magnusson, G., Noori, G., Dahmen, J., Frejd, T., and Lave, T., *Acta. Chem. Scand (B)*, **1981**, 35, 213-216.

233. Smits, E., Engberts, J. B. F. N., Kellogg, R. M., and Doren, H. A., *J. Chem. Soc., Perkin Trans. 1*, **1996**, 2873.

234. Negre, É., Monsigny, M., and Mayer, R., *Tetrahedron*, **1993**, 49, 3991-7000.

235. Thaisrivongs, S., Pals, D. T., Ducharme, D. W., Turner, S. R., Degraaf, G. L., Lawson, J. A., Couch, S. J., and Williams, M. V., *J. Med. Chem.*, **1991**, 34, 633-642.

236. Dean, B., Oguchi, H., Cai, S., Otsuji, E., Tashiro, K., Hakomori, S.-I., and Toyokuni, T., *Carbohydr. Res.*, **1993**., 245, 175-192.

237. Lee, Y. C., Stowell, C. P., and Krantz, M. J., *Biochemistry*, **1976**., 15, 3956-3963.

238. Habeeb, A. F. S. A., *Methods Enzymol.*, **1972**, 25, 463.

239. Augustyns, K., Krass, W., and Jung, G., *J. Pept. Res.*, **1998**, 51, 127-133.

240. Dixon, M., *Biochem. J.*, **1972**, 129, 197-202.

241. Spadaro, A. C. C., Draghetta, W., Nassif del Lama, S., Camargo, A. C. M., and Greene, L. J., *Anal. Chem.*, **1979**, 96, 317-321.

242. Diment, S. and Stahl, P. D., *J. Biol. Chem.*, **1985**, 260, 15311-15317.

243. Buktenica, S., Olenick, S. J., Salgia, R., and Frankfater, A., *J. Biol. Chem.*, 262, **1987**, 9469-9476.

244. Girolomoni, G., Lutz, M. B., Pastore, S., Assmann, C. U., Cavani, A., and Ricciardi-Castagnoli, P., *Eur. J. Immunol.*, **1995**, 25, 2163-2169.

245. Lutz, M. B., Assmann, C. U., Girolomoni, G., and Ricciardi-Castagnoli, P., *Eur. J. Immunol.*, **1996**, 26, 586-594.

246. Free, P., Hurley, C. A., Kageyama, T., Chain, B. M., and Tabor, A. B., *Org. Biomol. Chem.*, **2006**, 4, 1817-1830.

247. Chain, B. M., Free, P., Medd, P., Swetman, C., Tabor, A. B., and Terrazzini, N., *J. Immunol.*, **2005**., 174, 1791-1800.

248. Kjeken, R., Brech, A., LØvdal, T., Roos, N., and Berg, T., *Exp. Cell. Res.*, **1995**, 216, 290-298.

249. Moss, C. X., Villadangos, J. A., and Watts, C., *Eur. J. Immunol.*, **2005**., 35, 3442-3451.

250. Erlanson, D. A., McDowell, R. S., He, M. H., Randal, M., Simmons, R. L., Kung, J., Waight, A., and Hansen, S. K., *JACS.*, **2003**., 125, 5602-5603.

251. Baggett, N., and Marsden, B. J., *Carbohydr. Res.*, **1983**, 285-291.

252. Tsuzuki, T., *Bull. Chem. Soc. Jpn.*, **1967**., 40, 1208-1210.